

Mechanisms regulating endothelial barrier integrity *in vitro*

A thesis submitted to the University of East Anglia
for the degree of Doctor of Philosophy

By
Irene Pla-Navarro

University of East Anglia
School of Biological Sciences
Norwich, NR4 7TJ

September 2018

© This copy of the thesis has been supplied on condition that anyone who consults it is understood to recognise that its copyright rests with the author and that no quotation from the thesis, nor any information derived there-from may be published without the author's prior, written consent.

Abstract

Loss of endothelial barrier integrity is of key importance in a number of neuropathological conditions. Blood-Brain barrier (BBB) disruption, in part driven by cytokines, is an early event in the pathogenesis of Multiple Sclerosis (MS), an inflammatory autoimmune disorder caused by the presence of multifocal demyelinating lesions within the CNS. Astrocyte-derived sonic hedgehog (Shh) promotes BBB formation and a reduction in Shh levels has been reported in MS patients. Low circulating levels of Vitamin D3 are associated with an increased risk of MS although the molecular pathways underlying Vitamin D3 effects on MS pathogenesis remain elusive. Interplay between Shh and Vitamin D3 pathways has been reported in other cell types but this has not been yet studied in the context of the BBB. Several microRNAs are regulated in MS but their function is not always clear.

The hypothesis that under inflammatory conditions, Shh and Vitamin D3 signalling pathways may interact in order to promote endothelial barrier stability and/or prevent cytokine-driven BBB disruption was tested. A murine and a human endothelial barrier model were established and explored in the context of inflammation. Shh and Vitamin D3 treatment prevented cytokine-induced endothelial barrier disruption, in both model systems, possibly through the regulation of metalloproteinase expression and/or localisation. In addition, analysis of the human endothelial BBB barrier model suggested that miR125b is a possible candidate to exacerbate cytokine-driven loss in barrier integrity. Analysis of microarray data with the human BBB model revealed that Shh and Vitamin D3 treatment could prevent cytokine-driven tissue factor (TF/F3) expression, suggesting that this could be an additional mechanism by which Shh and Vitamin D3 can mediate their protective synergy against cytokine-driven barrier dysfunction.

Overall the data suggests that cross-talk between Shh and Vitamin D3 may provide a new approach to reducing loss off BBB integrity.

Acknowledgements

First of all, I would like to express my gratitude to my primary supervisor Dr. Jelena Gavrilovic, not only for guiding and supervising this work but also for being a constant source of support and inspiration through this whole project. I am also extremely grateful to all the members of the Gavrilovic lab (past and present), in particular to Dr. Damon Bevan for all his guidance, patience and laughs.

I would also like to thank my secondary supervisors Dr. Mohammad Hajihosseini and Dr. Mette Mogensen for their insightful comments, constant support, availability and generosity every time a resource was needed. Special thanks to Dr. Martin Lee for his invaluable guidance in all the clinical aspects of this work, Dr. Simon Moxon for all his help and advice with the bioinformatic aspects of the microarray analysis and Dr. Paul Thomas for all his guidance and insightful comments on imaging.

None of this would have been possible without all the support from friends and family. Thanks to Tope (for all those coffees), Ben (for all those walks), Stuart (for all the banter) Estela (por esos cigarritos), Maria (por todo el salseo), Sente (por tantísimas cosas que no me caben) and Raquel (porque estando lejos estás muy cerca). Special thanks to my mum for unconditionally being there when needed; my dad, for always supporting me and being the inspiration that pushed me through this project; and James, for putting up with me in the worst moments and always finding a way to make me smile.

Finally, thanks to Finn and Morty, because no matter how desperate I was, you kept purring.

List of Abbreviations

ADAM	-	A Disintegrin And Metalloproteinases
ADAMTS	-	A Disintegrin And Metalloproteinase with Thrombospondin motifs
AJ	-	Adherens Junction
ANG	-	Angiotensin
APC	-	Antigen-Presenting Cell
BBB	-	Blood-Brain Barrier
BCA	-	Bicinchoninic Acid Assay
BE	-	Bromoacetate
BSA	-	Bovine Serum Albumin
CASK	-	Ca ²⁺ -dependent serine protein kinase
CNS	-	Central Nervous System
CRE	-	CREB Responsive Element
CREB	-	cAMP Response Element Binding Protein
CytoD	-	Cytochalasin D
DBP	-	Vitamin D Binding Protein
ddH ₂ O	-	Double distilled water
DMEM	-	Dublecco's Modified Eagle Medium
EAE	-	Experimental Autoimmune Encephalomyelitis
EBM	-	Endothelial Basal Medium
EC	-	Endothelial Cell
ECGS	-	Endothelial Cell Growth Supplement
FCS	-	Fetal Calf Serum

FITC	-	Fluorescein Isothiocyanate
F3	-	Tissue factor (TF) or Coagulation Factor III
GA	-	Glatiramer Acetate
GSK	-	Glycogen Synthase Kinase
hCMEC/D3	-	Human Microvascular Endothelial Cell Line
HH	-	Hedgehog
HUVEC	-	Human Umbilical Vein Endothelial Cell Line
ICAM	-	Intracellular Adhesion Molecule
IGF1	-	Insulin-Like Growth Factor 1
IL	-	Interleukin
INF β	-	Interferon β
INF γ	-	Interferon γ
JAM	-	Junctional Adhesion Molecule
LFA1	-	Leukocyte Function-associated Antigen 1
LPL	-	Low-density Lipoprotein
LRP1	-	Low-density lipoprotein Receptor-related protein 1
MBP	-	Myelin Binding Protein
MCEC1	-	Mouse Cardiac Endothelial Cell Line 1
MHC	-	Major-Histocompatibility-Complex
mRNA	-	Messenger RNA
miRNA	-	Micro RNA
MLC	-	Myosin Light Chain
MLCK	-	Myosin Light Chain Kinase
MMP	-	Matrix Metalloproteinase

MOG	-	Myelin Oligodendrocyte Glycoprotein
MRI	-	Magnetic Resonance Imaging
MS	-	Multiple Sclerosis
NPC1	-	Niemann-Pick disease type C1
NR2F2	-	Nuclear Receptor subfamily 2 group F member 2
PDGF	-	Platelet Derived Growth Factor
PECAM	-	Platelet Endothelial Cell Adhesion Molecule
PI3K	-	Phosphoinositide 3-kinase
PKA	-	Protein Kinase A
PKB	-	Protein Kinase B
PLP	-	Proteolipid Protein
PPMS	-	Primary Progressive Multiple Sclerosis
PTCH	-	Patched
PVDF	-	Polyvinylidene fluoride
qRT-PCR	-	Quantitative Reverse Transcription Polymerase Chain Reaction
RISC	-	miRNA-Induced Silencing Complex
ROS	-	Reactive Oxygen Species
RORC	-	RAR Related Orphan Receptor C
RRMS	-	Relapsing Remitting Multiple Sclerosis
RXR	-	Retinoid X Receptor
TCA	-	Trichloroacetic Acid
TF	-	Tissue Factor
SHH	-	Sonic Hedgehog
SMO	-	Smoothened

TEER	-	Transendothelial Electrical Resistance
TGF β	-	Transforming Growth Factor β
TIMP	-	Tissue Inhibitor of Metalloproteinases
TJ	-	Tight Junction
Th1	-	Type 1 Helper
Th2	-	Type 2 Helper
TNF α	-	Tumour Necrosis Factor α
tPA	-	tissue-type Plasminogen Activator
VCAM	-	Vascular Cell Adhesion Molecule
VDR	-	Vitamin D Receptor
VDRE	-	Vitamin D response Elements
VEGF	-	Vascular Endothelial Growth Factor
ZO1	-	Zona Occludens 1
7DCH	-	7-dihydroxycholesterol

Table of Contents

ABSTRACT	ii
ACKNOWLEDGEMENTS.....	iii
LIST OF ABBREVIATIONS.....	iv
TABLE OF CONTENTS	viii
LIST OF FIGURES AND TABLES	xvi
1.Introduction	1
1.1. The Blood-Brain Barrier	2
1.2. Multiple Sclerosis, histopathological aspects.....	4
1.3. Vitamin D and Multiple Sclerosis	7
1.4. Modelling Multiple Sclerosis	7
1.5 Immune-mediated injury mechanisms during Multiple Sclerosis	8
1.6. Matrix Metalloproteinases play a key role during Blood Brain Barrier disruption.....	17
1.7. Vitamin D, a dual protective effect in the pathology of Multiple Sclerosis	26
1.7.1. Vitamin D reduces leukocyte’s ability to enter the CNS	29
1.7.2. Vitamin D increases the stability of the Blood Brain Barrier.....	29
1.8. Shh plays an anti-inflammatory role during Multiple Sclerosis pathogenesis	30
1.8.1. Shh pathway enhances Blood Brain Barrier maintenance.....	33
1.8.2. Shh pathway modulates the infiltration of pro-inflammatory cells	34
1.9. Shh and Vitamin D, a regulatory cross-talk.....	34
1.10. miRNAs dysregulated in Multiple Sclerosis	39
1.10.1 miR125b and miR326 target Hedgehog and Vitamin D pathways	42
1.11. Thesis Aims	44

2. Materials and Methods	45
2.1. Cell culture.....	46
2.1.1. MCEC-1.....	46
2.1.2. hCMEC/D3.....	46
2.2. Treatments	47
2.2.1. Cytokines.....	47
2.2.2. Cyclopamine	47
2.2.3. Sonic Hedgehog	48
2.2.4. Vitamin D3.....	48
2.2.5. MK-2206.....	48
2.2.6. GM6001.....	49
2.2.7. hTIMP3	49
2.2.8. Cytochalasin D.....	49
2.3. Cell viability assay	50
2.4. Immunocytochemistry.....	50
2.5. Total RNA purification.....	51
2.6. Reverse Transcription.....	52
2.7. Quantitative Reverse Transcription Polymerase Chain Reaction	53
2.8. Dextran Extravasation assay	58
2.9. Transendothelial Electrical Resistance assay.....	60
2.10. Protein detection by Western Blotting.....	60
2.10.1. Preparation of cell lysates	60
2.10.2. Protein quantification	61
2.10.3. Trichloroacetic Acid Precipitation	61
2.10.4. Protein resolution by SDS-PAGE	62
2.10.5. Semi-dry transfer of polyacrylamide gels onto PVDF membranes	62

2.10.6. Proteins immunodetection.....	62
2.10.7. Membrane stripping	63
2.11. Transfection of hCMEC/D3 cells.....	66
2.12. Microarray analysis.....	66
2.13. Statistical analysis	67
3. Development of an in vitro murine endothelial cell barrier model	68
3.1. INTRODUCTION	69
3.1.1. Endothelial barriers	69
3.1.2. MCEC-1: an endothelial cell line.....	69
3.1.3. Endothelial barriers are disrupted under inflammatory conditions..	69
3.1.4. Shh as an endothelial barrier promoting agent	72
3.1.5. Vitamin D3 and endothelial barrier integrity.....	72
3.1.6. Shh and Vitamin D3, an unexplored cross-talk	73
3.1.7. Transwell Cell Culture System.....	73
3.1.8. Aims.....	75
3.2. RESULTS	76
3.2.1. Tight Junction modulation in MCEC-1 confluent monolayers	76
3.2.1.1. MCEC-1 cells form a monolayer with responsive tight junctions when grown to confluence.....	76
3.2.1.2. Treatment with Shh or Vitamin D3 enhances Tight Junction protein expression/integrity formation	80
3.2.1.3. Abrogation of Hedgehog pathway (cyclopamine) has no effect on tight junction integrity.....	82
3.2.1.4. Tight junction integrity is compromised under inflammatory conditions	84
3.2.1.5. Cytokine driven loss of junctional ZO-1 can be synergistically enhanced by Hedgehog pathway abrogation (cyclopamine)	86

3.2.1.6. Preliminary observations show that a combination of Shh and Vitamin D3 may be needed to rescue cytokine and cyclopamine driven loss of junctional integrity.....	88
3.2.1.7. Akt activation in the Cytokine, Vitamin D3 and Hedgehog pathways..	90
3.2.1.8. Cytokine/cyclopamine driven loss of junctional stability could be metalloproteinase-dependent	92
3.2.2. Gene expression changes which may underly cytokine- and cyclopamine-driven effects	96
3.2.2.1. Cytokine and cyclopamine synergistically increase metalloproteinase expression	94
3.2.2.2. Cytokine-driven decrease in ZO-1 gene expression can be synergistically enhanced by cyclopamine	98
3.2.2.2. Cytokine-driven decrease in ZO-1 gene expression can be synergistically enhanced by cyclopamine	98
3.2.2.3. Regulation of steady state mRNA levels of Hedgehog pathway components.....	100
3.2.2.4. Barrier formation in the MCEC-1 in vitro mode.....	102
3.2.2.5. Barrier integrity is compromised after cytokine treatment in our in vitro model.....	104
3.2.2.6. Cyclopamine synergises with cytokines to further compromise barrier integrity.....	106
3.2.2.7. Cytokine/cyclopamine mediated loss of barrier integrity is metalloproteinase-dependent	108
3.2.2.8. Addition of hTIMP3 partially reverses cytokine/cyclopamine driven barrier disruption.....	110
3.2.2.9. Shh and Vitamin D3 synergistically protect against cytokines and cyclopamine driven barrier dysfunction.....	112
3.3. DISCUSSION	115
3.3.1. Mimicking an inflammatory environment reduces barrier stability	115
3.3.2. Shh and Vitamin D3 promote barrier structure	117

3.3.3. Hedgehog pathway abrogation (cyclopamine) furthers inflammation-driven barrier disruption.....	119
3.3.4. Shh and Vitamin D3 synergistically rescue cytokines and cyclopamine driven barrier disruption.	122
3.4. KEY FINDINGS	125
3.5. FUTURE STUDIES.....	127
4. Establishing an <i>in vitro</i> model with a human brain endothelial cell line	128
4.1. INTRODUCTION	129
4.1.1. The Blood-Brain Barrier	129
4.1.2. hCMEC/D3: a brain endothelial cell line.....	129
4.1.3. The BBB is disrupted under inflammatory conditions	130
4.1.4. Shh enhances BBB integrity.....	130
4.1.5. Vitamin D3 promotes BBB integrity	131
4.1.6. Shh and Vitamin D3, an unexplored cross-talk	131
4.1.7. Aims.....	132
4.2. RESULTS	133
4.2.1. Functional changes in an in vitro model of the BBB	133
4.2.1.1. Barrier formation in an in vitro model of the BBB.....	133
4.2.1.2. TEER resistance is reduced under inflammatory conditions.....	137
4.2.1.3. TEER resistance is enhanced by Shh and Vitamin D3.....	139
4.2.1.4. Shh and Vitamin D3 synergistically rescue cytokine-driven loss in TEER resistance	143
4.2.1.5. Cell viability assay.....	145
4.2.2. Tight Junction formation in confluent hCMEC/D3 monolayers ...	147
4.2.2.1. Immunofluorescent assessment of junctional integrity	147
4.2.2.1. ZO-1 gene expression is reduced under inflammatory conditions	152
4.2.3. Cytokines-driven barrier disruption is metalloproteinase-dependent	154

4.2.3.1. Metalloproteinase inhibition rescues cytokine-driven TEER reduction	154
4.2.3.2. Metalloproteinase gene expression is increased under inflammatory conditions	156
4.2.3.3. Cytokine-driven increase in metalloproteinase expression can be partially reduced by a combination of Shh and Vitamin D3	158
4.2.3.4. Cytokine-driven increase in secreted metalloproteinase protein levels can be partially reduced by a combination of Shh and Vitamin D3.....	162
4.2.3.5. A combination of Shh and Vitamin D3 partially blocked cytokine-driven increase in MMP3 intracellular levels	167
4.2.3.6. Cytokine-mediated reduction in LRP1 mRNA levels can be blocked by addition of a combination of Shh and Vitamin D3.....	169
4.2.3.7. Endocytosis mechanisms could be underlying the observed variations in secreted MMP3 levels	171
4.3. DISCUSSION	173
4.3.1. hCMEC/D3 as a model of the BBB.....	173
4.3.1.1. Pro-inflammatory cytokines can enhance barrier permeability in hCMEC/D3 monolayers	174
4.3.1.2. Vitamin D3 as a BBB enhancing agent	175
4.3.1.3. Shh promotes BBB stability.....	175
4.3.1.4. Cytokine-driven loss in barrier integrity can be synergistically rescued by a combination of Shh and Vitamin D3.....	177
4.3.2. hCMEC/D3 and junctional ZO-1 visualization	178
4.3.3. Metalloproteinases and BBB integrity	180
4.3.3.1. Cytokine-driven loss in barrier integrity is metalloproteinase dependent	180
4.4. KEY FINDINGS	189
4.5. FUTURE STUDIES.....	190
5. miR125b as a possible mediator of endothelial barrier integrity – microarray analysis	192
5.1. INTRODUCTION	193

5.1.1. miRNAs	193
5.1.2. miRNAs and Multiple Sclerosis	193
5.1.3. Expression of miRNAs in Norfolk and Norwich University Hospital Multiple Sclerosis patients.....	194
5.1.4. miR125b and miR326 in Multiple Sclerosis	197
5.1.5. Aims	198
5.2. RESULTS	199
5.2.1. miR125b and miR326 in a BBB <i>in vitro</i> model	199
5.2.2. miR125b transfection optimization in hCMEC/D3 cells	201
5.2.3. miR125b dependent barrier modulation in hCMEC/D3 confluent monolayers	206
5.2.4. Microarray analysis of hCMEC/D3 confluent monolayers	210
5.2.5. Effect of cytokines, Shh and Vitamin D3 on steady state mRNA levels in hCMEC/D3 cells	219
5.3. DISCUSSION	226
5.3.1. miR125b as a mediator of BBB stability.....	226
5.3.2. Microarray analysis of cytokine-mediated effects on hCMEC/D3 monolayers	226
5.3.3. Microarray analysis of miR125b-mediated effects of cytokines- treated hCMEC/D3 monolayers.....	227
5.4. KEY FINDINGS	230
5.5. FUTURE STUDIES.....	231
6. Discussion.....	232
6.1. ZO-1 regulation and cytoskeletal rearrangements	233
6.2. ZO-1 phosphorylation: possible role in VitD3 and Shh effects on barrier integrity	234
6.3. Actin and junctional integrity	235
6.4. Roles of RhoA activation and CREB in barrier integrity	239

6.5. Regulation of metalloproteinase activity	241
6.6. F3 as a regulator of BBB integrity	243
6.7. FUTURE STUDIES.....	247
7. APPENDIX.....	250
8. REFERENCES	273

List of Figures and Tables

CHAPTER 1

Figure 1.1 - Schematic representation of the architecture of the blood-brain barrier (BBB).....	3
Figure 1.2 - Schematic representation of the different events implicated in the migration of activated circulating leukocytes across the blood-brain barrier in the context of Multiple Sclerosis.....	12
Figure 1.3 - Graphic representation of the injury and repair mechanisms taking place during the pathogenesis of Multiple Sclerosis (MS).....	13
Figure 1.4 - Schematic representation of Metzincin structural domains	18
Table 1.1 - Key findings regarding metalloproteinases effect in BBB integrity and BBB related disease	22
Figure 1.5 - Synthesis, activation and catabolism of Vitamin D3.....	26
Figure 1.6 - Vitamin D3 mediated regulation of gene transcription.....	27
Figure 1.7 - Schematic representation of the molecular elements involved in the intracellular cascade of the Shh pathway.....	32
Figure 1.8 – Schematic representation of Hh and Vitamin D3 pathways cross-talk	38
Table 1.2 – miRNAs and Multiple Sclerosis.....	40

CHAPTER 2

Table 2.1 - Murine primer and probe sequences used for qRT-PCR.....	54
Table 2.2 - Human primer and probe sequences used for qRT-PCR	56
Figure 2.1 - Cytokines treatment does not alter barrier permeability to Dextran-FITC at 4h and 24h	59
Table 2.3 - Details of primary antibodies used in Western Blotting.....	64
Table 2.4 - Details of secondary antibodies used in Western Blotting	65

CHAPTER 3

Figure 3.1 – Cell viability assay in MCEC-1 cells	71
Figure 3.2 – In vitro modeling of the Blood-Brain Barrier (BBB)	74
Figure 3.3 - MCEC-1 cells form confluent monolayers with tight junctions..	77
Figure 3.4 – Analysis of ZO-1 junctional levels	79
Figure 3.5 – Shh or Vitamin D3 enhance tight junction integrity.....	81
Figure 3.6 – Hedgehog pathway abrogation has no effect in tight junction stability	83
Figure 3.7 – Tight junction stability is compromised under inflammatory conditions.....	85
Figure 3.8 – Hedgehog pathway abrogation in the presence of cytokines can further reduce tight junction stability.....	87
Figure 3.9 – Shh and Vitamin D3 synergistically rescue cytokines and cyclopamine driven loss of junctional stability	89
Figure 3.10 - Cytokines, Shh and Vitamin D3 driven modulation of junction stability is Akt dependent	91
Figure 3.11 – Cytokines and cyclopamine driven loss of tight junction stability could be metalloproteinase dependent	93
Figure 3.12 - Hedgehog pathway abrogation in the presence of cytokines can further reduce tight junction stability.....	95
Figure 3.13 – Cytokine and cyclopamine effects in TIMPs gene expression..	97
Figure 3.14 - Cytokines-driven decrease in ZO-1 gene expression can be synergistically enhanced by cyclopamine	99
Figure 3.15 – Cyclopamine reduces gene expression levels of Hedgehog pathway components	101
Figure 3.16 – Barrier formation was achieved in MCEC-1 confluent monolayers	103
Figure 3.17 - Cytokine treatment induce MCEC-1 barrier permeability	105
Figure 3.18 - Cytokine-driven reduction in MCEC-1 barrier permeability can be further enhanced by addition of cyclopamine.....	107
Figure 3.19 – Cytokines and cyclopamine driven loss in barrier stability is metalloproteinase-dependent	109

Figure 3.20 – hTIMP3 can partially block cytokine/cycloamine driven barrier disruption	111
Figure 3.21 – Shh and Vitamin D3 promote MCEC-1 barrier formation	113
Figure 3.22 – Shh and Vitamin D3 can synergistically rescue cytokines and cycloamine driven barrier dysruption	114
Figure 3.23 - Schematic representation of Chapter's 3 key findings	126

CHAPTER 4

Figure 4.1 – Confluent hCMEC/D3 monolayers form a barrier.....	134
Figure 4.2 – FCS concentration during culture does not affect hCMEC/D3 barrier formation.....	136
Figure 4.3 - Cytokine treatment induce hCMEC/D3 reduction in TEER resistance	138
Figure 4.4 – Shh and/or Vitamin D3 increase TEER resistance.....	140
Figure 4.5 - Shh increases TEER resistance regardless of site of addition	142
Figure 4.6 – Shh and Vitamin D3 synergistically rescue cytokines-driven loss of TEER	144
Figure 4.7 - Cell viability assay in hCMEC/D3 monolayers	146
Figure 4.8 – Tight junction stability is compromised under inflammatory conditions.....	148
Figure 4.9 – Optimization of junctional ZO-1 staining in hCMEC/D3 monolayers	149
Figure 4.10 – Optimization of ZO-1 protein levels analysis by Western Blotting	151
Figure 4.11 – Cytokines, Shh and Vitamin D3 effects in ZO-1 gene expression	153
Figure 4.12 – Metalloproteinase inhibition rescues cytokine-driven loss of barrier integrity	155
Figure 4.13 - Metalloproteinase mRNA levels are elevated under inflammatory conditions.....	157
Figure 4.14 – A combination of Shh and Vitamin D3 can partially block cytokines-driven increase in metalloproteinase expression	160

Figure 4.15 - A combination of Shh and Vitamin D3 can partially block cytokines-driven decrease in TIMPs expression.....	161
Figure 4.16 - A combination of Shh and Vitamin D3 can partially protect against cytokine-driven metalloproteinase extracellular accumulation.....	163
Figure 4.17 - A combination of Shh and Vitamin D3 can partially protect against cytokines-driven increase in MMP10 expression.....	165
Figure 4.18 – Modulation of MMP1, 3 and 10's basal secreted levels	166
Figure 4.19 - A combination of Shh and Vitamin D3 partially blocks cytokines driven increase in MMP3 intracellular levels	168
Figure 4.20 - Cytokines, Shh and Vitamin D3 modulate LRP1 expression at early time-points.....	170
Figure 4.21 – Shh and Vitamin D3 protective effect in MMP3 secreted levels is endocytosis-dependent	172

CHAPTER 5

Table 5.1 - miRNA expression levels in blood samples from Multiple Sclerosis (MS) patients.....	196
Figure 5.1 – miR125b and miR326 regulation under inflammatory conditions	200
Figure 5.2 – Optimization of miR125b Mimic Control transfection conditions	202
Figure 5.3 – Optimization of miR125b Inhibitor Control transfection conditions	203
Figure 5.4 – Optimization of miR125b Inhibitor Control transfection efficiency	205
Figure 5.5 – miR125b impairs barrier properties in an in vitro model of the BBB.....	207
Figure 5.6 – miR125b may be underlying cytokine-driven loss of barrier integrity.	209
Figure 5.7 – Cytokine signalling in immune system pathway (A) retrieved by Genomatix	211

Figure 5.8 - Cytokine signalling in immune system pathway (B) retrieved by Genomatix	214
Figure 5.9 – Extracellular matrix remodelling pathway retrieved by Genomatix	213
Table 5.2 - List of cytokine up-regulated genes associated with the pathogenesis of Multiple Sclerosis (MS) and retrieved from Genomatix pathway analysis.....	215
Table 5.3 - List of cytokine down-regulated genes associated with the pathogenesis of Multiple Sclerosis (MS) and retrieved from Genomatix pathway analysis.....	218
Table 5.4 - Individual genes selected from microarray analysis associated with Multiple Sclerosis (MS) pathology and/or Blood Brain Barrier (BBB) disruption	220
Figure 5.10 – Notch3 mRNA levels are modulated by cytokines but not by combination of Shh and Vitamin D3.....	222
Figure 5.11 – F3 mRNA levels are modulated by cytokines and a combination of Shh and Vitamin D3.....	223
Figure 5.12 – A combination of Shh and Vitamin D3 can partially protect against cytokines-driven increase in F3 expression.....	225

CHAPTER 6

Figure 6.1 - Possible mechanisms underlying cytokine, Shh and Vitamin D3 interactions regulating junctional ZO-1 in the BBB.....	237
Figure 6.2 - Possible mechanisms underlying cytokine, Shh and Vitamin D3 interactions regulating metalloproteinase levels in the BBB.....	241
Figure 6.3 - Schematic representation of the Tissue Factor (F3) mediated pathway of the coagulation cascade	245
Figure 6.4 - Possible mechanisms underlying cytokine, Shh and Vitamin D3 interactions regulating F3 levels in the BBB.....	246

APPENDIX

Appendix 3.A – Variations in MCEC-1 cell size	251
Appendix 3.B - Shh or Vitamin D3 increase junctional fluorescent intensity	252

Appendix 3.C - Hedgehog pathway abrogation in the presence of cytokines can further reduce tight junction stability	253
Appendix 3.D - A combination of Shh and Vitamin D3 rescues cytokines and cyclopamine driven loss of junctional stability	254
Appendix 3.E - Shh or Vitamin D3 cannot rescue cytokines and cyclopamine driven loss of junctional stability individually	255
Appendix 3.F - Cytokines, Shh and Vitamin D3 driven modulation of junction stability is Akt dependent	256
Appendix 3.G - Cytokines and cyclopamine driven loss of tight junction stability is metalloproteinase dependent	258
Appendix 3.H - Raw Ct Values for the measured genes in MCEC-1 monolayers	259
Appendix 3.I - Shh or Vitamin D3 addition had no effect in ZO-1 expression levels.....	260
Appendix 3.J - Gli3 or Ptch1 gene expression levels were not altered by addition of cytokines or Hedgehog pathway abrogation.....	261
Appendix 3.K - Gli2 or Smo gene expression levels were not altered by addition of Shh or Vitamin D3	262
Appendix 4.A - ZO-1 Raw Ct Values in hCMEC/D3 monolayers.....	263
Appendix 4.B - Raw Ct Values for the measured metalloproteinases and their inhibitors in response to cytokines	264
Appendix 4.C - Raw Ct Values for the measured metalloproteinases and their inhibitors in response to Shh and Vitamin D3	265
Appendix 4.D - Raw Ct Values for MMP3 and MMP10 in response to cytokines, Shh and Vitamin D3	266
Appendix 4.E - Raw Ct Values for TIMP2 and TIMP4 in response to cytokines, Shh and Vitamin D3.....	267
Appendix 4.F - LRP1 Raw Ct Values in hCMEC/D3 monolayers	268
Appendix 5.4 - Cumulative plot analysis for miR125 targets	269
Appendix 5.B - Gene symbol and full name of cytokine regulated genes and associated with the pathology of Multiple Sclerosis (MS) reported in table 5.2 and 5.3.....	270
Appendix 5.C - List of possible candidates regulated by miR125b.....	271

1. Introduction

1.1. The Blood-Brain Barrier

The Blood-Brain Barrier (BBB) is a tightly regulated interface between the Central Nervous System (CNS) and the circulating blood that ensures a highly selective paracellular and transcellular exchange of molecules between the two compartments. Structurally, the BBB is formed by a wall of highly specialised capillary endothelial cells (ECs) discontinuously wrapped by a cellular layer of pericytes (it is this discontinuous wrapping that allows a continuous interaction between the different cellular levels). Together, ECs and pericytes synthesise a basement lamina (comprising extracellular matrix components including collagen IV, laminin and heparan sulphate proteoglycan) that provide structural support and contribute to barrier formation. Astrocyte foot processes externally cover this basement membrane acting as intermediates between the blood vessels and the CNS and promoting BBB stability through the secretion of trophic factors (Park et al., 2003; Pla-Navarro et al., 2018; Seo et al., 2012) (**Figure 1.1.**)

The presence of close contacts between neighbouring ECs results in a polarized phenotype and very limited transcellular diffusion, resulting in the BBB's limited permeability. Tight (TJ) and adherens (AJ) junctions link adjacent ECs together (Kniesel & Wolburg, 2000). TJs comprise transmembrane proteins such as occludins, junctional adhesion molecules (JAMs) and claudins which are anchored to actin filaments via adaptor proteins including cingulin, zona occludens proteins (ZO-1, -2 and -3) and Ca²⁺-dependent serine protein kinase (CASK). Endothelial AJs link to the cytoskeleton through transmembrane proteins including vascular-endothelial (VE)-cadherin and catenins (α , β and p120) (Dejana et al., 2000; Kniesel & Wolburg, 2000) (**Figure 1.1.**) For a detailed review of endothelial tight junctions, see Stamatovic et al. (Stamatovic et al., 2016).

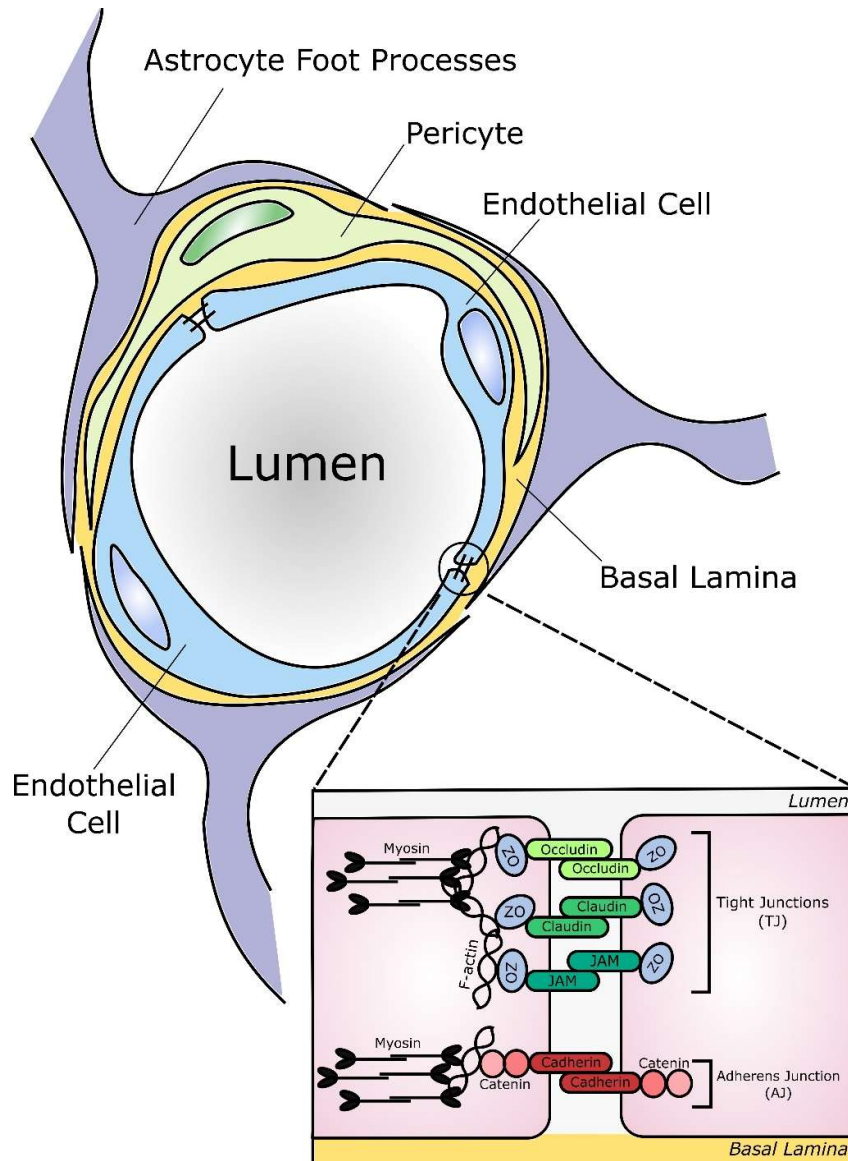


Figure 1.1 - Schematic representation of the architecture of the blood-brain barrier (BBB). Endothelial Cells (ECs) forming the capillaries establish intercellular contacts known as tight junctions. ECs and pericytes are surrounded by a basement membrane, which in turn is also wrapped by astrocyte foot processes. Astrocytes play a major role in BBB maintenance through the secretion of several factors including Shh (not shown) (Image from Pla-Navarro et al., 2018).

The development of the BBB is a tightly regulated process. In the developing brain, neural progenitor cells secrete Vascular Endothelial Growth Factor (VEGF), which guides embryonic ECs migration into the developing brain (Raab et al., 2004). Sprouting, angiogenesis and BBB maturation are promoted by Wnt secreted by neural progenitor cells, which induces transcription of genes implicated in BBB maintenance, such as TJ molecules (Liebner et al., 2008). ECs from emerging vessels release Platelet Derived Growth Factor-b (PDGF-b), promoting pericyte recruitment to the vessels surface (Hellström et al., 1999). Transforming Growth Factor- β (TGF- β)-mediated cross-talk between ECs and surrounding pericytes promotes VE-cadherin upregulation in ECs (increasing pericyte adhesion) and pericyte deposition of ECM components (Hill et al., 2014). Once vessels are formed, neighbouring astrocytes support BBB maturation through the secretion of Sonic Hedgehog (Shh), a trophic factor responsible for increased TJ protein expression in ECs (Alvarez, Dodelet-Devillers, et al., 2011).

Although the BBB is a tightly regulated barrier, a low flow of selective transendothelial transport across this barrier has been described (reviewed in De Bock et al., 2016). During transcytosis, a cargo-packed endocytosed vesicle moves across the cell cytoplasm towards the opposite membrane of a polarised cell. The cargo-packed vesicle will eventually fuse with the target membrane releasing its cargo into the extracellular environment, transporting the cargo molecule from one side of a polarised monolayer to the other (reviewed in De Bock et al., 2016). Interestingly, studies conducted within the context of hypoxia/ischemia point at altered transcytosis as one of the possible mechanisms responsible for the increase in barrier permeability observed in these conditions. In a murine model of stroke, Reeson et al. 2015 described an increase in transcytosis vesicles that accounted for the observed increase in BBB permeability since junctional integrity was preserved at the ultrastructural level (Reeson et al., 2015).

1.2. Multiple Sclerosis, histopathological aspects

Under physiological conditions, the central nervous system (CNS; composed of the brain and spinal cord) depends on a high level of connectivity

achieved through axonal myelination. The myelin sheath is comprised of a highly modified plasma membrane (including specific components such as myelin basic protein) that wraps around axonal segments, insulating them and increasing the speed of axonal conduction (reviewed in Abu-Rub & Miller, 2018). Multiple Sclerosis (MS) is an inflammatory autoimmune disorder caused by the presence of multifocal demyelinating lesions within the CNS. There are a great variety of clinical symptoms associated with this pathology that will depend on the neurological region affected. Regardless of their location, pro-inflammatory lesions are characterized by the presence of immune cell infiltrates which initiate a neuro-inflammatory process that will lead to myelin degradation and, eventually, neuronal loss (Hafler, 2004; Larochelle et al., 2011; Lassmann et al., 2007). In physiological conditions, the entry of pro-inflammatory cells into the CNS is tightly regulated by the BBB. During MS pathogenesis, a reduction in the levels of TJ proteins expressed by ECs will lead to the formation of small gaps that will diminish the BBB isolating properties. In patients, the location and degree of this disruptions can be measured by gadolinium-enhanced magnetic resonance imaging (MRI), showing that BBB breakdown is usually located near new active demyelinating lesions, but not near old ones (active or inactive). Thus, supporting the idea that BBB disruption is an early event in MS pathogenesis that facilitates the entrance of activated inflammatory cells into the CNS (Daneman, 2012). Thus, the pathological entry of self-reactive immune cells (such as T cells) into the CNS can be triggered by a breakdown of the BBB, which has been described as a crucial early event in the development of MS (Abbott et al., 2010; Larochelle et al., 2011).

It has been described that 85% of patients with MS exhibit acute neurological syndrome followed by a series of remission events that will eventually lead to a partial recovery and a period of clinical stability, known as relapsing remitting MS (RRMS). However, as the pathology evolves, recovery periods becomes rarer, generating an elongation of the clinical episode known as secondary progressive MS. The remaining 15% of MS patients will experience primary progressive MS (PPMS), characterised by an absence of remissions and relapses leading to a gradual clinical progression from the

initial stages of the disease (Nylander & Hafler, 2012). The majority of available treatments are effective for the RRMS form of the disease, including the disease modifying interferon β (IFN- β) and the immunomodulatory glatiramer acetate (GA) treatment. IFN- β treatment is effective against RRMS and in some PPMS patients since it modulates the immune system at several levels: reduced ability of activated immune cells to cross the BBB, enhanced regulatory T-cell and B-cell activation, impaired expression of pro-inflammatory cytokines (Kieseier, 2011; Kasper & Reder, 2014). GA (synthetic polymer of four myelin basic protein amino acids; Caporro et al., 2014)) has only shown efficient action in the treatment of RRMS, primarily by inducing the secretion of anti-inflammatory cytokines by reactive T cells and by preventing major histocompatibility complex class II molecule-mediated recognition of myelin antigens (Caporro et al., 2014). Thus, there is a need for treatments to delay neurodegeneration in PPMS patients (Feinstein et al., 2015). Non-specific suppressors of the immune system are able to rapidly decrease progression in PPMS patients, but their efficiency is drastically reduced in long term treatments (Feinstein et al., 2015). The secondary effects derived from immune-suppressive treatments led to the development of a new generation of treatments such as Natalizumab; a humanized monoclonal antibody that inhibits the entry of activated immune cells into the CNS by physically blocking the interaction between the endothelial vascular cell adhesion molecule-1 (VCAM-1) and the Very Late Antigen-4; VLA-4) protein expressed in transmigrating leukocytes (Pilz et al., 2012; Yednock et al., 1992). VLA-4 (or $\alpha 4\beta 1$ integrin) is composed by a $\alpha 4$ chain (CD49d) associated with a $\beta 1$ chain (CD29). When activated, VLA-4 undergoes a conformational change that allows it to bind to its natural ligand VCAM-1. However, Natalizumab's ability to target the $\alpha 4$ chain of integrins can prevent the VLA-4/VCAM-1 interaction blocking the extravasation of activated leukocytes across the BBB. Natalizumab also targets the interaction of $\alpha 4$ -expressing leukocytes with the connecting segment (CS)-1 isoform of fibronectin and osteopontin, further limiting leukocytes' recruitment into the CNS (Abram & Lowell, 2009; McCormack, 2013).

Despite Natalizumab's high efficiency in preventing disability progression and relapse rates, natalizumab-treated patients can generate neutralising antibodies (NAB) against this drug, developing resistance to this therapy (Calabresi et al., 2007). More recently, oral administration of the sphingosine 1-phosphate (S1P) receptor modulator Fingolimod (or FTY720) has been shown to be an efficient therapy against RRMS: Fingolimod prevents T cells release from lymphoid organs into the bloodstream by promoting the internalization of the S1P1-receptor, and it can also be sensed by astrocytes, oligodendrocytes and microglia, possibly promoting remyelination and repair within the CNS (Kipp & Amor, 2012). However, despite all the available treatments previously mentioned, there is an urgent need for more efficient MS therapies, particularly for PPMS.

1.3. Vitamin D and Multiple Sclerosis

Although the aetiology of MS remains unknown, recent observations suggest that the development of this disease may be determined by a combination of genetic susceptibility and environmental risk factors (Oksenberg et al., 2001; Marrie, 2004). Epidemiological studies have reported a strong association between low levels of Vitamin D and increased MS susceptibility (Munger et al., 2006). Additionally, experimental autoimmune encephalomyelitis (EAE, the murine and most common model for MS) can be treated and completely prevented by the bioactive form of Vitamin D; 1,25-dihydroxyvitamin D₃ (1,25-(OH)₂D₃) (Lemire & Archer, 1991; Pedersen et al., 2007), although treatment termination leads to prompt onset of disease symptoms (Grishkan et al., 2013). Further supporting these ideas, some polymorphisms present in the Vitamin D receptor have been correlated with enhanced risk of MS (Niino et al., 2000; Tajouri et al., 2005).

1.4. Modelling Multiple Sclerosis

MS is a highly complicated disease with an extremely variable clinical hallmark. Hence, suitable experimental models are needed in order to clarify the pathological mechanisms underlying this disease and to generate effective therapies.

The most common animal model of MS is known as experimental autoimmune encephalomyelitis (EAE) and, although it can be induced in multiple animal species, is mostly studied in rodents previously immunised with CNS antigens combined with an adjuvant to enhance the immune response. Clinically, it is characterised by inflammation, neurological impairment and myelin damage leading to paralysis and reduced activity. However, there is a broad spectrum of clinical symptoms determined by the genetic context of the recipient and the autoantigen inoculated - the most common of which are purified myelin or myelin proteins such as myelin binding protein (MBP), myelin oligodendrocyte glycoprotein (MOG) and proteolipid protein (PLP) (Wekerle & Kurschus, 2006; McCarthy et al., 2012; van der Star et al., 2012). Additionally, it is been proposed that virus or toxin-induced damage in individuals with a specific susceptibility can activate an inflammatory response that will eventually lead to the formation of a MS lesion. Thus, some animal models, like Theiler's virus-induced encephalitis, have been developed in order to assess the bases of the relationship between CNS autoimmunity and the pathogenic effect of viral antigens or toxins (Altmann & Boyton, 2004; Kipp et al., 2012; McCarthy et al., 2012).

However, despite the invaluable information provided by animal models, the complexity of this syndrome generates a need for a more simplistic approach, in which particular and specific pathological aspects can be assessed independently and in a more controllable environment. This is why in vitro models have been developed, among which BBB models are of great importance due to the central role of BBB breakdown in the pathogenesis of MS. Some models consist of a single culture of endothelial cells, and others incorporate co-cultured endothelial cells together with astrocytes in collagen-coated membranes, allowing the study of the BBB's dynamics and physiology (Naik & Cucullo, 2012; van der Star et al., 2012).

1.5 Immune-mediated injury mechanisms during Multiple Sclerosis

The sequence of events underlying the origin of MS's pathological cascade is largely unknown. It has been broadly accepted that Multiple Sclerosis could be originated by the de-regulated entry of autoreactive T

lymphocytes into the CNS, triggering lesion formation in an outside-in pattern. However, other studies have suggested that MS could be initiated by a neuronal alteration or primary infection within the CNS, which could result in the activation of an inflammatory response. Thus, the inflammatory response responsible for tissue damage would be generated in an inside-out fashion (Mahad et al., 2015) (**Figure 1.2 & Figure 1.3**).

Genetic and/or environmental factors can enhance the ability of circulating autoreactive T cells to cross the BBB and enter the CNS. Adhesion molecules of the selectin family (such as P-selectin, L-selectin or E-selectin) expressed by circulating activated lymphocytes can interact with their respective ligands presented on the vascular side of ECs comprising the BBB (Arpino et al., 2016; Engelhardt & Ransohoff, 2012; Man et al., 2007). The close interaction with the ECs allows circulating leukocytes to detect a signature of chemokines and cytokines (released by the damaged tissue) which enhances leukocyte tethering via the expression of integrins. In the absence of any stimuli, integrins exist in a bent conformation in which the cytoplasmic tails of their α and β subunits are kept together by a salt bridge between residues located in the membrane proximal region. Upon chemokines activation, GTP-bound Rap1 and activated talin are recruited to the integrin's cytoplasmic tail, leading to the separation of the α and β subunits. This conformational change in the cytoplasmic region is transmitted through the transmembrane domain to the extracellular region, leading to an open or activated state capable of high-affinity ligand binding (Abram & Lowell, 2009; Engelhardt, 2006; Prendergast & Anderton, 2009).

The increased affinity between the immune cell and the endothelium strengthens leukocyte adhesion to the vascular wall, leading to a crawling process mainly mediated by alpha L (Leukocyte Function-associated Antigen-1; LFA-1) and alpha 4 integrins (expressed at the leukocyte cell surface) and their respective endothelial partners Intercellular Adhesion Molecules (ICAMs) and Vascular Cell Adhesion Proteins (VCAMs) (Man et al., 2007; Hauser & Goodin, 2008; Engelhardt & Ransohoff, 2012). During this stage, crawling immune cells scan the endothelial surface looking for a permissive site for extravasation (or diapedesis), where protrusions from the endothelium's

membranes surround the adherent leukocyte helping it to migrate across the BBB. This extravasation can take place through two different routes: paracellular diapedesis and transcellular diapedesis. Whereas the molecular mechanisms underlying transcellular diapedesis are less understood, during paracellular diapedesis the activated leukocyte disrupts the endothelial junctions between adjacent ECs, generating a gap in the BBB that allows its transmigration (Man et al., 2007; Hauser & Goodin, 2008; Engelhardt & Ransohoff, 2012). Once the circulating autoreactive T cells have entered the CNS, they secrete proinflammatory cytokines such as interferon- γ (INF- γ) and tumour necrosis factor- α (TNF- α) (Engelhardt, 2006; Man et al., 2007; Engelhardt & Ransohoff, 2012). The released cytokines can then activate antigen-presenting cells (APCs) and further promote the migration of T cells across the BBB by increasing the expression of adhesion molecules in both circulating lymphocytes and ECs (reviewed in Vestweber (Vestweber, 2015)). These activated APCs then express class II major-histocompatibility-complex (MHC) molecules containing the presumed “MS antigen” (myelin basic protein, myelin oligodendrocyte glycoprotein (MOG), or myelin-associated glycoprotein among others), which can be recognised by the T-cell receptor complex located in the autoreactive T cell surface. Interestingly, this interaction results in an enhanced or reduced (anergy) immune response against the MS antigen depending on the combination of co-stimulatory molecules expressed at the APC and T cell surfaces: T cell activation leads to differentiation into CD4+ type 1 helper (Th1) or type 2 helper (Th2) cells, which can enhance or impair the immune response through the secretion of pro-inflammatory or anti-inflammatory cytokines respectively. Whereas Th2 cells can induce the production of B cells (characterised by their antibody production) and send anti-inflammatory signals to APCs, Th1 cells orchestrate a myelin and oligodendrocyte immune-mediated injury through the secretion of pro-inflammatory cytokines such as TNF- α and INF- γ . These pro-inflammatory cytokines can in turn trigger macrophage activation, which damage myelin membranes and oligodendrocytes via phagocytic mechanisms, secretion of proteases and production of reactive oxygen species (ROS). However, APCs can also interact with CD8+ T cells, leading to the activation of CD8+ T cells or cytotoxic T cells, triggering apoptosis of cells expressing the targeted

antigen via the Fas-ligand signalling pathway (reviewed in Noseworthy et al., 2000). Thus, cytokines play a crucial role initiating and promoting the entry of pro-inflammatory cells into the CNS.

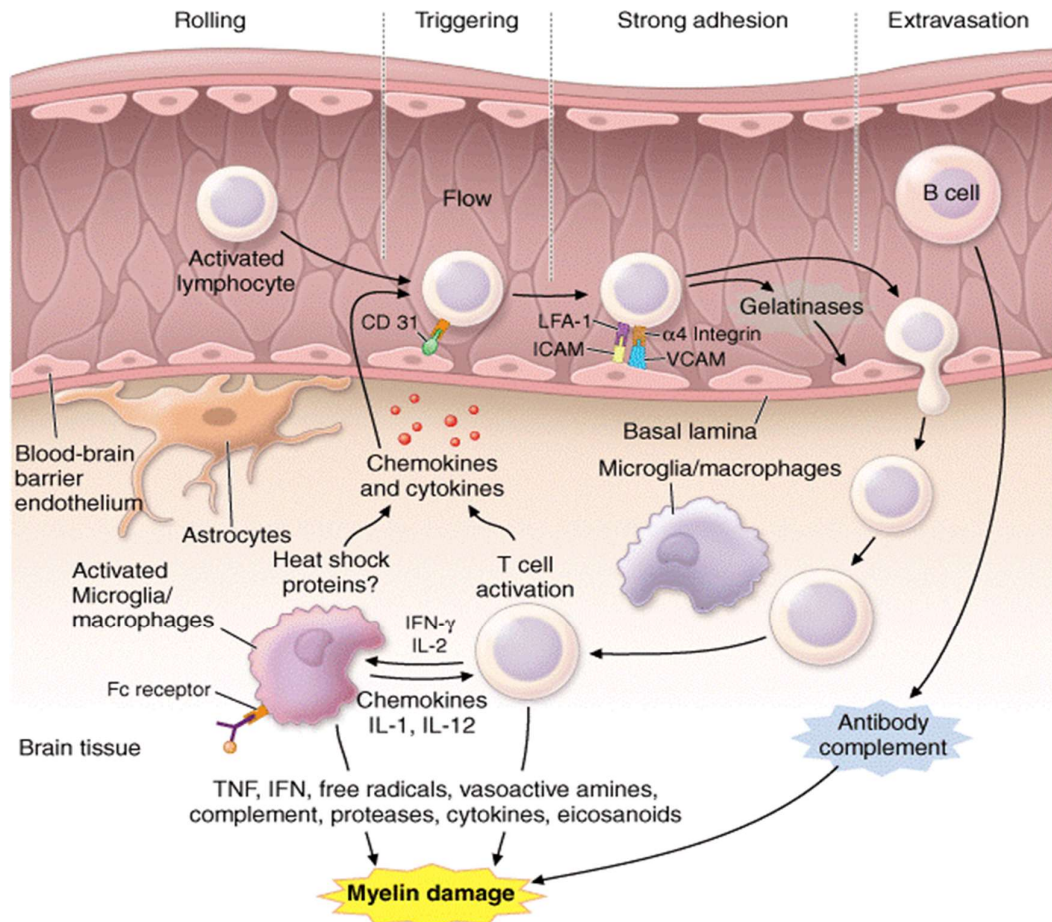


Figure 1.2 - Schematic representation of the different events implicated in the migration of activated circulating leukocytes across the blood-brain barrier in the context of Multiple Sclerosis. Activated leukocytes adhere to the vascular side of the endothelial cells (EC) composing the blood-brain barrier (BBB) through the expression of adhesion molecules and their respective endothelial ligands (triggering stage). Leukocytes are now in close contact with the endothelium, which allows them to detect a signature of cytokines and chemokines released by the activated microglia in the damaged tissue. This enhances leukocyte adhesion via the expression of integrins, leading to a crawling process (strong adhesion stage) mainly mediated by alpha L (Leukocyte Function-associated Antigen-1; LFA-1) and alpha 4 integrins (expressed at the leukocyte cell surface) and their respective endothelial partners Intercellular Adhesion Molecules (ICAMs) and Vascular Cell Adhesion Proteins (VCAMs). Through the secretion of gelatinases (and other metalloproteinases), activated leukocytes degrade the tight cell-to-cell contacts between adjacent ECs and basal lamina components, helping them to migrate across the BBB (extravasation). Once they have entered the central nervous system (CNS), activated leukocytes enhance the recruitment of additional activated immune cells through the secretion of chemokines and cytokines into the extracellular environment, establishing a pro-inflammatory feedback loop (Image from Hauser & Goodin, 2008).

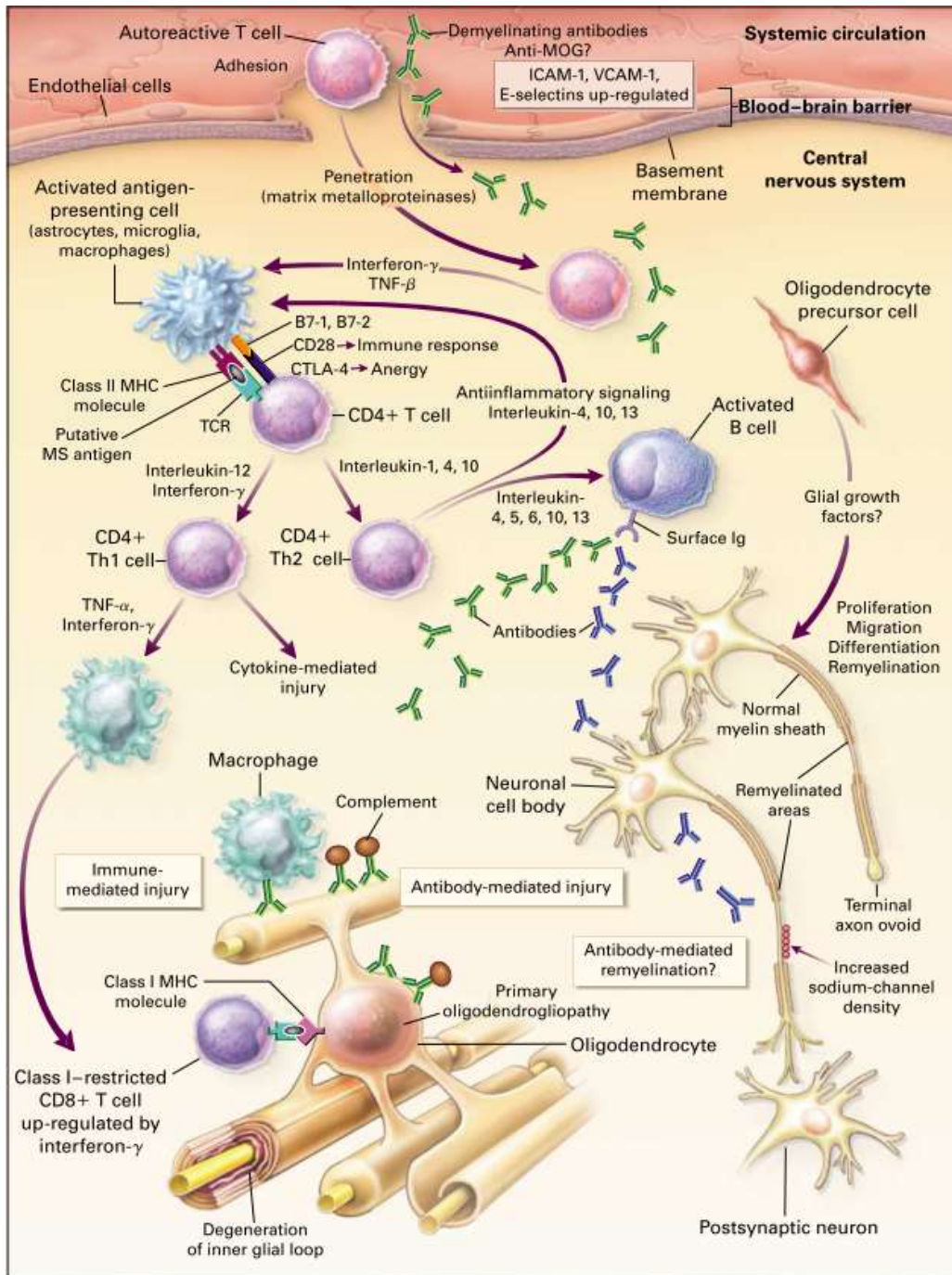


Figure 1.3 Graphic representation of the injury and repair mechanisms taking place during the pathogenesis of Multiple Sclerosis (MS). Genetic and environmental factors (such as viral infection) can activate and promote the movement of autoreactive T cells from the blood stream into the central nervous system (CNS) across the blood-brain barrier (BBB) through the upregulation endothelial adhesion molecules such as Intercellular adhesion molecule 1 (ICAM-1), vascular cell adhesion molecule 1 (VCAM-1) and E-selectin. Proteases, such as matrix metalloproteinases (MMPs), can enhance the trans migration of activated T cells across the BBB by degrading extracellular matrix components. Once in the CNS, pro-inflammatory cytokines released by activated T cells (interferon- γ [INF γ] and tumour necrosis factor β [TNF- β]), may trigger an increase in cell-surface molecules on surrounding lymphocytes and antigen-presenting cells. Binding of putative multiple sclerosis (MS) antigens (such as myelin basic protein among others) by the class II major-histocompatibility-complex (MHC) and the T-cell receptor (TCR) may trigger an enhanced immune response through the differentiation of T cells into Th1 (pro-inflammatory) or Th2 (anti-inflammatory) cells depending on the signature of costimulatory molecules present (e.g. CD28 or CTLA-4). Th2 cells can promote an anti-inflammatory response (anergy) through production of anti-inflammatory cytokines (e.g. interleukin [IL]-1, -4 or -10) and the consequent activation of antibody-producing B cells. However, if the signature of costimulatory molecules triggers an enhancement of inflammation, T cells will differentiate into Th1 cells through the secretion of pro-inflammatory cytokines (e.g. INF γ , TNF α or IL-12), triggering a cascade of signalling events that will result in the proliferation of Th1 cells and activation of macrophages (microglia in the CNS) that will ultimately lead to immune-mediated degeneration of oligodendrocytes and myelin. Several mechanisms of immune-mediated injury have been suggested: macrophages-mediated degradation of myelin antigens; complement-mediated injury; or direct injury by activated T cells (CD4+ or CD8+). Injury to the myelin membrane will result in denuded axons no longer capable of transmitting action potentials, which will lead to neurological symptoms. Additionally, denuded axons will be susceptible to further injury by soluble mediators (such as cytokines, chemokines, complement and/or proteases), leading to irreversible axonal damage. However, before axonal damage occurs, several mechanisms of myelin repair have been described: resolution of the inflammatory response followed by remyelination; restored conduction by an increased expression of sodium channels that will recover denuded axon segments and restore conduction; antibody-mediated remyelination; and proliferation, migration and differentiation of resident oligodendrocyte precursor cells (image from Noseworthy et al., 2000).

Release of pro-inflammatory mediators is widely-agreed to be an early event in MS pathology, leading to BBB disruption (Minagar & Alexander, 2003; Abbott et al., 2010; Larochelle et al., 2011). This immune-mediated damage will result in enhanced demyelination and impaired axonal conduction (axons are no longer transmit axon potentials and saltatory conduction is lost) resulting in characteristic neurological symptoms. These denuded axons become highly susceptible to damage by soluble factors (e.g. proteases or chemokines), resulting in some instances, in irreversible axonal transection. However, more frequently partial remyelination may occur following resolution of the inflammatory response with proliferation and differentiation of oligodendrocyte precursor cells resulting in the generation of a substitutive thin myelin sheet; and increased density of sodium-channels in the demyelinated regions in an attempt to restore a normal axonal conduction (reviewed in Noseworthy et al., 2000).

Many studies have reported the role of cytokines in BBB disruption, not only in MS but also in other neuroinflammatory disorders. Cytokines released by activated microglia (TNF α , IL-1 and -6) can lead to increased BBB permeability in Hepatic Encephalopathy (Butterworth, 2015; Jayakumar et al., 2015). During ischemic stroke activated perivascular astrocytes and microglia release cytokines such as TNF α and IL-1 triggering BBB breakdown (Amantea et al., 2015). Meningitis and BBB breakdown in rat can be induced by elevated levels of IL-1 (Quagliariello et al., 1991). In particular, increased levels of IL-1 α have been associated with increased BBB permeability in *in vitro* studies with brain ECs (Al-Obaidi & Desa, 2018; Ravindran, Agrawal, Gupta, & Lakshmana Rao, 2011) and combined secretion of IL-1 α and TNF α by activated leukocytes can trigger an increase in BBB's paracellular permeability, transcellular migration and loss of junctional stability (Afonso et al., 2007). Elevated levels of circulating TNF α , IL-17A and decreased levels of circulating IL-10 were reported in Multiple Sclerosis patients (Trenova et al., 2018). Although the exact mechanisms by which cytokines trigger BBB disruption are incompletely understood, reduced levels of TJ proteins (such as ZO-1, claudin-5 and occludin) have been reported (Forster et al., 2008; Aslam et al., 2012; Cohen et al., 2013; Labus et al., 2014). Despite the generally accepted effect of

cytokines on BBB stability, a small number of studies have reported TNF α stimulation had no effect on TJ protein levels such as ZO-1 (Labus et al., 2014) or VE-cadherin (Forster et al., 2008). In some instances, IL-1 β disrupts TJs and can mediate up-regulation of other cytokines including TNF α and IL-6 (Cohen et al., 2013). Additionally, TNF α stimulation increased occludin levels in bovine retinal ECs (Aveleira et al., 2010) while increased levels of claudin-5 were reported after IL-6 stimulation in ovine microvessels (Cohen et al., 2013). Taken together, the detrimental effects of cytokines on BBB stability seems compelling, although there may be exceptions in certain complex environmental conditions: overexpression of anti-inflammatory cytokines such as IL-4 and IL-10 was capable of ameliorating brain lesions and cellular infiltration in a murine model of Multiple Sclerosis (Hosseini et al., 2017), and termination of inflammation together with repair mechanisms can be promoted by microglial secretion of IL-10, transforming growth factor β (TGF β) and insulin-like growth factor 1 (IGF1) (Amantea et al., 2015). For an overview of factors controlling BBB permeability, see Almutairi *et al.* (Almutairi et al., 2016).

Proving the importance of auto-reactive immune cells in the pathology of MS, autologous hematopoietic stem cell transplantation (HSCT) has been shown to ameliorate MS progression particularly in RRMS patients (Radaelli et al., 2014). Prior to HSCT, patients undergo an immunosuppressive conditioning regimen that temporarily eradicates auto-reactive T cells. Additionally, autologous hematopoietic stem cells (HTS) collected from the patient (either directly from the bone marrow or by leukapheresis from the peripheral blood) are re-infused following a conditioning regimen with high-dose chemotherapy by which the remaining auto-reactive T cells are depleted. Thus, a combination of high-dose immune ablation and autologous HSCT has been reported to be efficacious in the treatment of MS through the elimination of pathogenic T cells and renewal of the immune system repertoire (for a review on HSCT and its clinical efficacy in the treatment of MS please see (Radaelli et al., 2014).

1.6. Matrix Metalloproteinases play a key role during Blood Brain Barrier disruption

Metzincins, comprising Matrix Metalloproteinases (MMPs), A Disintegrin And Metalloproteinases (ADAMs) and A Disintegrin And Metalloproteinase with Thrombospondin motifs (ADAMTS), are a family of proteinases widely implicated in the biology of the nervous system (reviewed in Rivera et al., 2010).

MMPs are synthesized as inactive enzyme precursors containing a signal peptide, directing secretion or localisation to the plasma membrane. Thus, MMP catalytic activities are mainly restricted to the extracellular environment and the cell surface (Fanjul-Fernandez et al., 2010). MMP activity, (as well as activation in some cases), is inhibited by the four Tissue Inhibitors of Metalloproteinases (TIMPs) (Larochelle et al., 2011). In humans, 23 different MMPs have been identified and classified according to differences in their domain structure and substrate specificity (**Figure 1.4**) (reviewed in Yong, 2005). MMPs are tightly regulated at three main levels: firstly, at the transcriptional level (e.g. cytokine-induced transcription); by proteolytic activation of their initial inactive form exposing their active catalytic domain; and through inhibition by TIMPs. Additionally, MMP activity can also be controlled by post-translational modifications, substrate availability and cellular localization (reviewed in Yong, 2005).

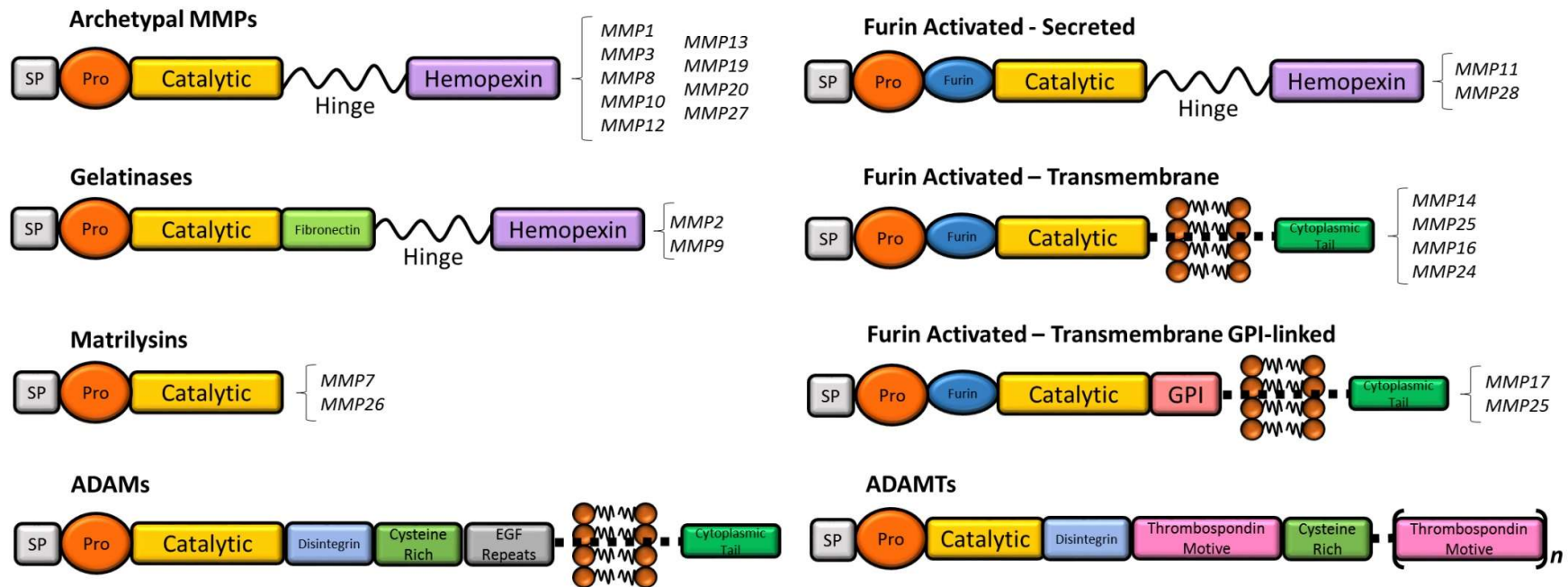


Figure 1.4 - Schematic representation of Metzincin structural domains. Metalloproteinases exhibit a high structural homology with a catalytic domain followed by a highly conserved methionine residue; a linker or hinge peptide; and a hemopexin domain with a calcium binding site. Differences in this consensus structure have been used to classify this family members in the above specified subgroups. The presence of a signal peptide (SP) directs their secretion or transmembrane anchorage. These metalloproteinases are activated proteolytically through cleavage of the pro-domain. Although MMPs are secreted, the presence of a transmembrane or glycosyl phosphatidylinositol (GPI) domain allows some members of this family to anchor to the cellular membrane. ADAMs have a disintegrin-like domain involved in cell adhesion together with a cysteine-rich region and Epidermal Growth Factor (EGF-) like repeats. Structurally similar to ADAMs, ADAMTs also contain a disintegrin-like and cysteine-rich regions (separated by a thrombospondin motive) but lack a transmembrane domain and are thus secreted (image from Pla-Navarro et al., 2018).

A major consequence of neuroinflammation is the up-regulation of MMPs (Rempe et al., 2016). Components of endothelial cell TJs and AJs as well as the extracellular matrix surrounding ECs and pericytes, can be degraded by members of this large family of zinc-dependent endoproteinases (Fanjul-Fernandez et al., 2010; Eisenach et al., 2012; Liu et al., 2012). Additionally, several studies using broad spectrum metalloproteinases inhibitors revealed metzincins to be major mediators of BBB pathological disruption: administration of a broad spectrum (M)MP inhibitor in a rat model of meningitis (Paul et al., 1998) or stroke (Pfefferkorn & Rosenberg, 2003), and a murine model of multiple sclerosis (Gijbels et al., 1994) impaired the increase in BBB permeability. Interestingly, studies conducted by Rosenberg *et al.* reported that the ability of LPS to trigger BBB damage and the ability of the tested broad spectrum (M)MP inhibitors to block LPS-induced BBB disruption could depend on murine strain, suggesting that genetic background could be playing an important role (Rosenberg et al., 2001). In any case, metzincins are prime candidates to for study in order to gain a better understanding of BBB integrity.

MMPs induction is associated with inflammation and brain injury: high levels of MMP9 together with a reduction in inhibitor levels (TIMP1) are seen in serum from Multiple Sclerosis (MS) patients (an autoimmune disorder in which early BBB breakdown is likely to precede invasion of autoreactive immune cells into the CNS) (M. A. Lee et al., 1999; Waubant et al., 1999). A prospective study in MS patients showed a reduction in MMP2, -3, -8, -9 and -10 after Natalizumab treatment (proven to reduce clinical and MRI signs of BBB disruption), with MMP12, -13 and particularly -9 serum levels correlating with relapses and disease score (Balasa et al., 2018). During ischemia MMP3 expression levels can be elevated triggering loss of BBB integrity (Rosenberg et al., 2001; Gurney et al., 2006). Observed dysregulation of MMP levels may initiate BBB damage since several members of this family are capable of degrading TJ and basement membrane elements. Claudins, occludins and ZO-1 proteins can be directly degraded by MMP1 (K. Wu et al., 2015), -2 (Yang et al., 2007), -9 (Yang et al., 2007; Bauer et al., 2010) and -13 (Lu et al., 2009) amongst others. Using a murine model of Multiple Sclerosis Membrane anchored MMPs also activate other MMPs, as well as degrading basement

membrane elements such as collagen IV and laminin (Y. Itoh, 2015). In the same murine model, MMP2 and -9 were reported capable of targeting dystroglycan (a transmembrane receptor responsible for astrocyte foot processes anchorage to the basement membrane) promoting leukocyte infiltration (Agrawal et al., 2006). Additionally, pro-inflammatory cytokines can also be proteolytically activated by mentzincins, suggesting the existence of a feedback loop mechanisms between (M)MPs and pro-inflammatory agents: TNF α can be cleaved and activated by ADAM17 together with MMP7, -12, -14 and -17; IL-1 β can be proteolytically activated by MMP2, -3 and -9; whereas MMP9 can mediate interferon- β inactivation (reviewed in Rodriguez et al., 2010). For further discussion of MMPs in brain disease see Rempe *et al.* (Rempe et al., 2016).

The ADAM family shares great structural similarities with MMPs (**Figure 1.4**) and has also been implicated in BBB disruption (reviewed in Reiss & Saftig, 2009). ADAMs have major roles in shedding molecules from the cell surface (for a new comprehensive sheddome database see Tien et al. 2017). Within the ADAM family, ADAM10 and ADAM17 are the principal shedding enzymes and during inflammatory conditions may be capable of promoting BBB leakage through the shedding of adhesion molecules expressed by ECs (reviewed in Drey Mueller et al., 2012). Interestingly, TNF α receptor can be shed by ADAM8 or -17, releasing its soluble form which can sequester extracellular TNF α ameliorating inflammation (Reddy et al., 2000; Bartsch et al., 2010). IL1R and IL6R can be shed by ADAM10 and/or -17, releasing a soluble fraction capable of stabilising IL1 or IL6 exacerbating inflammation (Reddy et al., 2000; Schumacher et al., 2015). In addition, the expression of ADAM17 has been found to be up-regulated in active lesions during MS (Plumb et al., 2006). Recent evidence indicates that Natalizumab (and anti-alpha 4 integrin antibody) treatment in patients with multiple sclerosis results in reduction in circulating soluble Vascular Cell Adhesion Molecule 1 (sVCAM-1) levels (Petersen et al., 2016), whose shedding from endothelial cells is ADAM17-dependent (Garton et al., 2003; R. J. Singh et al., 2005). If Natalizumab effects on VCAM-1 levels are ADAM17 mediated remains to be studied, although it could be speculated that Natalizumab blockade of

activated immune cells recruitment could lead to a local decrease in secreted cytokines, leading to a downregulation in ADAM17 activation and a possible reduction in VCAM-1 shedding.

A Disintegrin and Metalloproteinase with Thrombospondin motifs (ADAMTS) proteinases are secreted extracellular enzymes with a characteristic thrombospondin type 1 sequence repeat (TSR) motif that share the same catalytic domain as MMPs and ADAMs (Kelwick et al., 2015). Several members of this family have been implicated in BBB disruption: genetic linkage studies in Multiple Sclerosis patients have associated ADAMTS14 (a procollagen aminoproteidase) with this disease (Goertsches et al., 2005) whereas studies in an ischemic murine model have reported that ADAMTS13 blocks tissue Plasminogen induced BBB disruption after cerebral stroke (L. Wang et al., 2013) (**Table 1.1**).

Despite recent advances in our understanding of metalloproteinases, the precise underlying mechanisms by which metzincins regulate BBB stability remain uncertain. Many pathways can regulate BBB integrity during adulthood. In this thesis we aim to highlight signalling pathways which are already implicated in metzincin-mediated regulation of BBB integrity as well as those which are deserving of further study.

Table 1.1 Key findings regarding metalloproteinases effects in BBB integrity and BBB related disease (adapted from Pla-Navarro et al., 2018)

	OBSERVATION	STUDIED IN	REFERENCES
MMP1	Capable of degrading claudins and occludins but not ZO-1 proteins	Co-culture of mBMEC with human breast cancer cells	Wu et al., 2015
MMP2	Required by monocytes, dendritic cells and activated T cells to induce BBB breakdown	EAE	Graesser et al., 2000
	Resistance to EAE in MMP-2 and MMP-9 in double knockout mice	EAE	Agrawal et al., 2006
	Positive feedback mechanism: cytokines produced by leukocytes induce MMP-9 and -2, which in turn can promote further infiltration of immune cells	EAE	Agrawal et al., 2006
	Capable of claudin-5 degradation	Cerebral artery occlusion and reperfusion in rats	Song et al., 2015
	Increase susceptibility to EAE in MMP2 ^{-/-} mouse due to a compensatory increase in MMP9 levels	EAE	Yang et al., 2007

	OBSERVATION	STUDIED IN	REFERENCES
MMP3	LPS intracerebral injection showed reduced BBB opening and neutrophil infiltration in MMP3 ^{-/-} mouse	Knockout mouse	Esparza et al., 2004
	Increased expression during brain ischemic insult	Ischemic rat brain	Gurney et al., 2006
	mRNA levels elevated during Relapsing Remitting Multiple Sclerosis	MS patients	Rosenberg et al., 2001
	Increased transcriptional up-regulation in a murine virus induced model of Multiple Sclerosis	Murine MS model	Reviewed in Larochelle et al., 2011
MMP7	Increased in lesions from post-mortem Multiple Sclerosis brains	Post-mortem brain	Hansmann et al., 2012
	mRNA levels elevated during Relapsing Remitting Multiple Sclerosis	MS patients	Lindberg et al., 2001
MMP8	Serum levels increased in Multiple Sclerosis patients	MS patients	Reviewed in Larochelle et al., 2011
	Up-regulated expression levels in the CNS of a mouse model of Multiple Sclerosis (EAE)	EAE	Reviewed in Larochelle et al., 2011
MMP9	Required by monocytes, dendritic cells and activated T cells to induce BBB breakdown	EAE	Toft-Hansen et al., 2004
	Resistance to EAE in MMP-2 and MMP-9 in double knockout mice	EAE	Agrawal et al., 2006
	Positive feedback mechanism: cytokines produced by leukocytes induce MMP-9 and -2, which in turn can promote further infiltration of immune cells	EAE	Graesser et al., 2000

	OBSERVATION	STUDIED IN	REFERENCES
	Higher levels in MS patients and associated with relapse	MS patients	Agrawal et al., 2006
	High serum levels correlated with BBB disruption in MS patients		
	Gene knockout is associated with a reduction in infarction and attenuation of BBB opening after focal cerebral ischemia	Transient focal ischemia in mice	Song et al., 2015
	ZO-1, occludin and claudin-5 degradation	Cerebral hypoxia mice Brain artery occlusion rats	Lee et al., 1999
	Reduced susceptibility to EAE, BBB damage and infarcts susceptibility in MMP9 ^{-/-} mouse	Knockout mouse	Waubant et al., 1999
	Polymorphisms in its promoter have been linked to increased susceptibility to Multiple Sclerosis	MS patients	Asahi et al., 2001
MMP10	Up-regulated expression levels in the CNS of a mouse model of Multiple Sclerosis (EAE)	EAE	Bauer et al., 2010
MMP12	Up-regulated expression levels in the CNS of a mouse model of Multiple Sclerosis (EAE)	EAE	Yang et al., 2007
	Increased susceptibility to EAE in MMP12 ^{-/-} mouse	EAE	Asahi et al., 2001

	OBSERVATION	STUDIED IN	REFERENCES
MMP13	Can enhance BBB permeability through ZO-1 fragmentation	Primary rat astrocytes and ARBECs co-culture	Dubois et al., 1999
MT-MMPs	Can degrade BBB basement membrane components such as laminin and collagen IV	<i>In vitro</i> studies	Fiotti et al., 2004
	Serum levels (MT-MMP1) can be elevated in Multiple Sclerosis patients	MS patient's serum	Toft-Hansen et al., 2004
TIMP1	Low serum levels correlated with BBB disruption in Multiple Sclerosis (MS) patients	MS patient's serum	Toft-Hansen et al., 2004
ADAM10	Promote BBB leakage through the shedding of adhesion molecules	HUVECs	Weaver et al., 2005
ADAM15	ADAM15 depletion can decrease endothelial permeability. This can be reversed by its overexpression	HUVECs	Lu et al., 2009
ADAM17	Promote BBB leakage through the shedding of adhesion molecules	HUVECs	Reviewed in Itoh, 2015
	Expressed in blood vessels of MS lesions	MS patients	
ADAMTS13	Capable of blocking tPA induced BBB disruption after cerebral ischemia in mice	Ischemia mouse model	Reviewed in Larochelle et al., 2011
ADAMTS14	Associated to Multiple Sclerosis through genetic linkage	MS patients	Waubant et al., 1999

1.7. Vitamin D, a dual protective effect in the pathology of Multiple Sclerosis

Despite the implication of Vitamin D3 in protection against MS pathogenicity, the molecular pathways underlying its effect have not been yet elucidated. Vitamin D3 (or cholecalciferol) is synthesised in the skin from its precursor 7,8-dehydrocholesterol through a photolytic conversion induced by the action of ultraviolet light. Vitamin D3 is transported through the blood stream by the Vitamin D Binding Protein (DBP) to the liver, where it is hydroxylated into 25-hydroxyVitamin D3 (25(OH)D₃) by one or more cytochrome P450 Vitamin D 25 hydroxylases. Once 25(OH)D₃ is synthesised, it is transported to the kidney by DBP, where it undergoes a second hydroxylation step, generating the hormonally active form of Vitamin D3: 1,25-dihydroxyVitamin D3 (1,25(OH)₂D₃). Interestingly, the enzyme responsible for this latter hydroxylation (cytochrome P450 monooxygenase 25(OH)D 1 α hydroxylase) is not only found in the kidney, but also in monocytes and macrophages. This final metabolite is once again carried by DBP to the target tissues or cells, where it is responsible for most of the biological actions of Vitamin D (**Figure 1.5**) (Brown et al., 1999; Dusso et al., 2005; Christakos et al, 2010).

When Vitamin D3 enters the cell, it binds to the cytoplasmic vitamin D receptor (VDR), and moves to the nucleus where a heterodimer forms with the retinoid X receptor (RXR) to target genes that contain Vitamin D3 response elements (VDRE) in their regulatory regions (**Figure 1.6**) (Dusso et al., 2005). Some of these genes are involved in the up-regulation of CD4+ T cells apoptosis (L B Pedersen et al., 2007), the inhibition of cytokine synthesis (Pedersen et al., 2007; Joshi et al., 2011), and the blockade of leukocyte transmigration into the CNS (Grishkan et al., 2013), suggesting several mechanisms by which vitamin D could exert its anti-inflammatory effects.

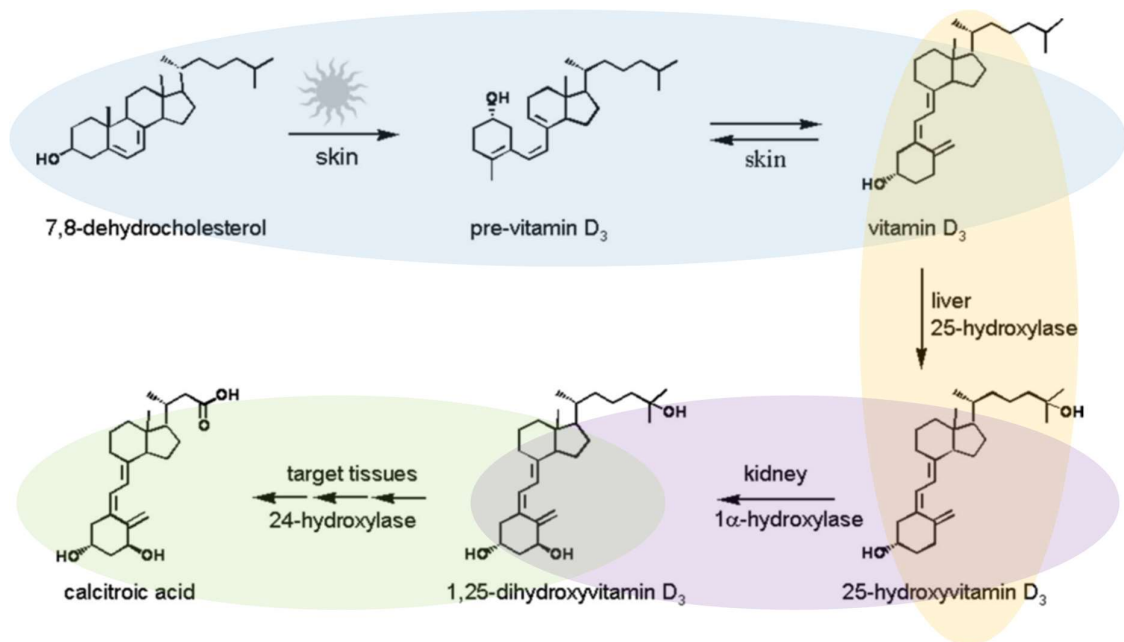


Figure 1.5 - Synthesis, activation and catabolism of Vitamin D₃. 7,8-dehydrocholesterol is photolytically cleaved and isomerised in the skin, generating Vitamin D₃. Vitamin D₃ is then transported into the liver, where it will undergo an hydroxylation and will be converted into 25-hydroxyvitamin D₃. Finally, 25-hydroxyvitamin D₃ is transported into the kidneys, where a final hydroxylation step takes place, forming 1,25-dihydroxyvitamin D₃ (the active form of Vitamin D₃). In the target tissues, a series of oxidation steps (catabolic steps) result in the cleavage of the side chain and the formation of calcitric acid (image adapted from Dusso et al., 2005).

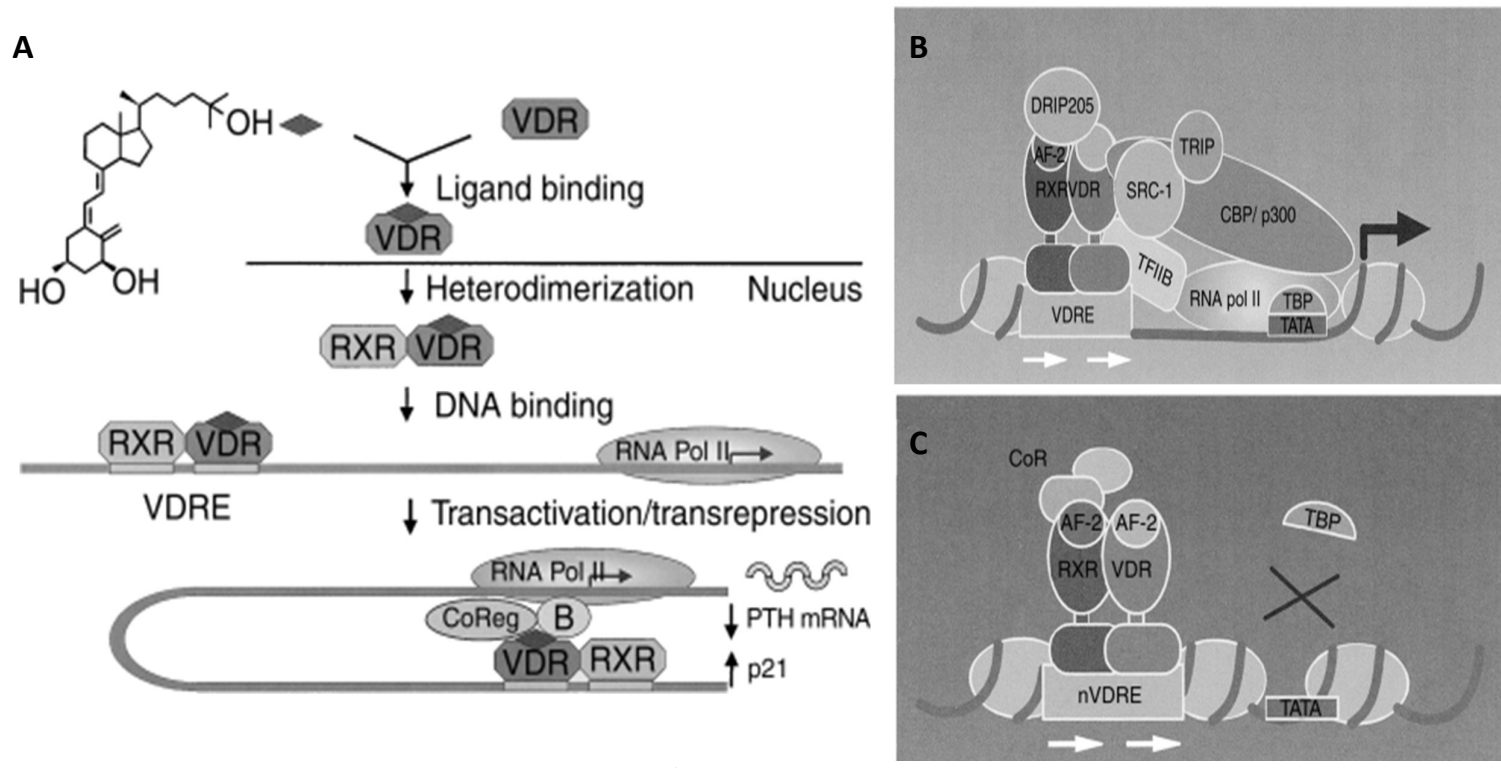


Figure 1.6 - Vitamin D3 mediated regulation of gene transcription. (A) Vitamin D3 binds to the vitamin D receptor (VDR) triggering its heterodimerization with the retinoid X receptor (RXR) and translocation into the nucleus, and activates the expression of those genes with a vitamin D responsive element (VDRE). Co-regulator molecules participating in the regulation of gene transcription mediated by VDR: co-activator molecules (B) and co-repressor molecules (C) are shown. Image from Dusso et al., 2005.

1.7.1. Vitamin D reduces leukocyte's ability to enter the CNS

Leukocyte trafficking into the CNS involves a coordinated interaction between the endothelial cells (ECs) of the BBB and the circulating leukocytes. As previously mentioned, under inflammatory conditions activated innate immune cells release cytokines into the neighbouring environment, inducing the expression of adhesion molecules on the surface of ECs and circulating leukocytes, allowing leukocyte anchoring and extravasation across the BBB (Engelhardt, 2006; Man et al., 2007; Palmer et al, 2013). Thus, Vitamin D3 could hinder the migration of leukocytes into the CNS by hindering the expression of adhesion molecule and/or chemokine receptors. In this regard, TNF α -mediated increase in ICAM-1 and VCAM-1 was blocked by 1,25-(OH) $_2$ D $_3$ addition in an *in vitro* culture of human umbilical vein endothelial cells (HUVEC) (Martinesi et al, 2006). However, oral administration of Vitamin D3 in patients with end-stage renal disease triggered a decrease in ICAM's and VCAM's serum levels (Naeini et al., 2017). In the presence of 1,25-(OH) $_2$ D $_3$, the expression of the chemokine receptor CXCR3 on Th circulating cells is significantly reduced, and this can be rapidly reversed on cessation of treatment (Grishkan et al., 2013). Interestingly, a great proportion of the Th cells present in MS active demyelinating lesions are CXCR3R $^+$ (Balashov et al., 1999; Simpson et al., 2000) and in EAE their migration into the CNS can be effectively blocked by CXCR3R antagonists or antibodies, reducing pathogenesis (J. Ni et al., 2009; Sporici & Issekutz, 2010).

1.7.2. Vitamin D increases the stability of the Blood Brain Barrier

Alternatively, Vitamin D3 could also impair MS development by enhancing the BBB isolating properties since 1,25(OH) $_2$ D $_3$ treatment has been shown to increase the expression of claudins (H. Fujita et al., 2008), occludins (Kong et al., 2008; Yin et al., 2011), and ZO proteins (Palmer et al., 2001) in several endothelial cell types (although there is no data available on brain microvascular ECs). In a human colon carcinoma epithelial cell line the presence of 1,25(OH) $_2$ D $_3$ increased translocation of nuclear ZO-1 and β -catenin to the plasma membrane has been described (Palmer et al., 2001). In

intestinal epithelial cells Vitamin D3 treatment triggers an increase in TEER (S Chen et al., 2015; Chirayath et al., 1998), whereas in airway epithelial cells no TEER effects were reported (R. Zhang et al., 2016).

Vitamin D3 can also protect BBB integrity by inhibiting the degradation of its extracellular matrix components and junctional complexes. During inflammation, the generation of a cytokine stimuli induces the secretion of the afore mentioned MMPs (Unemori et al., 1991), by activated pro-inflammatory cells. In this context, population studies have described that vitamin D deficiency can be associated with increased serum levels of MMP2 and MMP9, which could be revoked by Vitamin D3 dietary supplementation. Additionally, circulating levels of TIMP-1 (and therefore MMP activity) can be strongly influenced by the VDR haplotype (Timms et al., 2002). Although not in the context of the BBB, Vitamin D3 has been reported to reduce MMP3 and TIMP1 expression levels in mice susceptible to myocarditis (Szalay et al., 2009), reduce MMP1 protein levels in rats with chronic renal failure (Panizo et al., 2013), increase MMP2 secreted levels in porcine aortic endothelial cells (Molinari et al., 2013), protect against VEGF-mediated increase in ADAM33 in airway smooth muscle cells (Kim et al., 2017) and promote MMP9 gene expression in a rat chondrogenic cell line (Lin et al., 2002). Thus, it is possible that Vitamin D3 can mediate changes in BBB stability through metzincin regulation.

Taken together, these observations suggest various mechanisms by which Vitamin D3 could be enhancing the structural stability of the BBB and, therefore, ameliorating neuro-inflammation.

1.8. Shh plays an anti-inflammatory role during Multiple Sclerosis pathogenesis

In ECs, the primary cilia are microtubule-based sensory organelles that extend from the cell surface and protrude into the lumen of the blood vessels, allowing ECs to sense and respond to external stimuli such as blood-flow variations, converting mechanosensory information into an intracellular signal

(Luu et al, 2018; Mohieldin et al., 2016). It is in these primary cilia where most components of the Hedgehog pathways localise (Ribes & Briscoe, 2009).

Sonic Hedgehog (Shh) is a small protein (20 kDa) that can remain associated to the external face of the cell membrane signalling adjacent cells, or it can be released into the extracellular environment and function as a long-range signalling molecule. Shh binds to a 12-pass transmembrane protein similar to the Niemann-Pick disease type C1 protein, involved in cholesterol trafficking, named Patched (Ptch). In the absence of Shh, Ptch works as an inhibitor of Smoothened (Smo), a 7-pass transmembrane protein that resembles a G-protein coupled receptor. However, upon Shh-Ptch binding, Smo is activated (often termed depressed), moves to the primary cilium initiates the Shh signalling cascade, which will result in the activation of the Gli family of transcription factors (Gli1, Gli2 and Gli3) (**Figure 1.7**) (Benson et al., 2004; Ribes & Briscoe, 2009; Choudhry et al., 2014).

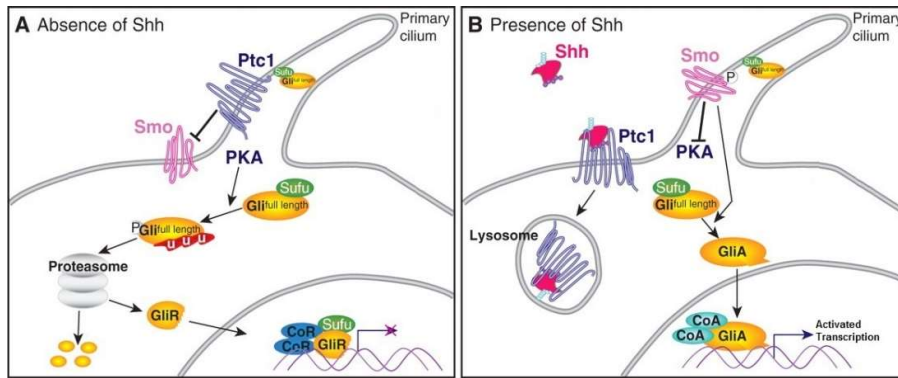


Figure 1.7 - Schematic representation of the molecular elements involved in the intracellular cascade of the Shh pathway. (A) In the absence of Sonic Hedgehog (Shh), the receptor Patched 1 (Ptc1) constitutively represses the activity of the transmembrane protein Smoothen (Smo) and the consequent translocation of Smo to the primary cilium of the cell. In context, active protein kinase A (PKA) promotes the proteasomal degradation of the Gli family of transcription factors, originating the truncated forms of these proteins (GliR). GliR can then translocate to the nucleus and repress the transcription of Shh signalling targets. Additionally, any full-length Gli proteins that could have escaped proteasomal degradation will then be repressed by SuFu. **(B)** When Shh is present, it will bind and inactivate Ptc1, releasing Smo from its repression and allowing Smo's translocation to the cell's primary cilium. Active Smo can then inhibit PKA-mediated proteolytic processing of Gli proteins. Active Gli transcription factors (GliA) can then translocate into the nucleus and activate target gene expression. Image modified from Ribes & Briscoe, 2009.

1.8.1. Shh pathway enhances Blood Brain Barrier maintenance

Under normal physiological conditions, astrocyte end-feet play a central role in the maintenance of the BBB integrity through direct physical contacts and the secretion of trophic factors such as Shh (Luissint et al., 2012). Thus, it has been reported that abrogation of the Shh pathway in ECs can trigger an acute disruption of the BBB integrity mediated by a diminished expression of junctional proteins (Alvarez, Dodelet-Devillers, et al., 2011). Shh can increase ZO-1 and occludin expression through the up-regulation of angiogenic cytokines principally in astrocytes, but also in ECs (Xia et al., 2013). One of these angiogenic cytokines is angiotensin-1 (Ang-1), whose production by ECs could potentially be impaired by the blockage of Smo. However, Smo abrogation had no effect in the levels of Ang-1 secreted by astrocytes, suggesting that the intracellular pathways underlying Shh effects on BBB integrity could vary depending on the cell type (Xia et al., 2013). Supporting this idea, studies in astrocytes have described Shh's ability to activate COUP transcription factor II (COUP-TFII also known as NR2F2); a transcription factor that contains a Shh response element different from that described for Gli and that is capable of inducing Ang-1 expression (Y. Li et al., 2013; Xia et al., 2013). Additionally, Shh could also impact on BBB stability through the regulation of metalloproteinases since Shh has been proven to increase MMP9 levels in human ECs (Renault et al., 2010) and human tissue samples from oral squamous cell carcinoma (Fan et al., 2014) and elevate MMP2 and -9 levels in human hepatoma and hepatocytes cell lines (Chen et al., 2013; Wang et al., 2015).

Regardless of the mechanism underlying Shh effects in the maintenance of the BBB, a reduction in the levels of Shh has been described in MS patients (Mastronardi et al., 2003). During inflammation, activated pro-inflammatory cells secrete interleukin-1 β , which impairs Shh production in astrocytes leading to the previously mentioned disruption of the BBB (Wang et al., 2014). Although there are probably more mechanisms involved, the latter observation reinforces the idea that Shh may be implicated in the pathological disruption of the BBB during inflammatory conditions.

1.8.2. Shh pathway modulates the infiltration of pro-inflammatory cells

As in the case of vitamin D, Shh can also modulate MS immunogenicity by altering leukocyte infiltration. It has been shown that when CD4⁺ T cells polarized into Th1 and Th17 lymphocytes in the presence of Shh, the latter exhibit a reduced capacity to adhere to the ECs forming the BBB (Alvarez, Dodelet-Devillers, et al., 2011). In agreement with this observation, abrogation of the Shh pathway in the EAE model led to a higher localization of activated lymphocytes to the CNS without affecting their proliferation (Alvarez, Dodelet-Devillers, et al., 2011). Thus, Shh appears to play a protective role by impairing the infiltration of pro-inflammatory cells into the CNS. Interestingly, in active demyelinating MS lesions, an increased secretion of Shh by the astrocyte end-feet was found, together with an enhanced expression of Ptch by ECs and infiltrating leukocytes (Alvarez, Dodelet-Devillers, et al., 2011). Taken together, these findings suggest that under inflammatory conditions, astrocytes increase their secretion of Shh in an attempt to restore physiological conditions by preventing leukocyte infiltration and promoting BBB repair.

In contrast to the protective role above, Shh has also been reported to be a potent chemoattractant for circulating monocytes since it can activate cell migration pathways in a Smo-dependent way (Dunaeva et al., 2010). However, as it has been stated above, Shh could exert its effects via different intracellular pathways depending on the cell type as well as environmental conditions. Thus, Shh ability to regulate the transmigration of pro-inflammatory cells across the BBB should be studied in this context.

1.9. Shh and Vitamin D, a regulatory cross-talk

As it has been stated above, in the absence of Shh, Ptch functions as a constitutive inhibitor of Smo. However, it seems unlikely that Ptch blockade of Smo occurs via a direct physical interaction, since Ptch is able to inhibit Smo in a sub-stoichiometrical manner and no physical association among them has ever been unambiguously proved (Taipale et al. 2002). Interestingly, Ptch bears a high structural homology with the Niemann-Pick disease type C1 (NPC1) protein, whose cholesterol trafficking and pump functions have been

previously described (Davies et al., 2000). Additionally, culture medium conditioned by Ptch-transfected cells was found to be enriched in 3 β -hydroxysteroids, suggesting that Ptch overexpression lead to an increased translocation of these compounds (Bijlsma et al., 2006). Taken together, these observations lead to the idea that Ptch could translocate a small cholesterol-like molecule across the cellular membrane that will act as a Smo antagonist (Bijlsma et al., 2006). The idea that a 3 β -hydroxysteroid is responsible for Smo inactivation is supported by the observation that Smo antagonists, like cyclopamine (a broadly known inhibitor of Gli activation), bear high structural resemblances with steroids (Incardona et al., 1998). Specifically, it is likely that the 3 β -hydroxysteroid translocated by Ptch is (pro)-Vitamin D3 (either 7-dihydroxycholesterol (7-DHC) or its metabolite Vitamin D3) or a precursor that is metabolised in the extracellular medium into a Smo repressor (Bijlsma et al., 2006) (**Figure 1.8**).

Ptch and Smo are not always expressed in the same cell, but depending on the biological context, Ptch-expressing cells are located in the vicinity of Smo-expressing cells. Thus, Ptch can mediate an autocrine or paracrine repression of Smo depending on the biological circumstance. However, Vitamin D3 is a highly hydrophobic molecule with an extremely reduced diffusion capacity in aqueous environments. Thus, in those cases of paracrine inhibition, a molecule able to transport this hydrophobic antagonist through the extracellular environment is needed. This is the case of the low-density lipoprotein (LDL), a carrier molecule that has been proven to be essential for intercellular blockage of Smo (Bijlsma et al., 2006). In any case, when the extracellular Vitamin D3 interacts with Smo, binds to the same site than the antagonist cyclopamine (which has been reported to have a higher affinity for Smo) (Bijlsma et al., 2006). Additionally, studies in hematopoietic stem and progenitor cells showed a specific ability of the Vitamin D3 cholecalciferol (but not active 1,25-dihydroxy vitamin D3) to antagonise Hh pathway through extracellular binding of Smo, triggering a loss in Gli-reporter activation (Cortes et al., 2015). However, despite this shared ability to repress Shh-signalling, these molecules should not be considered biologically

equivalent, since cyclopamine is incapable of activating VDR signalling (Uhmann et al., 2012).

Taking the above observation into consideration, Shh effects should perhaps not only be considered in terms of Smo activation but also in terms of Ptch blockade, since this will lead to an inhibition of Ptch-mediated export and an increase in the intracellular levels of Vitamin D3.

Smo inhibition is not the only point where the signalling pathways of Shh and Vitamin D3 converge. Once Smo is released from Ptch repression, it transduces a signal that ends with the activation of the Gli family of transcription factors. Although the exact mechanisms underlying this intracellular transduced signal are not well understood, previous studies have shown that upon Smo activation, Akt (or Protein Kinase B, PKB) becomes phosphorylated in a phosphoinositide 3-kinase (PI3K)-dependent manner (Kanda et al., 2003; Riobo et al., 2006). The initiation of the Akt pathway leads to the phosphorylation and inhibition of the Protein Kinase A (PKA) and the Glycogen Synthase Kinase 3 β (GSK-3), two kinases that sequentially phosphorylate and repress Gli transcriptional activity (Riobo et al., 2006; Yoo et al., 2011). Despite the reported capacity of Akt to mediate Shh signalling, it remains to be clarified if Akt effects on the activity of the Gli transcription factors equally impacts in all the members of this family and, if this modulation, is maintained among different cellular types and biological contexts. Remarkably, Vitamin D can also regulate Akt phosphorylation, although the effect on Akt activity depends on the studied cell type: Akt phosphorylation is promoted by Vitamin D in osteoblasts (Zhang & Zanello, 2008) whereas it is inhibited in keratinocytes by the Vitamin D synthetic analogue 1 α ,25-dihydroxy Vitamin D3-3-bromoacetate (BE) (Datta Mitra et al., 2013). Thus, although it is not fully understood how vitamin D-mediated regulation of Akt may impact on the transcriptional activity of the Gli family members, or different transcription factors, these data support the existence of a possible cross-talk between Vitamin D and Shh signalling pathways (**Figure 1.8**).

Interestingly, the members of the Gli family are not the only transcription factors that can respond to Shh signalling, since Shh-response element has been identified in the promoter region of the Nuclear Receptor subfamily 2 group F member 2 (NR2F2 or COUP-TFII) transcription factor (Krishnan et al., 1997). NR2F2 is implicated in the up-regulation of various angiogenic factors after Shh activation (Y. Li et al., 2013), but it is also involved in the inhibition of VDR on three different stages: direct transcriptional inhibition; competition for the DNA binding region; formation of non-functional heterodimers with Retinoid X Receptor (RXR), a VDR co-regulator that enhances VDR's transcriptional activity and DNA affinity (Cooney et al., 1993). However, the biological significance of NR2F2 regulation of VDR and Shh's role on this interaction remains to be elucidated.

Therefore, these observations lead to the possibility that the Shh pathway could integrate a great variety of positive and negative signals from the surrounding environment in order to generate a final cellular response through the function of the Gli family members or even another transcription factors not yet identified.

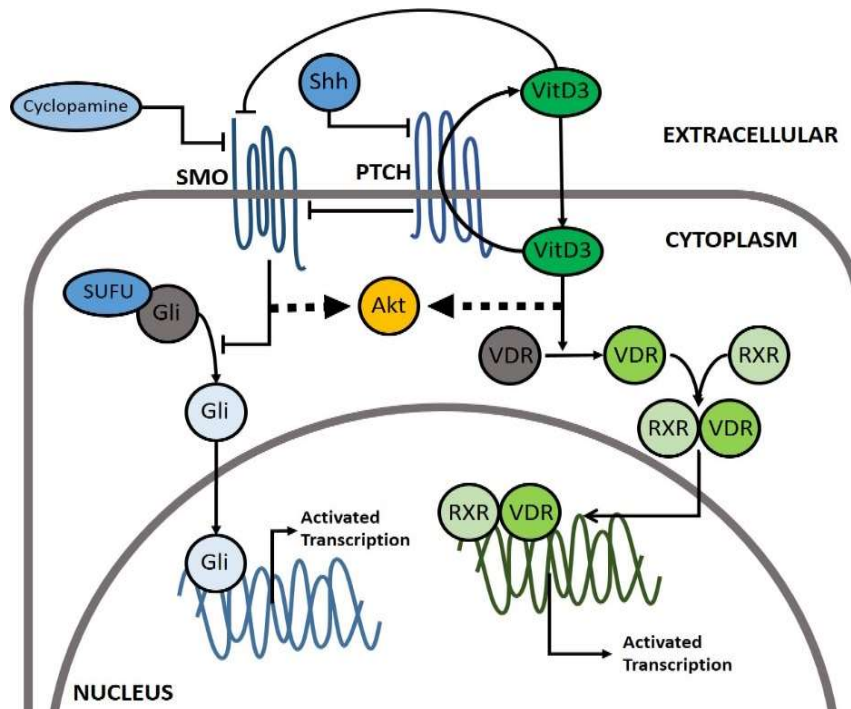


Figure 1.8 - Schematic representation of Hh and Vitamin D3 pathways cross-talk. In the absence of Sonic Hedgehog (Shh), Patched (Ptch) works as an inhibitor of the transmembrane protein Smoothened (Smo), which becomes activated and able to initiate a signalling cascade that will result in the activation of the Gli family of transcription factors. Hh pathway can be pharmacologically inhibited through cyclopamine-mediated blocage of Smo. When Vitamin D3 (VitD3) enters the cell binds to Vitamin D Receptor (VDR), which upon activation (depicted in green) can dimerize with the Retinoid X Receptor (RXR) forming an heterodimer capable to target a those genes with a Vitamin D3 response element. . Patched can work as a Vitamin D3 (or direct metabolite) translocator. Once in the extracellular environment, Vitamin D3 (or its metabolite) can directly bind and inactivate Smo, truncating Hh signalling. Additionally, both Hh and Vitamin D3 pathways converge on the activation of Akt. Hh and Vitamin D3 pathways showed in blue and green respectively. Grey circles indicate inactive transcription factors. (Note that the primary cilium has been omitted for simplicity).

1.10. miRNAs dysregulated in Multiple Sclerosis

MicroRNAs (miRNAs) are a group of non-protein coding RNAs with a length comprised between the 19 and 25 nucleotides. miRNAs play a central role in the regulation of gene expression since they are capable of promoting post-transcriptional gene silencing: miRNAs can block the translation of specific target messenger RNAs (mRNAs) or induce their degradation through the selective binding of their nucleotide sequences. Thus, miRNAs are capable of regulating protein synthesis in a specific manner, without altering the transcription of target mRNAs, allowing them to play a central role in several biological functions (reviewed in Cui et al., 2006; Friedman et al., 2009).

The miRNAs ability to regulate such a wide range of cellular processes has led to the idea that their function, regulation and/or expression patterns may be altered during pathological conditions. This is the case of MS, where several studies showed that the expression of several miRNAs were up- or down-regulated in samples from patients as well as in EAE mice, suggesting that this pathogenesis may be characterised by a particular signature of altered miRNAs (**Table 1.2**) (reviewed in Ma et al., 2014).

Table 1.2 - miRNAs and Multiple Sclerosis. Key miRNA reported in the literature to be up-regulated and /or down-regulated in samples from MS patients and EAE mice. PBMCs refers to Peripheral Blood Mononuclear Cells. Table modified from Ma et al., 2014.

SAMPLE	UP-REGULATED	DOWN-REGULATED	SAMPLE	UP-REGULATED	DOWN-REGULATED
Blood	miR20a, miR186	miR15a, miR15b, miR16, miR17 miR20a, miR20b, miR93, miR140-5p miR624, let-7g, let-7i	Tregs	miR15a, miR19a, miR22 miR210, miR223	-
Plasma	miR22, miR155 miR210, let-7i	miR15b, miR23a miR1979	B Cells	miR497	miR15a, miR16, miR93 miR140-5p, miR152, miR363 miR624, let-7i
Blood Cells	miR125b, miR145, miR223	miR20b	Brain Lesions	miR15a, miR21, miR22 miR142-3p, miR146a, miR146b miR155, miR193a, miR200c miR223, miR125a-5p miR326	miR181c, miR328
PBMCs	miR19a, miR21, miR142-3p miR145, miR146a, miR146b miR155, miR200c, miR326 miR629, let-7f	miR150, miR152, miR181c miR197, miR328, miR363 let-7g	EAE mice	miR21, miR142-3p, miR146a miR146b, miR155, miR326	-
Total T Cells	miR17, miR125b, miR193a miR497, miR629	miR15a, miR15b, miR23a miR150, miR197, miR1979			

According to the literature, there is a wide range of miRNAs with an altered expression during MS pathogenesis and, interestingly, a great proportion of this deregulated population is implicated in the modulation of components of the immune response (reviewed in Ma et al., 2014). This is the case of miR326, a miRNA with increased expression in MS patients and whose silencing or overexpression is capable of ameliorating or enhancing EAE pathology, respectively. Mechanistically, miR326 can promote inflammation by targeting Ets-1, a negative regulator of Th17 differentiation (another subset of T cells as critical in MS pathogenesis alongside Th1 cells) (C. Du et al., 2009). Remarkably, miR326's expression was found to be reduced in a cohort of patients after glucocorticoid treatment, indicating that overall, this miRNA could be a potential biomarker for diagnosis and evaluation of drug responses in patients with MS (C. Du et al., 2009). Additionally, analysis of peripheral blood mononuclear cells of RRMS patients (Waschbisch et al., 2011) and active MS lesions (Junker et al., 2009) showed an upregulation of miR326. Another miRNA capable of modulating immune responses in the context of MS is miR125b, whose expression is increased in samples of peripheral blood T-cells from RRMS patients (assessed by analysis of Gene Expression Omnibus database; Sheng et al., 2015) and can promote macrophage activation (reviewed in Essandoh et al., 2016).

However, not all the miRNAs altered during MS pathogenesis are involved with the direct modulation of the immune response, since some of them have been described to be able to modulate the permeability of the BBB under inflammatory conditions (Eadon et al., 2014). Studies of mRNAs expression in brain capillaries isolated from MS patients showed a reduction in the expression levels of miR-125a-5p (among others), corroborated by analysis of ECs from MS active lesions (Reijerkerk et al., 2013). In addition to miR-125a-5p role modulating inflammatory processes (Chen et al., 2009; Zhao et al., 2010), this miRNA can enhance BBB formation: silencing of miR-125a-5p leads to a reduction in the density and continuity of tight junction complexes, whereas its overexpression triggers the opposite effect (Reijerkerk et al., 2013). Another miRNA capable of alter BBB structure is miR155, one of the most elevated miRNAs in acute lesions of MS (Junker et al., 2009) and

partially protective against EAE when silenced (O'Connell et al., 2010; Murugaiyan et al., 2011). At the functional level, miR155 can enhance inflammation by promoting Th17 differentiation (Yao et al., 2012) and impairing Th2 responses (Rodriguez et al., 2007; Thai et al., 2007) but also reduce BBB permeability by targeting annexin-2, claudin-1 (both of them involved in the maintenance of cell-cell contacts between adjacent ECs), syntenin-1 and dedicator of cytokinesis-1 (equally responsible for the maintenance of cell-to-extracellular matrix contacts) (M A Lopez-Ramirez et al., 2014).

Taken together, these observations lead to the idea that perhaps a cohort of deregulated miRNAs could be underlying MS pathogenesis by principally targeting the integrity of the BBB and components of the immune response, and result in a signature of altered miRNAs that could be used with diagnostic purposes. However, it is important to consider that miRNAs exhibit redundancy when interacting with their targets (Lim et al., 2005) and that some of them are capable of binding to a promoter stimulating gene expression (Fazi & Nervi, 2008). Thus, further research is needed in order to fully understand miRNAs biological mechanisms and how these can be used as diagnostic markers or possible therapeutic targets.

1.10.1 miR125b and miR326 target Hedgehog and Vitamin D pathways

Previous data from the literature and from our laboratory had identified two key miRNAs that could be intimately related with the regulation of MS pathogenesis: miR125b and miR326. Particular interest has been taken in miR125b and miR326 also because of their reported ability inhibit Hedgehog signalling. Using a medulloblastoma cell line, Ferretti *et al.* demonstrated that miR125b and miR326 (together with miR324-5p) could inhibit Hedgehog signalling pathway through the targeting of Smo (Ferretti et al., 2008). Additionally, miR125b and miR326 have been also associated with Vitamin D signalling: although not yet validated, miR326 has been predicted to target Vitamin D Receptor (VDR) (Sebastiani et al., 2011); treatment with Vitamin D3 active form can increase miR125b levels in epithelium from patient prostate tissue (Giangreco et al., 2013); overexpression of miR-125b significantly decreased the endogenous VDR protein level in a breast adenocarcinoma cell

line (Mohri et al., 2009), although no miR125b-dependent regulation of VDR was observed in a melanoma cell line (Essa et al., 2012) suggesting some cell type-dependent variations.

1.11. Thesis Aims

- To develop an in vitro model for endothelial barrier formation using murine endothelial cells to enable the study of vitamin D3 and the Shh-pathway interactions to modulate B endothelial barrier integrity under physiological and inflammatory conditions, with a focus on metzincin expression/function.
- To exploit a human brain endothelial cell model of the BBB to assess the Shh/Vitamin D3 link and to understand mechanisms underpinning their effects
- To explore expression, modulation and function of key MS-relevant miRNAs in response to Shh and Vitamin D treatment in the human endothelial BBB model.
- To expand knowledge of gene expression modulated by these miRNAs and by inflammatory cytokines through an analysis of genome-wide RNA expression in the human brain microvascular endothelial cells model system.

2. Materials and Methods

2.1. Cell culture

2.1.1. MCEC-1

The murine endothelial cell line MCEC-1 (Lidington et al., 2002) was grown on surfaces previously coated with 1% Type A Gelatin from Porcine Skin (Sigma) for 1h at 37°C. MCEC-1 cells were cultured in Duplecco's Modified Eagle Medium (DMEM) liquid medium with high glucose (4.5g/L) (Invitrogen), containing a mix of Penicillin (50u/ml) and Streptomycin (50µg/ml) antibiotics (Life Technologies), L-Glutamine (2mM) (Life Technologies), supplemented with 10% (v/v) Fetal Bovine Serum (FBS) (PAA) and Endothelial Cell Growth Supplement (ECGS; 30µg/ml) (Sigma). Cells were incubated at 33°C, 5% CO₂ and passaged at a 1:5 ratio approximately every four days. The MCEC-1 cell line was previously established from transgenic mice expressing a thermolabile strain (tdA58) of the simian virus (SV) 40 large T antigen, meaning that cell proliferation was only possible at the reduced temperature of 33°C (Lidington et al., 2002). For experiments cells were transferred to 37°C 24h prior to treatment addition.

2.1.2. hCMEC/D3

The human cerebral microvascular endothelial cell line hCMEC/D3 (Weksler et al., 2005) (CELLutions Biosystems) was grown in surfaces previously coated with 150µg/ml Rat Collagen I Low Viscosity (R&D Systems) for 1h at room temperature. hCMEC/D3 cells were cultured in Endothelial Basal Medium (EBM-2) (Lonza) containing a mix of Penicillin (50u/ml) and Streptomycin (50µg/ml) antibiotics (Life Technologies), L-Glutamine (2mM) (Life Technologies), supplemented with 5% (v/v) Fetal Bovine Serum (FBS) (A15-104 PAA), Chemically Defined Lipid Concentrate (1/100; Life Technologies), Ascorbic Acid (5µg/ml; Sigma), human Basic Fibroblast Growth Factor (bFGF; 1ng/ml; Sigma), HEPES (10mM; Life Technologies) and Hydrocortisone (1.4µM; Sigma). Cells were incubated at 37°C, 5% CO₂ and passaged at a 1:5 ratio approximately every four days.

2.2. Treatments

All experiments performed in either MCEC-1 or hCMEC/D3 cells were performed in the relevant cell culture media as described in 2.1 until treatment addition. For hCMEC/D3s, treatments were added in media without foetal bovine serum (0% FBS).

2.2.1. Cytokines

Human recombinant Interleukin-1 α (IL-1 α ; R&D Systems) and mouse recombinant Tumour Necrosis Factor- α (TNF α ; Life Technologies) purified from *E. Coli* were combined as described below. Due to availability of resources and since IL-1 α has been described capable of modulating BBB integrity (Afonso et al., 2007; Al-Obaidi & Desa, 2018; Ravindran et al., 2011) and metalloproteinase expression in the context of the CNS (Giraudon et al, 1996) this interleukin (instead of IL-1 β) will be used throughout this thesis.

IL1 α was dissolved to a 4 μ g/ml stock solution in Phosphate Buffer Saline (PBS) with Bovine Serum Albumin (BSA; 0.1% (w/v)) as a carrier protein for storage at -20 $^{\circ}$ C until later use. TNF α was dissolved to a 100 μ g/ml stock solution in ddH $_2$ O for storage at -20 $^{\circ}$ C until later use. TNF α stock solution was later diluted to 100ng/ml in the appropriate culture media. IL1 α or TNF α when then added to adherent MCEC-1, hCMEC/D3 or the top of a cell culture insert containing either of the mentioned cell lines. MCEC-1 or hCMEC/D3 remained exposed to the cytokines mixture for the duration of the experiment before assessing Transendothelial Electrical Resistance (TEER), imaging, collection of conditioned media, RNA or protein extraction.

2.2.2. Cyclopamine

The Hedgehog pathway pharmacological inhibitor cyclopamine (Zhu et al., 2014; PromoKine) was dissolved in Ethanol (100% (v/v)) to a 1mM stock solution for storage at -20 $^{\circ}$ C until later use. This stock solution was added to adherent MCEC-1, hCMEC/D3 or the top of a cell culture insert containing either of the mentioned cell lines. MCEC-1 or hCMEC/D3 remained exposed

to cyclopamine treatment for the duration of the experiment before assessing TEER imaging, collection of conditioned media, RNA or protein extraction.

2.2.3. Sonic Hedgehog

Human recombinant Sonic Hedgehog (Shh; PromoKine) purified from *E. Coli* was dissolved to a 50µg/ml stock solution with double distilled water (ddH₂O) and bovine serum albumin (BSA) (0.1% (w/v)) as a carrier protein for storage at -20°C until later use. This stock solution was added to adherent MCEC-1, hCMEC/D3 or the top of a cell culture insert containing either of the mentioned cell lines. MCEC-1 or hCMEC/D3 remained exposed to Shh treatment for the duration of the experiment before assessing TEER, imaging, collection of conditioned media, RNA or protein extraction.

2.2.4. Vitamin D3

Vitamin D3 active form 1α,25-Dihydroxyvitamin D₃ (Sigma) was used in the experiments described in this thesis and referred to hereafter as Vitamin D3.

Vitamin D3 was dissolved in Ethanol (95% (v/v)) to a 1mM solution that was then aliquoted and stored in amber glass ampules under an inter gas (N₂) at -20°C until later use. Vitamin D3 stock solution was later diluted to 100µM in the appropriate culture media and then added to adherent MCEC-1, hCMEC/D3 or the top of a cell culture insert containing either of the mentioned cell lines. MCEC-1 or hCMEC/D3 remained exposed to Vitamin D3 treatment for the duration of the experiment before assessing TEER imaging, collection of conditioned media, RNA or protein extraction.

2.2.5. MK-2206

Akt pharmacological inhibitor MK-2206 (Shelleckchem) was dissolved in Dimethyl Sulfoxide (DMSO) to a 5mM stock solution stored at -80°C until later use. The inhibitor was added at the indicated final concentrations to adherent MCEC-1, hCMEC/D3 or the top well of a cell culture insert containing either of the cells. MCEC-1 or hCMEC/D3 remained exposed to MK-2206 treatment for

the duration of the experiment before assessing TEER, imaging, collection of conditioned media, RNA or protein extraction.

2.2.6. GM6001

The broad-spectrum metalloproteinase inhibitor GM6001 and its negative control (Merck Millipore) were dissolved to a 5mg/ml stock solution in DMSO and stored at -20°C until later use. GM6001 and control were independently added to adherent MCEC-1, hCMEC/D3 or the top well of a cell culture insert containing cells. MCEC-1 or hCMEC/D3 remained exposed to GM6001 treatment for the duration of the experiment before assessing TEER, imaging, collection of conditioned media, RNA or protein extraction.

2.2.7. hTIMP3

Human recombinant TIMP3 (kindly provided by Prof Gill Murphy) (Lee et al., 2003) at a stock concentration of 50.4µM and stored at -80°C until later use. hTIMP3 was added at the indicated final concentrations to the top well of a cell culture insert containing MCEC-1 confluent monolayers 30min (at 37°C) prior to addition of the remaining treatments. MCEC-1 remained exposed to the added treatments for the duration of the experiment before assessing TEER values.

2.2.8. Cytochalasin D

The broad-spectrum endocytosis inhibitor cytochalasin D (Sigma) was dissolved in DMSO to a 1mg/ml stock solution stored at -20°C in the dark until later use. Cytochalasin D stock solution was after diluted to 10mM in the appropriate culture media and added to the top hCMEC/D3 confluent monolayers. hCMEC/D3 cells remained exposed to cytochalasin D3 treatment for the duration of the experiment before conditioned media collection and protein extraction.

2.3. Cell viability assay

Cell viability of MCEC-1 or hCMEC/D3 confluent monolayers was determined with Presto Blue (ThermoFisher), following manufacturer's instructions. Eight thousand cells were plated in a previously coated 96-well together with 200µl of the appropriate media and allowed to reach confluence for 24h. Once confluence was reached, treatments were added and incubated for further 24h. At this point, 1/10th volume (20µl) of cell viability reagent (Presto Blue 10X; room temperature) was added directly to the cells and incubated at 37°C and in the dark for 2h as assay sensitivity is greater at longer incubation times. Fluorescence was measured at 560nm and results analysed.

2.4. Immunocytochemistry

Immunocytochemistry was carried out essentially as described in (Gomez et al., 2013); unless otherwise stated, 100,000 cells were plated in a 50µl drop of the appropriate culture media onto 13mm glass coverslips (VWR) coated as previously indicated: with 1% Type A Gelatin from Porcine Skin (Sigma) for 1h at 37°C for MCEC-1 cells or with 150µg/ml Rat Collagen I Low Viscosity (R&D Systems) for 1h at room temperature for hCMEC/D3. Seeded cells were then allowed to adhere for 4h before addition of 450µl of the relevant culture media to flood the coverslips. Cells were incubated overnight at 33°C (for MCEC-1) or 37°C (for hCMEC/D3), 5% CO₂. After 24h, treatments were added and cells were incubated for further 24h at 37°C, 5% CO₂. Coverslips were then fixed and permeabilised in 90% (v/v) ice-cold methanol solution at -20°C for 30min and washed three times in PBS. Non-specific binding was blocked by a 30min incubation in Normal Goat Serum (NGS; 10% (v/v)) followed by a 1h incubation with a rabbit anti-ZO1 primary antibody diluted 1:100 (Invitrogen) without washing. Coverslips were then washed three times with PBS and incubated with an anti-rabbit Alexa Fluor-488 (Abcam) conjugated secondary antibody diluted at 1:1000 for 45min before washing three times with PBS. Coverslips were then incubated with 4',6-diamidino-2-phenylindole (DAPI) 1:10,000 and quickly washed with PBS before mounting on microscope slides with Hydromount mounting solution (National Diagnostics). Samples were left to set at 4°C overnight and stored at 4°C in the dark until ready to use.

Coverslips were viewed with the AxioCam ICm1 monochrome CCD camera attached to Widefield microscope Zeiss AxioPlan 2ie (exposing the entire sample to the light source) using the AxioVision 4.8.2 software (all Carl Zeiss Ltd, Herts, UK). A 20x objective was used for visualisation of a wider field of view and instrument parameter settings (contrast and intensity) were kept the same between experiments for comparability. A detailed explanation of the procedure followed in the quantification of fluorescence can be found in Section 3.2.1.1,

2.5. Total RNA purification

Total RNA purified from MCEC-1 or hCMEC/D3 cell lysates following RNeasy Minikit (Quiagen) according to manufacturer's instructions. Conditioned cultured media was collected from cells at the end of experiments and stored at -20°C until later use. Cells were washed with PBS before being lysed with the provided buffer RLT (a cell lysis buffer containing guanidium isothiocyanate and supplemented with 10% (v/v) β -mercaptoethanol). Cell lysates were homogenised by vortexing before being transferred to a gDNA eliminator column. After centrifugation, an equal volume of 70% (v/v) ethanol was added to the sample to promote RNA precipitation and binding to the membrane of the RNeasy mini-spin column. RNA was further purified by repeated washing of the spin-column with high salt buffers. Using RNase-free ddH₂O, RNA was eluted and stored at -20°C. RNA yield was measured using the Nanodrop 2000 spectrophotometer (Thermo Scientific). RNA concentration was measured at 260nm and the ratios of absorbance at 260/280 (used to assess the presence of contaminant proteins), and 260/230 (used to assess the presence of organic contaminants) were used to ensure RNA quality.

In Chapter 5, mirVana miRNA isolation kit (Life Technologies) kit was used to isolate total miRNA following manufacturer's instructions. Conditioned cultured media was collected and stored at -20°C until later use. Cells were kept on ice and washed with PBS before being lysed with buffer Lysis/Binding solution. Cell lysates were homogenised by vortexing before adding 1/10 volume of miRNA Homogenate Additive and incubate on ice for 10min. A

volume of Acid-Phenol:Chloroform equal to the lysate volume was added before vortexing and carefully centrifuging the samples in order to retrieve the aqueous phase. 1.25 volumes of 100% (v/v) ethanol were added to the aqueous phase before transferring into a filter cartridge. miRNA was further purified by repeated washing of the filter cartridge with various washing solutions. Using RNase-free ddH₂O, miRNA was eluted and stored at -20°C. RNA yield was measured using the Nanodrop 2000 spectrophotometer (Thermo Scientific). miRNA concentration was measured at 260nm and the ratios of absorbance at 260/280, and 260/230 were used to ensure miRNA quality.

2.6. Reverse Transcription

500ng of the isolated RNA was diluted with RNase-free ddH₂O to a final volume of 15µl. Samples were then incubated with random primers (1µg; Invitrogen) at 70°C for 10min. After denaturation, samples were immediately kept in ice to allow random primers annealing. Following annealing, samples were reversed transcribed to complementary DNA (cDNA) using dNTP mix (0.8mM; Bioline), RNase inhibitor (0.8u/µl; Promega), Maloney Murine Leukaemia Virus (M-MLV; 4u/µl; Promega) and MMLV Buffer (Promega) in a 25µl reaction. Samples were then incubated at 42°C for 50min. Enzyme activity was stopped by a 10min incubation at 70°C. Samples were stored at -20°C until further use.

For miRNA extracted samples, 10ng of the isolated miRNA was diluted with RNase-free ddH₂O to a final volume of 5µl. Samples were then incubated with 3µl of primers specific to each miRNA of interest (5x; Applied Biosystems) at 80°C for 5min and at 60°C for 5min. After denaturation, samples were immediately kept in ice to allow random primers annealing. Following annealing, samples were reversed transcribed to complementary DNA (cDNA) using dNTP mix (2mM; Applied Biosystems), RNase inhibitor (0.5u/µl; Applied Biosystems), MultiScribe™ Reverse Transcriptase (7u/µl; Applied Biosystems) and Reverse Transcription Buffer (Applied Biosystems) in a 12µl reaction. Samples were then incubated at 16°C for 30min followed by 30min

at 42°C. Enzyme activity was stopped by a 5min incubation at 85°C. Samples were diluted 1/3 with RNase-free ddH₂O and stored at -20°C until further use.

2.7. Quantitative Reverse Transcription Polymerase Chain Reaction

Quantitative Reverse Transcription Polymerase Chain Reaction (qRT-PCR) was performed using a 7500 RT-PCR system (Applied Biosystems) following manufacturer's instructions. 5ng of each cDNA sample were loaded into each well of a TaqMan® plate (Applied Biosystems) together with 8.3µl of 2x qRT-PCR MasterMix (Applied Biosystems), 100nM of probe and 250nM of forward and reverse primers in a final volume of 20µl (a full list of the primers and probes employed is provided in **Table 2.1 & Table 2.2**). Samples were then incubated at 95°C for 10min in order to activate the polymerase component of the MasterMix, followed by 40 cycles of 15sec melting at 95°C and 1 minute of annealing. Data was collected using the 7500 Software (v2.0.5 Applied Biosystems).

Table 2.1 Murine primer and probe sequences used for qRT-PCR. Probes designed by the Universal Probe Library (UPL) are indicated. All the probes were labelled with FAM (5') and TAMRA (3'). Primer Forward (PF); Primer Reverse (PR).

NAME	SEQUENCE (5' - 3')
18s	PF: GCCGCTAGAGGTGAAATTCTTG PR: CATTCTTGGCAAATGCTTTTCG Probe: ACCGGCGCAAGACGGA
MMP3	PF: GGAAATCAGTTCTGGGCTATACGA PR: TAGAAATGGCAGCATCGATCTTC Probe: AGGTTATCCTAAAAGCATTACACCCTGGGTCT
MMP10	PF: CCTGCTTTGTCCTTTGATTCACT PR: CGGGAT TCCAATGGGATCT Probe: TCCTATTCTTTAAAGACAGGTA CTCTGGCGCA
MMP13	PF: GGGCTCTGAATGGTTATGACATTC PR: AGCGCTCAGTCTCTTCACCTCTT Probe: AAGGTTATCCAGAAAAATATCTGACCTGGGATTC
TIMP1	PF: CATGGAAAGCCTCTGTGGATATG PR: AAGCTGCAGGCACTGATGTG Probe: CTCATCACGGGCCCGCCTAAGGAAC
TIMP3	PF: GGCCTCAATTACCGCTACCA PR: CTGATAGCCAGGGTACCCAAAA Probe: TGCTACTACTTGCCTTGTTTTGTGACCTCCA
ZO-1	PF: ATGCAGACCCAGCAAAGGT PR: TGACCAAGAGCTGGTTGTTTT Probe: UPL Probe #12
Shh	PF: CCAATTAACCCCGACATC PR: GCATTTAACTTGTCTTTGCACCT Probe: UPL Probe #32
Dhh	PF: CACGTATCGGTCAAAGCTGA PR: TAGTTCCTCAGCCCCTTC Probe: UPL Probe #75

NAME	SEQUENCE (5' - 3')
Ihh	PF: TGCATTGCTCTGTCAAGTCTG PR: GCTCCCCGTTCTCTAGGC Probe: UPL Probe #83
Ptch1	PF: TGACAAAGCCGACTACATGC PR: GTACTIONGATGGGCTCTGCTG Probe: UPL Probe # 64
Smo	PF: GCAAGCTCGTGCTCTGGT PR: GGGCATGTAGACAGCACACA Probe: UPL Probe #3
Gli1	PF: CAGGGAAGAGAGCAGACTGAC PR: CGCTGCTGCAAGAGGACT Probe: UPL Probe #84
Gli2	PF: GCAGACTGCACCAAGGAGTA PR: CGTGGATGTGTTTCATTGTTGA Probe: UPL Probe #68
Gli3	PF: ACCGTTCAAAGCCCAGTACA PR: GGCTTTTGTGCAACCTTCA Probe: UPL Probe #7

Table 2.2 - Human primer and probe sequences used for qRT-PCR. Probes designed by the Universal Probe Library (UPL) are indicated. All the probes were labelled with FAM (5') and TAMRA (3'). Primer Forward (PF); Primer Reverse (PR).

NAME	SEQUENCE (5' - 3')
18s	PF: GCCGCTAGAGGTGAAATTCTTG PR: CATTCTTGGCAAATGCTTTTCG Probe: ACCGGCGCAAGACGGA
MMP1	PF: AAGATGAAAGGTGGACCAACAATT PR: CCAAGAGAATGGCCGAGTTC Probe: CAGAGAGTACAACCTTACATCGTGTGCGGCTC
MMP2	PF: AACTACGATGACGACCGCAAGT PR: AGGTGTAAATGGGTGCCATCA Probe: CTTCTGCCCTGACCAAGGGTACAGCC
MMP3	PF: TTCCGCCTGTCTCAAGATGATAT PR: AAAGGACAAAGCAGGATCACAGTT Probe: TCAGTCCCTCTATGGACCTCCCCCTGAC
MMP10	PF: GGACCTGGGCTTTATGGAGATAT PR: CCCAGGGAGTGGCCAAGT Probe: CATCAGGCACCAATTTATTCCTCGTTGCT
MMP12	PF: CGCCTCTCTGCTGATGACATAC PR: GGTAGTGACAGCATCAAACTCAA Probe: TCCCTGTATGGAGACCCAAAAGAGAACCA
MMP14	PF: AAGGCCAATGTTCGAAGGAA PR: GGCCTCGTATGTGGCATACTC Probe: CAACATAATGAAATCACTTTCTGCATCCAGAATTA
ADAM8	PF: AAGCAGCCGTGCGTCATC PR: AACCTGTCCTGACTATTCCAAATCTC Probe: AATCACGTGGACAAGCTATATCAGAACTCAACTT
TIMP1	PF: GACGGCCTTCTGCAATTCC PR: GTATAAGGTGGTCTGGTTGACTTCTG Probe: ACCTCGTCATCAGGGCCAAGTTCGT

NAME	SEQUENCE (5' - 3')
TIMP2	PF: GAGCCTGAACCACAGGTACCA PR: AGGAGATGTAGCACGGGATCA Probe: CTGCGAGTGCAAGATCACGCGC
TIMP4	PF: CACCCTCAGCAGCACATCTG PR: GGCCGGA ACTACCTTCTCACT Probe: CACTCGGCACTTGTGATTCTGGGC
ZO-1	PF: CATGAAGATGGGATTTCTTTCG PR: GCCAGCTACAAATATTCCAACA Probe: UPL Probe #20
LRP1	PF: GATGAGACACACGCCAACTG PR: CGGCACTGGA ACTCATCA Probe: UPL Probe #83
F3	PF: GCCAACTGGTAGACATGGAGA PR: GCTGCCACAGTATTTGTAGTGC Probe: UPL Probe #15
Notch	PF: CCAAGGGTGAGAGCCTGAT PR: CCATGCCTGGCTCCTCTA Probe: UPL Probe #10
RORC	PF: GAGGCTCTCAGGCTTTATCC PR: AACCAGCACC ACTTCCATTG Probe: UPL Probe #53
SMAD6	PF: TTAGGTTTTGTTTGGGATTTCTT PR: AAGGCAGGCTTGTGATACC Probe: UPL Probe #24

2.8. Dextran Extravasation assay

Hundred thousand MCEC-1 cells were plated on the inner chamber of 0.3µm PET cell culture inserts (Greiner Bio-One) together with 200µl of the appropriate media. Each insert was then placed in a 24 well plate already containing 800µl of the same culture media and incubated at 33°C for 48h to promote a high confluence. After 48h incubation, 150µl of the media from the insert inner chamber was aspirated, to avoid disturbance of the endothelial cell monolayer, and replaced with 150µl of fresh culture media containing Dextran-FITC (Life Technologies) to a final concentration of 10µg/ml together with the appropriate treatment. The cellular inserts were then transferred to a new 24 well plate containing 800µl of fresh culture media and MCEC-1 cells were then incubated during 24h (37°C, 5% CO₂). After 24h, a 100µl aliquot from the cellular insert lower chamber was taken, placed in a 96 well white plate and measured using Wallac EnVision spectrophotometer with an excitation of 492nm and an emission of 530nm. A cell-free coated-insert was used as a negative control.

Preliminary Dextran extravasation experiments in non-treated and cytokine-treated MCEC-1 monolayers showed no differences between conditions (**Figure 2.1**). However, as it will be discussed in the following chapters, cytokines did seem to affect endothelial barrier integrity. This apparent controversy could be explained by the fact that conjugated dextran was added in combination with the treatments and incubated for 24h. Dextran extravasation assays reported in the literature typically measure concentration of transmigrated dextran between 30min and 2h after addition (Mark & Miller, 1999; Trickler et al., 2005; Sajja et al., 2014; Ni et al., 2017) as longer incubations could allow for diffusion and transcytosis mechanisms to take place and increase dextran concentrations on the lower compartment chamber, obscuring any possible differences in actual barrier function. Due to this, an alternative method (Transendothelial Electrical Resistance measurements) will be used to assess modulations in endothelial barrier stability.

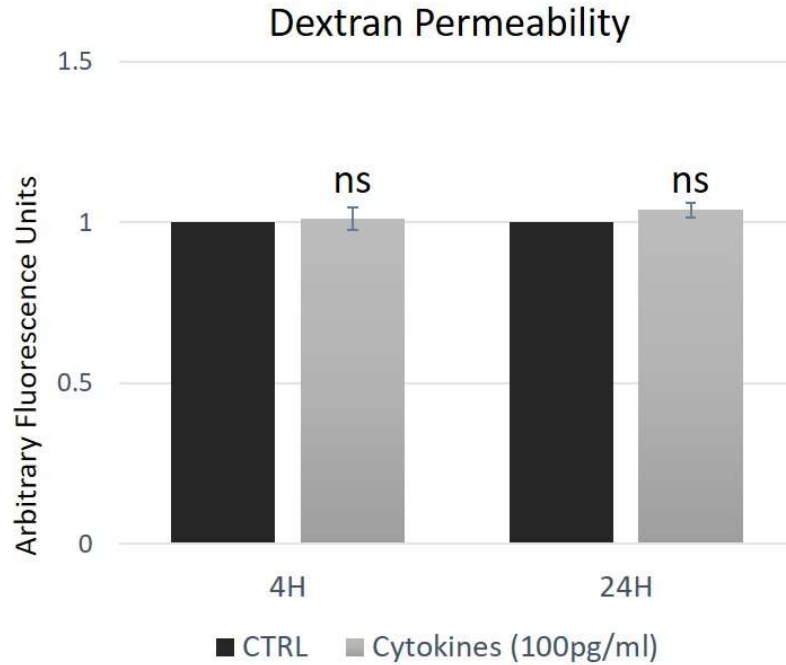


Figure 2.1 - Cytokines treatment does not alter barrier permeability to Dextran-FITC at 4h and 24h. MCEC-1 cells were cultured on cell culture inserts (0.3 μ m porous). Upon confluency, MCEC-1 monolayers were treated with a cytokines mix (TNF α and IL1 α at 100pg/ml) and Dextran-FITC (4kDa) was loaded onto the luminal side of the insert. At 4h and 24h after treatment addition Dextran-FITC levels on the albumnal side were analysed. Statistically significant differences were assessed via t-test. Each bar represents the mean \pm SEM for 3 wells. ns $p > 0.5$. Representative experiment depicted. Experiment replicated 2 times.

2.9. Transendothelial Electrical Resistance assay

Hundred thousand cells (MCEC-1 or hCMEC/D3), together with 200µl of the appropriate media, were plated on the inner chamber of 0.3µm PET cell culture inserts (Greiner Bio-One) coated as previously indicated: with 1% Type A Gelatin from Porcine Skin (Sigma) for 1h at 37°C for MCEC-1 cells or with 150µg/ml Rat Collagen I Low Viscosity (R&D Systems) for 1h at room temperature for hCMEC/D3. Each insert was then placed in a 24 well plate already containing 800µl of the same culture media and incubated for 48h at 33°C (for MCEC-1) or 37°C (for hCMEC/D3), 5% CO₂ to promote a high confluence. After 48h incubation, treatments were added into the inner chamber of the cell culture insert and incubated for further 24h at 37°C, 5% CO₂. 24h after treatment addition Transendothelial Electrical Resistance (TEER) was measured across the generated endothelial barrier using an EVOM & EVOMX system equipped with chopstick electrodes (World Precision Instruments). A cell-free coated-insert was used as a negative control. To minimise cell exposure to variable conditions outside the incubator, TEER measurements were taken in intervals of 24h.

2.10. Protein detection by Western Blotting

Western Blotting (WB) was performed essentially as described in Baker *et al.* (Baker *et al.*, 2012). Further details are given below.

2.10.1. Preparation of cell lysates

Confluent hCMEC/D3 monolayers treated for 24h were washed in ice cold PBS and lysed in RIPA buffer: 50mM Tris-Hydrochloride (Tris-HCl; pH 8), 150mM NaCl, 1% (v/v) Triton X100, 0.5% (w/v) Sodium Deoxycholate, 0.1% (w/v) SDS containing Halt™ Protease and Phosphatase Inhibitor Cocktail (Pierce). Protein extraction was performed on ice for a total of 30min with one intermediate scraping step at 15min. Cell lysates were then cleared to remove debris by centrifugation at 4°C (13,000rpm) for 10min after which, supernatant was transferred to a new tube.

2.10.2. Protein quantification

Protein concentration in the lysed samples was determined using a Pierce Bicinchoninic Acid (BCA) Protein Assay Kit (Thermo Fisher) following manufacturer's instructions. 10 μ l of protein standards of known concentrations of Bovine Serum Albumin (BSA; ranging from 0 to 2000 μ g/ml) were prepared and plated in duplicate into a 96 well clear plate. 5 μ l of the lysed samples together with 5 μ l of ddH₂O were also plated. 200 μ l of Working Reagent (50:1; Reagent A; Reagent B) were prepared and added to each standard or cell lysate sample and incubated at 37^oC for 30min. Absorbance at 562nm was then measured using a Wallac EnVision spectrophotometer.

In order to calculate protein concentration in the cell lysed samples, the absorbance reading from the 0 μ g/ml BSA standard (control) was subtracted from all measurements. The average values of known BSA standards were plotted against their absorbance values and used to generate a standard curve, which trendline equation was then used to interpolate the concentration of the unknown samples.

After quantification, the volume corresponding to 30 μ g of protein was taken from each sample and mix with 4x Reducing Sample Buffer: 625mM Tris-HCl (pH 6.8); 2% (w/v) SDS; 10% (v/v) glycerol; bromophenol blue; 12.5% (v/v) β -mercaptoethanol. Samples were then stored at -80^oC until needed.

2.10.3. Trichloroacetic Acid Precipitation

Before RNA or protein extraction, conditioned media from hCMEC/D3 treated monolayers was collected and incubated with 5% (v/v) Trichloroacetic Acid (TCA) overnight at 4^oC under agitation. Media was then centrifuged and the protein pellet was thoroughly washed with acetone, let to air dry and further washed with 0.5M Tris-Hydrochloride (Tris-HCl; pH 9). Pellet was then resuspended in Reducing Sample Buffer followed by denaturation at 95^oC for 5min.

2.10.4. Protein resolution by SDS-PAGE

Quantified protein samples or total TCA-precipitates of conditioned media were loaded onto polyacrylamide gels (7% or 10% resolving gels and 5% stacking gel). The pre-stained molecular weight marker (10kDa to 250kDa) Precision Plus Protein™ Ladder (Bio-Rad) was also loaded onto each gel. Gels were run (BioRad mini gel apparatus) at a constant 30mAmp per gel until the dye front reached the lower end of the gel.

2.10.5. Semi-dry transfer of polyacrylamide gels onto PVDF membranes

Polyvinylidene fluoride (PVDF) membranes (Bio-Rad) were activated in 100% (v/v) methanol for 10min at room temperature. After activation, PVDF membranes together with thick filter paper (Bio-Rad) and the polyacrylamide gels were equilibrated in semi-dry transfer buffer for another 10min at room temperature. Proteins were then transferred at constant 15V for 50min using a Transblot SD Semi-Dry Transfer Cell (Bio-Rad).

2.10.6. Proteins immunodetection

PVDF membranes containing the transferred proteins were blocked under different conditions depending on the primary antibody: 1h at room temperature in 5% (w/v; dried, skimmed) milk for F3, β -actin and GADPH antibodies; 2h at room temperature in 5% (w/v; dried, skimmed) milk for ZO-1 antibody; and 3h at room temperature in 5% (w/v; dried, skimmed) milk with 3% BSA for MMPs antibodies. After blocking, membranes were incubated overnight at 4°C with primary antibody diluted in 2% (w/v; dried, skimmed) milk (for F3 or ZO-1) or 5% (w/v; dried, skimmed) milk with 3% BSA (for MMPs). Membranes were then washed with TBS-T (0.1% (v/v) Tween-20) and incubated with the secondary antibody conjugated with horse radish peroxidase (HRP) diluted in 2% (w/v; dried, skimmed) milk for 60min at room temperature. After washing again with TBS-T, membranes were incubated in ECL (Pierce) for 5min and developed using the ChemiDoc™ Imaging System (Bio-Rad). A full list of primary and secondary antibodies can be found in **Table 2.3 & Table 2.4**.

2.10.7. Membrane stripping

In order to re-probe the membranes for different proteins, membranes were incubated with 10ml of ReBlot Plus Strong (Merck Millipore) stripping buffer for 15min before re-incubating with the appropriate blocking buffer for 5min (twice). Membranes were then incubated with the desired primary antibody followed by the previously described immunodetection protocol.

Table 2.3 - Details of primary antibodies used in Western Blotting. List of primary antibodies used in protein immunoblotting together with their most relevant details. Metalloproteinase antibodies were provided by Dr Gavrilovic.

Target	Supplier	Product Number	Host Species	Clonality	Isotype	Dilution
MMP1	In-house made	Limb et al., 2005	Sheep	Polyclonal	IgG	50µg/ml
MMP3	In-house made	Bord et al.,1998	Sheep	Polyclonal	IgG	50µg/ml
MMP10	In-house made	Bord et al.,1998	Sheep	Polyclonal	IgG	50µg/ml
F3	R&D Systems	MAB2339	Mouse	Monoclonal	IgG	1:250
ZO-1	Invitrogen	61-7300	Rabbit	Polyclonal	IgG	1:500
β-Actin	Abcam	ab8227	Rabbit	Polyclonal	IgG	1:10000
GADPH	Abcam	ab70699	Rabbit	Polyclonal	IgG	1:2000

Table 2.4 - Details of secondary antibodies used in Western Blotting. List of secondary antibodies used in protein immunoblotting together with their most relevant details.

Target	Supplier	Product Number	Host Species	Clonality	Isotype	Dilution
α -Rabbit (HRP)	Sigma	12-348	Goat	Polyclonal	IgG	1:10000
α -Sheep (HRP)	R&D Systems	HAF016	Donkey	Polyclonal	IgG	1:10000
α -Mouse (HRP)	Sigma	12-349	Goat	Polyclonal	IgG	1:10000

2.11. Transfection of hCMEC/D3 cells

hCMEC/D3 cells were transfected with 200nM of hsa-miR125b-5p (Exiqon), hsa-miR125b-5p miRCURY LNA microRNA mimics Negative Control 4 (Exiqon), hsa-miR125b-5p miRCURY LNA Power Inhibitor (Exiqon), or the fluorescently labelled hsa-miR125b-5p miRCURY LNA Power Inhibitor Control (Exiqon). 500,000 hCMEC/D3 cells in PBS were transfected using programme V-001 of the Nucleofector™ 2d Device (Lonza), although other transfection media were trialled as part of the optimization process including serum-free cell culture media and Nucleofector™ Kit V (Lonza). Immediately after transfection, cells were transferred to a 6 well cell culture insert (previously coated as described) containing the appropriate cell culture media previously equilibrated at 37°C. Transfected cells were then incubated at 37°C (5% CO₂) for 48h prior to treatment addition.

2.12. Microarray analysis

RNA was extracted (as described above) from transfected hCMEC/D3 cells stimulated with cytokines for 24h. Extracted RNA was checked for quality (A260/A280 and A260/A230 ratios above 1.8 with a minimum concentration of 50ng/μl) before sending 10μl to Cambridge Genomic Services (Cambridge, UK) for microarray analysis using the Genechip WT Plus Kit from Affymetrix. Each condition consisted of three biological replicates and were confirmed to pass the quality control requirements. Initial statistical analysis was performed by Cambridge Genomic Services.

Bioinformatic cumulative plot analysis for miR125 targets between mimic and inhibitor transfected cells was performed by Dr Simon Moxon. Additionally, genes showing a significant change (adjusted p value <0.05) greater than 1.5-fold were inputted into Genomatix© NGS Analysis and Pathway System in order to visualise regulated pathways, networks and processes.

2.13. Statistical analysis

Statistical analysis was performed with two-tailed Students' t test for two-sample unequal variance using Microsoft Office Excel 2010. Alternatively, statistical analysis for multiple comparisons were performed with one-way ANOVA followed by Tukey's post hoc test using GraphPad Prism (v. 6). Significance was only accepted for p-values of less than 0.05.

3. Development of an in vitro murine endothelial cell barrier model

3.1. INTRODUCTION

3.1.1. Endothelial barriers

Endothelial barriers are not only found in the Blood-Brain barrier (BBB) but widely spread across the body, including the lung and cardiac systems. The cardiac endothelium or endocardium, forms a blood-heart barrier maintaining the correct ionic homeostasis needed for cardiomyocyte contractility (Kuruvilla & Kartha, 2003). Thus, endocardial dysfunction has been reported to underline several cardiac pathologies such as congestive heart failure, myocardial infarction or myocarditis among others (Kuruvilla & Kartha, 2003). Thus, cardiac endothelial cells can serve as a useful model for endothelial barrier studies.

3.1.2. MCEC-1: an endothelial cell line

A murine cardiac endothelial cell line (MCEC-1) was previously established from transgenic mice (expressing a thermolabile strain (tdA58) of the simian virus (SV) 40 large T antigen, meaning that cell proliferation is only possible at the reduced temperature of 33°C (Lidington et al., 2002). MCEC-1 cells, are capable of tubule formation, express the endothelial marker CD31 together with E-, P-selectin, intercellular adhesion molecule (ICAM)-2 and vascular cell adhesion molecule (VCAM)-1 corroborating their endothelial phenotype (Lidington et al., 2002).

3.1.3. Endothelial barriers are disrupted under inflammatory conditions

Endothelial barrier disruption under inflammatory conditions has been broadly described in the literature (Mark & Miller, 1999; Trickler et al., 2005; Forster et al., 2008; Sajja et al., 2014; Ni et al., 2017). *In vitro* studies in endothelial monolayers have shown that one of the mechanisms by which cytokines may be mediating endothelial barrier disruption is through a reduction in the levels of tight junction proteins (such as ZO-1, claudin-5 and occludin) (Forster et al., 2008; Aslam et al., 2012; Cohen et al., 2013; Labus et al., 2014). Junctional proteins provide endothelial barriers with close contacts between neighbouring ECs, resulting in a polarized phenotype and

very limited transcellular diffusion (Kniesel & Wolburg, 2000). Thus, cytokine-mediated loss of junctional proteins could disrupt these cell-cell contacts resulting in increased endothelial permeability. To model these events, cytokine-dependent modulation of the tight junction protein ZO-1 will be explored and correlated with overall measurements of barrier integrity.

An alternative mechanism by which cytokines can mediate endothelial barrier disruption is through increased levels of metzincins (reviewed in Rempe et al., 2016). Some members of the metzincin family (which comprises Matrix Metalloproteinases (MMPs), A Disintegrin And Metalloproteinases (ADAMs) and A Disintegrin And Metalloproteinase with Thrombospondin motifs (ADAMTS)) can degrade junctional proteins and basal lamina elements, leading to loss of cell-cell contacts and endothelial barrier opening (Yang et al., 2007; Lu et al., 2009; Bauer et al., 2010; Wu et al., 2015). For these reasons, the role of metalloproteinases (and their inhibitors TIMPs) in barrier permeability under inflammatory conditions will be explored in our *in vitro* model of an endothelial barrier.

In this thesis, inflammatory conditions will be mimicked through the addition of a cytokines mix consisting of TNF α (100pg/ml) and IL1 α (100pg/ml). MCEC-1 cells have been previously stimulated with similar cytokines combinations (TNF α and IL1 β at 10ng/ml) in the published literature (Gomez et al, 2017; R. J. Singh et al., 2005). However, preliminary analysis of cell viability (Presto Blue) revealed a slight decrease in cell viability when high doses of cytokines similar to those used in previously published literature (10ng/ml) were used (**Figure 3.1**). Additionally, a significant decrease in MCEC-1 viability was seen when a combination of cytokines (10ng/ml) and cyclopamine (an inhibitor of the Hedgehog pathway that will be further discussed in the following sections) was used (**Figure 3.1**). Since an experimentally chosen lower concentration of cytokines (100pg/ml) was able to trigger changes in gene expression (see **sections 3.2.2.1 and 3.2.2.2**) and MCEC-1 monolayer's integrity (see **section 3.2.1.4**) without compromising cell viability (**Figure 3.1**) this will be the concentration used through the following chapter (**Chapter 3**).

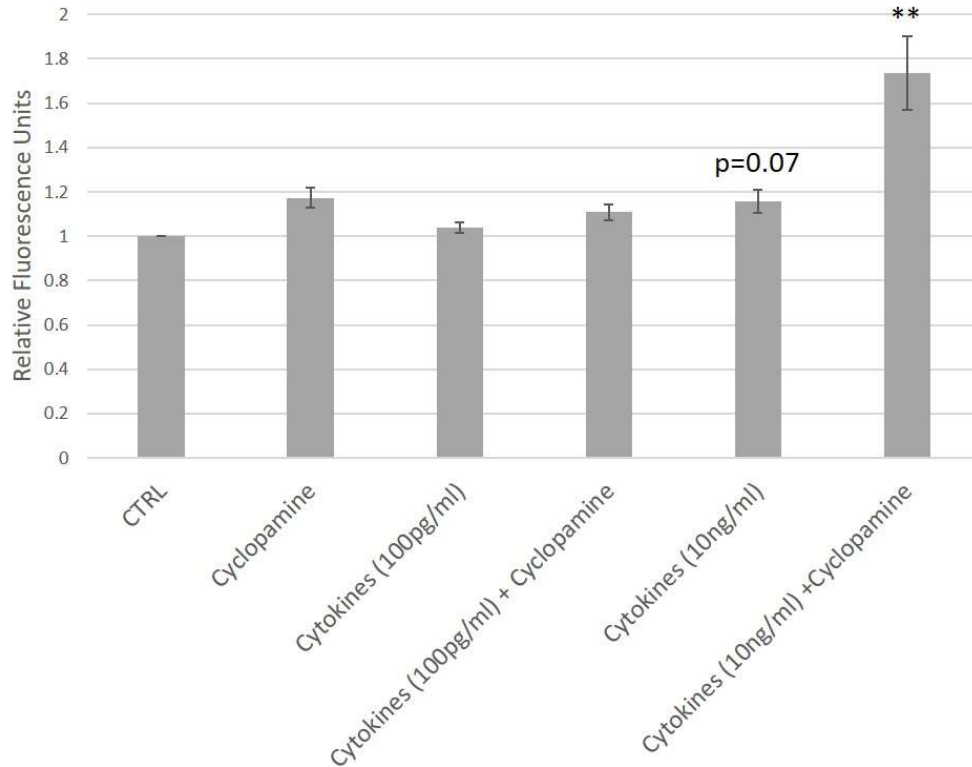


Figure 3.1 – Cell viability assay in MCEC-1 cells. Confluent MCEC-1 monolayers untreated (CTRL) and treated with a mixture of cytokines (TNF α and IL1 α) (100pg/ml or 10ng/ml), the hedgehog pathway inhibitor cyclopamine (4 μ M) or a combination of both during 24h. Following treatment, cells were incubated with Presto Blue reagent for 2h and fluorescence measured. Each bar represents the mean \pm SEM for 4 wells measured. ** $p < 0.01$. Statistically significant differences were assessed via t-test. Preliminary experiment (1 replica).

3.1.4. Shh as an endothelial barrier promoting agent

In order to understand potential roles of hedgehog pathway signalling in vascular endothelial barrier integrity (see Chapter 1 for details) a pharmacological approach was taken to explore the effect of Shh in this murine endothelial cell barrier model. Shh is a small secreted protein that can be released into the extracellular environment, where it can target a transmembrane protein named Patched (Ptch). In the absence of Shh, Ptch works as an inhibitor of the transmembrane protein Smoothed (Smo), which becomes activated and able to initiate a signalling cascade that will result in the activation of the Gli family of transcription factors (Gli1, Gli2 and Gli3) (Luissint et al., 2012). The importance of the Hedgehog (Hh) pathway in the maintenance of endothelial barrier integrity will be tested in our *in vitro* model in the presence or absence of inflammation.

3.1.5. Vitamin D3 and endothelial barrier integrity

Vitamin D3 is a steroid hormone capable of crossing the cell membrane and bind to the intracellular vitamin D receptor (VDR), which interacts with the retinoid X receptor (RXR) in order to form a heterodimer able to target genes that contain the vitamin D3 response elements (VDRE) in their regulatory regions (Dusso et al., 2005). Although the underlying mechanisms by which Vitamin D3 may promote endothelial barrier integrity remain unknown, treatment with Vitamin D3 active form (1,25(OH)₂D₃) has been shown to increase the expression of several tight junction proteins such as claudins (Fujita et al., 2008), occludins (Kong et al., 2008; Yin et al., 2011), and ZO proteins (Palmer et al., 2001) in several endothelial cell types. Due to this, Vitamin D3 effects on the tight junction protein ZO-1 will be explored and correlated with overall measurements of barrier integrity.

Another mechanism by which Vitamin D3 could be promoting endothelial barrier integrity is through the impairment of the degradation of its extracellular matrix components and junctional complexes. As it has been previously mentioned, inflammatory cytokines can promote metalloproteinase secretion (Unemori et al., 1991). In this context, Vitamin D3 deficiency has

been associated with increased metalloproteinase serum levels, which could be revoked by Vitamin D3 dietary supplementation (Timms et al., 2002). Additionally, circulating levels of TIMP-1 (and therefore MMP activity) can be strongly influenced by the VDR haplotype (Timms et al., 2002). For this reasons, Vitamin D3 effects on metalloproteinase levels (in the presence and absence of inflammation) will be also explored.

3.1.6. Shh and Vitamin D3, an unexplored cross-talk

It has been suggested that Ptch-driven inhibition of Smo could be mediated by a Ptch-dependent translocation of Vitamin D3 (or a precursor) across that will act as a Smo antagonist once in the extracellular environment (Bijlsma et al., 2006). Thus, according to Bijlsma *et al*, these two endothelial barriers promoting signalling pathways could be opposing each other. Shh and Vitamin D3 possible cross-talk will be explored in the context of endothelial barrier and inflammatory conditions, together with its possible impact on metalloproteinase regulation.

3.1.7. Transwell Cell Culture System

In this model, a monolayer of ECs is grown in a previously coated transwell insert. Cell polarization is achieved through the existence of two separated chambers: the inside of the insert mimics the capillary lumen whereas the well containing the insert represents the brain parenchyma. The presence of microporous (typically 0.3-0.4 μ m) on the insert membrane prevents cell migration between the different compartments while allowing the exchange of small molecules (**Figure 3.2**) (reviewed in He et al., 2014)). It is very common to co-culture ECs together with other cell types that impact on BBB maintenance such as astrocytes, providing the model with a more accurate physiological environment. However, a monolayer reductionist approach could be an ideal first step in the study of raw barrier responses to different stimuli.

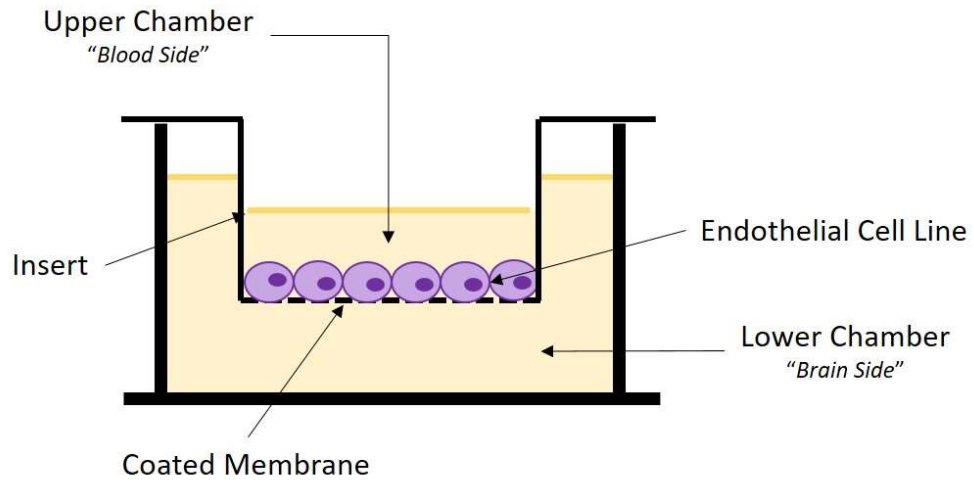


Figure 3.2 – In vitro modeling of the Blood-Brain Barrier (BBB). Endothelial cells (ECs) are seeded onto the microporous membrane of a culture insert and grown to confluence to promote barrier formation. The insert membrane is typically coated with extracellular matrix components to mimic the basal lamina. EC polarization is achieved through the presence of two separated chambers: the upper and lower chambers, representing the luminal and parenchymal sides respectively. Any exchange between these two chambers will be tightly regulated by the cultured endothelial barrier.

3.1.8. Aims

1. Using a Mouse Cardiac Endothelial Cell Line (MCEC-1) we aim to take the first approach to the establishment of an *in vitro* model of an endothelial barrier.
2. The model will be then exposed to barrier-enhancing (Hh pathway and Vitamin D3 stimulation) and barrier-impairing conditions (cytokine stimulation to model inflammation and Hh pathway pharmacological inhibition through cyclopamine) conditions in order to explore function.
3. Different methods to assess barrier integrity, such as dextran permeability and TEER measurements, will be tested. Additionally, ZO-1 junctional levels in response to the afore mentioned stimuli will be also assessed and correlated with overall barrier functional dynamics.
4. Metalloproteinase role in endothelial barrier impairment under inflammatory conditions, and its response to Shh and/or Vitamin D3 will be also studied.

After optimization, this model will be used to further our study of BBB dynamics by using a brain microvascular EC line.

3.2. RESULTS

3.2.1. Tight Junction modulation in MCEC-1 confluent monolayers

3.2.1.1. MCEC-1 cells form a monolayer with responsive tight junctions when grown to confluence

As a first approach, MCEC-1 ability to form structured tight junctions in confluent monolayers was tested. As shown in bright field images, MCEC-1 cells grown for a period of 24h form confluent single-cell monolayers (**Figure 3.3**). Confluent MCEC-1 cells' ability to form structured tight junctions (a marker of endothelial barrier integrity) after 24h culture was also assessed through the staining of the junctional protein ZO-1. MCEC-1 cells grown in these conditions formed structurally viable tight junctions in which ZO-1 localization was restricted to the cell membrane (with very little detectable cytoplasmic staining) originating a continuous and homogeneous staining around the cellular periphery (**Figure 3.3**). Non-treatment dependent variation in cell size was reported in different areas of the studied coverslips (**Appendix 3.A**), we aimed to take images from equivalent areas of the coverslip in order to minimise this effect.

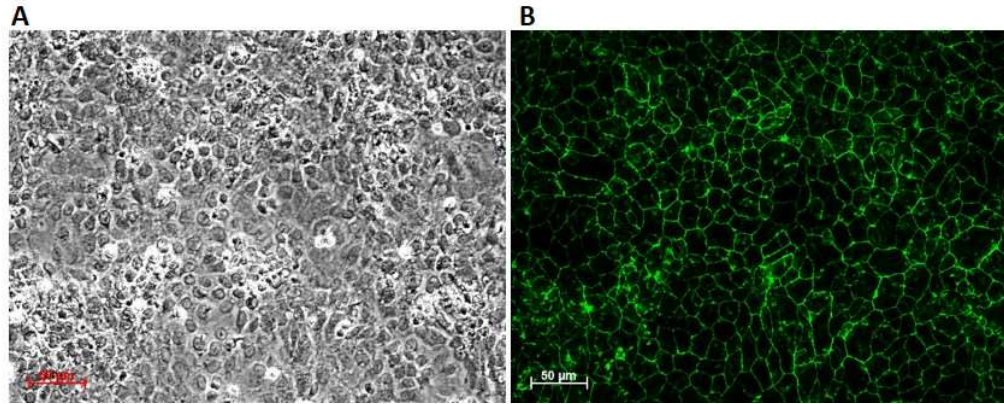


Figure 3.3 - MCEC-1 cells form confluent monolayers with tight junctions. (A) Bright field image of MCEC-1 confluent monolayers cultured for 24h. (B) Confluent MCEC-1 monolayers were immunolabelled forZO-1 protein to visualise tight junctions.

An unbiased approach was developed in order to quantify ZO-1 junctional levels. Bright field images of MCEC-1 monolayers were used to draw lines between adjacent cells, assuring that the point of cell-to-cell contact (where junctions are expected to be found) would be located approximately in the middle of the line. Maintaining this line, bright field images would be replaced by the corresponding fluorescent image, stained against ZO-1. The usage of bright field images during the line placement instead of the ZO-1 stained images assured an unbiased placement of the draw lines across the whole image, making sure that the measurements were not concentrated on cells with more obvious or prominent signal. Now, the fluorescent intensity across the draw line could be quantify, originating bell curves with a peak corresponding with the centre of a particular junction. This way, loss or delocalization of junctional ZO-1 would produce curves with lower peaks than those with higher ZO-1 levels (**Figure 3.4**). Andor IQ2 software was used for this analysis. In order to facilitate the understanding of the following sections, the differences between the curves' peaks will be represented using bar graphs, but the original bell curves can be found in the appendix (**Appendix 3.B to 3.G**). For comparability, contrast and brightness parameters were kept constant between experiments. However, in order to incorporate a normalisation procedure in ZO-1 staining, future analysis could consider a normalisation of ZO-1 signal based in the intensity levels of DAPI.

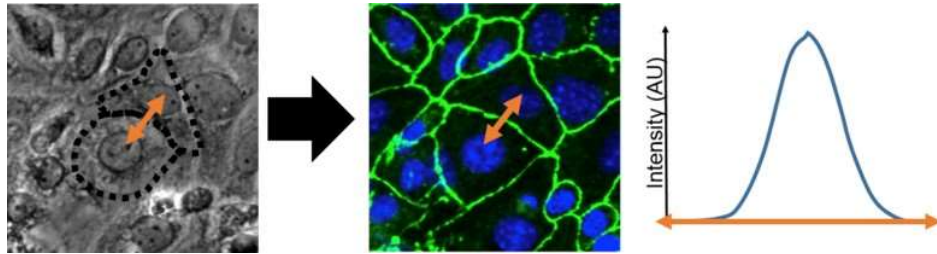


Figure 3.4 – Analysis of ZO-1 junctional levels. Bright field images of MCEC-1 monolayers were used to draw a line between adjacent cells, assuring that the expected junction would be included in the draw line in an unbiased manner. Bright fields images were replaced by the fluorescent image (stained against ZO-1) and fluorescence intensity across the line was quantified. Bell curves were originated, the peak of which was used to assess ZO-1 junctional levels and, thus, junctional integrity.

3.2.1.2. Treatment with Shh or Vitamin D3 enhances Tight Junction protein expression/integrity formation

The effects of Shh or Vitamin D3 on tight junction protein expression in MCEC-1 cells was explored. Confluent MCEC-1 monolayers were treated with either Shh or Vitamin D3 for 24h. After treatment, MCEC-1 monolayers were immunolabelled for ZO-1 and fluorescence intensity was measured as previously described. Monolayers exposed to Shh showed significantly enhanced levels of ZO-1 when compared with controls (1.58 ± 0.20 vs 1.00 ± 0.00 , $p < 0.05$). Similarly, treatment with Vitamin D3 significantly increased ZO-1 levels when compared with untreated monolayers (1.50 ± 0.18 vs 1.00 ± 0.00 , $p < 0.05$) (**Figure 3.5**). Treatment with either Shh or Vitamin D3 did not alter ZO-1 subcellular localization when compared with controls as in all cases ZO-1 signal was restricted to the cellular membrane (with nearly undetectable cytoplasmic staining). Additionally, a continuous and homogeneous staining around the cellular periphery was described for all the treatments (**Figure 3.5**).

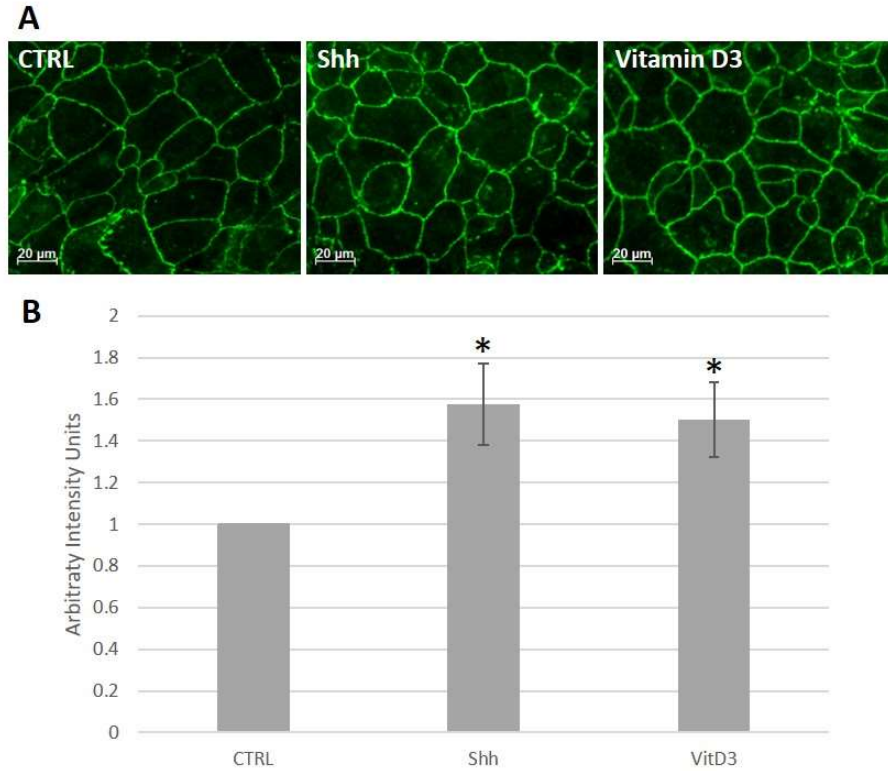


Figure 3.5 – Shh or Vitamin D3 enhance tight junction integrity. (A) Confluent MCEC-1 monolayers untreated (CTRL) and treated with either Shh (100ng/ml) or Vitamin D3 (100nM) for 24h. Cells were stained against ZO-1 to visualise tight junction integrity. Representative images shown. (B) Quantification of junctional ZO-1 signal intensity showed a significant increase in ZO-1 levels after Shh or Vitamin D3 exposure. Analysis performed with Andor IQ2 software. Each bar represents the mean \pm SEM for 3 independent experiments. Statistically significant differences were assessed via t-test. * $p < 0.05$; ** $p < 0.01$.

3.2.1.3. Abrogation of Hedgehog pathway (cyclopamine) has no effect on tight junction integrity

To test the important of Hedgehog signalling in tight junction maintenance, a confluent monolayer of MCEC-1 cells was treated for 24h with a Hedgehog pathway pharmacological inhibitor known as cyclopamine. As before, monolayers were immunolabelled for ZO-1 to visualise tight junction integrity. No significant differences in ZO-1 levels or subcellular localization were observed between cyclopamine-treated and untreated monolayers (0.98 ± 0.18 vs 1.00 ± 0.00) (**Figure 3.6**). This observation suggests that an absence of endogenous Hedgehog signalling. Additionally, several molecules with potential implications in barrier functions were also explored and will be discussed (**Figures 3.6 to 3.9**).

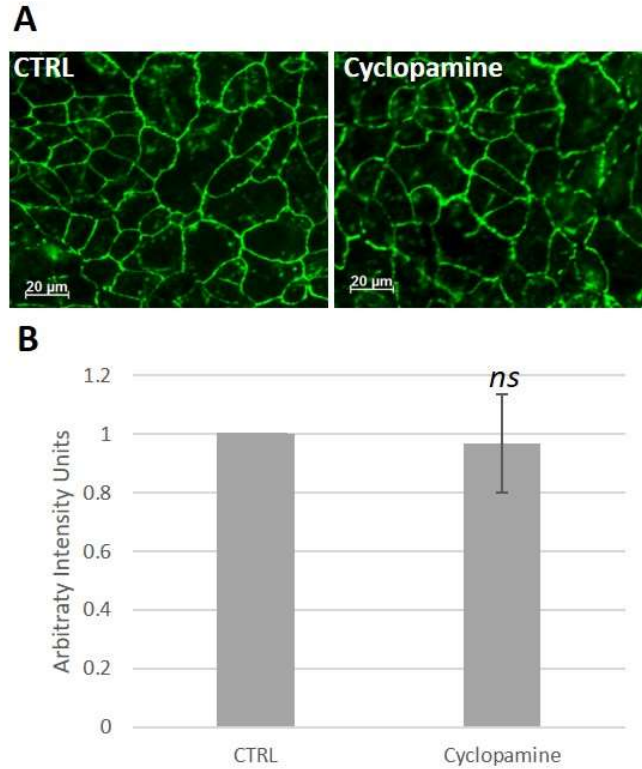


Figure 3.6 – Hedgehog pathway abrogation has no effect in tight junction stability. (A) Confluent MCEC-1 monolayers untreated (CTRL) or treated with the Hedgehog pathway inhibitor Cyclopamine (4 μ M) for 24h. Immunolabelling for ZO-1 to visualise tight junction integrity. Representative images shown. (B) Quantification of junctional ZO-1 signal intensity showed no variation ZO-1 levels after cyclopamine treatment. Statistically significant differences were assessed via *t*-test. Analysis performed with Andor IQ2 software. Each bar represents the mean \pm SEM for independent experiments.

3.2.1.4. Tight junction integrity is compromised under inflammatory conditions

Inflammation has major effects on endothelial barrier integrity. Inflammatory conditions were simulated by addition of a cytokines mix containing TNF α and IL1 α at 100pg/ml. After 24h treatment, monolayers were immunolabelled for ZO-1 to study junctional integrity. Addition of cytokines significantly reduced junctional ZO-1 levels when compared with untreated conditions (0.80 ± 0.04 vs 1.00 ± 0.00 , $p < 0.01$) (**Figure 3.7**). In the presence of cytokines, ZO-1 junctional immunostaining was disrupted, losing the continuous peripheral distribution characteristic of untreated monolayers and promoting the appearance of “gaps” between adjacent cells (**Figure 3.7**). While no cytoplasmic signal was detected in untreated monolayers, in the presence of cytokines a fraction of the cellular ZO-1 localised in the cytoplasm (**Figure 3.7**).

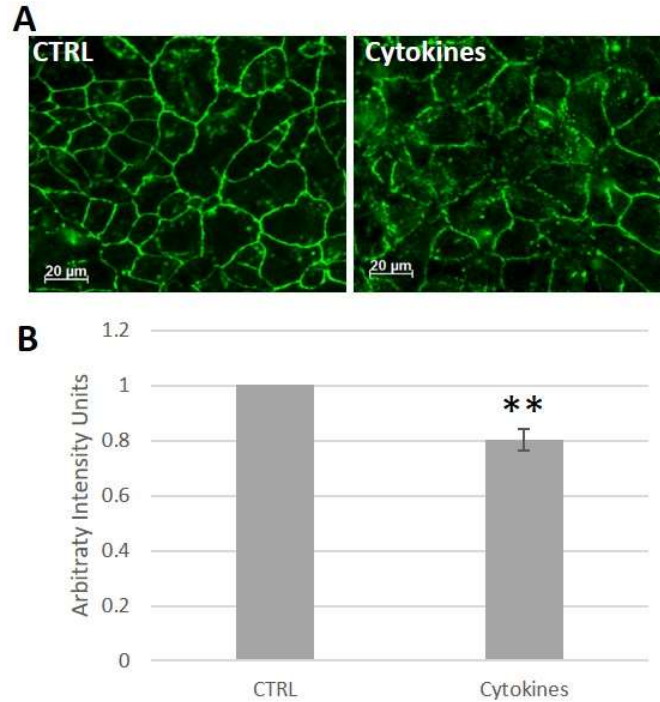


Figure 3.7 – Tight junction stability is compromised under inflammatory conditions. (A) Confluent MCEC-1 monolayers treated with a combination of cytokines (TNF α and IL1 α) (100pg/ml) for 24h or untreated (CTRL). Cells immunolabelled for ZO-1 to visualise tight junction integrity. Representative images shown (B) Quantification of junctional ZO-1 signal intensity showed a significant reduction in ZO-1 levels after cytokines exposure. Analysis performed with Andor IQ2 software. Statistically significant differences were assessed via t-test. Each bar represents the mean \pm SEM for 3 independent experiments. * $p < 0.05$.

3.2.1.5. Cytokine driven loss of junctional ZO-1 can be synergistically enhanced by Hedgehog pathway abrogation (cyclopamine)

The addition of cyclopamine (pharmacological inhibitor of the Hedgehog pathway), under inflammatory conditions was explored. After 24h treatment, monolayers were immunolabelled for ZO-1 to study junctional integrity. As before, the addition of a combination of cytokines significantly reduced ZO-1 junctional levels when compared with untreated monolayers (0.80 ± 0.04 vs 1.00 ± 0.00 , $p < 0.01$) (**Figure 3.8**). As previously reported, abrogation of Hedgehog pathway had no effect in ZO-1 junctional levels (0.91 ± 0.04 vs 1.00 ± 0.00). Abrogation of Hedgehog pathway in the presence of cytokines also reduced ZO-1 junctional levels when compared with untreated monolayers (0.59 ± 0.08 vs 1.00 ± 0.00 , $p < 0.001$), and when compared with the previously reported cytokines-driven decrease (0.59 ± 0.08 vs 0.80 ± 0.04 , $p < 0.05$) (**Figure 3.8**). Cytokine-driven loss of ZO-1 junctional staining was further enhanced by abrogation of the Hedgehog pathway: ZO-1 subcellular localization was mainly cytoplasmic, losing nearly all junctional staining (**Figure 3.8**). This suggests that cytokine-driven loss of tight junction stability can be synergistically enhanced by the addition of cyclopamine (Hedgehog pathway abrogation).

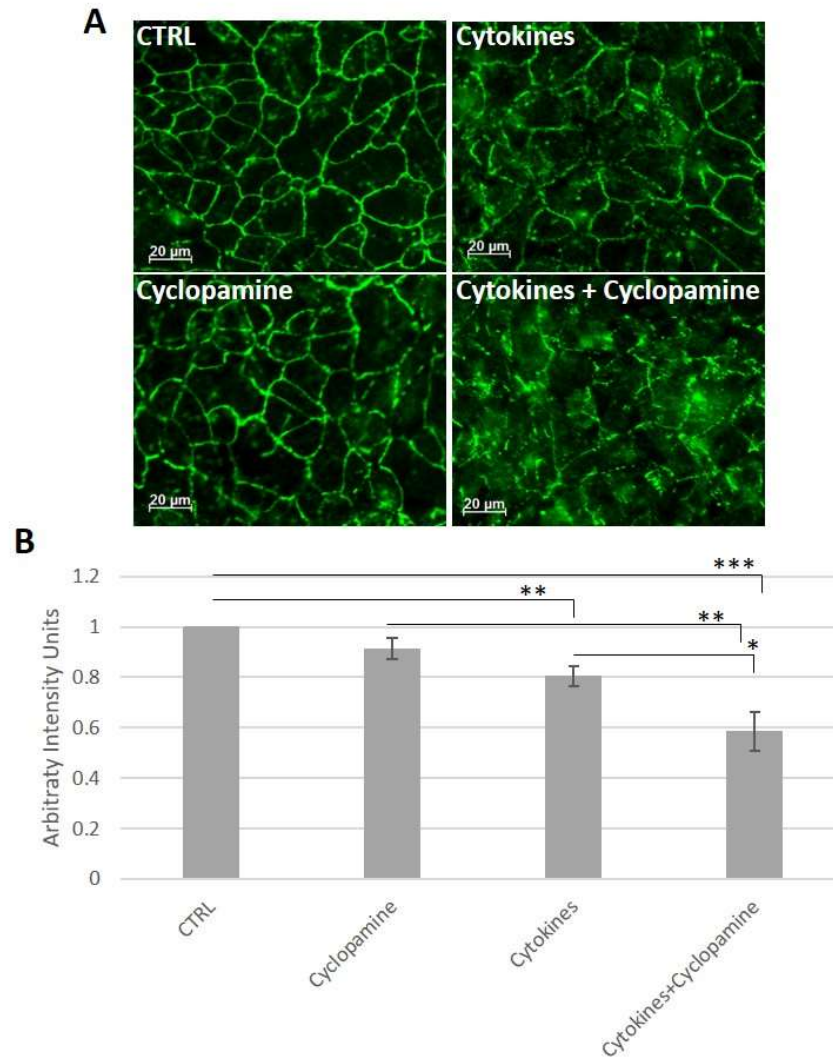


Figure 3.8 – Hedgehog pathway abrogation in the presence of cytokines can further reduce tight junction stability. (A) MCEC-1 monolayers incubated with a mixture of cytokines (TNF α and IL1 α) (100pg/ml), the hedgehog pathway inhibitor cyclopamine (4 μ M) or a combination of both during 24h. CTRL, untreated cells. Monolayers immunolabelled for ZO-1 as described in Methods. (B) Quantification of junctional ZO-1 signal intensity. Analysis performed with Andor IQ2 software. Statistically significant differences were assessed via One-way ANOVA with post-hoc Tukey. Each bar represents the mean \pm SEM for 3 independent experiments. ** $p < 0.01$; *** $p < 0.001$.

3.2.1.6. Preliminary observations show that a combination of Shh and Vitamin D3 may be needed to rescue cytokine and cyclopamine driven loss of junctional integrity

Following the interesting observations with cyclopamine treatment the effect of Shh and Vitamin D3 on junctional integrity was explored. After 24h treatment, confluent MCEC-1 monolayers were immunolabelled for ZO-1 to visualise tight junction integrity. As before, the addition of a combination of cytokines and cyclopamine reduced ZO-1 junctional levels when compared with untreated monolayers. Individual addition of Shh or Vitamin D3 did not trigger any observable changes in cytokines and cyclopamine driven loss of ZO-1 junctional levels. However, combined addition of Shh and Vitamin D3 (in the presence of cytokines and cyclopamine) seemed to increased ZO-1 junctional levels not only when compared with cytokine-cyclopamine treated monolayers but also when compared with untreated conditions (**Figure 3.9**). A combination of Shh and Vitamin D3 not only rescued cytokine/cyclopamine-induced ZO-1 cytoplasmic accumulation but also restored ZO-1 homogeneous distribution around the cellular periphery, contrasting with the discontinuous distribution characteristic of cytokine/cyclopamine-treated monolayers (**Figure 3.9**). These effects were observed in two independent preliminary experiments (**Appendix 3.D** and **3.E**).

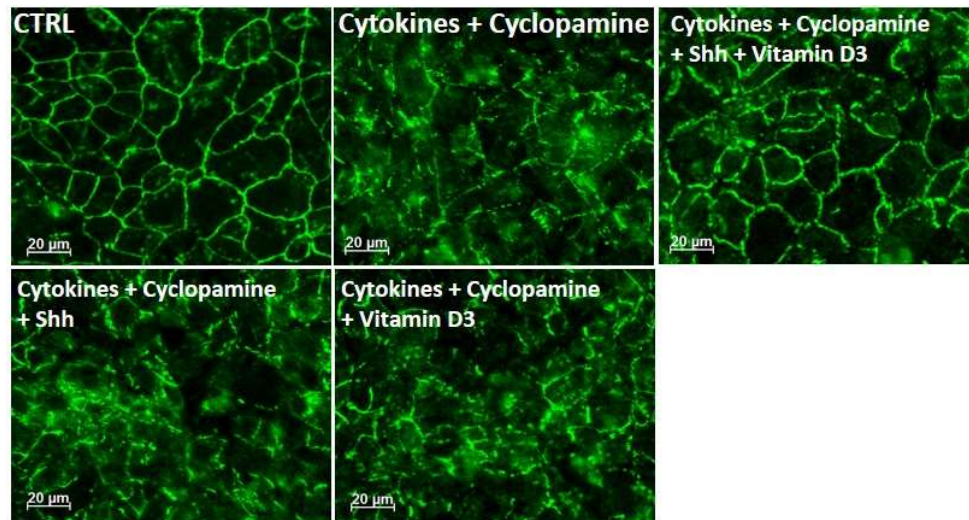


Figure 3.9 – Shh and Vitamin D3 synergistically rescue cytokines and cyclopamine driven loss of junctional stability. MCEC-1 monolayers incubated with a mixture of cytokines (TNF α and IL1 α) (100pg/ml) and the hedgehog pathway inhibitor cyclopamine (4 μ M) in the absence and presence of Shh (100ng/ml) and/or Vitamin D3 (100nM) for 24h. Untreated monolayers are represented as controls (CTRL). Monolayers were immunolabelling for ZO-1 to visualise tight junction integrity (n=2).

3.2.1.7. Akt activation in the Cytokine, Vitamin D3 and Hedgehog pathways

A pharmacological approach was taken to investigate if cytokines, Vitamin D3 or Hedgehog pathways signal through Akt in MCEC-1 monolayers with the Akt specific inhibitor MK-2206. As previously described, treatment with Shh (1.33 ± 0.07 vs 1.00 ± 0.00 , $p<0.05$) or Vitamin D3 (1.28 ± 0.05 vs 1.00 ± 0.00 , $p<0.01$) triggered a significant increase in junctional ZO-1 levels when compared with untreated monolayers whereas treatment with a mixture of cytokines triggered a significant decrease in junctional ZO-1 levels (0.55 ± 0.08) compared to untreated monolayers (vs 1.00 ± 0.00 , $p<0.01$) (**Figure 3.10**). Remarkably, Akt inhibition with MK-2206 significantly reduced junctional ZO-1 levels when compared with untreated controls (0.70 ± 0.03 vs 1.00 ± 0.00 , $p<0.05$) suggesting that a basal level of Akt activation is needed to maintain tight junctions (**Figure 3.10**).

Addition of an Akt inhibitor in the presence of Shh (0.84 ± 0.22), or cytokine (0.81 ± 0.08) abrogated the effect of these treatments, restoring ZO-1 junctional levels to similar values of those observed in untreated monolayers (**Figure 3.10**), suggesting a possible role of Akt in the activation of these pathways. Inhibition of Akt in the presence of Vitamin D3 significantly reduced junctional ZO-1 levels to values below those reported for untreated (0.66 ± 0.06 vs 1.00 ± 0.00 , $p<0.01$) and Vitamin D3-treated monolayers (0.66 ± 0.06 vs 1.28 ± 0.05 , $p<0.001$) (**Figure 3.10**), suggesting that Akt could be also playing a role in the activation of the Vitamin D3 pathway in MCEC-1 monolayers. However, it is important to take into account that this reduction was similar to the one observed for MK-2206 alone (0.66 ± 0.06 vs 0.70 ± 0.03 , $p>0.05$), suggesting that MK-2206's effects could be obscuring any other subtle modulations.

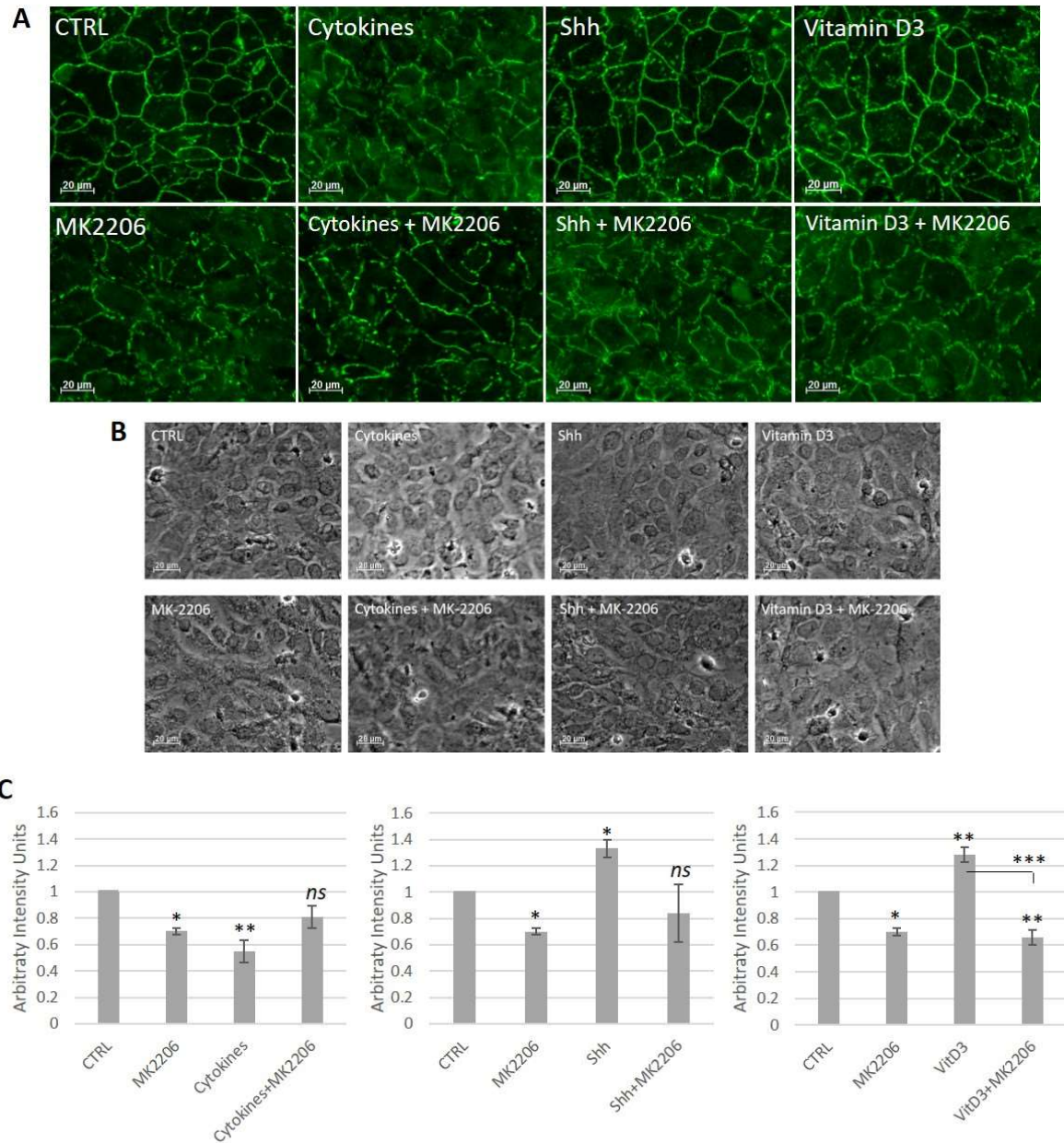


Figure 3.10 - Cytokine, Shh and Vitamin D3 driven modulation of junction stability is Akt dependent. (A) MCEC-1 monolayers incubated with a mixture of cytokines (TNF α and IL1 α) (100pg/ml), Shh (100ng/ml) and Vitamin D3 (100nM) alone or in combination with the Akt inhibitor MK-22016 (5 μ M) for 24h. Untreated monolayers are represented as controls (CTRL). Monolayers were stained against ZO-1 to visualise tight junction integrity. (B) Corresponding bright field images of MCEC-1 confluent monolayers. (C) Quantification of junctional ZO-1 signal intensity. Analysis performed with Andor IQ2 software. Statistically significant differences were assessed via One-way ANOVA with post-hoc Tukey. Each bar represents the mean \pm SEM for 3 independent experiments. * $p < 0.05$; ** $p < 0.01$; *** $p < 0.001$.

3.2.1.8. Cytokine/cyclopamine driven loss of junctional stability could be metalloproteinase-dependent

Metalloproteinases are implicated in endothelial barrier disruption. To test whether an increase in metalloproteinase activity could underlie cytokine/cyclopamine the observed effects on tight junction integrity, MCEC-1 monolayers were incubated with GM6001 (broad spectrum metalloproteinase inhibitor). However, due to high variability between the compared experiments, no significant changes were reported despite the clear differences in ZO-1 junctional levels (**Figure 3.11**): addition of a combination of cytokines and cyclopamine reduced ZO-1 junctional levels by 20-40% (normalised average values ranged from 0.81 ± 0.06 to 0.43 ± 0.03 between experiments) when compared with untreated monolayers (normalised to 1); whereas addition of GM6001 seemed to reverse cytokine/cyclopamine driven reduction in junctional ZO-1 levels (normalised averaged values ranged from 1.52 ± 0.08 to 0.72 ± 0.05 between experiments). Although not statistically significant, addition of GM6001 to cytokines and cyclopamine treated monolayers induced a reversal in cytokines/cyclopamine-driven loss of ZO-1 staining that ranged from approximately 20% (0.68 ± 0.06 vs 0.84 ± 0.05) to 70% (0.81 ± 0.06 vs 1.52 ± 0.08) between experiments. Addition of a GM6001 negative control to the cytokine/cyclopamine combination retrieved similar values to those observed for cytokine/cyclopamine in its absence (normalised average values ranged from 0.71 ± 0.05 to 0.44 ± 0.03 between experiments) (**Figure 3.11**). In any case, treatments triggered similar trends between experiments, following the same increases or decreases, regardless of the high variability observed in the range of these modulations.

Although no significant changes were reported following quantification of ZO-1 junctional levels due to the great variation between experiments, visualisation of ZO-1 junctional staining seemed to suggest that in the presence of cytokines and cyclopamine, GM6001-mediated metalloproteinase inhibition not only increased ZO-1 junctional levels but also reduced cytoplasmic ZO-1 immunolabelling and favouring continuous junctional localisation between adjacent cells (**Figure 3.11**).

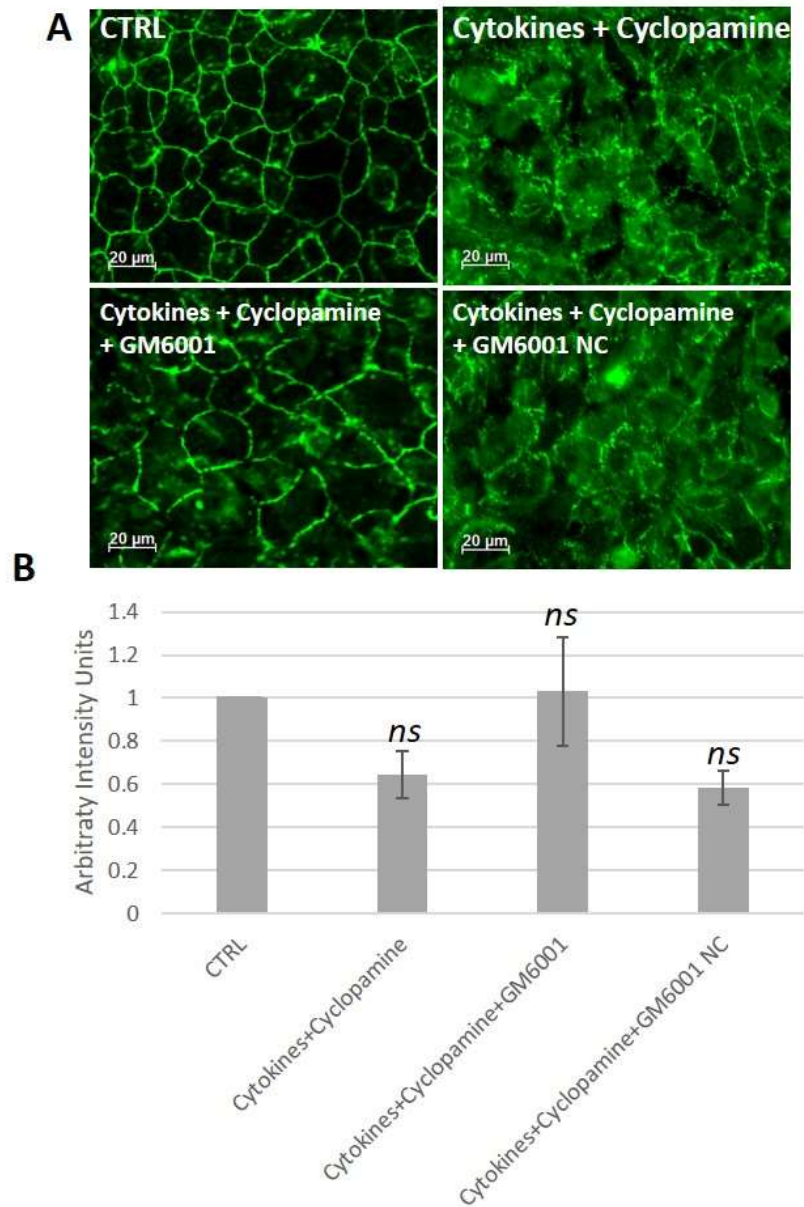


Figure 3.11 – Cytokines and cyclopamine driven loss of tight junction stability could be metalloproteinase dependent. (A) MCEC-1 monolayers incubated with a mixture of cytokines (TNF α and IL1 α) (100pg/ml) and the hedgehog pathway inhibitor cyclopamine (4 μ M) in the presence or absence of a broad-spectrum metalloproteinase inhibitor (GM6001) for 24h. GM6001 negative control (NC) and untreated monolayers (CTRL) were used as controls. Monolayers immunolabelled for ZO-1 to visualise tight junction integrity. (B) Quantification of junctional ZO-1 signal intensity. Analysis performed with Andor IQ2 software. Statistically significant differences were assessed via One-way ANOVA with post-hoc Tukey. Each bar represents the mean \pm SEM for 3 independent experiments. ns $p > 0.05$.

3.2.2. Gene expression changes which may underly cytokine- and cyclopamine-driven effects

3.2.2.1. Cytokines and cyclopamine synergistically increase metalloproteinase expression

As seen above, cytokines and cyclopamine mediated disruption of tight junction stability is at least partially metalloproteinase-dependent. In order to explore metalloproteinase expression under the test conditions of interest steady state mRNA levels of a range of metalloproteinases selected from the literature (including MMPs, ADAMs and ADAMTSs) and their inhibitors (TIMPs) were assessed in MCEC-1 treated monolayer cultures.

Cyclopamine treatment significantly increased the mRNA levels of MMP3, -10 and -13 when compared with untreated monolayers (3.62 ± 0.70 vs 1.05 ± 0.23 , $p < 0.05$; 11.26 ± 1.25 vs 1.01 ± 0.10 , $p < 0.01$; 6.33 ± 0.30 vs 1.05 ± 0.25 , $p < 0.001$) (**Figure 3.12**). Following cytokine treatment, MMP3 expression levels were upregulated when compared with untreated controls (2.50 ± 0.30 vs 1.05 ± 0.23 , $p < 0.05$) (**Figure 3.12**). Interestingly, the cytokine/cyclopamine combination triggered a further increase in MMP3, -10 and -13 expression levels when compared with untreated monolayers (9.34 ± 1.23 vs 1.05 ± 0.23 , $p < 0.01$; 382.97 ± 69.09 vs 1.01 ± 0.10 , $p < 0.01$; 86.82 ± 16.33 vs 1.05 ± 0.25 , $p < 0.001$) which appeared to be a synergistic effect for MMPs -10 and 13 (**Figure 3.12**) (raw Ct values can be found in **Appendix 3.H**). No changes in metalloproteinase gene expression were observed after treatment with Shh and/or Vitamin D3 (data not shown).

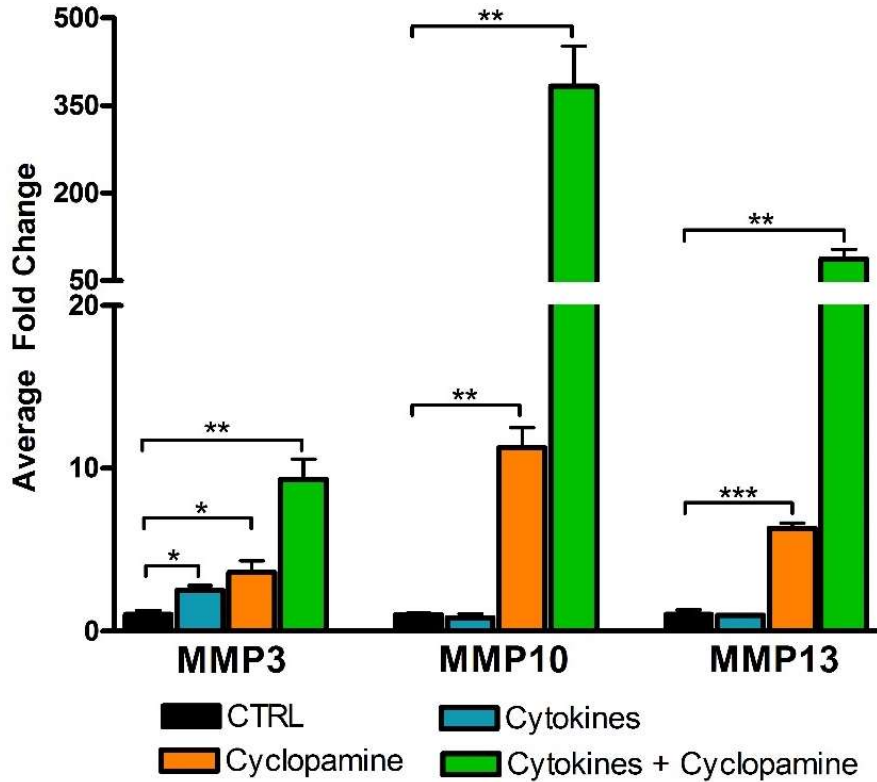


Figure 3.12 - Hedgehog pathway abrogation in the presence of cytokines can further reduce tight junction stability. MCEC-1 cells confluent monolayers incubated with a mixture of cytokines (TNF α and IL1 α) (100pg/ml), cyclopamine (4 μ M) alone or in combination. Untreated monolayers (CTRL) were used as control. After 24h treatment, MMP3, 10 and 13 steady-state mRNA levels were determined by qRT-PCR with normalisation to 18s expression. Fold-change is depicted relative to untreated control. Statistically significant differences were assessed via t-test. Each bar represents the mean \pm SEM for 3 wells. * $p < 0.05$; ** $p < 0.01$; *** $p < 0.001$. Representative experiment depicted. Experiment replicated 3 times.

Addition of cytokines triggered contrasting effects on TIMP levels with a significant increase in TIMP1 (2.26 ± 0.03 vs 1.14 ± 0.04 , $p < 0.01$) and a significant decrease in TIMP3 (0.66 ± 0.04 vs 1.15 ± 0.04 , $p < 0.05$) mRNA levels when compared with untreated monolayers (**Figure 3.13**). Treatment with cyclopamine alone had no significant effect. However, when treated with a combination of cytokines and cyclopamine TIMP3 expression levels were further reduced, reaching significantly lower values than those seen for cytokine-treated (0.34 ± 0.05 vs 0.66 ± 0.04 , $p < 0.05$) and untreated monolayers (0.34 ± 0.05 vs 1.15 ± 0.04 , $p < 0.05$) (**Figure 3.13**) (raw Ct values can be found in **Appendix 3.H**). Thus, cyclopamine treatment in the presence of inflammatory conditions can synergistically downregulate TIMP3 expression levels. No changes in gene expression levels were observed for TIMP2 or -4 (data not shown). Treatment with Shh and/or Vitamin D3 triggered no significant changes (data not shown).

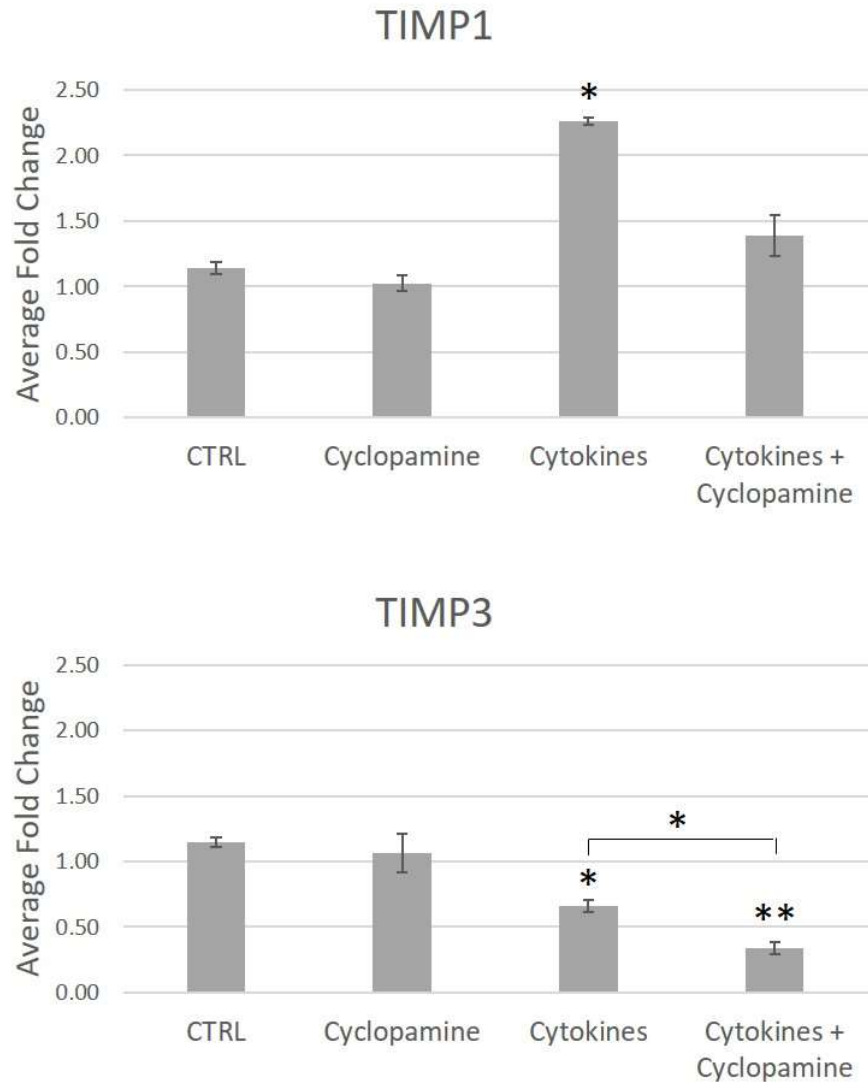


Figure 3.13 – Cytokine and cyclopamine effects in TIMPs gene expression. MCEC-1 cells confluent monolayers incubated with a mixture of cytokines (TNF α and IL1 α) (100pg/ml), cyclopamine (Hedgehog pathway abrogation) (4 μ M), or a combination of both during 24h. Untreated monolayers (CTRL) were used as control. After treatment, TIMP1 and -3 mRNA steady-state levels were determined by qRT-PCR with normalisation to 18s expression. Fold-change is depicted relative to untreated control. Statistically significant differences were assessed via One-way ANOVA with post-hoc Tukey. Each bar represents the mean \pm SEM for 3 wells. * $p < 0.05$; ** $p < 0.01$. Representative experiment depicted. Experiment replicated 3 times.

3.2.2.2. Cytokine-driven decrease in ZO-1 gene expression can be synergistically enhanced by cyclopamine

In order to explore if variations in gene expression were observed alongside changes in junctional stability, ZO-1, claudin-5, occludin or VE-cadherin mRNA steady-state levels were measured in MCEC-1 confluent monolayers. Cells were treated with a mixture of cytokines (TNF α and IL1 α at 100pg/ml), the Hedgehog pathway inhibitor cyclopamine (4 μ M), Shh (100ng/ml) and Vitamin D3 (100nM) (individually or in combination) before measuring steady state mRNA levels by qRT-PCR. All measurements were normalised to 18S endogenous control. Treatment with either Shh or Vitamin D3 did not trigger any significant changes in ZO-1 mRNA levels (**Appendix 3.I**). Addition of cytokines significantly diminished ZO-1 mRNA levels when compared with untreated controls (0.71 ± 0.03 vs 1.05 ± 0.03 , $p < 0.01$) (**Figure 3.14**), suggesting that this decrease in gene expression could be at least partially responsible for the observed reduction in ZO-1 junctional levels. Although addition of cyclopamine alone had no effect on ZO-1 expression levels, ZO-1 expression levels were further reduced by a combination of cytokines and cyclopamine, reaching significantly lower values than those reported for cytokine-treated (0.43 ± 0.05 vs 0.71 ± 0.03 , $p < 0.05$) and untreated monolayers (0.43 ± 0.05 vs 1.05 ± 0.03 , $p < 0.001$) (**Figure 3.14**) (raw Ct values can be found in **Appendix 3.H**). This seems to indicate that cytokine/cyclopamine driven decrease in junctional ZO-1 levels could also be mediated by a reduction in ZO-1 gene expression levels, explaining why GM6001-dependent metalloproteinase inhibition failed to restore junctional ZO-1 levels back to control values. No changes in gene expression levels were reported for either claudin-5, occluding or VE-cadherin (data not shown).

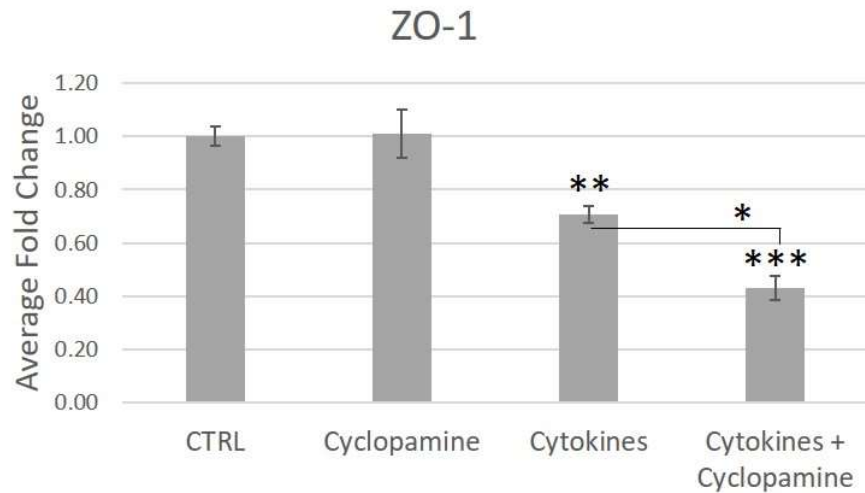


Figure 3.14 - Cytokines-driven decrease in ZO-1 gene expression can be synergistically enhanced by cyclopamine. MCEC-1 cells confluent monolayers incubated with a mixture of cytokines (TNF α and IL1 α) (100pg/ml), cyclopamine (Hedgehog pathway abrogation) (4 μ M), or a combination of both during 24h. Untreated monolayers (CTRL) were used as control. After treatment, ZO-1 mRNA steady-state levels were determined by qRT-PCR with normalisation to 18s expression. Fold-change is depicted relative to untreated control. Statistically significant differences were assessed via One-way ANOVA with post-hoc Tukey. Each bar represents the mean \pm SEM for 3 wells. ** $p < 0.01$; *** $p < 0.001$. Representative experiment depicted. Experiment replicated 3 times.

3.2.2.3. Regulation of steady state mRNA levels of Hedgehog pathway components

To study the implication of Hedgehog pathway in the regulation of tight junction stability in MCEC-1 confluent monolayers, mRNA steady-state levels of the following Hedgehog signalling pathway components were measured by qRT-PCR: Ptch, Smo, Gli1, -2 and -3. Cells were treated with a mixture of cytokines (TNF α and IL1 α at 100pg/ml), the Hedgehog pathway inhibitor cyclopamine (4 μ M), Shh (100ng/ml) and Vitamin D3 (100nM) (individually or in combination). All measurements were normalised to 18S endogenous control. Gli1 was undetected in MCEC-1 monolayers (data not shown) while Ptch and Gli3 were expressed but unmodulated by any added treatment (**Appendix 3.J**).

Addition of a cytokines mix, Shh and/or Vitamin D3 (with/without cytokines) had no effect in Gli2 or Smo gene expression levels (**Appendix 3.K**). However, cyclopamine treatment significantly reduced Gli2 (0.25 \pm 0.04 vs 1.04 \pm 0.21, p<0.05) and Smo (0.54 \pm 0.14 vs 1.02 \pm 0.15, p<0.05) mRNA levels when compared with untreated cells (**Figure 3.15**). Although addition of cytokines did not enhance cyclopamine-driven decrease of Smo gene expression, it did significantly reduce Gli2 mRNA levels under those reported for cyclopamine-treated (0.11 \pm 0.03 vs 0.25 \pm 0.04, p<0.05) and untreated monolayers (0.11 \pm 0.03 vs 1.04 \pm 0.21, p<0.05) (**Figure 3.15**) (raw Ct values can be found in **Appendix 3.H**). Thus, cyclopamine and cytokines could be synergistically reducing Hedgehog signalling through a decrease in Gli2 gene expression.

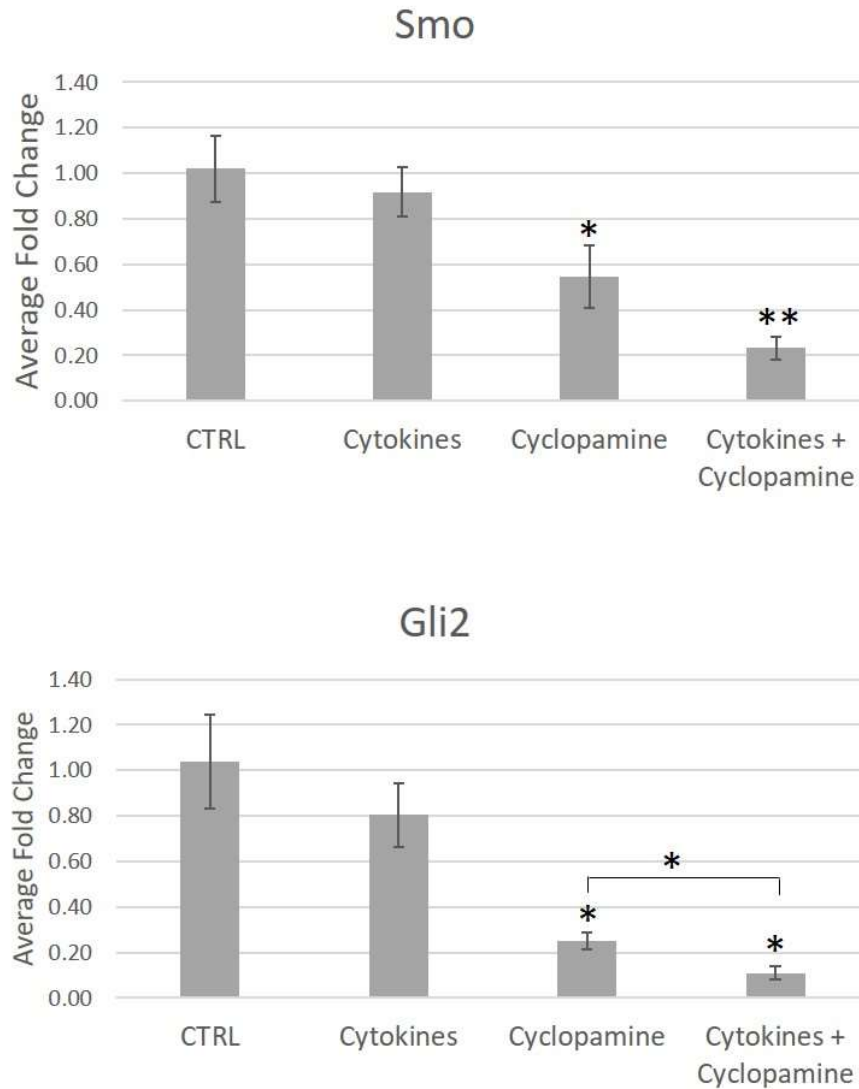


Figure 3.15 – Cyclopamine reduces gene expression levels of Hedgehog pathway components. MCEC-1 cells confluent monolayers incubated with a mixture of cytokines (TNF α and IL1 α) (100pg/ml), cyclopamine(4 μ M), or a combination of both during 24h. Untreated monolayers (CTRL) were used as control. After treatment, Smo and Gli2 mRNA steady-state levels were determined by qRT-PCR with normalisation to 18s expression. Fold-change is depicted relative to untreated control. Statistically significant differences were assessed via One-way ANOVA with post-hoc Tukey. Each bar represents the mean \pm SEM for 3 wells. * $p < 0.05$; ** $p < 0.01$. Representative experiment depicted. Experiment replicated 3 times.

3.2.2.4. Barrier formation in the MCEC-1 *in vitro* model

MCEC-1 ability to form a functional barrier in our *in vitro* model was tested by TEER. A significant increase in TEER was detected at 24h and 48h after seeding, suggesting that the cultured MCEC-1 monolayer is forming a functional barrier. A cell-free coated-insert was used as a negative control (**Figure 3.16**).

Interestingly, monolayers cultured for 24h and 48h reached similar TEER levels, suggesting the formation of a stable and sustained barrier (**Figure 3.16**). This supports the idea that the previously discussed increase in dextran extravasation (**Figure 3.16**) between 4h and 24h measurements could be due to a diffusion effect between the insert compartments rather than a less functional barrier, as if this was the case it would have an impact on TEER levels.

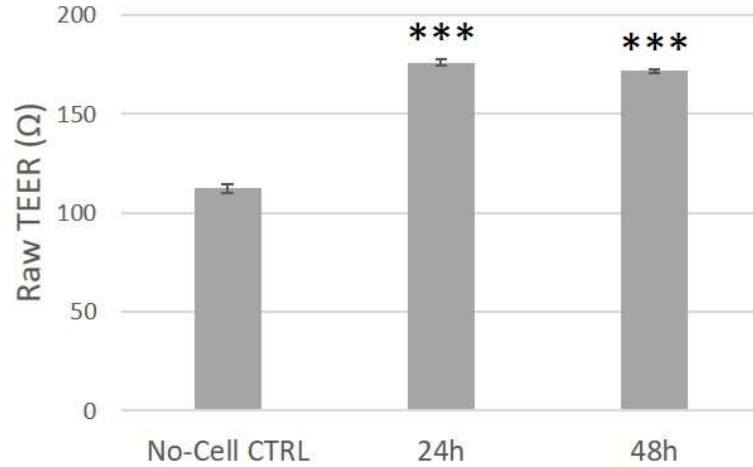


Figure 3.16 – Barrier formation was achieved in MCEC-1 confluent monolayers. Transendothelial Electrical Resistance (TEER) measurements of MCEC-1 monolayers cultured for 24h and 48h. Statistically significant differences were assessed via t-test. Each bar represents the mean \pm SEM for 3 wells. * $p < 0.05$; *** $p < 0.001$. Representative experiment depicted. Experiment replicated >3 times.

3.2.2.5. Barrier integrity is compromised after cytokine treatment in our in vitro model

In order to assess TEER sensitivity to cytokine-driven barrier disturbances, cells were incubated with a mix of cytokines (TNF α and IL1 α at 100pg/ml and 10ng/ml) for a total of 24h. A significant cytokines-dependent reduction in TEER values was detected at 24h after stimulation (26.03 ± 0.97 vs 35.02 ± 0.73 Ω/cm^2 , $p<0.01$) (**Figure 3.17**). Thus, it seems that cytokines can mediate barrier disruption, supporting the previously observed effect in ZO-1 junctional stability.

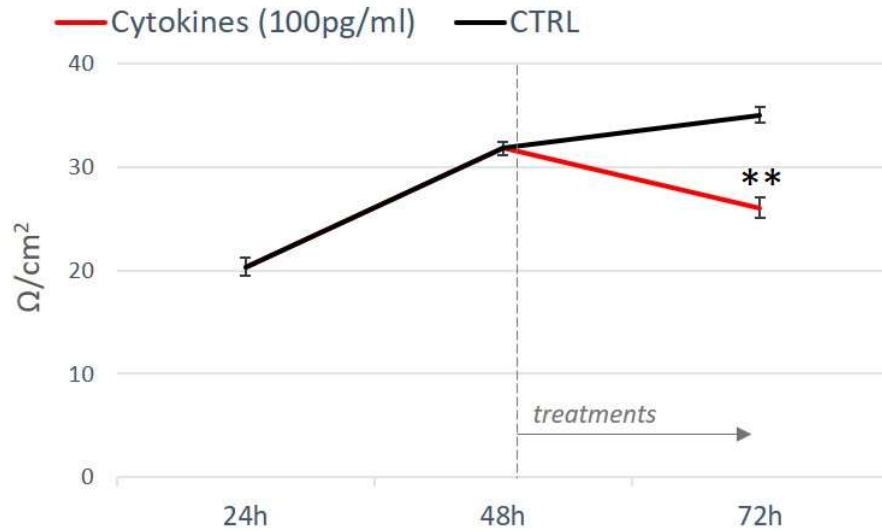


Figure 3.17 - Cytokine treatment induces MCEC-1 barrier permeability. MCEC-1 were seeded onto cell inserts (0.3 μ m porous) and grown for 48h until confluent in order to promote barrier formation. MCEC-1 monolayers were then treated with a cytokines mix (TNF α and IL1 α at 100pg/ml). Untreated monolayers (CTRL) were used as control. Transendothelial Electrical Resistance (TEER) was measured to assess barrier integrity at 24h after seeding and at 24h after treatments addition. Statistically significant differences were assessed via t-test. Each point represents the mean \pm SEM for 3 wells. * $p < 0.05$; ** $p < 0.01$. Representative experiment depicted. Experiment replicated >3 times.

3.2.2.6. Cyclopamine synergises with cytokines to further compromise barrier integrity

In order to determine whether the effects seen on ZO-1 junctional integrity have a functional outcome in barrier stability, the cells were treated with cyclopamine in the presence and absence of cytokines. Abrogation was achieved through cyclopamine (4 μ M) exposure, a pharmacological inhibitor of the Hedgehog pathway. TEER measurements were taken at after 24h treatment in order to assess barrier responses. As previously reported, cytokines addition significantly lowered TEER values when compared with untreated monolayers (26.03 \pm 0.97 vs 35.02 \pm 0.73 Ω /cm², p<0.01) (**Figure 3.18**). Cyclopamine treatment had no measurable effect on TEER levels when compared with controls (36.12 \pm 0.49 vs 35.02 \pm 0.73 Ω /cm²) (**Figure 3.18**). However, addition of cyclopamine in the presence of cytokines synergistically enhanced the cytokine effect, triggering a significant reduction in TEER values when compared with cytokines-treated (16.32 \pm 1.02 vs 26.03 \pm 0.97 Ω /cm², p<0.01) and untreated monolayers (16.32 \pm 1.02 vs 35.02 \pm 0.73 Ω /cm², p<0.001) (**Figure 3.18**).

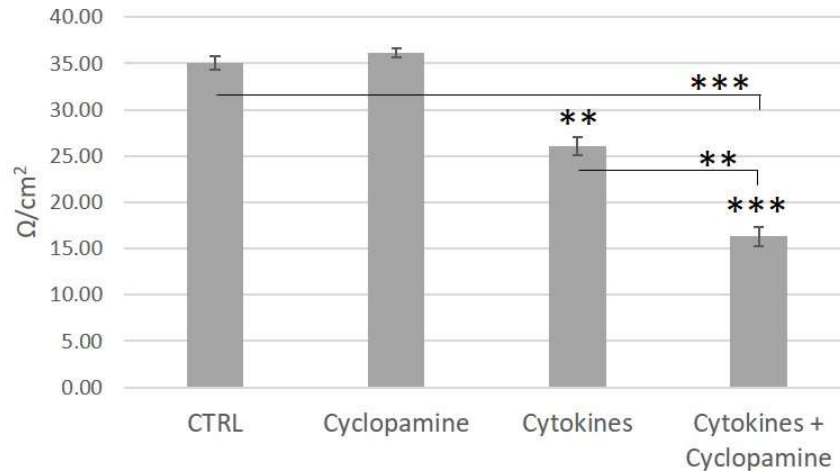


Figure 3.18 – Cytokine-driven reduction in MCEC-1 barrier permeability can be further enhanced by addition of cyclopamine. MCEC-1 were seeded onto cell inserts (0.3μm porous) and grown for 48h until confluent in order to promote barrier formation. MCEC-1 monolayers were then treated with a cytokines mix (TNFα and IL1α at 100pg/ml), the Hedgehog pathway inhibitor cyclopamine (4μM) or a combination of both for 24h. Untreated monolayers (CTRL) were used as control. Transendothelial Electrical Resistance (TEER) was measured to assess barrier integrity. Statistically significant differences were assessed via One-way ANOVA with post-hoc Tukey. Each bar represents the mean ±SEM for 3 wells. ** p < 0.1; *** p < 0.001. Representative experiment depicted. Experiment replicated >3 times.

3.2.2.7. Cytokine/cyclopamine mediated loss of barrier integrity is metalloproteinase-dependent

To test if cytokines and cyclopamine effect in barrier stability was metalloproteinase-dependent, confluent MCEC-1 monolayers were incubated with GM6001 (broad spectrum metalloproteinase inhibitor) in the presence and absence of the cytokines and cyclopamine combination. TEER measurements of confluent MCEC-1 monolayers were taken 24h after treatment addition in order to assess barrier stability. As before, the presence of a combination of cytokines and cyclopamine significantly reduced TEER values when compared with untreated monolayers (26.77 ± 1.28 vs 78.28 ± 0.66 Ω/cm^2 , $p < 0.001$) (**Figure 3.19**). Addition of GM6001 fully reversed cytokines and cyclopamine driven impairment of barrier stability (26.77 ± 1.28 vs 71.13 ± 1.20 Ω/cm^2 , $p < 0.001$) (**Figure 3.19**). Addition of GM6001 negative control (NC) had no detectable effect in cytokines and cyclopamine driven barrier disruption (26.03 ± 1.63 vs 26.77 ± 1.28 Ω/cm^2) (**Figure 3.19**). These results agree with the previously described protective effect of GM6001 against cytokines and cyclopamine mediated loss of ZO-1 junctional stability.

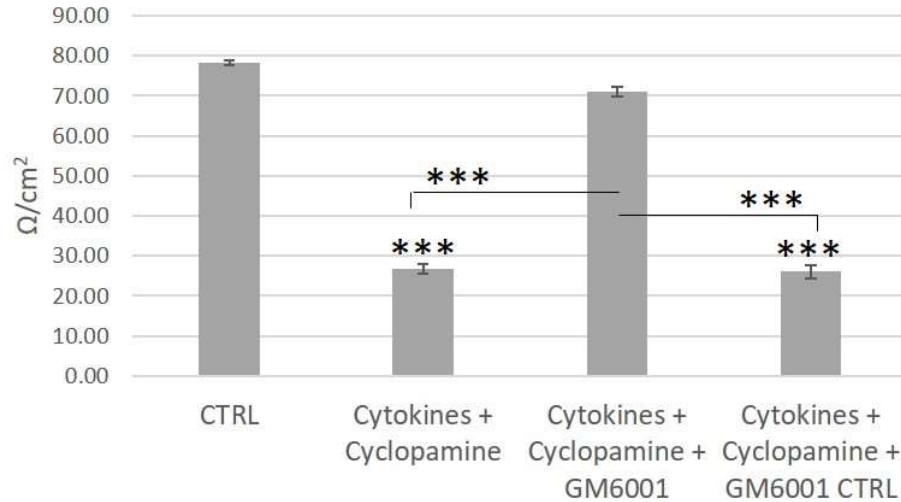


Figure 3.19 – Cytokines and cyclopamine driven loss in barrier stability is metalloproteinase-dependent. MCEC-1 were seeded onto cell inserts (0.3µm porous) and grown for 48h until confluent in order to promote barrier formation. Monolayers were incubated with a mixture of cytokines (TNFα and IL1α) (100pg/ml) and cyclopamine (4µM) in the presence or absence of a broad-spectrum metalloproteinase inhibitor (GM6001) for 24h. GM6001 negative control (NC) and untreated monolayers (CTRL). Transendothelial Electrical Resistance was measured 24h after treatment to assess barrier integrity. Statistically significant differences were assessed via One-way ANOVA with post-hoc Tukey. Each bar represents the mean ±SEM for 3 wells. * $p < 0.5$; *** $p < 0.001$. Representative experiment depicted. Experiment replicated 3 times.

3.2.2.8. Addition of hTIMP3 partially reverses cytokine/cyclopamine driven barrier disruption

Cytokine/cyclopamine mediated effects on barrier stability seem to be accompanied not only by an upregulation in MMP3, -10 and -13 gene expressions but also by a downregulation in TIMP3 mRNA levels. Thus, it is possible that metalloproteinase-dependent impairment in barrier structure could be mediated by an increase in metalloproteinase activity through a downregulation of their inhibitor TIMP3. To test the hypothesis, that TIMP3 may play an important role in barrier integrity, confluent MCEC-1 monolayers were pre-treated with human recombinant TIMP3 (hTIMP3) (0.5 μ M) before the addition of a combination of cytokines (TNF α and IL1 α at 100pg/ml) and cyclopamine (4 μ M) with TEER measurements 24h later. Although only performed once, preliminary results show the previously seen reduction in TEER values in the presence of a combination of cytokines and cyclopamine when compared with untreated monolayers (26.77 \pm 1.28 vs 78.28 \pm 0.66 Ω /cm², p<0.001) (**Figure 3.20**). Pre-treatment with hTIMP3 partially reversed the cytokine/cyclopamine driven reduction in TEER values (52.8 \pm 1.38 vs 26.77 \pm 1.28 Ω /cm², p<0.001) although control levels were not fully restored (52.8 \pm 1.38 vs 78.28 \pm 0.66 Ω /cm², p<0.001) (**Figure 3.20**). No effect in barrier stability was reported for monolayers pre-treated with hTIMP3 in the absence of any other stimuli (77.55 \pm 1.38 vs 78.28 \pm 0.66 Ω /cm²) (**Figure 3.20**). Thus, it seems TIMP3 plays an important role in cytokine/cyclopamine driven barrier disruption.

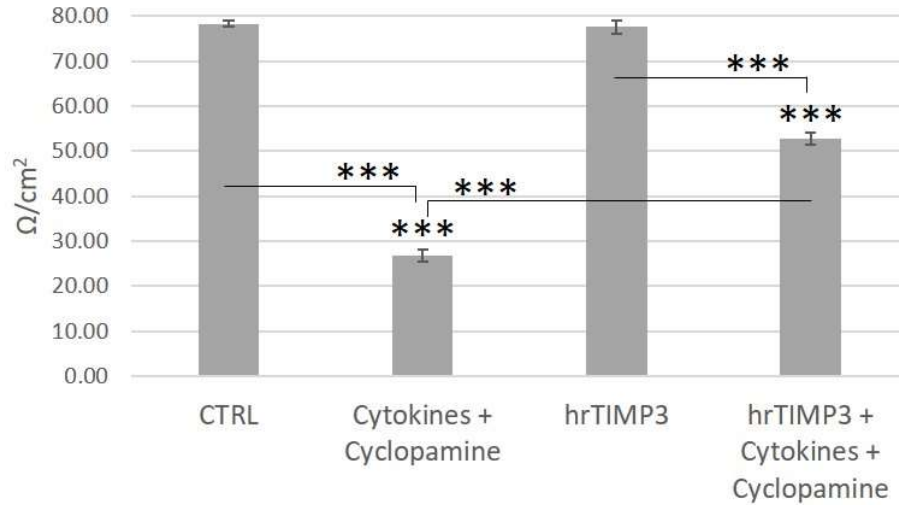


Figure 3.20 – hTIMP3 can partially block cytokine/cyclopamine driven barrier disruption. MCEC-1 were seeded onto cell inserts (0.3μm porous) and grown for 48h until confluent in order to promote barrier formation. Upon confluency human recombinant TIMP3 (hTIMP3) (0.5μM) was added for 30min prior to a combination of cytokines (TNFα and IL1α) (100pg/ml) and cyclopamine (4μM). Untreated monolayers (CTRL) were used as control. Transendothelial Electrical Resistance (TEER) was measured 24h after treatment to assess barrier integrity. Statistically significant differences were assessed via One-way ANOVA with post-hoc Tukey. Each bar represents the mean ±SEM for 3 wells. * p < 0.5; *** p < 0.001. Representative experiment depicted. Preliminary data from experiment replicated 1 time.

3.2.2.9. *Shh and Vitamin D3 synergistically protect against cytokines and cyclopamine driven barrier dysfunction*

To further test our barrier *in vitro* model, the responsiveness to previously described barrier promoting agents was tested through exposure to Shh (100ng/ml) and Vitamin D3 (100nM). After 24h treatment, both Shh (115.32±1.43 vs 98.63±0.66 Ω/cm^2 , $p<0.001$) and Vitamin D3 (114.95±0.84 vs 98.63±0.66 Ω/cm^2 , $p<0.001$) were capable of promote barrier integrity by significantly increasing TEER when compared to untreated cells (**Figure 3.21**). No further enhancement was obtained by a Shh and Vitamin D3 combination (115.68±0.80 vs 98.63±0.66 Ω/cm^2 , $p<0.001$) (**Figure 3.21**). Thus, it seems that both Shh and Vitamin D3 can enhance barrier stability in this *in vitro* model. This confirms not only their previously described role in the literature as barrier promoting agents but also agrees with the previously reported individual ability of Shh and Vitamin D3 to enhance tight junction formation. To further challenge Shh and Vitamin D3 protective effect, in a single experiment the individual effects of Shh and VitD3 to protect against cytokines and cyclopamine synergistic barrier disruption were explored. Although only repeated once, after 24h treatment exposure neither Shh nor Vitamin D3 were capable of rescue cytokines and cyclopamine disruptive effect on barrier stability (48.95±1.14 or 50.42±1.20 vs 98.63±0.66 Ω/cm^2 , $p<0.001$) (**Figure 3.22**). However, when combined, Shh and Vitamin D3 were not only completely reversed the cytokine/cyclopamine synergistic impairment of barrier integrity but also significantly increased TEER measurements above untreated levels (113.48±1.75 vs 98.63±0.66 Ω/cm^2 , $p<0.01$) (**Figure 3.22**). Hence, in this preliminary experiment and agreeing with the effects on seen ZO-1 junctional stability, it seems that Shh and Vitamin D3 can synergise to protect against cytokines and cyclopamine driven barrier disruption. It should be mentioned that it seems that TEER measurements reach a maximum level, in which barrier structure cannot be further enhanced.

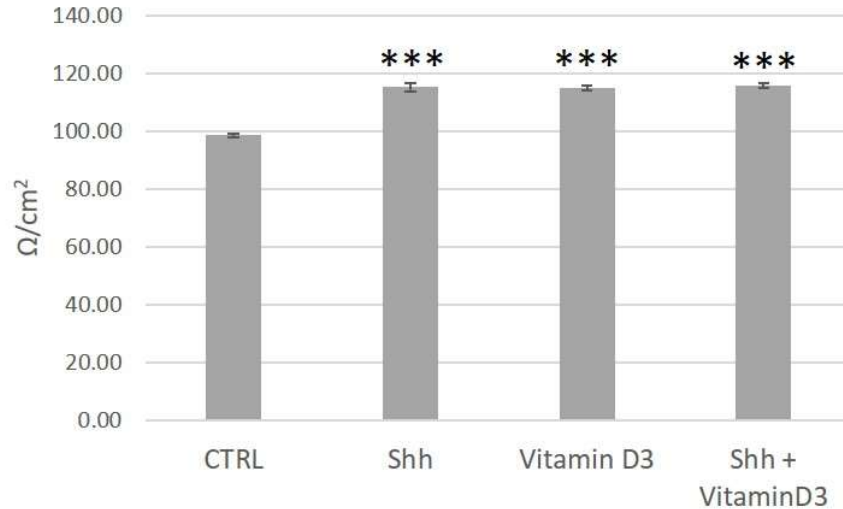


Figure 3.21 – Shh and Vitamin D3 promote MCEC-1 barrier formation. MCEC-1 were seeded onto cell inserts (0.3µm porous) and grown for 48h until confluent in order to promote barrier formation. Upon confluency human recombinant Sonic Hedgehog (hShh)(100ng/ml) and Vitamin D3 (100nM) were added alone or in combination. Untreated monolayers (CTRL) were used as control. Transendothelial Electrical Resistance (TEER) was measured 24h after treatment to assess barrier integrity. Statistically significant differences were assessed via One-way ANOVA with post-hoc Tukey. Each bar represents the mean ±SEM for 3 wells. * $p < 0.5$; *** $p < 0.001$. Representative experiment depicted. Experiment replicated >3 times.

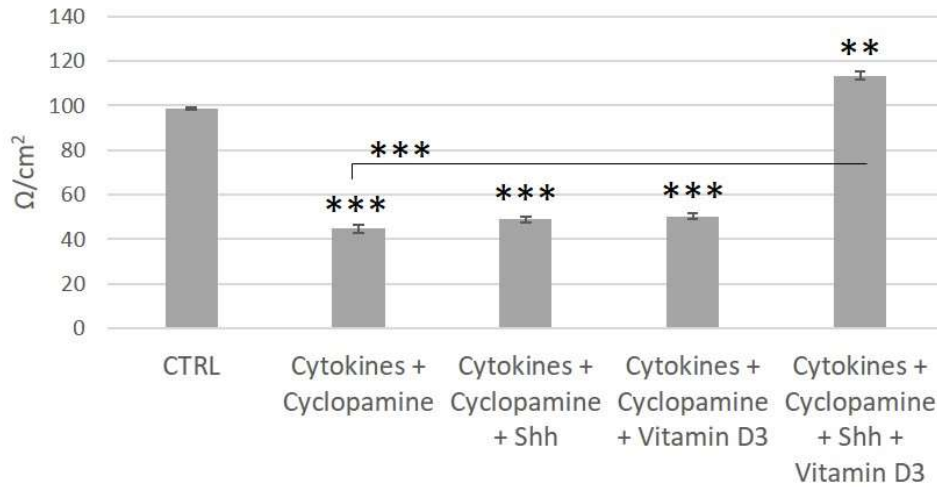


Figure 3.22 – Shh and Vitamin D3 can synergistically rescue cytokines and cyclopamine driven barrier disruption. MCEC-1 were seeded onto cell inserts (0.3µm porous) and grown for 48h until confluent in order to promote barrier formation. Upon confluency combinations of the following treatments were added: human recombinant Sonic Hedgehog (hShh)(100ng/ml), Vitamin D3 (100nM), the Hh pathway pharmacological inhibitor cyclopamine (4µM) and a cytokines mix (TNFα and IL1α at 10ng/ml). Untreated monolayers (CTRL) were used as control. Transendothelial Electrical Resistance (TEER) was measured after 24h treatments to assess barrier integrity. Statistically significant differences were assessed via One-way ANOVA with post-hoc Tukey. Each bar represents the mean ±SEM for 3 wells. * p < 0.5; *** p < 0.001. Representative experiment depicted. Experiment replicated 3 times.

3.3. DISCUSSION

3.3.1. Mimicking an inflammatory environment reduces barrier stability

Previous studies using brain microvascular endothelial cells have shown an ability of cytokines to impair cellular barrier stability in similar *in vitro* settings (Mark & Miller, 1999; Trickler et al., 2005; Forster et al., 2008; Sajja et al., 2014; Ni et al., 2017). Addition of cytokines to endothelial monolayers triggers reduced levels of tight junction proteins (such as ZO-1, claudin-5 and occludin) (Forster et al., 2008; Aslam et al., 2012; Cohen et al., 2013; Labus et al., 2014). Both ZO-1 junction localisation and steady state mRNA levels were down-regulated by cytokine treatment of MCEC-1 cells suggesting that effects of cytokines on barrier disruption, through junctional impairment, could be conserved in our model.

These data suggested that barrier integrity may have been modulated and this was apparent when TEER was assessed. Correlating with the observed reduction in ZO-1 junctional levels, TEER measurements revealed a significant loss in barrier properties in the presence of cytokines (**Figure 3.17**). As previously mentioned, other tight or adherens junction components are susceptible to cytokine-mediated regulation and could be playing a role in the observed loss of barrier integrity. However, no changes in gene expression were observed for claudin-5, occludin or VE-cadherin at 24h after treatment, but mRNA variations at earlier time-points and changes in their protein levels and subcellular localisation should also be studied to be completely certain of their role in the observed cytokine-mediated barrier disruption.

A major consequence of inflammation is the up-regulation of metalloproteinases (reviewed in Rempe et al., 2016), which can degrade junctional and basement membrane elements such as claudins, occludins, ZO-1 proteins and laminins (Yang et al., 2007; Lu et al., 2009; Bauer et al., 2010; Wu et al., 2015) among others. From all the measured metalloproteinases, only MMP3 was significantly increased 24h after cytokines addition (**Figure 3.11**). In a murine model of Parkinson's disease (a

pathology associated with neuroinflammation) BBB disruption was ameliorated after MMP3 genetic ablation, suggesting that MMP3 could play an important role in BBB breakdown under inflammatory conditions (Chung et al., 2013). Many MMPs have been described to be up-regulated under inflammatory conditions but different time-points and cytokine concentrations may need to be studied in our endothelial barrier model to observe a wider range of cytokines-mediated responses in MMPs gene expression. Regarding TIMP expression, cytokine treatment triggered a significant increase in TIMP1 and a significant decrease in TIMP3 when compared with untreated controls (**Figure 3.13**). TIMP3 expression has previously been shown in our lab to be down-regulated by cytokines in MCEC-1 cells (Singh et al. 2005). TIMP3^{-/-} mice showed an increased pulmonary microvascular leakage when compare with controls, and isolated pulmonary microvascular ECs from TIMP3 null mice exhibited a lower TEER and increased permeability to fluorescently labelled dextran and albumin (Arpino et al., 2016). In this regard, it is important to consider that TIMP3 not only inhibits MMPs, but also several members of the ADAM family. Thus, the reported cytokine-mediated loss of endothelial barrier integrity could be exerted not only through a direct regulation of metalloproteinases production/distribution but also through disinhibition of their proteinase activities mediated by a reduction in TIMP3 protein levels, although this was not explored here. TIMP1, low serum levels of TIMP1 have been previously correlated with endothelial barrier disruption in various clinical studies (Lee et al., 1999; Waubant et al., 1999; Toft-Hansen et al., 2004). However, more recent studies showed an increase in TIMP-1 serum from HIV-patients under inflammation (Xing et al., 2017) and previous data from our laboratory indicates cytokine-mediated elevation of TIMP1 in expression MCEC-1 cells (Singh et al., 2005). Additionally, studies in TIMP1-deficient mice showed an increased in activated immune cells transmigration across the BBB during viral encephalomyelitis (Savarin et al., 2013). This study reported no compensatory expression of other TIMPs, altered MMP expression or impaired chemokine production when compared with WT mice, and a possible MMP-independent role of TIMP1 has been postulated (Savarin et al., 2013). In any case, the observed loss in ZO-1 junctional levels and barrier properties after cytokines stimulation could be mediated by a broad

dysregulation of metalloproteinases activities. It should be also be noted that low serum levels of TIMP1 have been previously correlated with endothelial barrier disruption in various clinical studies (Lee 1999; Waubant 1999; Toft-Hansen 2004).

3.3.2. Shh and Vitamin D3 promote barrier structure

To test responses to barrier promoting agents, confluent MCEC-1 monolayers were treated with Shh or Vitamin D3. Incubation with either Shh (Alvarez et al., 2011; Xia et al., 2013) or Vitamin D3 (Palmer et al., 2001; Zhang et al., 2013) triggered an increase in ZO-1 junctional levels (**Figure 3.5**) as previously described in the literature. Correlating with these observations, Shh exposure triggered an increase in electrical resistance (**Figure 3.21**), indicative of an enhanced barrier structure as previously described in the literature (Alvarez et al., 2011; Wang et al., 2014). Incubation with Vitamin D3 significantly enhanced barrier structure (**Figure 3.21**). Although Vitamin D3 ability to promote TJ formation in ECs has been previously reported (Palmer et al., 2001; Fujita et al., 2008; Yin et al., 2011), its impact on barrier functionality has only been studied on epithelial cells. Supporting our observations, in intestinal epithelial cells Vitamin D3 treatment triggers an increase in TEER (Chirayath et al., 1998; Chen et al., 2015), whereas in airway epithelial cells no TEER effects were reported (Zhang et al., 2016). Overall, Vitamin D3 seems a very well-established promoter of barrier integrity, and some of the mentioned discrepancies may be due to cell line associated variations. Shh and Vitamin D3 combined effects on modulation of barrier permeability have not been as yet reported in the literature, but deserved to be assessed. A combination of Shh and Vitamin D3 increased TEER but this did not exceed effects seen with the individual stimuli (**Figure 3.21**). It is possible that, in order to trigger a greater increase in barrier structure, a higher dosage is required. However, the fact that individual and combined Shh and Vitamin D3 treatments trigger such similar increases could be indicative of a limit in TEER, above which no further enhancement can be reached regarding barrier structure. Additionally, this could be also suggestive of shared

mechanisms/pathways between Shh and Vitamin D3, but further studies are needed to clarify this point.

Both Shh and Vitamin D3 have been reported to modulate metalloproteinase expression in endothelial cells: Shh can promote angiogenesis through the up-regulation of MMP2 protein levels and MMP9 gene expression (Renault et al., 2010; Yi et al., 2016). Conversely, Vitamin D3 blocked LPS-mediated increase in MMP14 expression in human umbilical vein endothelial cells (Stach et al., 2011). Clinical studies showed that Vitamin D deficiency can be associated with increased serum levels of MMP2 and MMP9, which were reversed by Vitamin D3 dietary supplementation (Timms et al., 2002). Intriguingly, in the current study, no alteration in metalloproteinase gene expression levels was observed after 24h of Shh or Vitamin D3 treatment. Thus, gene expression at earlier time-points should be studied to fully clarify Shh and Vitamin D3 effects on metalloproteinase gene expression in our *in vitro* model of an endothelial barrier.

No changes were reported after incubation with either Shh or Vitamin D3 in the gene expression of junctional proteins (data not shown). However, previous data from the literature show that addition of Shh can induce mRNA levels of ZO-1 and occludin in a rat model of cerebral artery occlusion and brain microvessel endothelial cells (Xia et al., 2013). These differences in response could be due to higher concentration of Shh used by Xia et al. (1µg/ml or 3µg/ml) or due to tissue origin of endothelial cells since the studies of Xia et al. (2013) were performed in brain slices or primary brain microvascular endothelial cells (Xia et al., 2013). Regarding Vitamin D3, studies performed in human airway epithelial cells showed no effect on ZO-1 gene expression levels (Zhou et al., 2011). Overall, it does not seem likely that the observed effects of Shh and Vitamin D3 in junctional and barrier stability could be mediated by the modulation of junctional protein gene expression although further studies at earlier time-points should be performed for confirmation.

3.3.3. Hedgehog pathway abrogation (cyclopamine) furthers inflammation-driven barrier disruption.

Evidence from several models suggests that astrocytes and pericytes secrete Shh amongst other trophic factors to promote formation and maintain of the BBB (Luissint et al., 2012). Thus, in order to test Hedgehog pathway effects in barrier stability a Hedgehog pathway pharmacological inhibitor (cyclopamine) was added. No significant changes were reported after addition of cyclopamine alone either on ZO-1 junctional levels or TEER measurements (**Figure 3.6** and **3.18**). Studies performed in vitro models of the BBB (including a co-culture of astrocytes and endothelial cells) have shown a reduction in ZO-1 protein levels and TEER values in the presence of cyclopamine (Alvarez et al., 2011; Zhen et al., 2018). However, it has to be considered that in these studies endothelial cells were co-cultured with astrocytes, a physiological source of Shh (Alvarez et al., 2011; Zhen et al., 2018). Taking this into account, the absence of cyclopamine effect in our model could be due to a lack of endogenous Shh signalling and the presence of a constitutively inactive Hedgehog pathway. To test this hypothesis expression levels of all the members of the Hedgehog family (Shh, Ihh and Dhh) were assessed but mRNA expression was not detectable for any of these ligands. Interestingly, cyclopamine treatment did trigger a significant decrease in expression levels of Smo and Gli2 (**Figure 3.15**). Thus, this seems to indicate that there could be an endogenous basal activation of the Hedgehog pathway although Hedgehog ligands were undetectable (only assessed at gene expression level). Interestingly, it has been previously reported that addition of cyclopamine can promote ciliary accumulation of Smo, priming cells for Hh pathway hyper-responsiveness after compound withdrawal (Peluso et al., 2014). Although Hh hyper-responsiveness does not seem to be relevant in our model (since no Hh ligands were detected), no Hh ligand was detected in our model, cyclopamine ability to modulate Smo subcellular localization certainly indicates that cyclopamine effects could be more complex than simple Smo inhibition.

However, abrogation of basal Hedgehog signalling does not seem to be sufficient to drive an effect in barrier stability (assessed by ZO-1 junctional levels or TEER measurements) although a significant increase in MMP3, -10 and -13 expression levels was observed (**Figure 3.12**). The observed cyclopamine-driven up-regulation of metalloproteinase expression could be related with the reported reduction in Gli2 mRNA levels. Previous studies have described a relationship between Gli2 and metalloproteinase expression as Gli2 could enhance metastasis through an increased expression of MMP2 and -9 (Dennler et al., 2007; Zhao et al., 2013). Although in a metastatic context Gli2 seems to enhance metalloproteinase expression, this does not need to be the case for endothelial cells or other metalloproteinases. Thus, further research is needed to fully clarify the relationship between Gli2 and metalloproteinase expression in endothelial cells. In any case, it needs to be mentioned that the observed increase in MMP3, -10 and -13 after cyclopamine addition was not sufficient to impact in endothelial barrier stability (measured as junctional ZO-1 and TEER levels) as perhaps a higher amount of time was required.

Cyclopamine synergistically enhanced cytokine-driven barrier disruption (measured as junctional ZO-1 levels and TEER values) (**Figure 3.8** and **3.18**) together with an enhanced reduction in *Gli2* and *ZO-1* gene expression (**Figure 3.14**). Thus, Hedgehog abrogation under physiological conditions may not be enough to trigger any detectable variations in barrier stability. However, if barrier integrity is already compromised by an inflammatory environment, the cyclopamine-driven reduction in Hedgehog signalling (decreased *Gli2* and *Smo* gene expression) could then be enough to further enhance cytokines detrimental effect, synergistically reducing TEER values and ZO-1 junctional and expression levels (**Figures 3.18, 3.8** and **3.14**).

Cytokines and cyclopamine can also synergise in order to up-regulate *MMP3*, -10 and -13 gene expression (**Figure 3.12**). As it has been mentioned before, previous studies have described an ability of Shh to enhance angiogenesis (Renault et al., 2010) or metastasis (Dennler et al., 2007; Zhao et al., 2013) through the enhanced expression of MMP2 and -9. Thus, it may seem a little counterintuitive that abrogation of Hedgehog pathway enhances

cytokines-driven increase in metalloproteinase expression levels (**Figure 3.12**). However, the effects of Hedgehog signalling in metalloproteinase expression could vary depending on the studied cell type or the physiological environment and endothelial cells could respond in different manners under pro-angiogenic or inflammatory conditions.

In any case, the observed results seemed to suggest that the cytokine/cyclopamine driven increase in metalloproteinase expression could be underlying the reported loss of barrier integrity (measured as TEER levels). Thus, in order to explore this hypothesis, cytokine/cyclopamine effects on barrier integrity were assessed in the presence of a broad-spectrum metalloproteinase inhibitor GM6001, revealing a partial restoration of ZO-1 junctional distribution. However, as it has been previously discussed, when quantified this partial restoration of ZO-1 junctional distribution was not reported to be significant due to a high variability between experiments, regardless of the clear visual differences in ZO-1 junctional levels (**Figure 3.10**). Future experiments should explore the effects of broad metalloproteinase inhibition using an alternative tight or adherent junction protein with more constant modulations. Regarding TEER measurements, GM6001 addition fully protected against cytokines/cyclopamine driven loss of barrier properties (**Figure 3.19**). As TEER values account for the integrity of both tight and adherens junctions, it is possible that the described reduction in ZO-1 gene expression does not account for a measurable effect in overall barrier integrity. Supporting these observations, Alluri *et al.* showed GM6001 ability to attenuate IL-1 β induced barrier permeability in rat brain microvascular endothelial cells (Alluri *et al.*, 2016). GM6001 is a broad-spectrum metalloproteinase inhibitor thus, although MMP3, -10 and -13 cytokines and cyclopamine mediated up-regulation makes them good candidates to mediate the observed barrier disruption, other metalloproteinases may be involved.

Regarding metalloproteinase inhibition, abrogation of Hedgehog pathway also accentuated cytokine-driven reduction of *TIMP3* gene expression levels and prevented the cytokine-mediated increase in *TIMP1* expression levels (**Figure 3.13**). The effects of Hedgehog pathway abrogation on TIMP's regulation in the presence or absence of inflammation have not been studied.

In vivo/in vitro deletion of TIMP3 results in a reduction in pulmonary endothelial barrier stability (Arpino et al., 2016). In our model, cytokines/cyclopamine driven barrier disruption was partially reversed by addition of hTIMP3 (**Figure 3.20**). In this regard, it needs to be considered that TIMP3 does not inhibit all metalloproteinases with the same affinity, as it has been reported to be a weaker inhibitor of MMP3 and -7 (reviewed in Brew & Nagase, 2010). Additionally, hTIMP3 may not be as efficient as GM6001 in its inhibition of metalloproteinases and different hTIMP3 concentrations and incubation times, together with siRNA experiments, should be tested in order to determine hTIMP3 relevance in the reported results.

3.3.4. Shh and Vitamin D3 synergistically rescue cytokines and cyclopamine driven barrier disruption.

In order to study Shh and Vitamin D3 role as barrier promoters, their ability to protect barrier integrity in the presence of cytokines and cyclopamine was tested. Shh protection against inflammatory-mediated loss of barrier stability has been recently reported in a murine model of Human Immunodeficiency Virus (a disorder characterized by chronic neuro-inflammation), where treatment with a pharmacological agonist of the Hedgehog pathway rescued claudin-5 expression, a marker of barrier integrity, to WT levels (Singh et al., 2016). Regarding Vitamin D3, no previous protective effect has been described in the context of ECs. However, *in vitro* studies with intestinal epithelial cells showed a Vitamin D3 barrier-protective effect (measured as TEER and dextran extravasation) against TNF α (Chen et al., 2015a), LPS (Chen et al., 2015b) and ethanol (Chen et al., 2015c) driven barrier dysfunction. Additionally, TNF α -driven loss in colonic barrier permeability was enhanced in mice carrying VDR deletion in colonic epithelial cells, which could not be rescued by treatment with the Vitamin D3 analogue paricalcitol (Du et al., 2015). Nonetheless, no Vitamin D3 protective effect against cytokines and cyclopamine associated lost on barrier integrity was reported in our *in vitro* model (measured either as ZO-1 junctional levels or TEER) (**Figure 3.9** and **3.22**).

Interestingly, when combined, Shh and Vitamin D3 were able not only to completely abrogate cytokine/cyclopamine driven loss in barrier integrity but also to promote barrier formation above control levels (measured either as ZO-1 junctional levels or TEER) (**Figure 3.9** and **3.22**). No changes in gene expression levels were detected in the presence of Shh and Vitamin D3 (**Appendix 3.J**). This protective synergy between Shh and Vitamin D3 has not yet been reported in the literature, but it supports the previously described existence of a cross-talk between the Hedgehog and Vitamin D3 pathways in the context of endothelial barriers (Bijlsma et al., 2006). It needs to be mentioned that Shh and Vitamin D3 protective synergy takes place despite the presence of cyclopamine, suggesting that Shh could be cooperating with Vitamin D3 in a non-canonical manner. In this regard, Bijlsma *et al.* observed that Ptch could be functioning as a translocator of Vitamin D3 (or one of its metabolites) (Bijlsma et al., 2006). Additionally, studies in hematopoietic stem and progenitor cells showed a specific ability of the Vitamin D3 cholecalciferol (but not active 1,25-dihydroxy vitamin D3) to antagonise the Hh pathway through extracellular binding of Smo, triggering a loss in Gli-reporter activation (Cortes et al., 2015). These observations open the possibility that Shh and Vitamin D3 synergy is operated through an Shh-mediated inhibition of Ptch, no longer able to work as a translocase, increasing intracellular levels of Vitamin D3 and decreasing extracellular Vitamin D3 concentrations together with its availability to inhibit Hh signalling through Smo binding. Further studies regarding the effects of Ptch inhibition in the presence of Vitamin D3, cyclopamine and cytokines are needed to test this hypothesis.

Alternatively, Shh and Vitamin D3 could be mediating their synergistic protective effects through modulation of Akt signalling. As it has been previously discussed (**Section 1.9**), Akt phosphorylation (and consequent activation) is a shared element between the cytokine (reviewed in Alvarez et al., 2011), Shh (Kanda et al., 2003; Riobo et al., 2006) and Vitamin D3 (Datta Mitra et al., 2013; Zhang & Zanella, 2008) signalling routes, pointing towards Akt as a possible molecular switch capable of integrating all these pathways. Experiments with the Akt inhibitor MK-2206 seem to support this hypothesis since cytokine, Shh and Vitamin D3 individual effects on MCEC-1 junctional

stability seem to be abrogated upon Akt's inhibition (**Figure 3.10**). Regarding MK-2206 blockage of Shh's or Vitamin D3's driven increase in ZO-1 junctional levels, it is important to mention that this not only involved a disruption in ZO-1 continuous peripheral staining but it was accompanied but an increase in of ZO-1's cytoplasmatic (delocalised) levels (**Figure 3.10**). Inhibition of Akt in the absence of any other stimuli also triggered a reduction in ZO-1 junctional levels (**Figure 3.10**), suggesting an Akt-endogenous control of ZO-1 that will be further explored and discussed in **Section 6.1**.

In any case, future experiments should study Shh and Vitamin D3's ability to abrogate cytokine/cyclopamine driven loss in barrier integrity when the different treatments are added sequentially. Thus, by adding Shh and Vitamin D3 in a sequential manner following cytokine/cyclopamine stimulation it could become apparent if the described Shh/Vitamin D3 protective synergy is mediated by a Shh-driven priming of the cell that increases intracellular levels of Vitamin D3 through the inhibition of Ptch or it is due to an overall modulation of Akt signalling.

3.4. KEY FINDINGS

- Barrier stability is compromised under inflammation. Measured as TEER and ZO-1 gene expression and junctional levels. This is accompanied by an increase in MMP3 and TIMP1 together with a decrease in TIMP3 gene expression, suggesting a possible dysregulation of metalloproteinase activities.
- Shh and Vitamin D3 promote barrier stability, measured as TEER and ZO-1 junctional levels.
- Hedgehog abrogation (cyclopamine) furthers inflammation-driven barrier disruption. This enhanced cytokine-driven reduction in ZO-1 and TIMP3 gene expression and cytokine-driven increase in MMP3 gene expression. An increase in MMP10 and -13 gene expression was also reported with a combination of cytokine and cyclopamine. This was accompanied by an overall decrease in Hh pathway components (Smo and Gli2) gene expression levels.
- Cytokines and cyclopamine driven loss of barrier integrity is metalloproteinase dependent since the observed loss of barrier integrity (measured as TEER) could be blocked by addition of the broad metalloproteinase inhibitor GM6001. Cytokines and cyclopamine driven loss of barrier integrity could also be partially blocked by a pre-treatment with exogenous hTIMP3.
- Shh and Vitamin D3 synergistically rescue cytokines and cyclopamine driven barrier disruption, measured as TEER and ZO-1 junctional levels.

A summary of the reported key findings can be found in **Figure 3.23**.

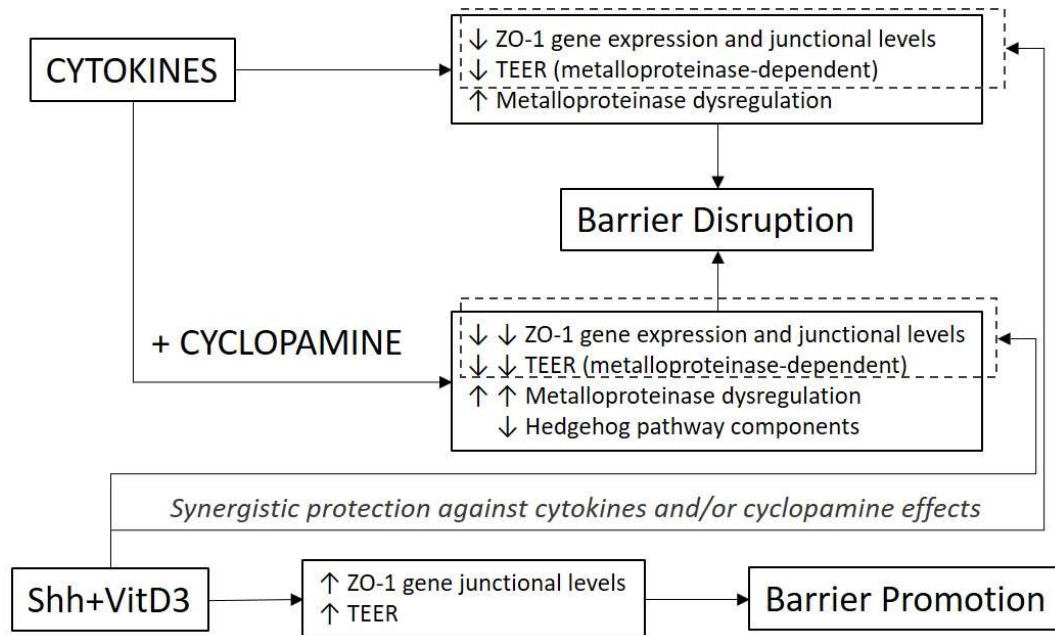


Figure 3.23 – Schematic representation of Chapter’s 3 key findings. Cytokines can lead to endothelial barrier disruption through reduction of ZO-1 gene expression and junctional levels, deregulation of metalloproteinase expression (increased MMP3 and TIMP1 together with a reduction in TIMP3 gene expression levels) and reduction in barrier stability (measured as transendothelial electrical resistance [TEER]) in a metalloproteinase-dependent manner. Cytokines effects can be synergistically enhanced by abrogation of the Hedgehog pathway (cyclopamine) triggering a further reduction in ZO-1 gene expression and junctional levels, further deregulation in metalloproteinase gene expression (further reduction in TIMP3 together with increased MMP3, -10 and -13 gene expression levels) and a further reduction in TEER levels also in a metalloproteinase-dependent manner. A combination of Shh and Vitamin D3 (VitD3) not only increased ZO-1 junctional levels but also increased TEER measurements leading to enhanced endothelial barrier properties. Additionally, Shh and Vitamin D3 combined were capable of synergistically rescue cytokines and cyclopamine driven barrier disruption (measured as TEER and ZO-1 junctional levels; dotted lines).

3.5. FUTURE STUDIES

- No effects were reported for Shh and/or Vitamin D3 dependent modulation of metalloproteinase gene expression despite some examples being previously described in the literature. Future experiments should assess gene expression changes at earlier time-points as well as changes in protein expression.
- Similarly, no changes in gene expression levels of claudin-5, occluding and VE-cadherin under any of the used treatments. Future experiments should assess gene expression changes at earlier time-points.
- GM6001 and hTIMP3 are broad inhibitors of metalloproteinase activity. To determine if one, or more, of the cytokines/cyclopamine upregulated metalloproteinases (MMP3, -10 or -13) are behind the observed changes in barrier stability siRNA experiments could elucidate their roles.
- Potential endogenous roles for TIMP3 role, could be explored through loss of function studies with siRNA experiments.
- Shh and Vitamin D3's combined ability to rescue cytokine/cyclopamine driven loss in barrier stability should be further studied through sequential addition of the different treatments.
- Future experiments will focus in the optimization of dextran extravasation as an alternative method to corroborate the observed changes in barrier function.

Although contrast and brightness parameters were kept constant between experiments, future experiments could incorporate a normalisation procedure for ZO-1 staining based in the non-changing intensity levels of DAPI.

4. Establishing an *in vitro* model with a human brain endothelial cell line

4.1. INTRODUCTION

4.1.1. The Blood-Brain Barrier

The Blood-Brain barrier (BBB) is formed by endothelial cells (ECs) wrapped on their abluminal side by a cellular layer of pericytes and a basement membrane (comprising extracellular matrix components), all in turn externally covered by astrocyte foot processes (Seo et al., 2012; Park et al., 2003). The ECs forming the BBB are form very tight cell-to-cell contacts, resulting in the BBB's limited permeability. Tight (TJ) and adherens (AJ) junctions link adjacent ECs together (Kniesel & Wolburg, 2000). TJs comprise transmembrane proteins such as occludins, junctional adhesion molecules (JAMs) and claudins which are anchored to actin filaments via adaptor proteins including cingulin, zona occludens proteins (ZO-1, -2 and -3) (reviewed in Stamatovic et al., 2016). Thus, ZO proteins can be considered the structural core of the junctional complex and, as such, modulations in their levels and cellular localization have been broadly used to assess junctional (and barrier) integrity.

4.1.2. hCMEC/D3: a brain endothelial cell line

The hCMEC/D3 cell line was developed from human temporal lobe microvessels isolated from tissue excised during surgery for control of epilepsy (Weksler et al., 2005). hCMEC/D3 cells express many endothelial markers characteristic of the brain endothelium such as: Platelet endothelial cell adhesion molecule (PECAM-1), VE-cadherin, β - and γ -catenins, ZO-1, JAM-A, claudin-5 and CD31 (among others) and no expression was detected for CD36 (which is absent from the brain endothelium) (Weksler et al., 2005). Additionally, hCMEC/D3 characterization showed that when grown to confluence in semi-permeable filters, these cells can form an endothelial barrier highly restrictive to a wide range of molecular sized (4 to 70 kDa) (Weksler et al., 2005). Thus, hCMEC/D3 is a well-characterised brain endothelial cell line that has been used in the *in vitro* modelling of the BBB (Forster et al., 2008; Eigenmann et al., 2013; Ni et al., 2017).

4.1.3. The BBB is disrupted under inflammatory conditions

Endothelial barrier disruption under inflammatory conditions has been previously established in a number of model systems (Mark & Miller, 1999; Trickler et al., 2005; Forster et al., 2008; Sajja et al., 2014; Ni et al., 2017). In this regard, the effects of pro-inflammatory conditions in *in vitro* in hCMEC/D3 mono-cellular models of the BBB have been previously reported, showing a cytokine-mediated reduction of barrier properties (Forster et al., 2008; Ni et al., 2017). One of the mechanisms by which cytokines may mediate endothelial barrier disruption is through a reduction in the levels of tight junction proteins (such as ZO-1, claudin-5 and occludin) (Forster et al., 2008; Aslam et al., 2012; Cohen et al., 2013; Labus et al., 2014). Thus, cytokine-mediated loss of junctional proteins could disrupt cell-cell contacts resulting in increased endothelial permeability.

As discussed in the previous chapter, an alternative mechanism by which cytokines can mediate endothelial barrier disruption is through metalloproteinase induction (reviewed in Rempe et al., 2016). Several studies using broad spectrum metalloproteinase inhibitors point to metalloproteinases as main mediators of BBB disruption both *in vivo* and *in vitro* (Gijbels et al., 1994; Paul et al., 1998; Pfefferkorn & Rosenberg, 2003; Alluri et al., 2016), and cytokine modulation of a wide range of metalloproteinases has been shown in the context of the BBB (reviewed in Leppert et al., 2001). For these reasons, the role of metalloproteinases (and their inhibitors TIMPs) in barrier permeability under inflammatory conditions will be explored in our *in vitro* model of the BBB.

4.1.4. Shh enhances BBB integrity

In order to understand potential roles of hedgehog pathway signalling in the BBB barrier integrity (see Chapter 1 for details) a pharmacological approach was taken to explore the effect of Shh in hCMEC/D3 monolayers. Shh is a small secreted protein that can be released into the extracellular environment, where it can target a transmembrane protein named Patched (Ptch). In the absence of Shh, Ptch works as an inhibitor of the transmembrane

protein Smoothed (Smo), which becomes activated and able to initiate a signalling cascade that will result in the activation of the Gli family of transcription factors (Gli1, Gli2 and Gli3) (Luissint et al., 2012). The importance of the Hedgehog (Hh) pathway in the maintenance of endothelial barrier integrity will be tested in our *in vitro* model in the presence or absence of inflammation.

4.1.5. Vitamin D3 promotes BBB integrity

Vitamin D3 is a steroid hormone capable of crossing the cell membrane and bind to the intracellular vitamin D receptor (VDR), which interacts with the retinoid X receptor (RXR) in order to form a heterodimer able to target genes that contain the vitamin D3 response elements (VDRE) in their regulatory regions (reviewed in Dusso et al., 2005). Although the underlying mechanisms by which Vitamin D3 may promote endothelial barrier integrity remain unknown, treatment with Vitamin D3 active form (1,25(OH)₂D₃) has been shown to increase the expression of several tight junction proteins such as claudins (Fujita et al., 2008), occludins (Kong et al., 2008; Yin et al., 2011), and ZO proteins (Palmer et al., 2001) in several endothelial cell types. Due to this, Vitamin D3 effects on BBB integrity will be explored in our *in vitro* system.

4.1.6. Shh and Vitamin D3, an unexplored cross-talk

It has been suggested that Ptch-driven inhibition of Smo could be mediated by a Ptch-dependent translocation of Vitamin D3 (or a precursor) across that will act as a Smo antagonist once in the extracellular environment (Bijlsma et al., 2006). Thus, according to Bijlsma *et al*, these two endothelial barriers promoting signalling pathways could be opposing each other. Shh and Vitamin D3 possible cross-talk will be explored in the context of the BBB and inflammatory conditions, together with its possible impact on metalloproteinase regulation.

4.1.7. Aims

1. The human brain microvascular endothelial cell line hCMEC/D3 will be used to generate an *in vitro* model of the BBB.
2. This model will be then used to study the effects of barrier promoting (Shh and Vitamin D3) and barrier disrupting (cytokines) agents in barrier integrity (measured as TEER and visualization of junctional ZO-1).
3. Additionally, Shh and Vitamin D3 role as protective agents against cytokine-driven effects on barrier stability will be also explored. In this context, modulation of the signature of metalloproteinases in response to cytokines, Shh and Vitamin D3 stimulation, and its effects on barrier stability, will be also assessed.

4.2. RESULTS

4.2.1. Functional changes in an in vitro model of the BBB

4.2.1.1. Barrier formation in an in vitro model of the BBB

In order to develop an in vitro model of the BBB, barrier formation by hCMEC/D3 cells was assessed by growth to confluency. Cells were seeded onto 0.3µm porous transwells and allowed to form an endothelial barrier for a period of 5 days as previously reported (Forster et al., 2008). Transendothelial Electrical Resistance (TEER) measurements were taken at 24h intervals to assess barrier formation. TEER measurements were normalised to a cell-free coated-insert used as a negative control. During the first 3 days after cell seeding, a drastic increase in TEER measurements suggests that barrier formation is taking place (19.75 ± 1.87 to 42.63 ± 2.16 Ω/cm^2 , $p < 0.001$) (**Figure 4.1**). After this point, TEER values seem to reach a plateau with no significant changes detected between days 3 and 5 (42.63 ± 2.16 to 49.50 ± 2.83 Ω/cm^2 , $p > 0.05$) (**Figure 4.1**). This data suggests that hCMEC/D3 cells can form a functional barrier which is sustained for up to 5days (**Figure 4.1**).

To enable analysis of secreted metalloproteinases culture in a lower Foetal Calf Serum (FCS) was necessary. Thus, barrier formation was by hCMEC/D3 cells was explored at the same density and time course as above. Cells were cultured in the presence of low (0.25%) and high (5%) FCS and TEER measurements were taken daily for a period of 5 days. TEER values gradually increased between day 1 and 3 for cells cultured with 5% FCS (19.75 ± 1.87 to 42.63 ± 2.16 Ω/cm^2 , $p < 0.001$) and 0.25% FCS (23.24 ± 1.59 to 46.15 ± 1.60 Ω/cm^2 , $p < 0.001$), indicating barrier formation during the first 3 days of culture with no differences derived from the concentration of FCS used (**Figure 4.2**). As before, cells cultured in the presence of 5% FCS reached a

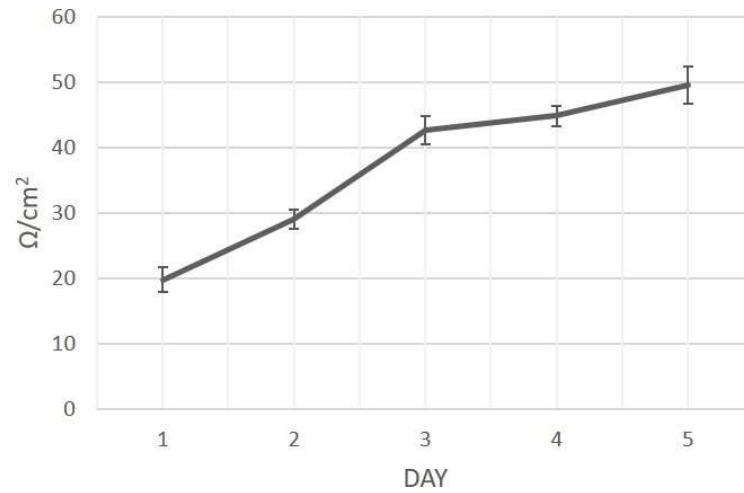


Figure 4.1 – Confluent hCMEC/D3 monolayers form a barrier. hCMEC/D3 cells were cultured on cell culture inserts (0.3 μm porous). Transendothelial Electrical Resistance (TEER) measured at 24h intervals. TEER measurements normalised to those of cell-free coated-insert. Each bar represents mean \pm SEM for 3 wells. Representative experiment depicted. Experiment replicated >3 times.

plateau with no significant variation detected between days 3 and 5 (42.63 ± 2.16 to $49.50 \pm 2.83 \text{ } \Omega/\text{cm}^2$, $p > 0.05$). However, a slight increase was observed for hCMEC/D3 monolayers cultured in lower (0.25%) FCS conditions between day 3 and 5 (46.15 ± 1.60 to $55.64 \pm 1.77 \text{ } \Omega/\text{cm}^2$, $p < 0.001$) which could be derived from some barrier maturation processes (**Figure 4.2**). Additionally, although no overall differences were detected between FCS concentrations, a higher TEER value was observed after 4 days of culture for cells grown in low FCS conditions (52.43 ± 1.52 vs $44.83 \pm 1.58 \text{ } \Omega/\text{cm}^2$, $p < 0.01$) (**Figure 4.2**). This could be an isolated event as no major differences in barrier formation were reported, suggesting that a low FCS concentration (0.25%) can be used in order to study metalloproteinase biology without compromising barrier properties.

Additionally, since barrier formation and maturation seem to be taking place largely on the first 3 days of culture (**Figure 4.1** and **4.2**), in further experiments monolayers were cultured for 3 days before treatment addition.

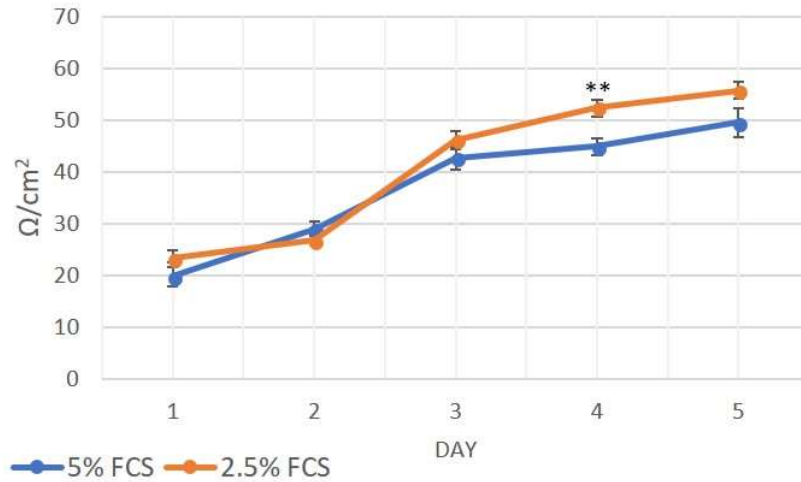


Figure 4.2 – FCS concentration during culture does not affect hCMEC/D3 barrier formation. hCMEC/D3 cells were cultured on cell culture inserts (0.3µm porous) under two different FCS concentrations (0.25 and 5%). Transendothelial Electrical Resistance (TEER) was measured at 24h intervals to assess barrier formation. TEER measurements normalised to a cell-free coated-insert was used as negative control. Each point represents the mean ±SEM for 3 wells. Statistically significant differences were assessed via t-test; ** p < 0.01. Representative experiment depicted. Experiment replicated 3 times.

4.2.1.2. TEER resistance is reduced under inflammatory conditions

In order to develop the *in vitro* BBB model for inflammatory conditions, confluent hCMEC/D3 monolayers were treated with a combination of cytokines (TNF α and IL1 α). Cells were seeded into 0.3 μ m porous transwells and cultured for 3 days (in order to allow for barrier formation) before cytokine (10ng/ml) addition. TEER measurements were taken at 24h intervals for up to 48h after treatment addition (5 days in total from cell seeding). TEER measurements were normalised to a cell-free coated-insert used as a negative control. Treatment with cytokines significantly reduced barrier integrity when compared with untreated monolayers at both, 24h (43.45 \pm 0.32 vs 66.00 \pm 0.32 Ω /cm², p<0.001) and 48h (43.27 \pm 0.97 vs 53.62 \pm 1.28 Ω /cm², p<0.001) (**Figure 4.3**). Thus, this seems to suggest that addition of cytokines can significantly impair barrier properties for the time-period measured.

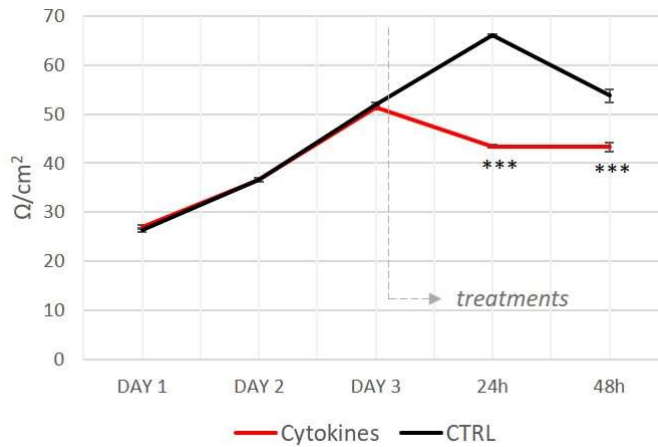


Figure 4.3 - Cytokine treatment induce hCMEC/D3 a reduction in TEER resistance. hCMEC/D3 were seeded onto cell inserts (0.3 μ m porous), grown for 3 days. hCMEC/D3 monolayers then treated with a cytokine mix (TNF α and IL1 α at 10 μ g/ml). Transendothelial Electrical Resistance (TEER) was measured to assess barrier integrity at 24h and 48h after treatment. Statistically significant differences were assessed via t-test. Each point represents the mean \pm SEM for 3 wells. * $p < 0.5$; *** $p < 0.001$. Representative experiment depicted. Experiment replicated >3 times.

4.2.1.3. TEER resistance is enhanced by Shh and Vitamin D3

To explore the potential roles of Shh and VitD3 signalling in our human endothelial cell BBB in vitro model, responses to Shh (100ng/ml), and Vitamin D3 (100nM) alone or in combination were assessed. Cells were seeded into 0.3µm porous transwells and cultured for 3 days (in order to allow for barrier formation) before Shh and/or Vitamin D3 addition. TEER measurements were made daily up to 48h after treatment addition and normalised to a cell-free coated-insert used as a negative control. After 24h treatment, addition of Shh (74.98 ± 1.20 vs 66.00 ± 0.32 Ω/cm^2 , $p < 0.001$) or Vitamin D3 (70.58 ± 0.49 vs 66.00 ± 0.32 Ω/cm^2 , $p < 0.001$) significantly increased TEER values when compared with untreated monolayers (**Figure 4.4**). Shh (61.05 ± 0.32 vs 53.72 ± 1.28 Ω/cm^2 , $p < 0.001$) and Vitamin D3 (60.87 ± 0.49 vs 53.62 ± 1.28 Ω/cm^2 , $p < 0.001$) barrier enhancing effects were maintained up to 48h after treatment (**Figure 4.4**). Interestingly, combined addition of Shh and Vitamin D3 did not promote barrier properties any further than Shh or Vitamin D3 individual treatment at neither 24h (73.15 ± 1.14 Ω/cm^2) or 48h (62.33 ± 1.81 Ω/cm^2) post-treatment, (**Figure 4.4**).

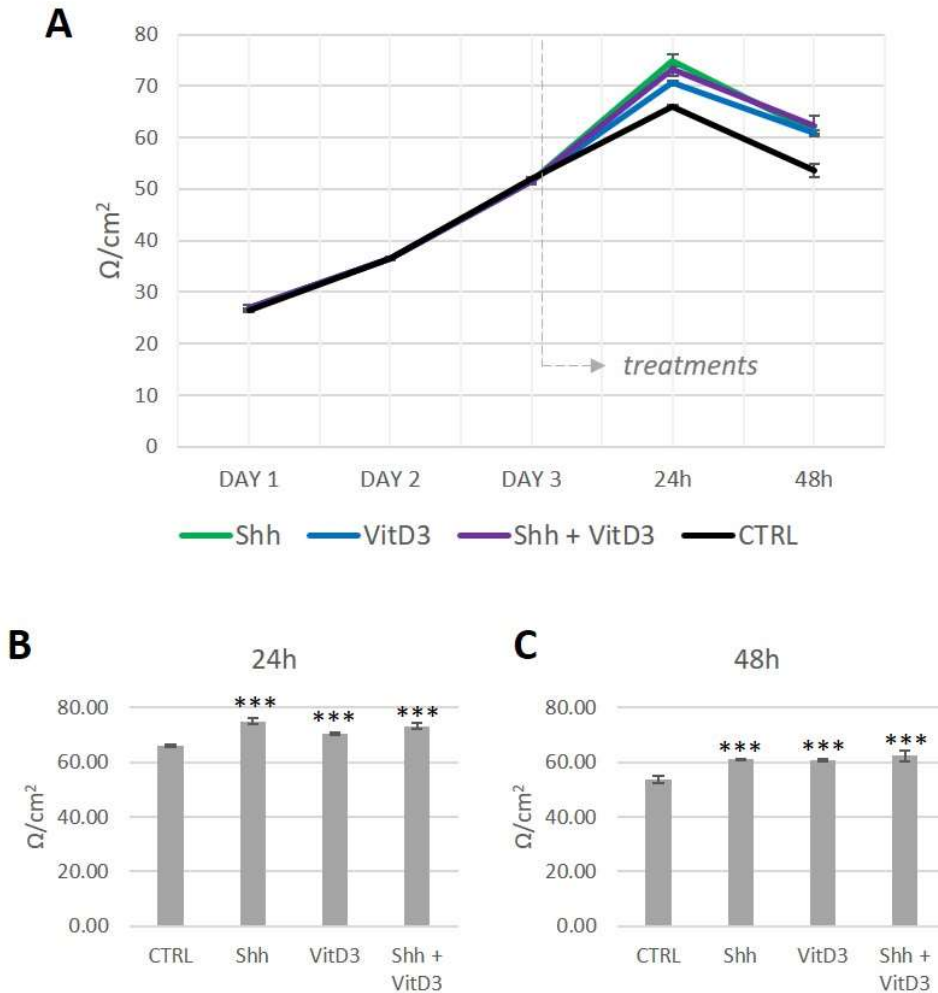


Figure 4.4 – Shh and/or Vitamin D3 increase TEER resistance. *hCMEC/D3* were seeded onto cell inserts (0.3 μ m porous) and grown for 3days until confluent in order to promote barrier formation. *hCMEC/D3* monolayers when then treated with Shh (100ng/ml), Vitamin D3 (100nM)(VitD3) or a combination of both for up to 48h. (A) Transendothelial Electrical Resistance (TEER) was measured to assess barrier integrity every 24h, including at (B) 24h and (C) 48h post-treatment. Statistically significant differences were assessed via One-way ANOVA with post-hoc Tukey. Each bar represents the mean \pm SEM for 3 wells. * $p < 0.05$; *** $p < 0.001$. Representative experiment depicted. Experiment replicated >3 times.

Under physiological conditions Shh is secreted by astrocytes (situated beneath the basal lamina underlying endothelial cells) and promotes BBB stability. However, thus far treatments in our *in vitro* model have been added to the apical side of the transwell system. Thus, to test if Shh's ability to modulate barrier integrity was dependent on the site of addition, Shh (100ng/ml) was added into the apical, basal or both sides of confluent hCMEC/D3 monolayers previously cultured for 3 days. After 24h treatment, Shh added to the apical (84.52 ± 1.12 vs 66.92 ± 1.86 Ω/cm^2 , $p < 0.01$), basal (83.78 ± 0.97 vs 66.92 ± 1.86 Ω/cm^2 , $p < 0.01$) or both (85.80 ± 0.64 vs 66.92 ± 1.86 Ω/cm^2 , $p < 0.001$) sides of the polarised barrier triggered a significant increase in TEER values when compared with untreated monolayers (**Figure 4.5**). The reported significant differences were maintained up to 48h post-treatment regardless of the site of addition: apical (72.23 ± 2.30 vs 55.37 ± 0.49 Ω/cm^2 , $p < 0.01$), basal (78.10 ± 4.37 vs 55.37 ± 0.49 Ω/cm^2 , $p < 0.01$), and both sides (79.93 ± 6.23 vs 55.37 ± 0.49 Ω/cm^2 , $p < 0.05$) (**Figure 4.5**). Interestingly, addition of Shh in the apical and/or basal sides of the polarised *in vitro* barrier did not trigger any detectable differences in Shh's ability to enhance barrier properties (**Figure 4.5**). Thus, Shh treatment was added in subsequent experiments to the upper transwell chamber (apical side) alongside the other treatments in order to minimise methodological variability.

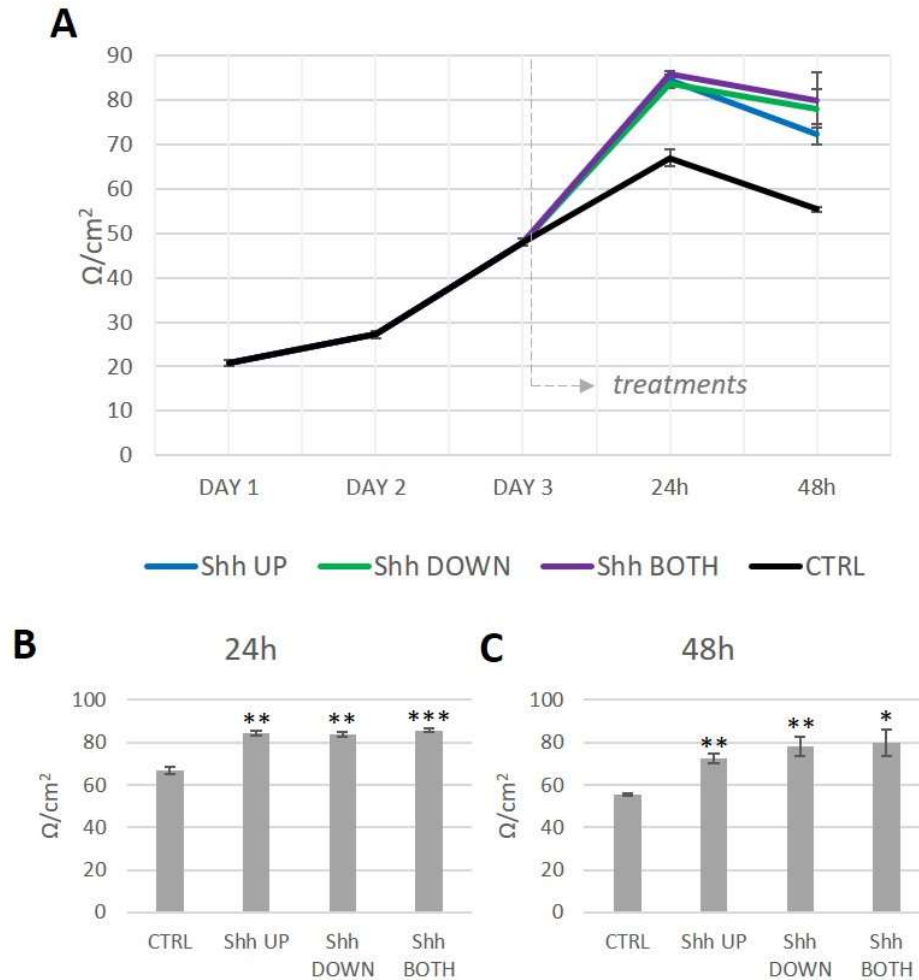


Figure 4.5 - Shh increases TEER resistance regardless of site of addition. hCMEC/D3 were seeded onto cell inserts (0.3 μ m porous) and grown for 3days until confluent in order to promote barrier formation. hCMEC/D3 monolayers when then treated with Shh (100ng/ml) added into the apical, basal or both sides of the transwells for 48h. (A) Transendothelial Electrical Resistance (TEER) was measured to assess barrier integrity every 24h, including at (B) 24h and (C) 48h post-treatment. Statistically significant differences were assessed t-test. Each bar represents the mean \pm SEM for 3 wells. * $p < 0.5$; ** $p < 0.01$; *** $p < 0.001$. Data from a single experiment.

4.2.1.4. *Shh and Vitamin D3 synergistically rescue cytokine-driven loss in TEER resistance*

In order to test Shh and Vitamin D3 barrier-enhancing role under inflammatory conditions, confluent hCMEC/D3 monolayers were treated with a combination of Shh (100ng/ml), Vitamin D3 (100nM) and cytokines (TNF α and IL1 α both at 10ng/ml). Cells were seeded into 0.3 μ m porous transwells and cultured for 3 days (in order to allow for barrier formation) before treatments addition. TEER measurements were made daily up to 48h post-treatment and normalised to a cell-free coated-insert used as a negative control. As previously described, monolayers exposed to cytokines showed significantly decreased TEER values when compared with untreated controls at 24h (47.85 \pm 0.84 vs 66.37 \pm 0.49 Ω /cm², p<0.001) and 48h (59.77 \pm 0.84 vs 76.82 \pm 0.97 Ω /cm², p<0.001) (**Figure 4.6A**). No protective effect against cytokine-driven barrier disruption was observed when Shh or Vitamin D3 were added individually at either 24h or 48h (**Figure 4.6A**). However, when added in combination, Shh and Vitamin D3 synergistically blocked the cytokine-driven effect (78.83 \pm 1.02 vs 47.85 \pm 0.84 Ω /cm², p<0.001) restoring TEER values above control levels (78.83 \pm 1.02 vs 66.37 \pm 0.49 Ω /cm², p<0.001) after 24h treatment (**Figure 4.6B**). Shh and Vitamin D3 observed protection against cytokines effects was maintained for up to 48h, when control levels were restored (75.35 \pm 0.32 vs 76.82 \pm 0.97 Ω /cm², p=0.22) (**Figure 4.6B**).

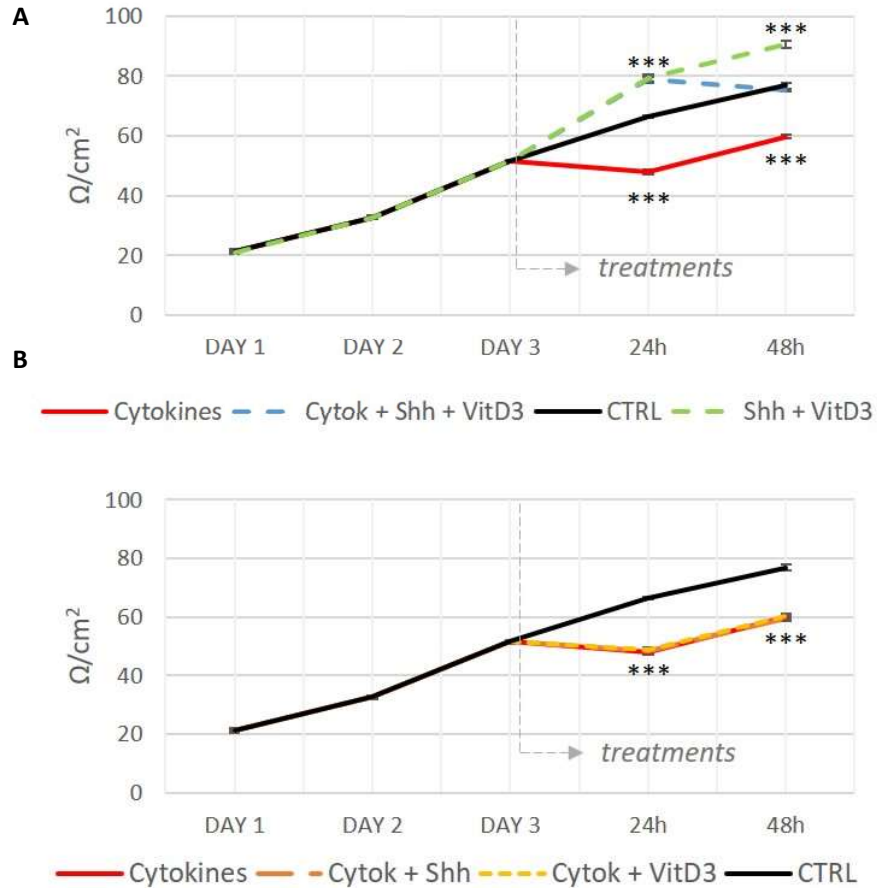


Figure 4.6 – Shh and Vitamin D3 synergistically rescue cytokines-driven loss of TEER. hCMEC/D3 were seeded onto cell inserts (0.3 μ m porous) and grown for 3days until confluent in order to promote barrier formation. hCMEC/D3 monolayers when then treated with with a cytokines mix (TNF α and IL1 α at 10 μ g/ml), Shh (100ng/ml), Vitamin D3 (100nM) (VitD3) or a combination of the above. Transendothelial Electrical Resistance (TEER) was measured to assess barrier integrity every 24h. Statistically significant differences were assessed via One-way ANOVA with post-hoc Tukey. Each bar represents the mean \pm SEM for 3 wells. * $p < 0.5$; *** $p < 0.001$. (A) Experiment replicated 3 times. (B) Data from a single experiment.

4.2.1.5. Cell viability assay

Since high concentrations of cytokines have been reported to promote apoptosis in endothelial cells (Chen & Easton, 2011; R&D, n.d; Chapter 3) cell viability assays were performed to assure that the observed reduction in TEER levels were not due to an increase in cell death but to a deterioration of the formed barrier. Similarly, Shh (Chinchilla et al, 2010; Renault et al., 2010; Zhu et al., 2015) and Vitamin D3 (Dehghani et al., 2013; Uberti et al., 2014) have been previously described to promote cell survival and angiogenesis. Thus, cell viability assays for these conditions were also performed to assure that the reported increase in TEER values were due to an increase in barrier stability rather than an increase in cell number. Combinations of the aforementioned treatments were also tested. Preliminary measurements showed no difference in cell viability in cells stimulated for 24h (not shown) or 48h (**Figure 4.7**) with any of the afore mentioned treatments.

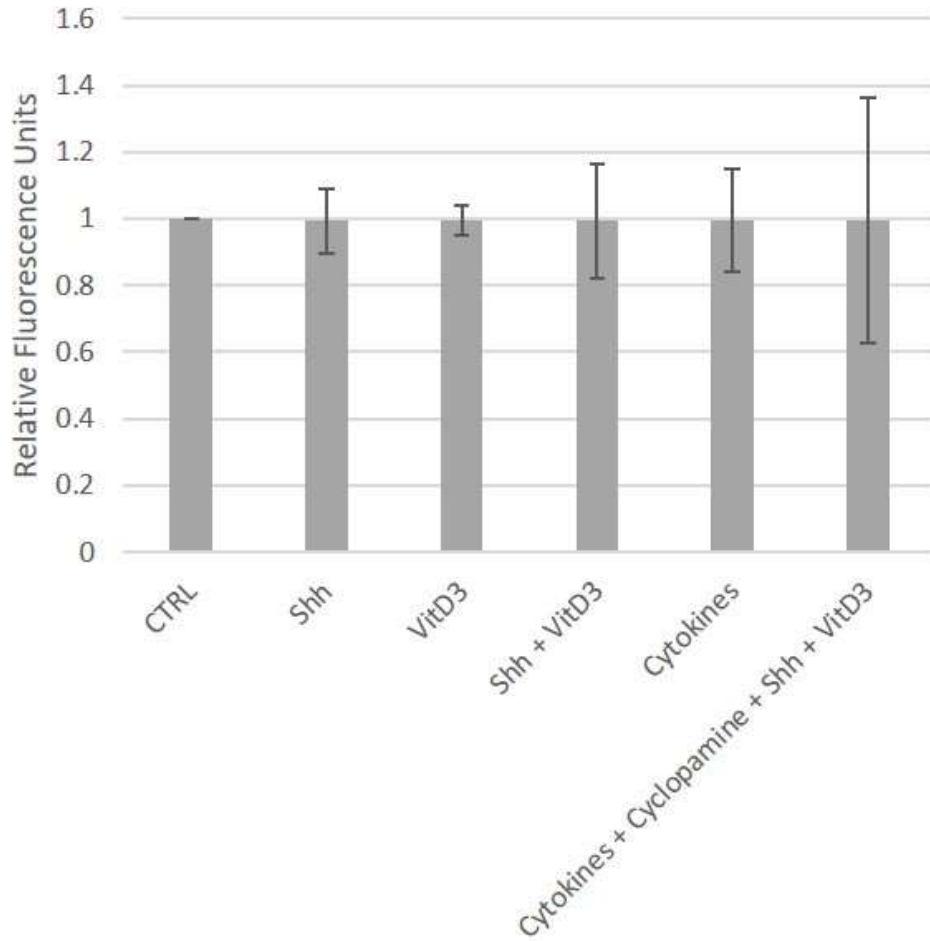


Figure 4.7 - Cell viability assay in hCMEC/D3 monolayers. hCMEC/D3 cell confluent monolayers treated with a mixture of cytokines (TNF α and IL1 α both at 10ng/ml), Shh (100ng/ml) and Vitamin D3 (100nM) (VitD3) alone or in combination during 48h. Following treatment, cells were incubated with Presto Blue reagent for 2h and fluorescence measured. Each bar represents the mean \pm SEM for 3 wells measured. Preliminary experiment (1 replica).

4.2.2. Tight Junction formation in confluent hCMEC/D3 monolayers

4.2.2.1. Immunofluorescent assessment of junctional integrity

In order to test if the reported changes in endothelial barrier stability were due to alterations in junctional protein distribution, hCMEC/D3 confluent monolayers were immunolabelled for the tight junction protein ZO-1. hCMEC/D3 cells were seeded into glass coverslips and cultured until confluent. Upon confluency, cells were treated with cytokines (TNF α and IL1 α both at 10ng/ml) for 48h. Immunofluorescent analysis revealed that the cultured cells were over-confluent, with cells growing in overlapping layers (**Figure 4.8**). Intriguingly, in some areas of the stained coverslip an underlying monolayer of confluent hCMEC/D3 cells could be observed through an opening in the top layers, revealing the formation of classic tight junctions (**Figure 4.8**). Under physiological conditions, hCMEC/D3 seemed to form structurally viable tight junctions (junctional ZO-1 was mainly localised in the cellular membrane in a continuous and homogeneous distribution between adjacent cells) (**Figure 4.8**). After cytokine addition, the continuous staining ZO-1 around the cell periphery was partially lost between adjacent cells (arrowheads in **Figure 4.8**).

The data from this experiment suggested that hCMEC/D3 cells may have been cultured at too high a density and thus, different seeding densities retrieved from the literature were tested in order to optimise ZO-1 staining in hCMEC/D3 confluent monolayers (**Figure 4.9**). Unfortunately, regardless of the employed method, hCMEC/D3 cells grown in coated glass coverslips did not form single-cell monolayers, as even when under confluent, some overlapping of cells was observed (**Figure 4.9**).

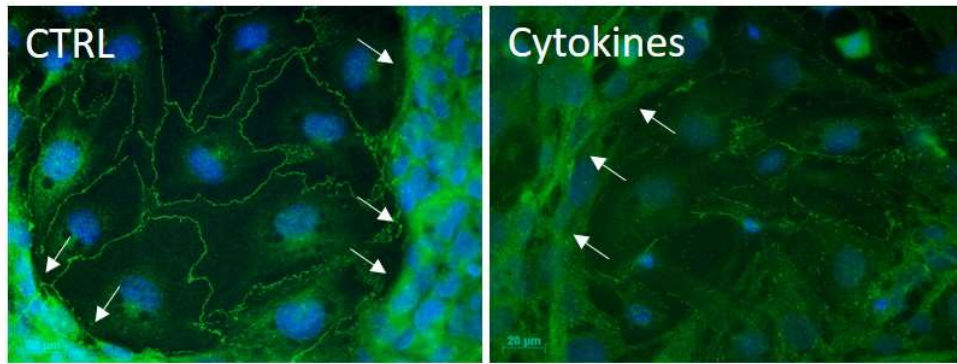


Figure 4.8 – Tight junction stability is compromised under inflammatory conditions. Over-confluent hCMEC/D3 monolayers untreated (CTRL) and treated with a mix of cytokines (TNF α and IL1 α both at 10ng/ml) for 48h. Cells were stained against ZO-1 to visualise tight junction integrity. White arrows point at overlapping cell layers.

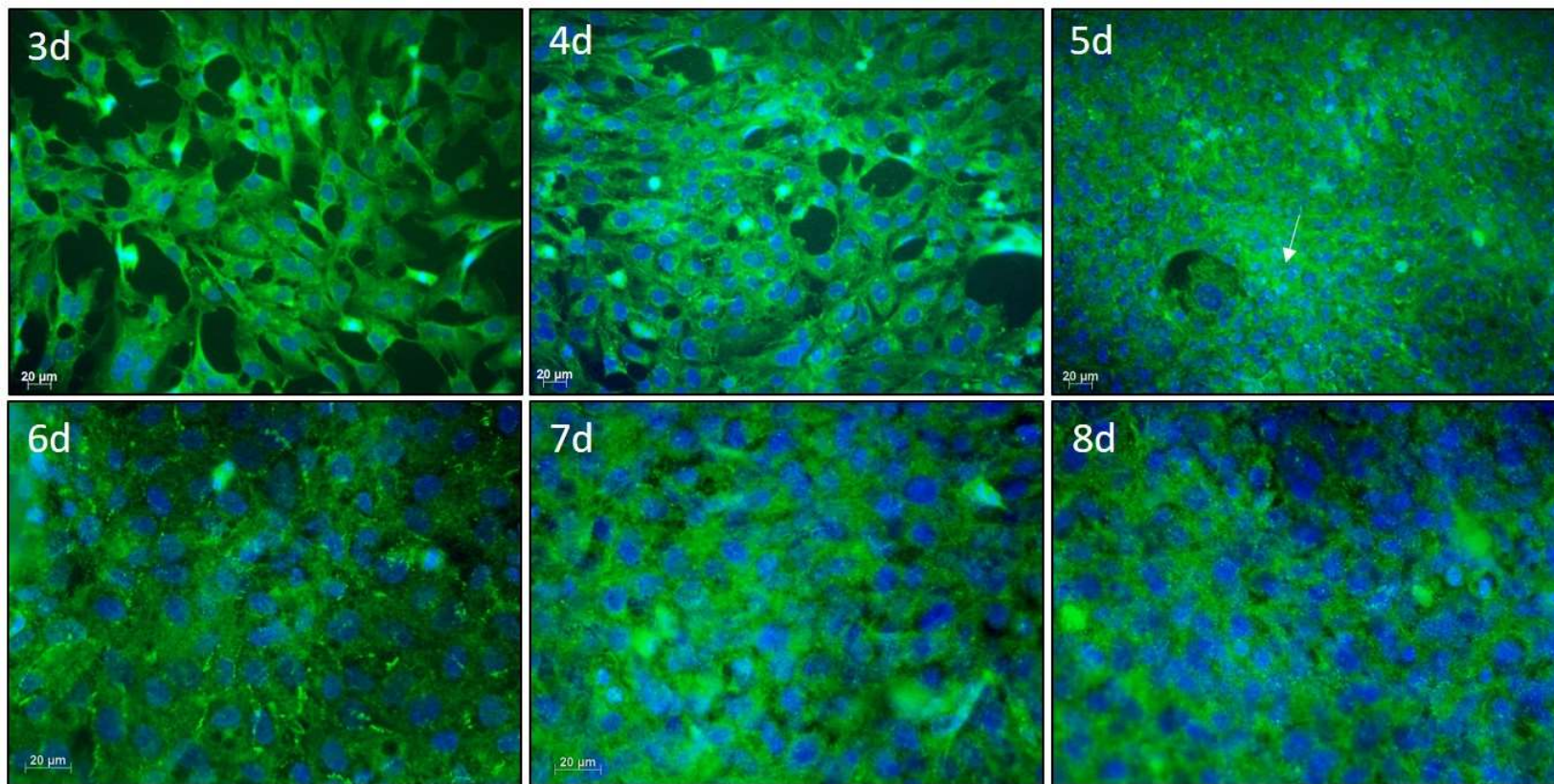


Figure 4.9 – Optimization of junctional ZO-1 staining in hCMEC/D3 monolayers. Sequential ZO-1 staining performed between 3 and 9 days after seeding. White arrow indicates the formation of a “gap” in the overlapping cells.

As an alternative method to assess ZO-1 protein levels, Western Blots were performed. However, due to time restraints, the methodology could not be fully optimised: not a clean ZO-1 detection was obtained and stripping of the membrane to visualise a loading control was not successful (**Figure 4.10**).

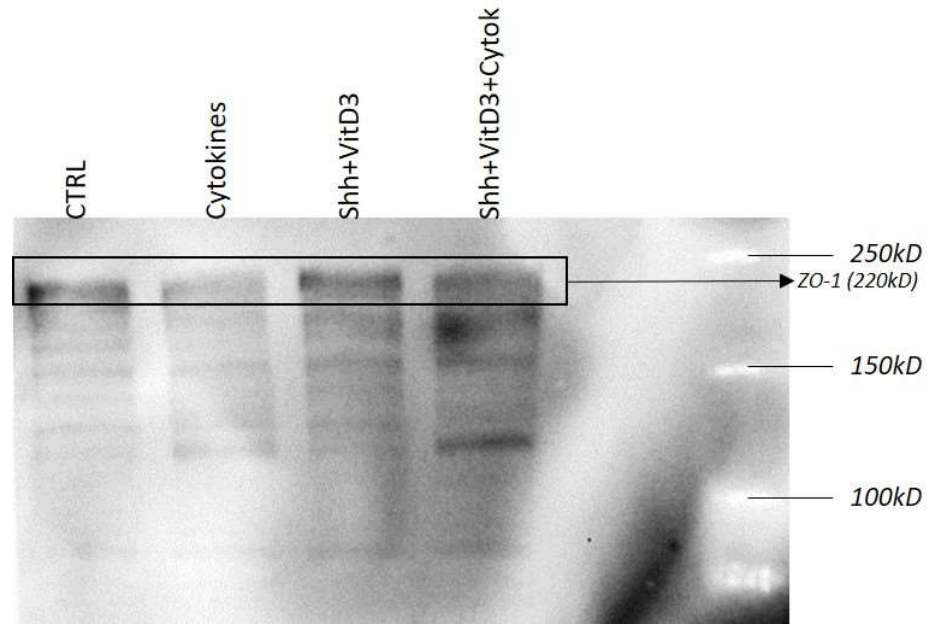


Figure 4.10 – Optimization of ZO-1 protein levels analysis by Western Blotting. hCMEC/D3 cell confluent monolayers treated with a mixture of cytokines (TNF α and IL1 α both at 10ng/ml) in the presence or absence of a combination of Shh (100ng/ml) and Vitamin D3 (100nM) (VitD3) during 24h. 24h after treatment total cellular levels of ZO-1 were determined by Western Blotting.

4.2.2.2. *ZO-1 gene expression is reduced under inflammatory conditions*

Due to the lack of an optimised protocol to directly visualise tight junction protein distribution, the gene expression of several tight junction (*ZO-1* and *CLDN5*) and adherens junction (*VE-CADHERIN*) proteins was explored. Confluent hCMEC/D3 monolayers were treated with cytokines (TNF α and IL1 α at 10ng/ml), Shh (100ng/ml) and/or Vitamin D3 (100nM) before measuring steady state mRNA levels by quantitative Reverse Transcription PCR (qRT-PCR) at 4h, 8h, 12h and 24h after treatment addition. A combination of Shh and Vitamin D3 significantly elevated *ZO-1* mRNA levels when compared with untreated monolayers after 4h exposure (2.38 ± 0.18 vs 1.01 ± 0.11 , $p<0.01$) (**Figure 4.11**) (**Appendix 4.A**). Additionally, 8h after treatment, cytokines significantly reduced *ZO-1* mRNA levels when compared with untreated controls (0.47 ± 0.08 vs 1.03 ± 0.18 , $p<0.05$). This cytokine-driven reduction was completely blocked by addition of a combination of Shh and Vitamin D3 (0.83 ± 0.05 vs 1.03 ± 0.18 , $p>0.05$). No changes in *ZO-1* gene expression were observed with longer treatment exposures (**Figure 4.11**) (**Appendix 4.A**). No changes were reported for *CLDN5* and *VE-CADHERIN* at any of the studied time-points (data not shown).

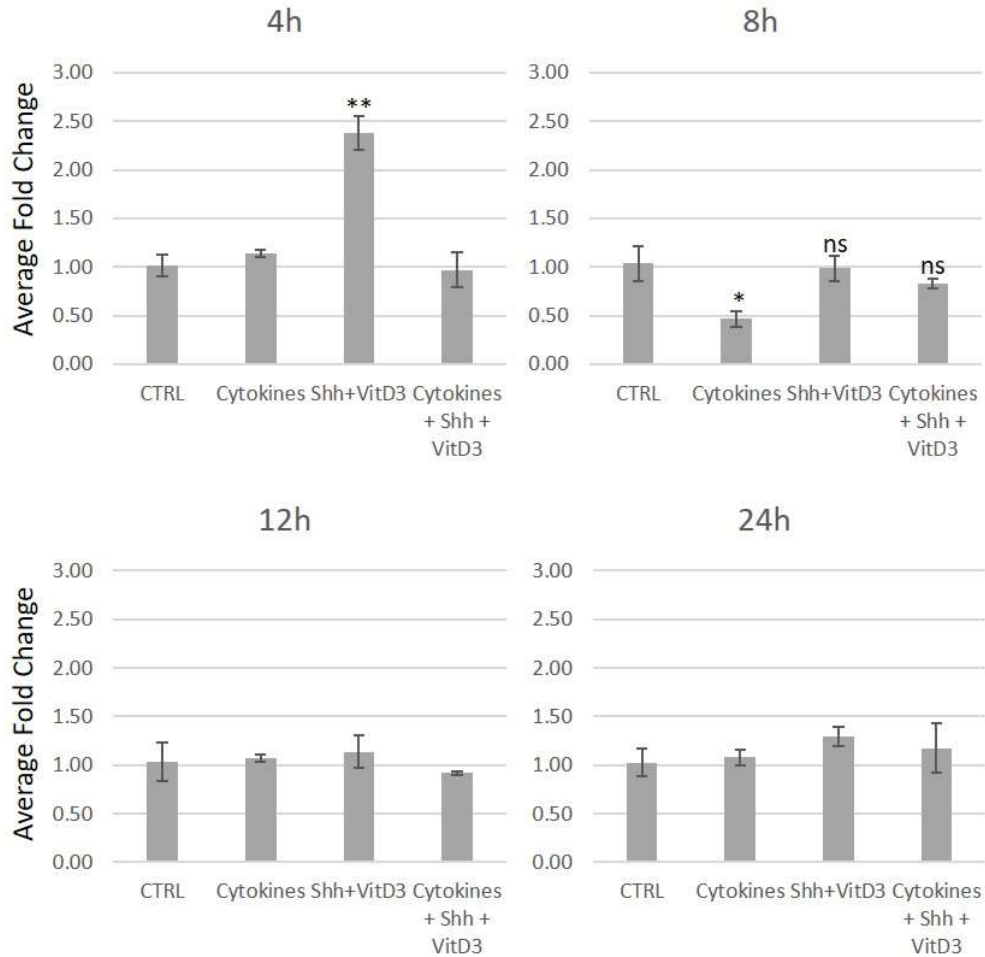


Figure 4.11 – Cytokines, Shh and Vitamin D3 effects in ZO-1 gene expression. hCMEC/D3 cells confluent monolayers were incubated with a mixture of cytokines (TNF α and IL1 α both at 10ng/ml) in the presence or absence of a combination of Shh (100ng/ml) and Vitamin D3 (100nM) (VitD3) during 4h, 8h, 12h and 24h. After treatment, mRNA steady-state levels of ZO-1 were determined by qRT-PCR. All measurements were normalised to 18S endogenous control. Statistically significant differences were assessed via One-way ANOVA with post-hoc Tukey. Each bar represents the mean \pm SEM for 3 wells. * $p < 0.5$; ** $p < 0.01$. Representative experiment depicted. Experiment replicated twice.

4.2.3. Cytokines-driven barrier disruption is metalloproteinase-dependent

4.2.3.1. Metalloproteinase inhibition rescues cytokine-driven TEER reduction

Metalloproteinases have been described to be one of the main mediators of BBB breakdown during inflammation. Thus, in order to assess if the cytokine-driven loss in BBB integrity (measured as TEER levels) observed in our *in vitro* model could be metalloproteinase dependent, a broad-spectrum metalloproteinase inhibitor (GM6001) was used. Cells were seeded into 0.3µm porous transwells and cultured for 3 days in order to allow for barrier formation. Confluent monolayers were then incubated with GM6001 in the presence and absence of cytokines (TNFα and IL1α both at 10ng/ml). TEER measurements were taken daily up to 48h post-treatment and normalised to a cell-free coated-insert used as a negative control. Cytokine addition triggered a significant reduction in TEER values when compared with untreated monolayers at 24h (47.85±0.84 vs 66.37±0.49 Ω/cm², p<0.001) and 48h (59.77±0.84 vs 76.82±0.97 Ω/cm², p<0.001) post-treatment (**Figure 4.12**). Remarkably, GM6001-mediated inhibition of metalloproteinase activities in the presence of cytokines fully restored TEER values to control levels at both, 24h (66.00±0.55 vs 66.37±0.49 Ω/cm², p>0.05) and 48h (75.17±1.60 vs 76.82±0.97 Ω/cm², p>0.05) after treatments addition (**Figure 4.12A**). Exposure to a GM6001 negative control (NC) had no detectable effects in cytokines-driven barrier disruption at either 24h (48.40±1.14 vs 47.85±0.84 Ω/cm², p=0.72) or 48h (58.67±0.49 vs 59.77±0.49 Ω/cm², p=0.18) after treatment when compared with untreated monolayers (**Figure 4.12B**). However, in the presence of cytokines, GM6001 treated monolayers had a significantly higher TEER value than GM6001 NC at both, 24h (66.00±0.55 vs 48.40±1.14 Ω/cm², p<0.001) and 48h post-treatment (75.17±1.60 vs 58.67±0.49 Ω/cm², p<0.001) (**Figure 4.12C**). Thus, this seems to suggest that cytokines-driven loss in barrier integrity could be mediated by an increase in metalloproteinase activity.

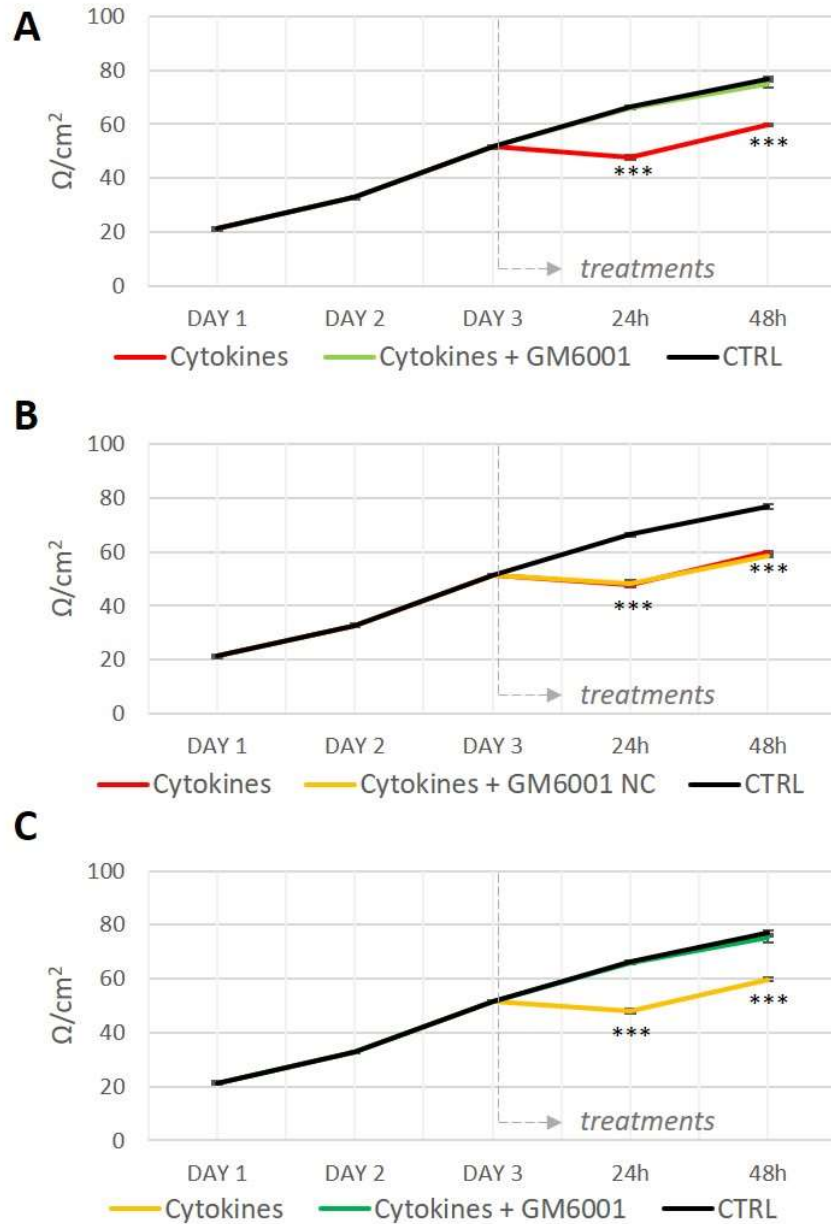


Figure 4.12 – Metalloproteinase inhibition rescues cytokine-driven loss of barrier integrity. hCMEC/D3 were seeded onto cell inserts (0.3µm porous) and grown for 3days until confluent in order to promote barrier formation. hCMEC/D3 monolayers when then treated with with a cytokines mix (TNFα and IL1α at 10µg/ml) in the presence or absence of a broad-spectrum metalloproteinase inhibitor (GM6001) for 24h and 48h. GM6001 negative control (NC) and untreated monolayers (CTRL) were used as controls Transendothelial Electrical Resistance (TEER) was measured to assess barrier integrity every 24h. Statistically significant differences were assessed via One-way ANOVA with post-hoc Tukey. Each bar represents the mean ±SEM for 3 wells. *** $p < 0.001$ to CTRL and/or cytokines and GM6001. Experiment replicated 3 times.

4.2.3.2. Metalloproteinase gene expression is increased under inflammatory conditions

Based on previous observations, it seems that cytokine mediated disruption of barrier stability could be metalloproteinase dependent. Thus, in order to identify possible candidates within the metalloproteinase family that could mediate the observed effects, steady state mRNA levels of a wide range of metalloproteinases selected from the literature (including MMPs, ADAMs and ADAMTSs) and their inhibitors (TIMPs) were measured in hCMEC/D3 treated monolayers at 24h after treatment coinciding with observed TEER effects. Confluent hCMEC/D3 monolayers were treated with cytokines (TNF α and IL1 α at 10ng/ml) before measuring steady state mRNA levels by qRT-PCR. Addition of cytokines significantly increased the expression levels of *MMP1* (53.70 ± 1.37 vs 1.02 ± 0.13 , $p < 0.001$), *-3* (1.78 ± 0.27 vs 1.00 ± 0.05 , $p < 0.05$), *-12* (3.56 ± 0.21 vs 1.01 ± 0.11 , $p < 0.001$), *-14* (2.08 ± 0.21 vs 1.07 ± 0.26 , $p < 0.05$), *ADAM8* (9.10 ± 0.16 vs 1.04 ± 0.20 , $p < 0.01$) and *TIMP1* (1.83 ± 0.09 vs 1.02 ± 0.15 , $p < 0.05$) when compared with untreated controls (**Figure 4.13**) (**Appendix 4.B**). In contrast, cytokine treatment significantly reduced *MMP2* (0.38 ± 0.01 vs 1.01 ± 0.12 , $p < 0.01$) and *TIMP2* (0.37 ± 0.01 vs 1.03 ± 0.16 , $p < 0.05$) mRNA levels when compared with untreated controls (**Figure 4.13**) (**Appendix 4.B**). *MMP10* expression was not detectable under physiological conditions but was induced after cytokine addition (average raw Cts measured went from undetected to 34.0; **Appendix 4.B**).

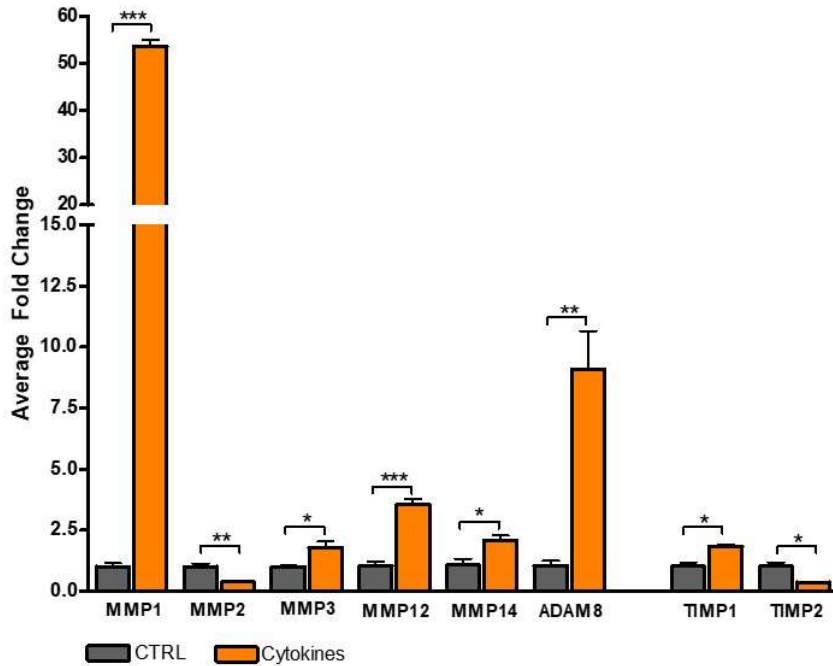


Figure 4.13 - Metalloproteinase mRNA levels are elevated under inflammatory conditions. hCMEC/D3 cells confluent monolayers were incubated with a mixture of cytokines (TNF α and IL1 α both at 10ng/ml) during 24h. After treatment, mRNA steady-state levels of a wide range of metalloproteinases and their inhibitors (TIMPS) were determined by qRT-PCR. All measurements were normalised to 18S endogenous control. Statistically significant differences were assessed via *t*-test. Each bar represents the mean \pm SEM for 3 wells. * *p* < 0.05; ** *p* < 0.01; *** *p* < 0.001. Representative experiment depicted. Experiment replicated >3 times.

4.2.3.3. Cytokine-driven increase in metalloproteinase expression can be partially reduced by a combination of Shh and Vitamin D3

A combination of Shh and Vitamin D3 was previously proven capable of rescuing cytokine-driven loss of barrier integrity. Since cytokine effects in barrier function were also metalloproteinase dependent, the effects of a combination of Shh and Vitamin D3 in metalloproteinase gene expression were assessed. Confluent hCMEC/D3 monolayers were treated with a mixture of cytokines (TNF α and IL1 α at 10ng/ml), Shh (100mg/ml) and Vitamin D3 (100nM) alone or in combination before measuring steady state mRNA levels by qRT-PCR. No effects of Shh and/or Vitamin D3 were reported in the presence or absence of cytokines 24h after treatment (**Appendix 4.C**). However, measurements at earlier time-points (4h, 8h and 12h) revealed an ability of combined Shh and Vitamin D3 to partially block cytokine-driven increase in *MMP3* (23.16 \pm 2.39 vs 39.98 \pm 5.14, p <0.05 at 8h and 20.64 \pm 3.14 vs 39.79 \pm 3.91, p <0.05 at 12h) and *MMP10* (93.33 \pm 13.43 vs 176.56 \pm 17.54, p <0.05 at 8h) mRNA levels (**Figure 4.14**) (**Appendix 4.D**). No Shh and Vitamin D3 mediated modulation was observed for other metalloproteinases at early time-points (data not shown).

Additionally, Shh and Vitamin D3 ability to modulate cytokines-mediated effects in TIMPs expression levels were also analysed. Interestingly, after 4h treatment, a combination of Shh and Vitamin D3 significantly increased *TIMP2* (2.52 \pm 0.08 vs 1.03 \pm 0.18, p <0.01) and *TIMP4* (2.51 \pm 0.36 vs 1.04 \pm 0.18, p <0.05) expression levels when compared with untreated controls (**Figure 4.15**) (**Appendix 4.E**). At 8h and 12h after treatment, cytokines addition significantly reduces *TIMP2* gene expression when compared with untreated controls (0.42 \pm 0.06 vs 1.03 \pm 0.18, p <0.05 at 8h and 0.46 \pm 0.08 vs 1.01 \pm 0.11, p <0.05 at 12h). A combination of Shh and Vitamin D3 did not alter the lower *TIMP2* levels seen with cytokine treatment (0.44 \pm 0.06 vs 1.03 \pm 0.18, p <0.05 at 8h and 0.47 \pm 0.09 vs 1.01 \pm 0.11, p <0.05 at 12h) (**Figure 4.15**) (**Appendix 4.E**). Interestingly, at 8h post-treatment, cytokine-driven reduction in *TIMP4* mRNA levels can be blocked by a combination of Shh and Vitamin D3 (0.44 \pm 0.09 vs 1.03 \pm 0.17, p <0.05; 0.95 \pm 0.27 vs 1.03 \pm 0.17, p =0.81), although this protection is lost at longer time-points (0.56 \pm 0.06 vs 1.00 \pm 0.05,

$p < 0.01$; 0.51 ± 0.01 vs 1.00 ± 0.05 , $p < 0.01$) (**Figure 4.15**). No Shh and Vitamin D3 mediated modulation was observed for other TIMPs at any of the studied time-points (data not shown).

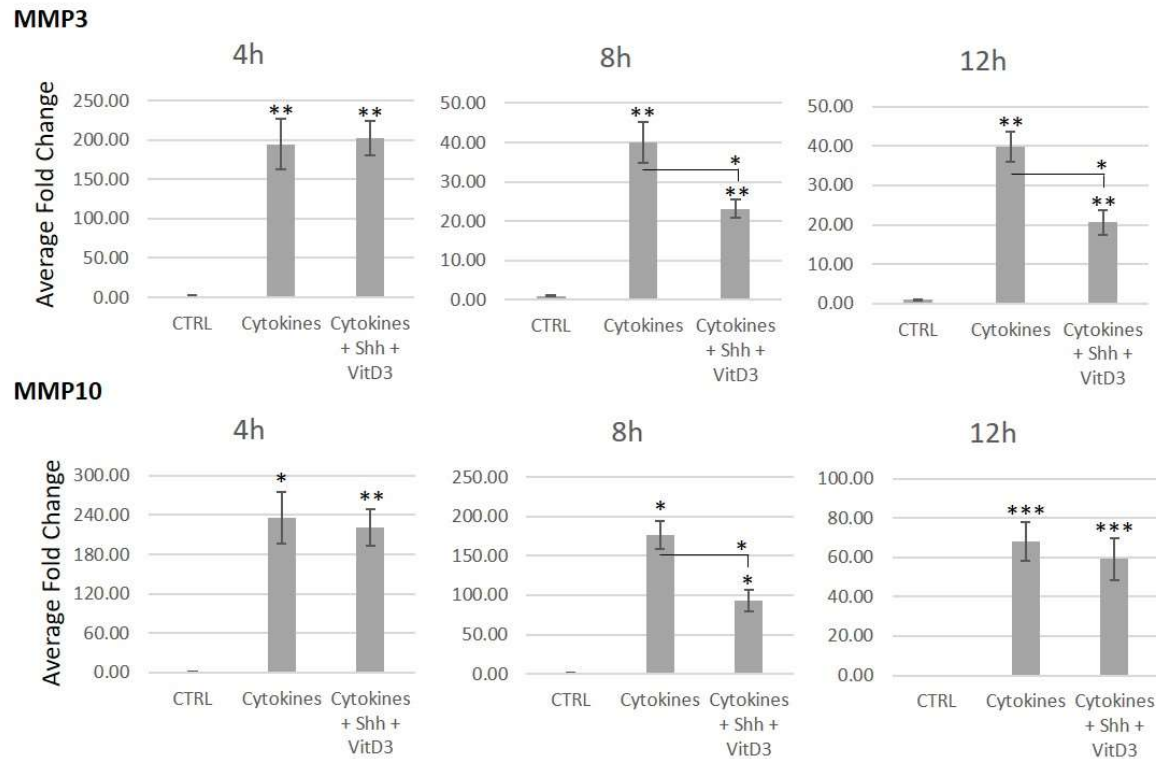


Figure 4.14 – A combination of Shh and Vitamin D3 can partially block cytokine-driven increase in metalloproteinase expression. hCMEC/D3 cells confluent monolayers were incubated with a mixture of cytokines (TNF α and IL1 α both at 10ng/ml) in the presence or absence of a combination of Shh (100ng/ml) and Vitamin D3 (100nM) (VitD3) during 4h, 8h and 12h. After treatment, mRNA steady-state levels of a MMP3 and -10 were determined by qRT-PCR. All measurements were normalised to 18S endogenous control. Statistically significant differences were assessed via One-way ANOVA with post-hoc Tukey. Each bar represents the mean \pm SEM for 3 wells. * $p < 0.5$; ** $p < 0.01$; *** $p < 0.001$. Representative experiment depicted. Experiment replicated 2 times.

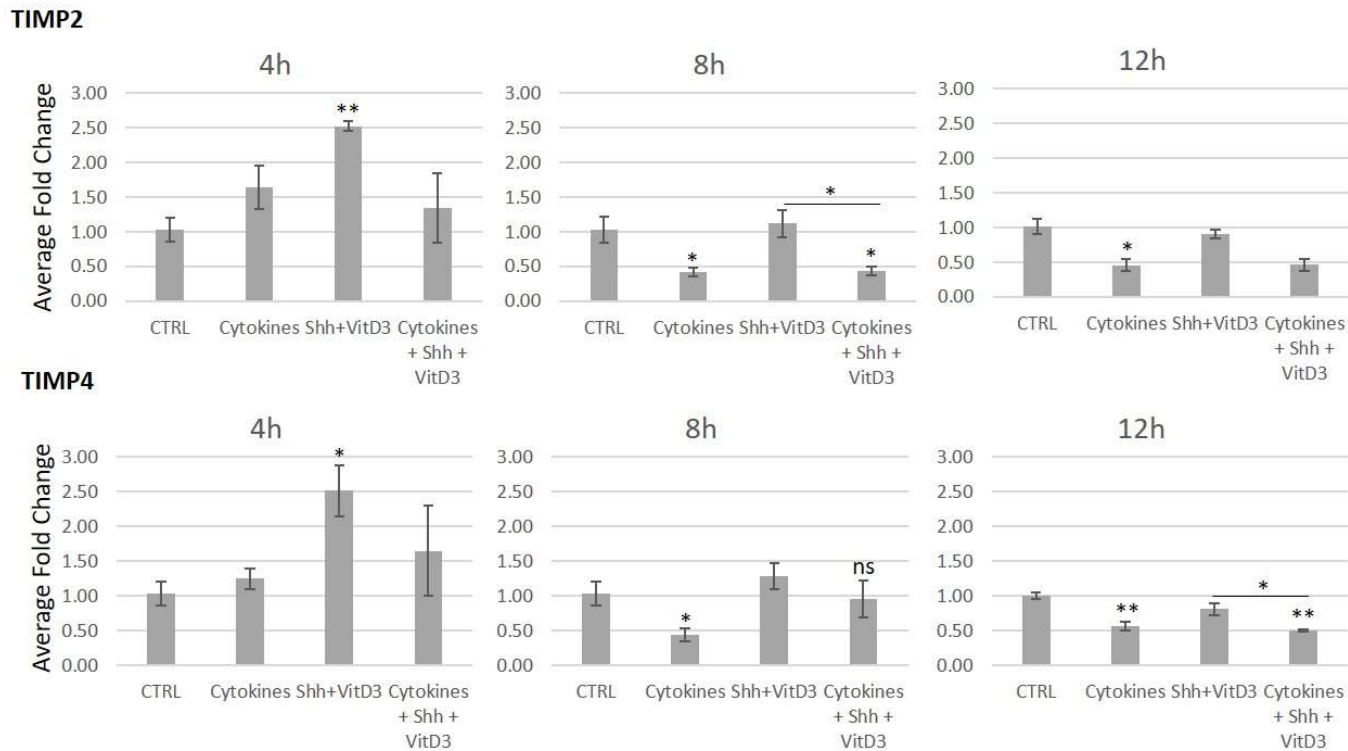


Figure 4.15 - A combination of Shh and Vitamin D3 can partially block cytokine-driven decrease in TIMP expression. hCMEC/D3 cells confluent monolayers were incubated with a mixture of cytokines (TNF α and IL1 α both at 10ng/ml) in the presence or absence of a combination of Shh (100ng/ml) and Vitamin D3 (100nM) (VitD3) during 4h, 8h and 12h. After treatment, mRNA steady-state levels of a TIMP2 and -4 were determined by qRT-PCR. All measurements were normalised to 18S endogenous control. Statistically significant differences were assessed via One-way ANOVA with post-hoc Tukey. Each bar represents the mean \pm SEM for 3 wells. * $p < 0.5$; ** $p < 0.01$; *** $p < 0.001$. Representative experiment depicted. Experiment replicated 2 times.

4.2.3.4. Cytokine-driven increase in secreted metalloproteinase protein levels can be partially reduced by a combination of Shh and Vitamin D3

In order to test if the observed regulation of *MMP1*, *3* and *10* mRNA levels correlated with protein changes, the levels of secreted MMP1, 3 and 10 into the upper Transwell chamber (“apical” side) were studied by Western blot of TCA precipitated hCMEC/D3 media. Addition of a combination of Shh and Vitamin D3 significantly reduced media levels of MMPs 1 and 3 (0.38 ± 0.14 vs 1.00 ± 0.00 , $p < 0.05$ for MMP1 and 0.32 ± 0.08 vs 1.00 ± 0.00 , $p < 0.05$ for MMP3; 50kDa band measured in all cases). In contrast, cytokine treatment triggered a significant increase in MMP1 and 3 media levels when compared with untreated controls (5.36 ± 1.49 vs 1.00 ± 0.00 , $p < 0.05$ for MMP1 and 3.87 ± 0.50 vs 1.00 ± 0.00 , $p < 0.05$ for MMP3) (**Figure 4.16**). Cytokines effect was completely blocked by the addition of a combination of Shh and Vitamin D3 (1.99 ± 0.71 vs 1.00 ± 0.00 , $p > 0.05$ for MMP1 and 1.70 ± 0.70 vs 1.00 ± 0.00 , $p > 0.05$ for MMP3) (**Figure 4.16**). Two protein bands for MMP3 were detected. Since metalloproteinases need to be proteolytically activated, the appearance of a smaller band at approximate 47kDa for MMP3 could correspond to a processed form. Thus, cytokines addition would predominantly increase MMP3’s potential active form, which was practically absent in the presence of a Shh and Vitamin D3 combination (**Figure 4.16**). Due to the high concentration of albumin (66kDa) in the TCA precipitated media, a white band (ghost band) can be observed above the 50kDa mark. Although this presence did not interfere with protein quantification, in some cases proteins of interest may seem to migrate slightly lower due to the albumin distortion.

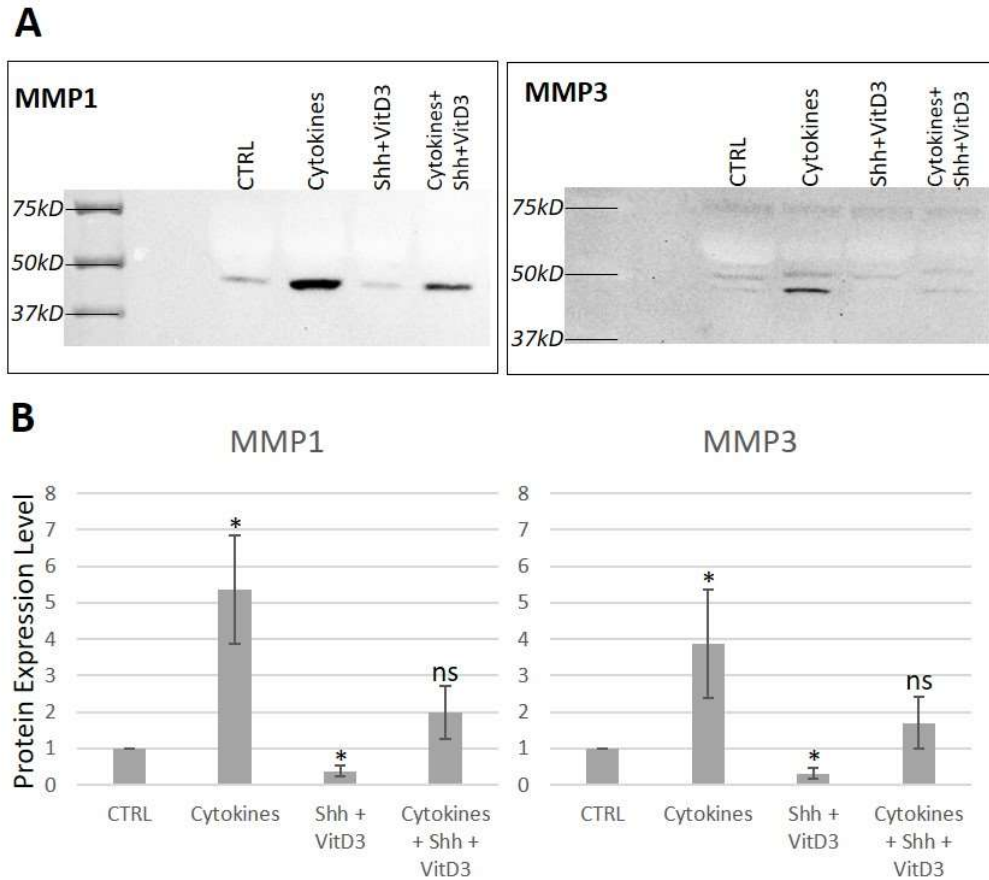


Figure 4.16 - A combination of Shh and Vitamin D3 can partially protect against cytokine-driven metalloproteinase extracellular accumulation. hCMEC/D3 cell confluent monolayers treated with a mixture of cytokines (TNF α and IL1 α both at 10ng/ml) in the presence or absence of a combination of Shh (100ng/ml) and Vitamin D3 (100nM) (VitD3) during 24h. (A) 24h after treatment extracellular apical levels of MMPs 1 and 3 were determined by Western Blotting. (B) Optical density of total protein was quantified and normalised to untreated controls (CTRL). Statistically significant differences were assessed via One-way ANOVA with post-hoc Tukey. Each bar represents the mean \pm SEM for 3 wells. * $p < 0.5$. Representative experiment depicted. Experiment replicated 3 times.

Regarding MMP10 secreted levels, preliminary WB analysis showed a potentially similar regulation to that observed for MMP1 and 3: addition of a Shh and Vitamin D3 seemed to decrease secreted MMP10 levels (**Figure 4.17**). As observed for MMP3, there is a MMP10 smaller band in the presence of cytokines but this does not correspond to the expected molecular mass for MMP10's fully processed form. The presence of a combination of Shh and Vitamin D3 seemed to reduce total MMP10 extracellular levels (**Figure 4.17**). However, due to the discrepancies between MMP10 mRNA levels (undetected in untreated cells) and observed levels of secreted protein no further experiments were performed regarding MMP10 protein.

Very low levels of secreted MMP1, and 3 were detected in the lower (basal) compartment of our *in vitro* BBB model, and were not modulated by any of the used treatments (**Figure 4.18**). Higher levels of MMP10 were secreted into the basal chamber (in comparison with MMP1 and MMP3 basal measurements) and addition of cytokines seemed to trigger an increase in MMP10 secreted basal levels that could be partially reduced by addition of Shh and Vitamin D3 (**Figure 4.18**). However, as it has been previously stated, due to the discrepancies between MMP10 mRNA levels (undetected in untreated cells) and observed levels of secreted protein no further experiments were performed regarding MMP10 protein. In any case, due to the low detection and lack of modulation on MMP1 and MMP3 secreted basal levels, future experiments will focus on the study of apical levels.

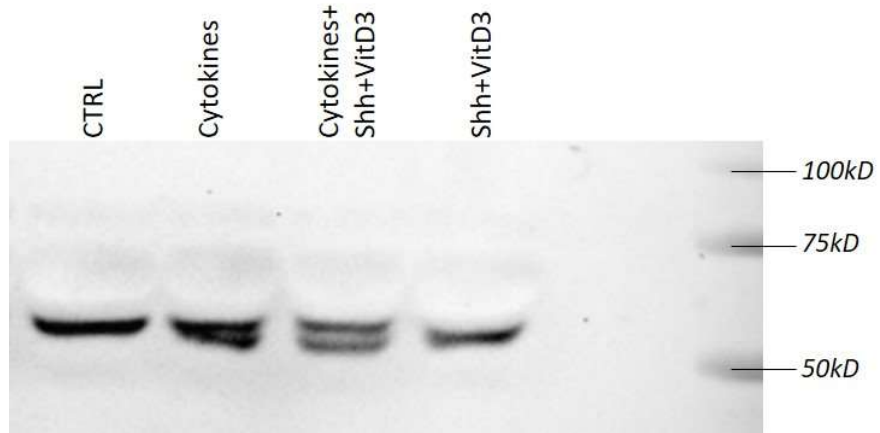


Figure 4.17 - A combination of Shh and Vitamin D3 can partially protect against cytokine-driven increase in MMP10 expression. hCMEC/D3 cells confluent monolayers were incubated with a mixture of cytokines (TNF α and IL1 α both at 10ng/ml) in the presence or absence of a combination of Shh (100ng/ml) and Vitamin D3 (100nM) (VitD3) during 24h. After treatment, secreted apical levels of MMP10 were determined by Western Blotting.

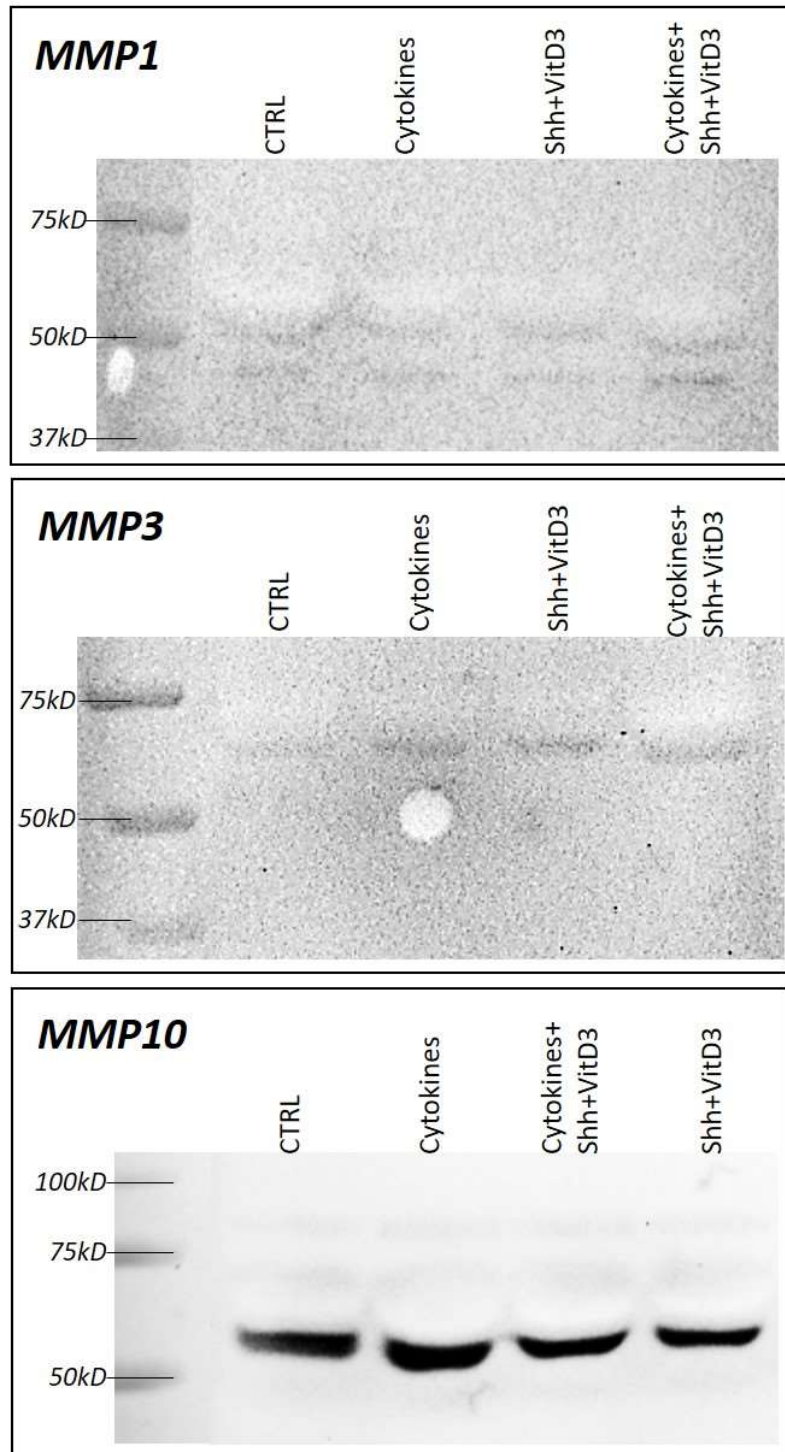


Figure 4.18 – Modulation of MMP1, 3 and 10's basal secreted levels. hCMEC/D3 cells confluent monolayers were incubated with a mixture of cytokines (TNF α and IL1 α both at 10ng/ml) in the presence or absence of a combination of Shh (100ng/ml) and Vitamin D3 (100nM) (VitD3) during 24h. After treatment, secreted basal levels of MMP1, 3 and 10 were determined by Western Blotting.

4.2.3.5. A combination of Shh and Vitamin D3 partially blocked cytokine-driven increase in MMP3 intracellular levels

As previously seen, a combination of Shh and Vitamin D3 triggered a reduction in MMP1 and -3 secreted protein levels. Conversely, no variation was reported in MMP1 and -3 gene expression levels at any of the studied time-points after Shh and Vitamin D3 exposure. Thus, in order to further investigate the observed disparity between gene expression and extracellular, secreted protein levels, intracellular levels of MMP1 and -3 were measured. MMP1 intracellular levels were too low to be detected (data not shown) but preliminary experiments showed a small cytokine-driven increase in MMP3 intracellular levels that could be partially blocked by addition of a combination of Shh and Vitamin D3 (**Figure 4.19**). No variations were observed in MMP3 intracellular levels after exposure to a combination of Shh and Vitamin D3 (**Figure 4.19**). Thus, changes in intracellular MMP3 levels seemed to follow similar trends to the variations observed in *MMP3* gene expression after the afore mentioned treatments.

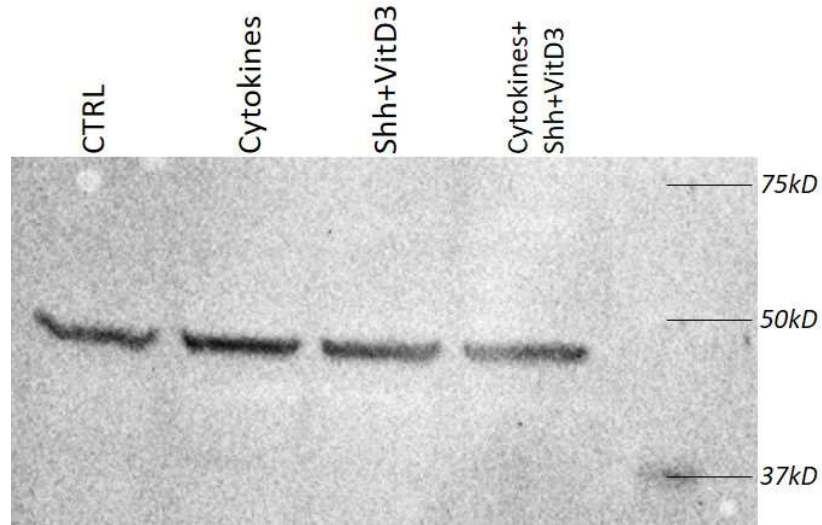


Figure 4.19 - A combination of Shh and Vitamin D3 partially blocks cytokine driven increase in MMP3 intracellular levels. hCMEC/D3 cells confluent monolayers were incubated with a mixture of cytokines (TNF α and IL1 α both at 10ng/ml) in the presence or absence of a combination of Shh (100ng/ml) and Vitamin D3 (100nM) (VitD3) during 24h. After treatment, total intracellular levels of MMP3 were determined by Western Blotting. Preliminary experiment shown.

4.2.3.6. Cytokines-mediated reduction in *LRP1* mRNA levels can be blocked by addition of a combination of Shh and Vitamin D3

The observed discrepancies between MMP3 intracellular and secreted protein levels, could be explained by alterations in MMP3 endocytosis mechanism. In order to study this hypothesis, expression levels of *LRP1* were analysed by qRT-PCR of hCMEC/D3 confluent monolayers treated with a combination of Shh (100ng/ml) and Vitamin D3 (100nM) in the presence and absence of a cytokines mix (TNF α and IL1 α both at 10ng/ml). After 4h treatment, addition of cytokines triggered a significant decrease in *LRP1* expression levels (0.44 ± 0.02 vs 1.01 ± 0.10 , $p<0.01$) that could be completely blocked by the addition of Shh and Vitamin D3 (1.43 ± 0.47 vs 1.01 ± 0.10 , $p=0.43$) (**Figure 4.20**). However, the Shh and Vitamin D3 effect against cytokine-driven reduction in *LRP1* mRNA levels was lost at longer incubation times (**Figure 4.20**). Interestingly, a small, but significant increase in *LRP1* gene expression levels was reported after 8h treatment with Shh and Vitamin D3 (1.39 ± 0.04 vs 1.01 ± 0.08 , $p<0.05$) (**Figure 4.20**). Thus, this observation opens the possibility that the observed modulation in MMP3 extracellular protein levels could be not only due to changes in *MMP3* gene expression but also to alterations in LRP1-mediated endocytosis.

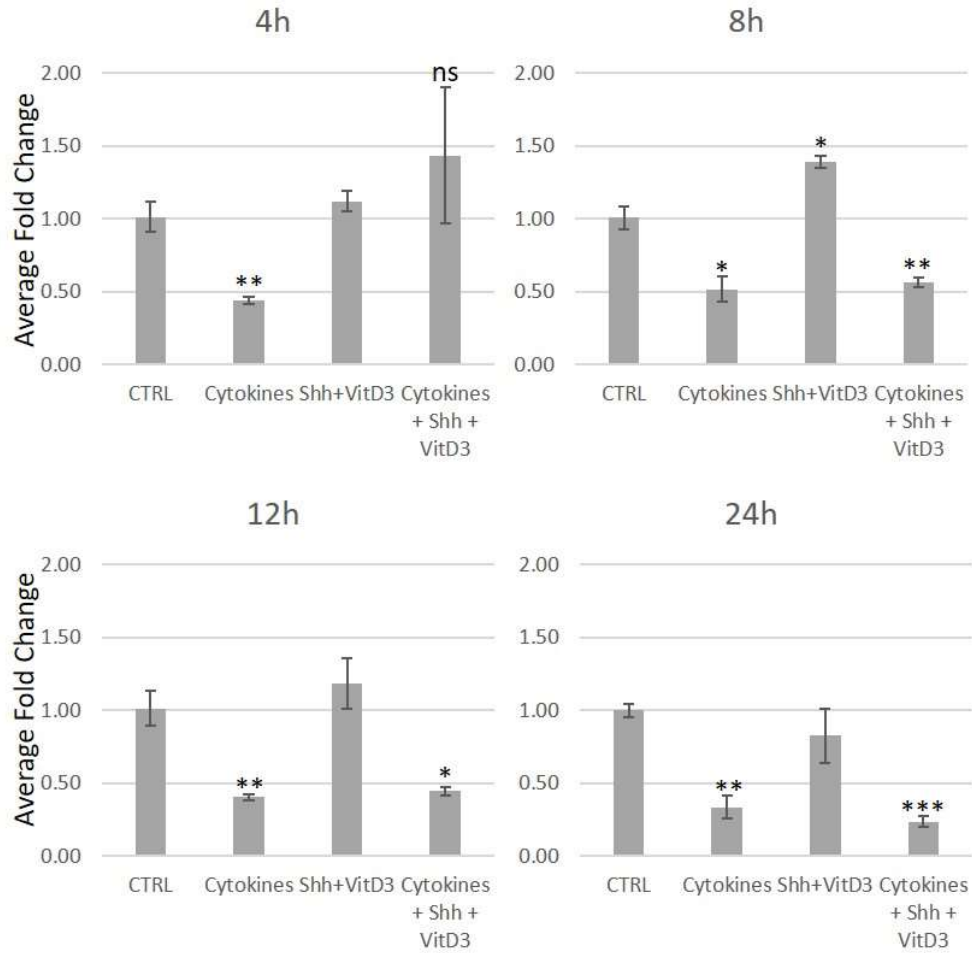


Figure 4.20 – Cytokines, Shh and Vitamin D3 modulate LRP1 expression at early time-points. *hCMEC/D3* cells confluent monolayers were incubated with a mixture of cytokines (TNF α and IL1 α both at 10ng/ml) in the presence or absence of a combination of Shh (100ng/ml) and Vitamin D3 (100nM) (VitD3) during 4h, 8h, 12h and 24h. After treatment, mRNA steady-state levels of a TIMP2 and -4 were determined by qRT-PCR. All measurements were normalised to 18S endogenous control. Statistically significant differences were assessed via One-way ANOVA with post-hoc Tukey. Each bar represents the mean \pm SEM for 3 wells. * $p < 0.5$; ** $p < 0.01$; *** $p < 0.001$. Representative experiment depicted. Experiment replicated 2 times.

4.2.3.7. Endocytosis mechanisms could be underlying the observed variations in secreted MMP3 levels

The observed modulation in *LRP1* levels seem to suggest that the reported changes in MMP3 extracellular protein levels could be at least partially explained by a deregulation of endocytic mechanisms. Preliminary experiments using Cytochalasin D (CytoD; a pharmacological inhibitor of endocytosis) showed that MMP3 extracellular levels were enhanced under CytoD-mediated broad inhibition of endocytosis (**Figure 4.21**). Intriguingly, Shh and Vitamin D3 driven reduction of MMP3 secreted levels in the presence of cytokines was less obvious than previously seen, but this could be attributed to experimental variation (**Figure 4.21**). In any case, Shh and Vitamin D3 seem to trigger a slight reduction in MMP3 secreted levels in the absence of cytokines that can be reversed by the addition of CytoD (**Figure 4.21**). Note that in the presence of CytoD more MMP3 is detected in media under all conditions.

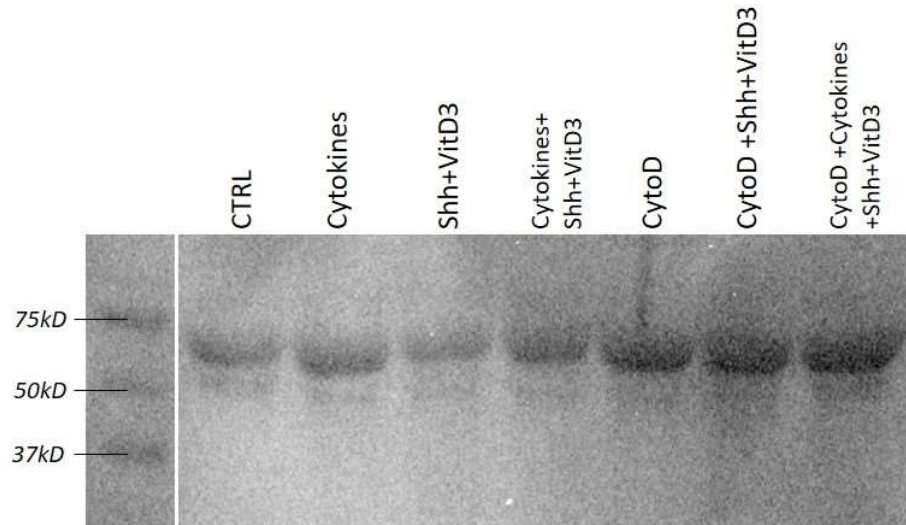


Figure 4.21 – Shh and Vitamin D3 effect in MMP3 secreted levels is endocytosis-dependent. hCMEC/D3 cells confluent monolayers were incubated with the inhibitor of endocytosis Cytochalasin D (CytoD; 1mM), a mixture of cytokines (TNF α and IL1 α both at 10ng/ml) and/or a combination of Shh (100ng/ml) and Vitamin D3 (100nM) (VitD3) during 24h. After treatment, total levels of secreted MMP3 were determined by Western Blotting.

4.3. DISCUSSION

4.3.1. hCMEC/D3 as a model of the BBB

Many immortalised cell lines have been used to generate *in vitro* models of the BBB. A currently available and well characterised brain endothelial cell line previously used in *in vitro* models of the BBB is hCMEC/D3 (reviewed in Weksler et al., 2013). Under static culture conditions like the ones used in our studies, hCMEC/D3 have been reported by previous studies to develop TEER values between 30-50 Ω /cm² when cultured for up to 5 days (reviewed in Weksler et al., 2013). In this regard, our monoculture of hCMEC/D3 behaved as previously described, retrieving TEER values of 50 Ω /cm² when cultured for 3-5 days. Since our *in vitro* BBB model reached the typical TEER values associated with hCMEC/D3 monolayers following 3 days of culture, this was the chosen incubation time to allow barrier formation before treatment addition. Occasionally, higher TEER values were observed for hCMEC/D3 monolayers (between 60-80 Ω /cm²) but, in our experience, these differences have been due to the addition of fresh culture media containing the relevant treatments and a slight reduction in TEER is observed as the monolayers equilibrate with the newly added media. Similar TEER values have been reported by Ni *et al.* although in their *in vitro* setting hCMEC/D3 monolayers were cultured for up to 7 days (Ni et al., 2017). Interestingly, a comparative study of 4 immortalised brain capillary endothelial cell lines reported TEER values for hCMEC/D3 around 10 Ω /cm² at days 3 and 4 after culture (Eigenmann et al., 2013). However, the striking difference in reported TEER values could be due to the use by Eigenmann *et al.* of an automated system (CellZscope) in the assessment of TEER rather than the classic chopstick electrode system (Eigenmann et al., 2013). Interestingly, Eigenmann *et al.* comparative studies also report a slight increase in TEER values of approximate 25% between days 3 to 4 after culture as the one observed in our model for days 3 to 5, attributing this to minor junctional maturation processes (Eigenmann et al., 2013). It is possible that the increase in TEER values detected during the first 3 days

of culture was not only due to the formation of an endothelial barrier but also to cell expansion. Although it is probably due to a combination of both, the fact that TEER values get stabilised between the third and fifth days of culture seems to indicate that cell expansion is inhibited by cell-to-cell contacts, allowing for the formation of a mature single-cell endothelial barrier.

Regarding serum concentrations, hCMEC/D3 have been previously reported to retrieve typical TEER values of 50-80 Ω /cm² when, after 5 days culture, serum concentration was lowered to 0.25% (Forster et al., 2008). Agreeing with this observation, culture with a lower serum concentration (0.25%FCS) for up to 5 days after cell seeding did not result in any significant differences in barrier formation and maturation when compared with cells cultured in the recommended serum concentration (5%FCS) (**Figure 4.2**).

4.3.1.1. Pro-inflammatory cytokines can enhance barrier permeability in hCMEC/D3 monolayers

The effects of pro-inflammatory cytokines in hCMEC/D3 mono-cellular models of the BBB have been broadly reported. Förster *et al.* studied the effects of TNF α addition in hCMEC/D3 monolayers, showing a significant reduction barrier stability assessed through both TEER and Dextran Extravasation measurements (Forster et al., 2008). Ni *et al.* also observed a significant reduction in *in vitro* BBB integrity in hCMEC/D3 monolayers treated with TNF α or IL1 β (Ni et al., 2017). Corroborating the previous observations, addition of a combination of TNF α and IL1 α to our *in vitro* monolayer of hCMEC/D3 cells triggered a significant reduction in TEER levels (**Figure 4.3**). In terms of the degree of disruption caused by the addition of pro-inflammatory cytokines, a similar reduction to that observed in the current study was reported by Förster *et al.* (\approx 60%), whereas the decrease in TEER values observed by Ni *et al.* was less acute (\approx 20%). These differences could be due to the different treatments employed in each study: while Förster *et al.* used TNF α (174ng/ml), Ni *et al.* individually stimulated hCMEC/D3 monolayers with TNF α (10ng/ml) or IL1 β (10ng/ml). Thus, it is possible that although at the same concentration, individual addition of TNF α or IL1 β cannot trigger barrier

disruption to the same extent than a combination of TNF α and IL1 α (also, differences between IL1 α and IL1 β should be considered). In this regard, the much higher concentration of TNF α used in Förster *et al.* could trigger a similar reduction in TEER values than the combination of TNF α and IL1 α used in our model (Forster et al., 2008; Ni et al., 2017). In any case, the barrier-disruptive effect of pro-inflammatory cytokines in BBB *in vitro* models seems to be well established.

4.3.1.2. Vitamin D3 as a BBB enhancing agent

Using our *in vitro* model of the BBB, we reported an ability of Vitamin D3 to enhance hCMEC/D3 barrier properties, as a significant increase in TEER values was detected in Vitamin D3 treated monolayers (**Figure 4.4**). Vitamin D3 has been shown previously to promote endothelial barrier formation through enhancement of tight junctions in endothelial cells from other sources (Palmer et al., 2001; Fujita et al., 2008; Yin et al., 2011). Vitamin D3 also impacts on epithelial cell barriers. Supporting our observations, Vitamin D3 treatment triggers an increase in TEER in intestinal epithelial cells (Chirayath et al., 1998; Chen et al., 2015), whereas in airway epithelial cells no TEER effects were reported (Zhang et al., 2016).

In the context of the BBB, Vitamin D3 ability to enhance barrier stability (measured as TEER values) in an *in vitro* model of the BBB has not been previously described in the published literature. However, supporting the observed role of Vitamin D3 as a BBB protective agent, intranasal Vitamin D3 administration in a rat model of subarachnoid haemorrhage significantly decreased brain oedema (measured as brain water content) and Evans blue extravasation (Enkhjargal et al., 2017). Overall, Vitamin D3 seems to be a very well-established promoter of barrier integrity, and some of the mentioned discrepancies may be due to cell line associated variations.

4.3.1.3. Shh promotes BBB stability

The ability of Shh to promote BBB formation has been broadly described in the literature: using primary BBB-ECs isolated from human patients and cultured in cell inserts, Alvarez *et al.* showed that addition of

human recombinant Shh can decrease barrier permeability measured as TEER and BSA-FITC Extravasation (Alvarez et al., 2011); addition of mShh could reverse IL1 β -induced permeability (measured as BSA-FITC permeability) in confluent mouse brain capillary ECs monolayers (Wang et al., 2014); *in vivo* studies showed that activation of Hedgehog pathway through a Smo agonist can rescue BBB integrity in HIV infected mice (Singh et al., 2016). In this regard, the observed effects of Shh in our *in vitro* system corroborate and extend those of previous studies, as addition of Shh triggered a significant increase in TEER values and, thus, BBB properties in hCMEC/D3 cells (**Figure 4.4**).

Under normal physiological conditions, Shh is provided to BBB-ECs through secretion from astrocyte end-feet (Luissint et al., 2012). In this regard, more complex *in vitro* BBB models have established a co-culture of hCMEC/D3 together with astrocytes, reporting a significant increase in barrier properties (measured as TEER values) (Hatherell et al., 2011) together with a significant reduction in paracellular permeability (Kulczar et al., 2017). In all these co-culture systems the source of Shh is located in the basal side of the ECs monolayer. However, when Shh is added as an external treatment to confluent ECs monolayers, the site of addition is not typically specified. Since in the current study Shh was added into the apical side of the hCMEC/D3 monolayer in order to minimise treatment variability, the effects of Shh's addition to the apical and/or basal side of a polarised ECs monolayer were assessed for the first time. No differences in Shh's ability to increase TEER values in confluent hCMEC/D3 monolayers were observed regardless of the site of addition (basal, apical or both) (**Figure 4.5**) possibly due to diffusion and/or transcytosis mechanisms that equilibrate treatments' concentration across both chambers of the insert. However, taking into account that this is an *in vitro* model in which only a monolayer of ECs are grown over a layer of collagen I, it is more likely that diffusion mechanisms (rather than transcytosis) are the ones allowing a small molecule such as Shh (20kDa) to trigger an effect in barrier permeability regardless of the site of addition.

4.3.1.4. Cytokine-driven loss in barrier integrity can be synergistically rescued by a combination of Shh and Vitamin D3

In order to study Shh and Vitamin D3 role as barrier promoters, their ability to protect barrier integrity in the presence of cytokines was tested. Shh ability to protect against inflammatory-mediated loss of barrier stability has already been reported by Singh et al. In a murine model of Human Immunodeficiency Virus (a disorder characterized by chronic neuro-inflammation), treatment with a pharmacological agonist of the Hedgehog pathway rescued claudin-5 expression, a marker of barrier integrity, to WT levels (Singh et al., 2016). Interestingly, in our *in vitro* barrier model exogenous Shh was not capable of protecting against cytokine-associated barrier dysfunction (measured as TEER) (**Figure 4.6**). Regarding Vitamin D3, no previous protective effect has been described in the context of ECs. However, *in vitro* studies with intestinal epithelial cells shown a Vitamin D3 barrier protective effect (measured as TEER and dextran extravasation) against TNF α driven barrier dysfunction (Chen et al., 2015a). Nonetheless, no Vitamin D3 protective effect against cytokines and cyclopamine associated lost on barrier integrity was reported in our *in vitro* model (measured as TEER) (**Figure 4.6**).

Interestingly, when combined, Shh and Vitamin D3 not only completely abrogated cytokine-mediated loss in barrier integrity but also promoted barrier formation above control levels at 24h (**Figure 4.6**). This protective synergy between Shh and Vitamin D3 has not yet been reported in the literature, but it supports the previously described existence of a cross-talk between the Hedgehog and Vitamin D3 pathways in the context of endothelial barriers (Bijlsma et al., 2006). In this regard, Bijlsma *et al.* observed that Ptch could be functioning as a translocator of Vitamin D3 (or one of its metabolites) (Bijlsma et al., 2006), opening the possibility that Shh and Vitamin D3 synergy is operated though an Shh-mediated inhibition of Ptch, no longer able to work as a translocase, increasing intracellular levels of Vitamin D3. Further studies regarding the effects of Ptch inhibition in the presence of Vitamin D3 and cytokines are needed to test this hypothesis.

4.3.2. hCMEC/D3 and junctional ZO-1 visualization

Since 2005, when human brain endothelial cells were immortalised to form the hCMEC/D3 cell line (Weksler et al., 2005), these cells have been established as an appropriate system for BBB *in vitro* modelling. Although the subject of several studies, there is a lack of consensus when it comes to the immunofluorescent analysis of Tight Junction proteins in cultured hCMEC/D3 monolayers. As recommended by the manufacturer, hCMEC/D3 monolayers should be cultured on collagen I coated surfaces, but no further mention is made regarding the nature of the culture surface. When looking in the literature, a wide range of cultured surfaces are used in tight junction immunostaining protocols. For example, collagen I coated transwells have been used to study ZO-1 junctional stability in hCMEC/D3 monolayers, although in the reported staining was too weak to observe junctional integrity (Miao et al., 2015) or was obscured by an elevated cytoplasmic localization of ZO-1 (Luissint et al., 2012). Collagen I coated glass slides are the most widely used cultured surface for the immunofluorescent study of tight junction stability in hCMEC/D3 monolayers, reporting a clear visualisation of ZO-1 in the peripheral and continuous distribution characteristic of confluent EC monolayers (Weksler et al., 2005; Lopez-Ramirez et al., 2012; Liu et al., 2014; Sajja et al., 2014). Trying to mimic these results, hCMEC/D3 cells were seeded on collagen I coated glass coverslips and incubated for 8 days as previously performed in the literature (Luissint et al., 2012; Sajja et al., 2014). Occasionally an under layer of confluent and differentiated hCMEC/D3 cells was visible with a classical junctional ZO-1 as previously reported in the literature (Weksler et al., 2005; Lopez-Ramirez et al., 2012; Liu et al., 2014; Sajja et al., 2014). Additionally, when the underlying layer of hCMEC/D3 was visible in cytokine-treated conditions, it revealed a more punctate and discontinuous ZO-1 membrane distribution with an increase in cytosolic levels (**Figure 4.8**). A similar effect of a mix of cytokines (TNF α and IFN γ) in junctional ZO-1 had been previously reported for hCMEC/D3 monolayers (Lopez-Ramirez et al., 2014).

In order to prevent cellular over-growth and overlapping, ZO-1 staining was performed in cells cultured from 3 to 8 days (**Figure 4.9**). Unfortunately, cellular overlapping was reported even in under confluent monolayers. Intriguingly, studies done in collagen I coated glass coverslips reported a blurry and faint ZO-1, without a clear membrane distribution or monolayer formation (Tai et al., 2010) very similar to the one observed in the current study. Thus, further scrutiny of the terminology used in the literature revealed that the term “glass slides” referred to the commercially available cell-culture treated Thermanox coverslips and not plain glass coverslips coated with collagen I like the ones used by Tai *et al* or in this study. Thus, it seems that hCMEC/D3 cells are not capable of forming single-cell monolayers when cultured on glass surfaces (despite the collagen I coating), growing in a multi-layered formation that impairs junctional study. Future studies should focus on the use of cell-culture treated coverslips suitable for microscopy.

Analysis of ZO-1 total protein levels were performed by Western Blotting (**Figure 4.10**). However, due to time restraints, the methodology could not be fully optimised. The observed decrease in ZO-1 mRNA levels (**Figure 4.11**) could account for the possible reduction in ZO-1 junctional levels observed in preliminary immunofluorescence assessments (**Figure 4.8**). Not many studies refer to Shh or Vitamin D3 effects on ZO-1 mRNA levels, as effects in junctional regulation are typically assessed through Western Blotting or immunofluorescence techniques. However, Shh has been shown to increase ZO-1 mRNA levels in a murine model of permanent middle cerebral artery occlusion (Xia et al., 2013). The few studies analysing Vitamin D3 ability to modulate ZO-1 gene expression may suggest variations in Vitamin D3-mediated regulation depending on the cell type studied. For example, no changes were reported for ZO-1 mRNA levels in Vitamin D3 treated human airway epithelial cells (Zhou et al., 2011) whereas studies in VDR knockout mice reported a decreased expression of occludin and ZO-1 in the corneal epithelium (Elizondo et al., 2014). To our knowledge data is not available regarding Shh and/or Vitamin D3 regulation of ZO-1 gene expression in BBB *in vitro* monolayers, but studies in a mouse brain EC cell line have shown Vitamin D3’s ability to protect against the increase in barrier permeability and

decrease in junctional protein levels (ZO-1, claudin 5 and occludin) reported after hypoxia (Won et al., 2015). Similarly, cytokine effects on ZO-1 levels are typically assessed at the protein level, although some data is available regarding gene expression regulation: ZO-1 mRNA levels were significantly reduced in TNF α stimulated human umbilical vein ECs (Zhang et al., 2017). Addition of TNF α to rabbit isolated corneas (Hu et al., 2013) or murine intestinal sections (Song & Liu, 2009) had no effect in ZO-1 mRNA levels. Again, cytokines effect on ZO-1 gene expression could be dependent on the tissue or cell type studied.

4.3.3. Metalloproteinases and BBB integrity

4.3.3.1. Cytokine-driven loss in barrier integrity is metalloproteinase dependent

Under inflammatory conditions, an up-regulation of a wide range of metalloproteinases have been reported by the literature (reviewed in Rempe et al., 2016). In turn, this increase in metalloproteinase levels can trigger the degradation of junctional and basement membrane elements such as claudins, occludins and ZO-1 proteins (Yang et al., 2007; Lu et al., 2009; Bauer et al., 2010; Wu et al., 2015) among others. Several studies using broad spectrum metalloproteinase inhibitors point to metalloproteinases as main mediators of BBB disruption: administration of a broad-spectrum metalloproteinase inhibitor in a rat model of meningitis (Paul et al., 1998), stroke (Pfefferkorn & Rosenberg, 2003), or a murine model of multiple sclerosis (Gijbels et al., 1994) (all pro-inflammatory disorders) resulted in suppression BBB permeability. Additionally, studies in rat brain microvascular ECs showed that IL-1 β induced permeability could be attenuated by the broad-spectrum MP inhibitor, GM6001 (Alluri et al., 2016). Here full inhibition of cytokine-mediated loss in barrier stability in the presence of GM6001 was also demonstrated in hCMEC/D3 cells (**Figure 4.12**).

Cytokines have been reported to modulate a wide range of metalloproteinases. In order to study which metalloproteinases could be behind of the observed cytokines-driven changes in TEER levels, the gene expression of a wide range of metalloproteinases reported to be linked with

BBB breakdown during pro-inflammatory disorders was measured. Of the assessed MPs, MMPs 1, 3, 12, 14 and ADAM8 were up-regulated by cytokines at 24h after treatment (**Figure 4.13**). In vitro studies in human microvascular ECs revealed an increase in secreted MMP1 following TNF α stimulation (Jackson & Nguyen, 1997), and studies in fibroblasts cultured under normoxic or hypoxic conditions reported an increase in MMP1 levels after IL1 β stimulation (Lee et al., 2012). TNF α has been previously reported to induce MMP3 (and MMP1) gene expression in mouse intervertebral disc (Fujita et al., 2012), human adult dermal fibroblasts (Ono et al., 2018) and in Nucleus Pulposus Cells (Wang et al., 2014). Studies on primary smooth muscle cells showed a TNF α and IL1 β -mediated increase in MMP12 levels (mRNA and protein) (Xie et al., 2005), and studies of gene expression in human microvascular ECs reported an increase in MMPs 3, 10 and -2 (Roy et al., 2006) or MMPs 3, 10 and 13 in human periodontal ligament cultured cells (Ahn et al., 2014). Studies in cultured callus cells and articular chondrocytes reported a TNF α -mediated increase in MMP14 mRNA levels (Lehmann et al., 2005) but information is lacking in endothelial cells. In brain regions affected by neurodegeneration, TNF α has been shown to trigger an increase in ADAM8 by neurons, astrocytes and microglia (Schlomann et al., 2000; Bartsch et al., 2010).

In contrast to the above data, cytokine treatment resulted in a reduction in MMP2 mRNA levels (**Figure 4.13**). Of interest here, MMP2 (together with MMP13 and -14), can participate in the resolution of inflammation through the cleavage of Macrophage chemoattractant protein 3 (MCP-3) (McQuibban et al., 2000) and the pro-inflammatory chemokine fractalkine, that can be cleaved by MMP2 into a soluble antagonist (Dean & Overall, 2007). However, MMP2's role during inflammation could be much more complex as a compensatory mechanism between MMP2 and -9 has been described in a murine model of MS (Yang et al., 2007). In addition, inhibition of TNF α signalling reduced hypoxia-associated increase in MMP2 secreted levels in human brain microvascular ECs (Abdullah et al., 2015).

Regarding TIMPs, cytokines-mediated an increase in TIMP1 but a decrease in TIMP2 expression levels (**Figure 4.13**). Conflicting with the

observed up-regulation of TIMP1, low serum levels of TIMP1 have been previously correlated with endothelial barrier disruption in various clinical studies (Lee et al., 1999; Waubant et al., 1999; Toft-Hansen et al., 2004). However, more recent studies showed an increase in TIMP-1 serum from HIV-patients under inflammation (Xing et al., 2017). Additionally, studies in TIMP-1 deficient mice showed an increased in activated immune cells transmigration across the BBB during viral encephalomyelitis. This study reported no compensatory expression of other TIMPs, altered MMP expression or impaired chemokine production when compared with WT mice, suggesting the existence of an MMP-independent role of TIMP1 (Savarin et al., 2013). That being said, it needs to be considered that Savarin *et al.* only study variations in the levels of MMP-3, -9 and -12, but not the levels of activation and/or substrate degradation of these MMPs or other metzincins inhibited by TIMP-1 (Savarin et al., 2013). Earlier studies conducted in microvascular ECs (using human microvascular endothelial cells derived from neonatal foreskin) reported an increase in TIMP1 secreted levels after TNF α stimulation (Jackson & Nguyen, 1997). Additionally, previous studies conducted by Singh *et al.* in our laboratory, as well as this thesis, reported an up-regulation in TIMP1's mRNA levels following cytokines stimulation in cardiac mouse ECs (Chapter 3; Singh et al., 2005). The effects of cytokines on TIMP2 levels in BBB-ECs are little studied, but *in vitro* studies performed in murine cardiac endothelial cells (Chapter 3; Singh et al., 2005), in rat synovial membranes (Hyc et al., 2011) and keratoconus fibroblasts (Feng et al., 2016) reported a reduction in TIMP2 mRNA or protein levels (respectively) after TNF α stimulation. Overall, the observed loss hCMEC/D3 barrier properties after cytokines stimulation could be mediated by a broad dysregulation of metalloproteinase activities.

Previous observations suggest that cytokine-mediated loss of barrier integrity could be metalloproteinase-dependent since this effect could be reversed by addition of a broad-spectrum metalloproteinase inhibitor (GM6001) and an overall increase in metalloproteinase gene expression was observed under inflammatory conditions. In this regard, it would be reasonable to speculate that the described protective effect of a combination of Shh and Vitamin D3 in the presence of cytokines could also be a result of modulation

of metalloproteinase levels and as discussed in Chapter 1, others have observed such effects. However, no detectable alteration in metalloproteinase expression was observed by the addition of Shh and Vitamin D3 after 24h treatments (in the presence or absence of cytokines) (**Appendix 4.C**). Analysis at shorter incubation times revealed a Shh and Vitamin D3 combined effect to block cytokine-driven increase in MMP3 and MMP10 mRNA levels at 8h post-treatment (**Figure 4.14**). This protective effect was maintained up to 12h after treatments in the case of MMP3 but lost after 8h incubation periods for MMP10 (**Figure 4.14**). There is no evidence in the published literature for a Shh-protective role against cytokine-driven increase in metalloproteinase gene expression, but some reports have described an ability for Vitamin D3 to reduce IL1 β induced increase in MMP1, -3 and -9 in human rheumatoid synovial tissues (Tetlow & Woolley, 1999), decrease MMP3 production in IL1 β treated human periodontal ligament cells (Hosokawa et al., 2015) and significantly reduce LPS-mediated increase in MMP14 in human umbilical vein ECs (Stach et al., 2012). In addition, VitD3 impedes hypoxia/reoxygenation induction of MMP9 through an NF κ B mechanism in bend3 endothelial cells (Won et al., 2015). Thus, it is possible that the observed effects of Shh and Vitamin D3 on MMP3 and 10 mRNA levels could be exclusive effect of Vitamin D3, the fact that Vitamin D3 was only capable of trigger a protective effect against cytokine-driven loss in barrier integrity (measured as TEER) when combined with Shh, leads to the idea of a possible synergistic effect. Future time-points experiments assessing Vitamin D3 and Shh individual effects in MMP3 and 10 gene expression in the presence of inflammatory conditions need to be performed.

Expression levels of TIMPs (-1, -2, -3 and -4) at shorter post-treatment times were also evaluated in order to uncover any possible Shh and/or Vitamin D3 mediated effects. Interestingly, a combination of Shh and Vitamin D3 was capable of increasing TIMP2 and -4 mRNA levels 4h after treatment (**Figure 4.15**). Although a cytokine-driven reduction in TIMP2 and -4 levels was observed at 8h and 12h time-points, a combination of Shh and Vitamin D3 abrogated cytokines-mediated decrease in TIMP4 gene expression levels at 8h after treatment, although no protection was observed at further

incubation times (**Figure 4.15**). Thus, this seems to suggest that Shh and Vitamin D3 may not only be mediating their protective effects through the described inhibition of cytokines-driven increase in MMP3 and MMP10 expression levels (8h post-treatment) but also through an increase of TIMP2 (4h post-treatment) and blocked cytokines-driven reduction in TIMP4 expression (8h post-treatment), leading to an overall reduction in metalloproteinase activity. Although no effects of Shh in TIMPs gene expression have been previously described, Vitamin D3 treatment in rats with induced endometriosis were observed to significantly reduce TIMP2 levels (Yildirim et al., 2014) whereas in cultured murine myoblasts, addition of Vitamin D3 significantly decreased TIMP3 expression (Garcia et al., 2013). Once again, the observed effects in TIMP2 and 4 expression levels could be mainly produced by the addition of Vitamin D3, but as before, the fact that Vitamin D3 was only capable of trigger a protective effect against cytokines-driven loss in barrier integrity (measured as TEER) when combined with Shh, leads to the idea of a possible synergistic effect. Future time-points experiments assessing Vitamin D3 and Shh individual effects in TIMP2 and 4 gene expressions in the presence of inflammatory conditions, together with a study of variations in TIMP2 and 4 protein levels need to be performed.

In order to further explore Shh and Vitamin D3 protective effect on MMP3 and 10 expression levels under inflammatory conditions, analysis of secreted proteins were performed by Western Blotting. Additionally, MMP1 secreted levels were also assessed despite of the lack of Shh and Vitamin D3 effect on its mRNA levels since it experienced the highest cytokine-driven induction (**Figure 4.16**). As it has been previously discussed, cytokines ability to induce MMP1 and -3 gene expression has been broadly described in the literature. Thus, the observed increase in MMP1 and -3 secreted protein levels observed under inflammatory conditions agreed with findings in the literature (**Figure 4.16**) (Jackson & Nguyen, 1997; Roy et al., 2006; Fujita et al., 2012; Lee et al., 2012; Ahn et al., 2014; Ono et al., 2018). Vitamin D3 can reduce MMP1 and 3 levels in the absence (Szalay et al., 2009; Panizo et al., 2013) or presence of inflammatory conditions (Tetlow & Woolley, 1999; Hosokawa et al., 2015). However, this is the first study reporting a combined ability of Shh

and Vitamin D3 to abrogate the cytokine-driven increase in MMP1 and 3 secreted levels (**Figure 4.16**). Again, a possible synergistic effect of vitamin D3 and Shh may be implicated here and future experiments assessing Vitamin D3 and Shh individual effects on MMP1 and 3 secreted protein levels under inflammatory conditions will shed light on mechanisms involved.

To further explore effects of Vitamin D3 and Shh on extracellular levels of MMP3 protein, intracellular MMP3 protein levels were assessed. Preliminary data showed that cytokine treatment resulted in an increase in MMP3 intracellular levels as seen for MMP3 mRNA and secreted protein levels (**Figure 4.19**). However, addition of a combination of Shh and Vitamin D3 did not seem to trigger any changes in MMP3 intracellular protein (**Figure 4.19**). A possible protective effect of Shh and Vitamin D3 against cytokine-driven increase was also observed. Further experiments will be needed in order to corroborate the observed changes and assess the extent of Shh and Vitamin D3 mediated protection against cytokine-driven increase in MMP3 intracellular levels.

In order to explore further the Shh and Vitamin D3 combination increasing MMP3 secreted protein levels without altering MMP3 mRNA, we hypothesised that the observed effects could be underlined by a modulation of endocytic mechanisms, affecting the levels of extracellular MMP3. Previous literature has reported a role for low-density lipoprotein receptor-related protein 1 (LRP1) regulating the extracellular activities of metalloproteinases through the endocytic clearance of secreted metzincins and TIMPs (reviewed in Yamamoto et al., 2015). To date, LRP1 has been shown to directly participate in the extracellular clearance of MMP2 (Yang et al., 2001; Emonard et al., 2005), -9 (Van den Steen et al., 2006), -13 (Barmina et al., 1999), TIMP1 (Thevenard et al., 2014), -2 (Emonard et al., 2005), -3 (Scilabra et al., 2013), ADAMTS4 (Yamamoto et al., 2014) and -5 (Yamamoto et al., 2013), but not, as yet, MMP3. Thus, as a first approach, expression levels of *LRP1* were measured in hCMEC/D3 *in vitro* monolayers. Here, we report a reduction in *LRP1* gene expression levels in the presence of cytokines at short and longer incubation times (**Figure 4.20**). Although the effect of cytokines such as TNF α or IL1 α in *LRP1* expression levels has not been previously reported, studies

conducted in murine isolated brain microvessels showed a reduction in LRP1 gene expression after LPS injections, a pro-inflammatory agent (Jaeger et al., 2009). Similarly, LPS treated mice showed an impairment in LRP1-mediated transport after LPS injections (Erickson et al., 2012). These results seem to agree with the observed reduction in LRP1 expression (and probably consequent reduction in LRP1 function) in the presence of a pro-inflammatory environment. Interestingly, addition of a combination of Shh and Vitamin D3 reversed the cytokine-driven decrease in *LRP1* expression levels at 4h after treatment, although no protection was detected at longer incubation times (**Figure 4.20**). Additionally, Shh and VitaminD3 increased *LRP1* expression in the absence of cytokines, although, again, this seemed to be a limited effect, as it was only observed at 8h post-treatment (**Figure 4.20**). Guo *et al.*, studying the BBB in Alzheimer's disease, observed that Vitamin D3 treatment increased LRP1 mRNA and protein levels in mouse hippocampal sections and cultured murine brain microvascular cells (respectively) under normoxic and hypoxic conditions (Guo et al., 2016). Guo *et al.*'s data could suggest that the observed effects in *LRP1* expression levels shown here could be mainly due to the presence of Vitamin D3, but as before, the fact that Vitamin D3 was only capable of triggering a protective effect against cytokine-driven loss in barrier integrity (measured as TEER) when combined with Shh, a possible synergistic effect seems likely. Future experiments assessing Vitamin D3 and Shh individual effects in *LRP1* mRNA levels in the presence and absence of inflammatory conditions need to be performed.

LRP1 levels are increased in the CNS of a murine model of MS (Gaultier et al., 2009; Chuang et al., 2016) and in the rims of chronic active lesions in MS patients (Hendrickx et al., 2013). In this regard, a broad range of possible mechanisms by which LRP1 could be playing a role in the development of MS have been suggested in the literature: LRP1 blockade with a specific antibody inhibited tPA-driven increase in ICAM-1 (adhesion molecule that facilitates activated leukocytes extravasation) in a brain-derived EC line (Wang et al., 2014); in an animal model of cerebral ischemia, an interaction between tPA and LRP in perivascular astrocytes can lead to an increase in BBB permeability through LRP direct activation of Akt (An et al.,

2008); *in vivo* studies in mice showed that BBB opening after tPA injection could be inhibited in the presence of an LRP1 antagonist (Yepes et al., 2003); LRP1 seems to play an essential role in the phagocytosis of degraded CNS myelin, whose accumulation may accelerate disease progression, (Fernandez-Castaneda et al., 2013; Gaultier et al., 2009); LRP1 may regulate the membrane levels of TNF α 's receptor through its endocytosis (Gaultier et al., 2008); and selective microglial deletion of LRP1 promoted a pro-inflammatory phenotype that exacerbated disease severity in a murine model of MS (Chuang et al., 2016). Altogether, the previous observations seem to suggest a role of LRP1 in the development of autoimmune disorders such as MS. However, it seems that protective or pathological effects can be associated to LRP1 depending on the region studied: whereas tPA-mediated BBB opening has been suggested to be LRP1-dependent, it also seems that LRP1 could play a protective role through the clearance of myelin debris and the maintenance of an anti-inflammatory microglial phenotype, among others.

To explore whether a modulation of endocytosis mechanisms was involved in Shh and Vitamin D3 mediated effects in MMP3 secreted levels, hCMEC/D3 confluent monolayers were incubated with cytokines, Shh and/or Vitamin D3 in the presence and absence of Cytochalasin D (CytoD; a broad pharmacological inhibitor of endocytosis). Preliminary results showed that addition of CytoD could itself be increasing MMP3 secreted levels above untreated controls, suggesting that endocytic clearance mechanisms take place endogenously in untreated hCMEC/D3 confluent monolayers (**Figure 4.21**). Interestingly, in the presence of CytoD, Shh and Vitamin D3 mediated reduction in MMP3 secreted levels (in the absence of cytokines) was partially reversed (**Figure 4.21**).

Although it is possible that the reported results could be LRP1-dependent, it is important to consider that CytoD is a broad inhibitor of endocytic activities. Thus, although gene expression measurements seem to point at LRP1 as a possible candidate, other endocytic mechanisms for MMP3 cannot be ruled out. Future experiments with specific inhibitors of LRP-mediated uptake such as Receptor-Associated Protein (RAP) and siRNA for LRP1 could be performed. In contrast with the speculated LRP1/MMP3

interaction, Suzuki *et al.* described a tissue-type plasminogen activator (tPA) induced increase in LRP1 together with MMP3 levels in a murine brain microvascular cell line and brain sections from tPA treated mice (Suzuki *et al.*, 2009). Thus, Suzuki *et al.* postulated that tPA could be inducing MMP3 secretion through an activation of the LRP/NF κ B pathway (Suzuki *et al.*, 2009). Although in our observations *LRP1* expression levels seem to oppose MMP3 modulation (suggesting that LRP1 could not be functioning as an inducer of MMP), it needs to be considered that LRP1-mediated regulation of MMP3 could be more complex than a simple endocytic mechanism.

Cytochalasin D may also be affecting the Shh signalling. When Shh binds to Ptch, the Shh-Ptch receptor complex is internalised in a clathrin-dependent manner (Christ *et al.*, 2012); LRP2 has been implicated not only in the enhancement of clathrin-dependent endocytosis of the Shh-Ptch complex but also in the recycling of Shh back to the plasma membrane, increasing its local concentration and potentiating its signal (Christ *et al.*, 2012). Following Ptch endocytosis, derepressed Smo is endocytosed through a clathrin-dependent mechanism and activated as part of the Shh signalling pathway (reviewed in Pedersen *et al.*, 2016). Thus, it needs to be considered that CytoD mediated abrogation of Shh and Vitamin D3 effect on MMP3 secreted levels (in the presence or absence of cytokines) could not be only due to an inhibition of MMP3 extracellular clearance but also to an inhibition of Shh signalling, since both Ptch and Smo endocytic internalization mechanisms would be impaired. Future experiments with specific inhibitors (such as the clathrin inhibitor Pitstop) should help to clarify these points.

4.4. KEY FINDINGS

- Human endothelial barrier stability is compromised under inflammatory conditions in an *in vitro* model of the Blood Brain Barrier (BBB). TEER measurements also reveal that barrier stability is dependent on metalloproteinase activity. Metalloproteinase expression is regulated by cytokines both at mRNA level and apparently at the level of secretion.
- A combination of Shh and Vitamin D3 can synergistically protect against cytokine-driven loss in endothelial barrier stability in an *in vitro* model of the BBB, demonstrated with TEER measurements. Shh and Vitamin D3 showed protective effects by regulating ZO-1, MMPs and TIMPs expression.
- Alterations in endocytosis mechanisms could underly the observed variations in secreted MMP3 levels in an *in vitro* model of the BBB. Shh and Vitamin D3 modulated LRP1 expression and MMP3 secretion.

4.5. FUTURE STUDIES

- The presented results focused on TEER values as a measurement of barrier integrity. Permeability to fluorescently labelled dextran molecules and/or Evans Blue could also be assessed as an alternative method to corroborate the observed changes in *in vitro* barrier stability. Additionally, cells grown in a transwell insert could be fixed with paraformaldehyde and stained with phalloidin (a toxin isolated from the 'death cap' mushroom and fluorescently labelled capable of binding to actin filaments with high affinity), providing a confirmation of the monolayer's confluence.
- Future studies could focus on tight junction regulation - optimization of immunofluorescent staining of hCMEC/D3 monolayers will allow further study of variations in the levels and cellular localization of junctional proteins (such as ZO-1) as a measurement of barrier stability. Alternatively, treatment-derived variations in the total levels of junctional proteins could be also assessed by Western Blotting or a different brain microvascular cell line (such as BMECs) that can be used to explore monolayer integrity as direct visualization of junctional status.
- Exploring the potential of Shh and Vitamin D3 individually in reversing cytokine-driven effects could provide a way forward for further mechanistic studies.
- As an alternative to Western Blotting, cytokine/Shh/Vitamin D3 regulation of metalloproteinase expression could be assessed by enzyme-linked immunosorbent assay (ELISA), avoiding albumin contamination and providing a more accurate measurement.
- Targeted deletion experiments (e.g. siRNA) could be employed to assess the individual importance of the deregulated metalloproteinases (with particular interest in MMP1, 3 and 10) in barrier integrity. Additionally, silencing of metalloproteinase inhibitors (TIMP2 and TIMP4) would help to clarify their possible implication in Shh and Vitamin D3 mediated protection against cytokines-driven barrier breakdown.

- The possible role of deregulated endocytosis mechanisms in the modulation of MMP3 secreted levels could be further clarified with the following approaches:
 - Shh and Vitamin D3 individual roles as protective agents against cytokines-mediated reduction in LRP1 gene expression levels needs to be assessed.
 - Future experiments with specific inhibitors of LRP-mediated uptake such as Receptor-Associated Protein (RAP) and siRNA for LRP1 could reveal a definitive role for this pathway.
 - Cytochalasin D effects on Shh signalling should be also assessed since both Ptch and Smo endocytic internalization mechanisms could be impaired under these conditions. Thus, future experiments studying Smo and Ptch subcellular localization upon Cytochalasin treatment should be considered.

5. miR125b as a possible mediator of endothelial barrier integrity – microarray analysis

5.1. INTRODUCTION

5.1.1. miRNAs

MicroRNAs (miRNAs) are a group of non-protein coding RNAs with a length comprised between the 19 and 25 nucleotides (reviewed in Nelson et al., 2008). Non-mature miRNAs (pre-miRNAs) are transcribed from intronic regions or miRNA genes by the RNA polymerase II and cleaved by RNase III (or Drosha) originating a short double-stranded stem-loop pre-miRNA that will then be translocated into the cytoplasm. Once in the cytoplasm, pre-miRNAs are again cleaved by a complex containing Dicer to generate the typical double-stranded miRNA. Mature miRNAs are composed by two miRNA sequences (5p and 3p) that can be individually recruited into an RNA-protein complex known as miRNA-Induced Silencing Complex (RISC) and composed by DICER and its co-factors. The RISC-miRNA complex can then bind to the miRNA complementary sequence in the 3'UTR region of the target mRNA, not only repressing the targeted mRNA translation but also triggering the mRNA degradation or storage by processing body (P-body). Interestingly, several mRNAs can be targeted by a single miRNA (reviewed in Nelson et al., 2008).

Since miRNAs can block the translation of specific target mRNAs or induce their degradation through the selective binding of their nucleotide sequences, miRNAs play a central role in the regulation of gene expression. Thus, miRNAs are capable of regulating protein synthesis in a specific manner, without altering the transcription of target mRNAs, allowing them to play a central role in several biological functions (Cui et al., 2006; Friedman et al., 2009).

5.1.2. miRNAs and Multiple Sclerosis

Many studies have showed altered expression of several miRNAs in samples from MS patients (and also in EAE mice, a murine model of MS), suggesting that this condition could be characterised by a particular signature of altered miRNAs (reviewed in Ma et al., 2014).

Previous literature has reported a role for these miRNAs in the pathogenesis of MS: using CD4⁺ T cells from MS patients, miR17 has been shown not only to be up-regulated in MS patients (Lindberg et al., 2010), but also to be downregulated under natalizumab (anti-alpha 4 integrin antibody) treatment and up-regulated during relapses (Meira et al., 2014). miR17 and miR20a are down-regulated in whole blood samples from all MS subtypes patients and can repress T cell activation (Cox et al., 2010). In addition, miR20a is down-regulated in whole blood samples from Relapsing-Remitting MS (RRMS) patients (Keller et al., 2014) and could be an essential regulator of cytokine production in CD4⁺ cells (Reddycherla et al., 2015). In contrast, more recent studies reported an up-regulation of miR20a in whole blood samples from MS patients (Yang et al., 2017); miR145 is up-regulated in Multiple Sclerosis patients, particularly in RRMS (Junker et al., 2009; Gandhi et al., 2013; Søndergaard et al., 2013; Keller et al., 2014); and miR186 was also up-regulated in whole blood samples from MS patients (Keller et al., 2014; Ma et al., 2014).

5.1.3. Expression of miRNAs in Norfolk and Norwich University Hospital Multiple Sclerosis patients

Previous preliminary studies undertaken by Dr. Damon Bevan (Gavrilovic group) assessed the expression of several miRNAs in blood samples from Multiple Sclerosis (MS) patients (visiting NNUH clinic under the care of Dr Martin Lee). The measured miRNAs were carefully selected from the literature based on correlation with MS previously reported in the literature. Expression levels of miR17, miR20a, miR125b, miR145, miR186 and miR326 were measured by qRT-PCR (**Table 5.1**; Bevan, Gage, Lee and Gavrilovic, unpublished observations). Amongst these miRNAs, of particular interest were miR125b and miR326 as they had been previously described to impair Hedgehog signalling through inhibition of Smo, a Hedgehog pathway component (Ferretti et al., 2008). Interestingly, preliminary analysis reported a positive correlation with disease duration or a significant increase in Relapsing-Remitting MS compared with Primary-Progressive MS patients for

miR125b and miR326 respectively (**Table 5.1**; Bevan, Gage, Lee and Gavrilovic, unpublished observations).

Table 5.1 – miRNA expression levels in blood samples from Multiple Sclerosis (MS) patients. Main observations from the literature and the pilot study of miRNA expression in blood samples from MS patients are summarised. Primary-Progressive MS (PPMS); Relapsing-Remitting MS (RRMS); positive correlation (+ve). Data provided by Bevan, Gage, Lee and Gavrilovic, unpublished observations.

miRNA	MS Literature	Expression in MS pilot	Disease Activity	Disease Duration
miR17	↑ Lindberg <i>et al.</i> 2010 ↓ Cox <i>et al.</i> 2010	-	+ve correlation (R=0.6, P=0.019, N=15)	-
miR20a	↓ Cox <i>et al.</i> 2010	↑ 2-fold PPMS vs CTRL ($F_{1,18}=3.2$, P=0.09)	-	-
miR125b	-	-	-	+ve correlation (R=0.46, P=0.048, N=19)
miR145	↑ Keller <i>et al.</i> 2009	-	+ve correlation (R=0.47, P=0.042, N=19)	-
miR186	↓ Keller <i>et al.</i> 2009	↓ 1.5-fold ($F_{1,18}=2.7$, P=0.118)	-	-
miR326	↑ Du <i>et al.</i> 2009 ↑ Junker <i>et al.</i> 2009 ↑ Waschbisch <i>et al.</i> 2011	↑ 1.6-fold RRMS vs PPMS ($F_{1,18}=3.55$, P=0.032)	-	-

5.1.4. miR125b and miR326 in Multiple Sclerosis

miR125b and miR326 have also been associated with MS pathogenesis. Analysis of Gene Expression Omnibus database revealed an up-regulation of miR125b in samples of peripheral blood T-cells from RRMS patients (Sheng et al., 2015); miR125b has been shown to promote macrophage activation (Essandoh et al., 2016); knockdown or overexpression of miR-326 alleviated or aggravated pathogenesis, respectively, in a murine model of MS through the targeting of Ets-1 and the consequent modulation of Th17 differentiation (Du et al., 2009); analysis of peripheral blood mononuclear cells of RRMS patients showed an upregulation of miR326 (Waschbisch et al., 2011); and miR326 was up-regulated in active lesions from MS patients when compared with normal white matter (Junker et al., 2009). Additionally, miR125b and miR326 have been also associated with Vitamin D signalling: although not yet validated, miR326 has been predicted to target Vitamin D Receptor (VDR) (Sebastiani et al., 2011); treatment with Vitamin D3 in its active form (1,25) can increase miR125b levels in the epithelium of patient prostate tissue (Giangreco et al., 2013); overexpression of miR-125b significantly decreased the endogenous VDR protein level in a breast adenocarcinoma cell line (Mohri et al., 2009), although no miR125b-dependent regulation of VDR was observed in a melanoma cell line (Essa et al., 2012) suggesting some cell type-dependent variations. Thus, the possibility that miR125b and miR326 could impact on both Hedgehog and Vitamin D3 signalling pathways, together with their implications in MS and the reported dysregulation in PBMCs isolated from MS patients (**Table 5.1**; Bevan, Gage, Lee and Gavrilovic, unpublished observations), supported our hypothesis that these miRNAs could be involved in the changes in barrier integrity reported in the previous chapter.

5.1.5. Aims

1. The levels of miR125b and miR326 and their response to cytokine stimulation will be studied in the human endothelial *in vitro* model of the BBB established in Chapter 4.
2. Transfection experiments will be used to assess the direct effects of miR125b and/or miR326 in barrier stability (measured as transendothelial electrical resistance; TEER) in the *in vitro* model of the BBB. This will be studied in the presence and absence of cytokines.
3. The most promising miRNA (miR125b or miR326) (based on the above results) will be selected for functional testing with microarray analysis of gene expression in the presence of inflammatory conditions in the *in vitro* model of the BBB.
4. Candidate genes and/or pathways emerging from microarray analysis will be validated and their implications in BBB maintenance will be further assessed using our BBB *in vitro* model.

5.2. RESULTS

5.2.1. miR125b and miR326 in a BBB *in vitro* model

Since disruption of the BBB has been described as one of the early events in MS pathogenesis, we speculated that perhaps the observed changes in our *in vitro* model of the BBB could involve alterations in miR125b or miR326 levels. To first approach this hypothesis, miR125b and miR326 levels were assessed in hCMEC/D3 confluent monolayers in the presence or absence of a mixture of cytokines (TNF α and IL1 α both at 10ng/ml). Initial analysis revealed higher detectable expression levels for miR125b (25.47 Average Raw Ct values) when compared with miR326 (31.46 Average Raw Ct values) (data not shown). In a second experiment, cytokine treatment revealed a small, but significant increase in miR125b levels when compared with untreated monolayers (1.14 ± 0.02 vs 1.00 ± 0.01 , $p<0.05$) (**Figure 5.1**). No alterations on miR326 levels were observed by addition of cytokines when compared with untreated controls (1.60 ± 0.067 vs 1.57 ± 0.69 , $p=0.97$) (**Figure 5.1**). Due to these observations further experiments focused on miR125b and its role in the observed loss of barrier functions in our BBB *in vitro* model under inflammatory conditions.

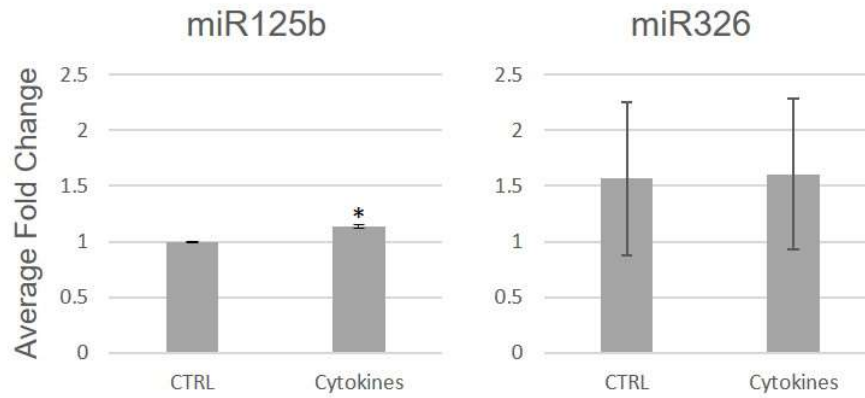


Figure 5.1 – miR125b and miR326 regulation under inflammatory conditions. hCMEC/D3 cells confluent monolayers were incubated with a mixture of cytokines (TNF α and IL1 α both at 10ng/ml) for 24h. miR125b and miR326 levels were determined by qRT-PCR. All measurements were normalised to RNU48 endogenous control. Statistically significant differences were assessed via t-test. Each bar represents the mean \pm SEM for 3 wells. * $p < 0.5$.

5.2.2. miR125b transfection optimization in hCMEC/D3 cells

In order to test miR125b effects on barrier permeability, hCMEC/D3 cells were transfected with 200nM of miR125b mimic (miR125b-M) or miR125b inhibitor (miR125b-I) and grown on 0.3µm porous transwells until confluence was reached.

As a first approach, hCMEC/D3 were transfected with 200nM of either miR125b mimic control (miR125b-MC) or miR125b inhibitor control (miR125b-IC) in order to optimise transfection and culture conditions. Three different transfection incubation media were tested (culture media with 0% FCS, PBS and Nucleofector Solution) and cell recovery was studied at 24h intervals after transfection for up to 3 days. For miR125b-MC, transfection in the presence of cell culture media (0%FCS) caused a high mortality rate that was not recovery at either 24h, 48h or 72h post-transfection (**Figure 5.2**). Similarly, very few cells transfected with miR125b-IC in the presence culture media with 0%FCS survived, with no improvement at either 24h, 48h or 72h post-transfection (**Figure 5.3**). Much better survival was achieved when hCMEC/D3 cells were transfected in the presence of either PBS or the recommended Nucleofector Solution (for miR125b-MC and miR125b-IC) (**Figure 5.2** and **5.3**). With the exception of 0% FCS cases, hCMEC/D3 monolayers were able to reach confluence at 72h post-transfection, although in those transfected in the presence of PBS monolayers were slightly less packed (**Figure 5.2** and **5.3**). In subsequent experiments, transfected cells were cultured for 72h after transfection in order to develop confluent monolayers.

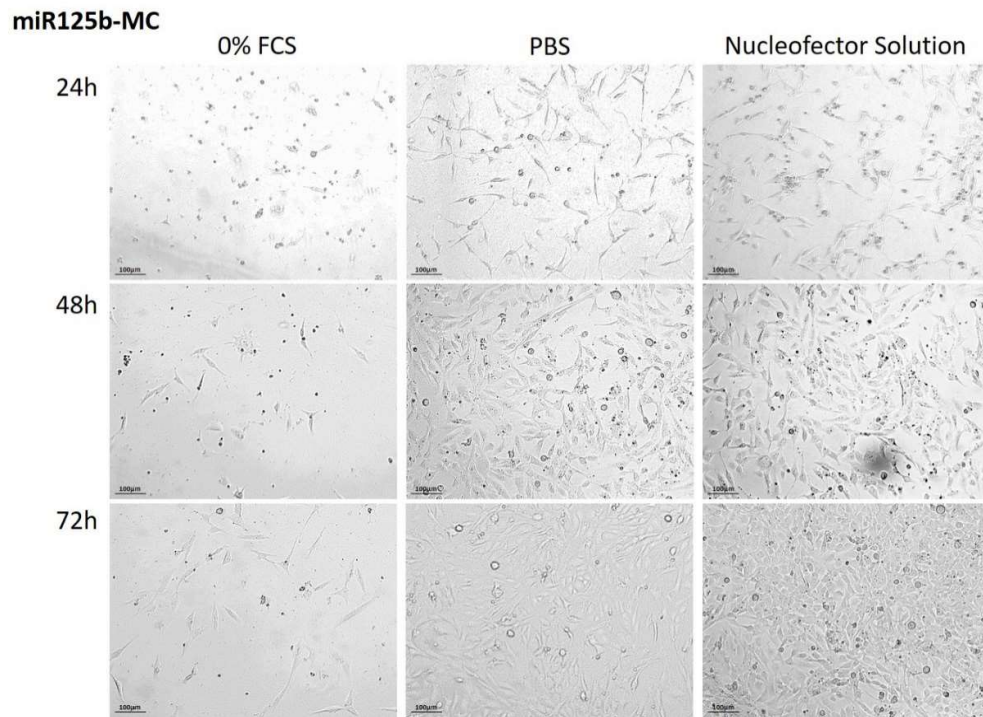


Figure 5.2 – Optimization of miR125b Mimic Control transfection conditions. hCMEC/D3 cells were transfected with miR125b mimic control (miR125b-MC) (200nM) in culture media with 0% FCS, PBS or Nucleofector Solution. Cells were imaged every 24h for up to 72h post-transfection.

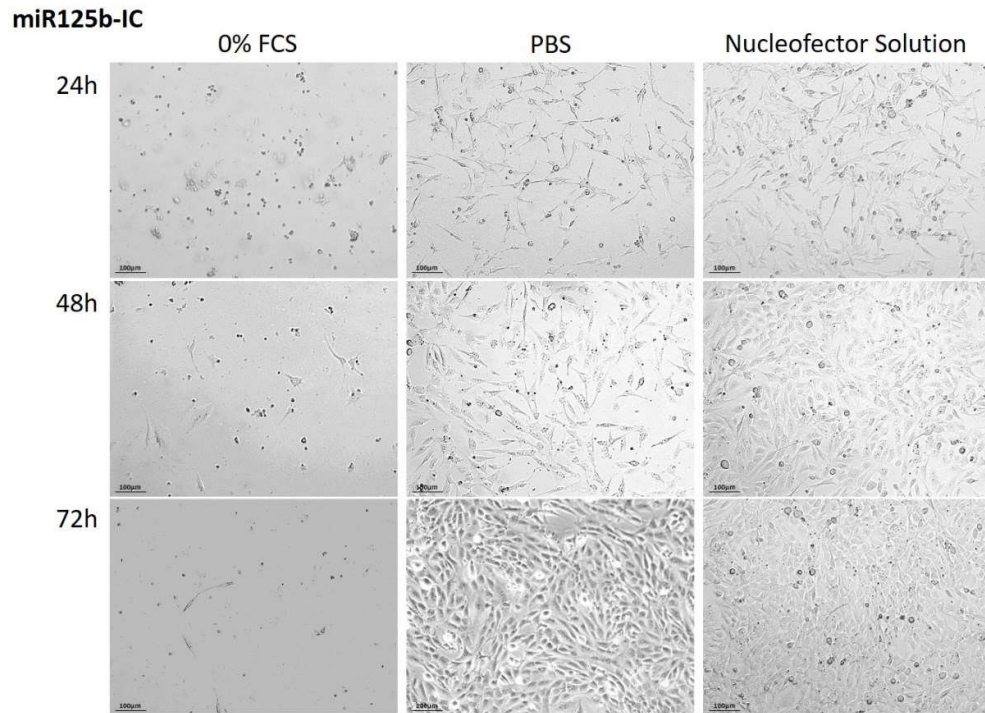


Figure 5.3 – Optimization of miR125b Inhibitor Control transfection conditions. *hCMEC/D3 cells were transfected with miR125b inhibitor control (miR125b-IC) (200nM) in culture media with 0% FCS, PBS or Nucleofector Solution. Cells were imaged every 24h for up to 72h post-transfection.*

In order to facilitate the study of transfection efficiency, the commercially available miR125b-IC was fluorescently tagged. Thus, transfection efficiency of hCMEC/D3 cells transfected with miR125b-IC in the presence of PBS or Nucleofector Solution was studied at 48h and 72h post-transfection. As previously described, confluence was reached at 72h for hCMEC/D3 cells transfected in the presence of PBS or Nucleofector Solution, although in the latter a slightly cell density was reached (**Figure 5.4**). Transfection efficiency rates seemed to increase between 48h and 72h but in any case, higher rates were reached for PBS transfections at both time-points (**Figure 5.4**). Differences in the number of transfected cells between 48h and 72h post-transfection could be due to cellular processing of miR125b-IC and/or cellular recovery effects.

Due to the apparently higher transfection rates reached for miR125b-IC (at 48h and 72h) when transfected in the presence of PBS rather than Nucleofector Solution (**Figure 5.4**), PBS was used in subsequent transfections despite the slightly lower cell density reached. This was also appropriate given the fact that over-confluent cells are known to be less responsive to stimulation in terms of their gene expression (Gavrilovic, personal communication). Thus, the level of confluence reached in PBS transfected hCMEC/D3 cells after 72h seems ideal to study miR125b driven changes in barrier integrity and gene expression levels.

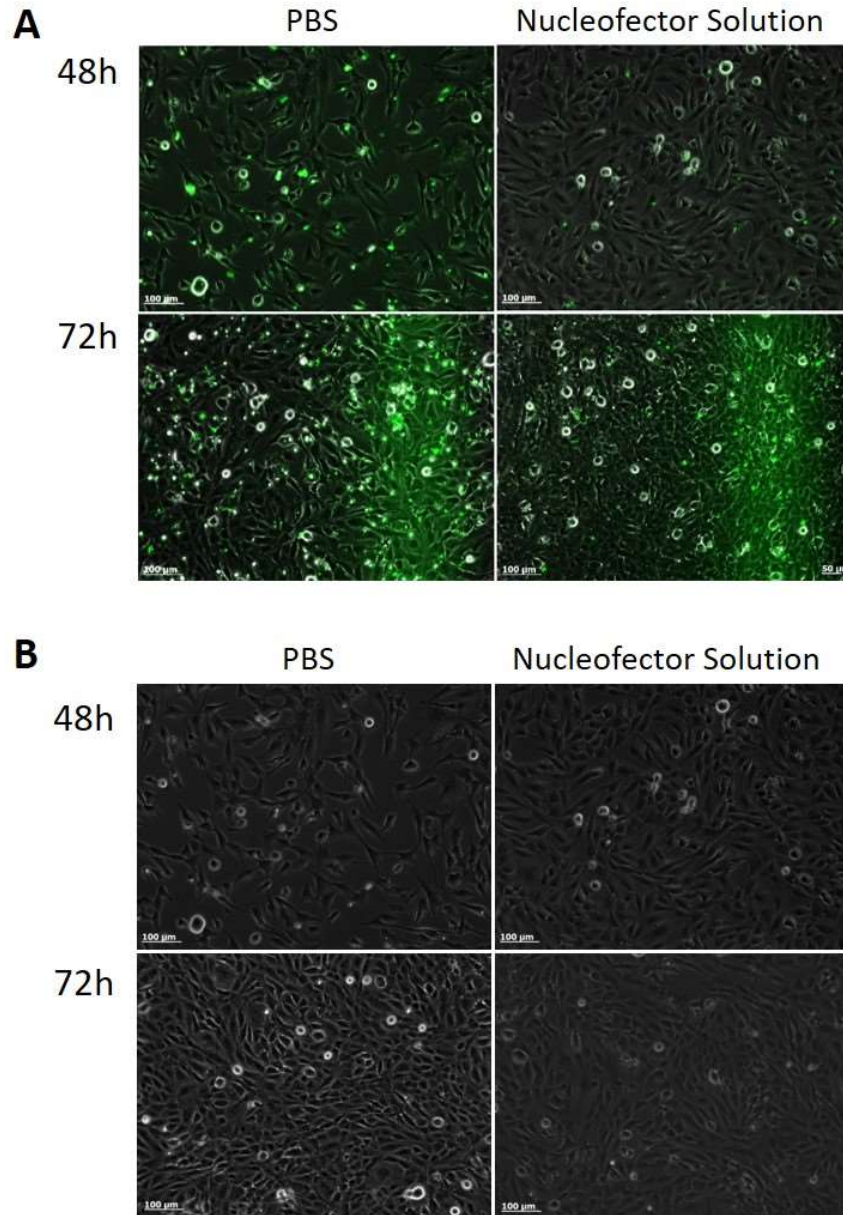


Figure 5.4 – Optimization of miR125b Inhibitor Control transfection efficiency. (A) hCMEC/D3 cells were transfected with fluorescently tagged miR125b inhibitor control (miR125b-IC) (200nM) in either PBS or Nucleofector Solution. Transfection efficiency was studied at 48h and 72h post-transfection. (B) Bright field images of hCMEC/D3 cells transfected with fluorescently tagged miR125b inhibitor control (miR125b-IC) (200nM) in either PBS or Nucleofector Solution at 48h and 72h post-transfection.

5.2.3. miR125b dependent barrier modulation in hCMEC/D3 confluent monolayers

In order to assess miR125b effects in our BBB *in vitro* model, hCMEC/D3 cells were transfected with miR125b-M (200nM), miR125b-I (200nM) and their respective controls (200nM). Cells were seeded onto 0.3µm porous transwells and cultured for 3days. TEER measurements were taken every 24h and normalised to a cell-free coated-insert used as a negative control. Transfection with the inhibitor of miR125b (miR125b-I) significantly increased TEER values by nearly 1.5-fold at 48h (630.50 ± 7.72 vs $430.84 \pm 20.71 \Omega/\text{cm}^2$, $p < 0.001$) and to a slightly lower extent at 72h (575.53 ± 27.20 vs $433.27 \pm 9.83 \Omega/\text{cm}^2$, $p < 0.001$) post-transfection when compared with control monolayers (**Figure 5.5**). Transfection with the mimic of miR125b (miR125b-M) triggered a significant disruption in barrier integrity (measured as TEER) at 72h when compared with un-transfected monolayers (315.25 ± 5.83 vs $433.27 \pm 9.83 \Omega/\text{cm}^2$, $p < 0.01$) (**Figure 5.5**). No effects were observed at either 24h or 48h, Thus, these observations suggest that miR125b may impair barrier integrity, since its inhibition increased TEER values above those of control hCMEC/D3 monolayers and transfection with miR125b-M significantly disrupted barrier properties. No differences in TEER values were reported after transfection with the appropriate controls, miR125b-MC or miR125b-IC, at any of the studied time points (**Figure 5.5**). A much higher TEER levels than the previously observed in this thesis was reported for hCMEC/D3 monolayers in these experiments. It is possible that the higher number of hCMEC/D3 cells used in order to compensate for the transfection-derived mortality or the transfection itself could be behind this effect.

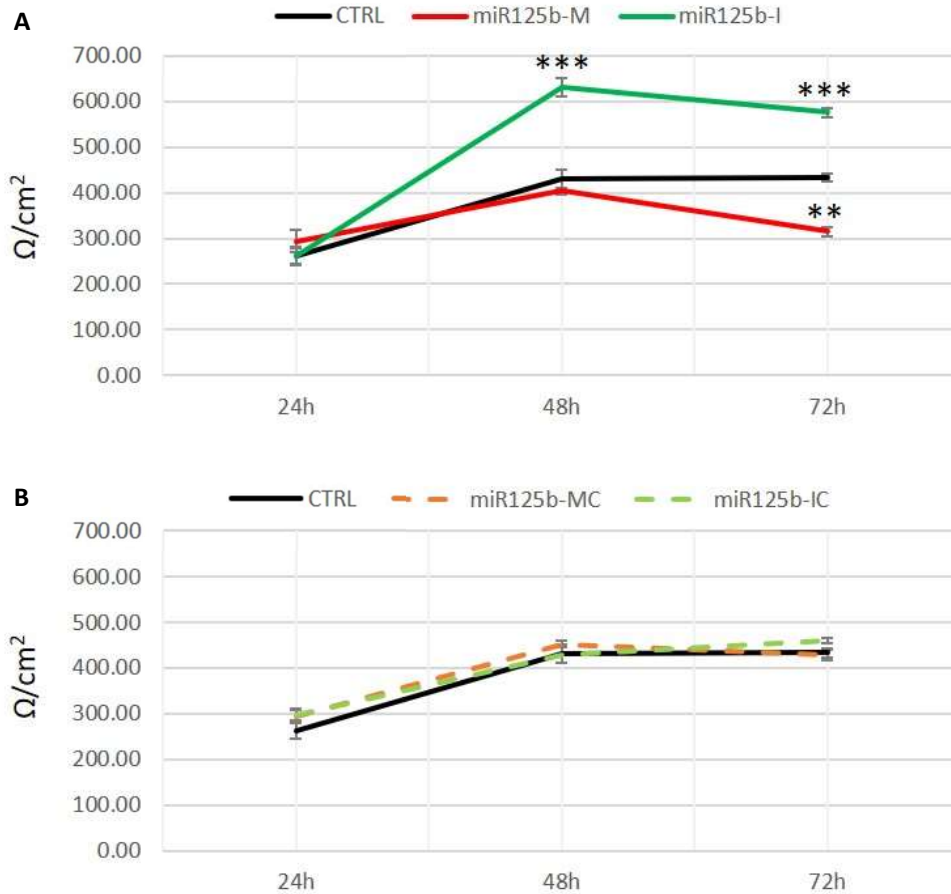


Figure 5.5 – miR125b impairs barrier properties in an *in vitro* model of the BBB. hCMEC/D3 transfected with 200nM of either a miR125b mimic (miR125b-M), a miR125b inhibitor (miR125b-I) (A), a miR125b mimic control (miR125b-MC) or a miR125b inhibitor control (miR125b-IC) (B) were seeded onto cell inserts (0.3µm porous) and grown for 3days. Cells were electroporated in the absence of miRNA were used as control (CTRL). Transendothelial Electrical Resistance (TEER) was measured to assess barrier integrity every 24h and normalised to a cell-free coated-insert used as a negative control. Statistically significant differences were assessed via One-way ANOVA with post-hoc Tukey. Each bar represents the mean ±SEM for 3 wells. * $p < 0.5$; ** $p < 0.01$; *** $p < 0.001$. Experiment replicated 5 times.

In order to test the role of miR125b in barrier dysfunction under inflammatory conditions, hCMEC/D3 cells were transfected with miR125b-M (200nM) and miR125b-I (200nM) and then treated with a mixture of cytokines (TNF α and IL1 α at 10ng/ml). After transfection cells were seeded into 0.3 μ m porous transwells and cultured for 3 days, with cytokines addition on the second day. TEER measurements were taken every 24h and normalised to a cell-free coated-insert. As previously described, addition of cytokines significantly reduced barrier properties when compared with untreated monolayers (281.30 \pm 1.98 vs 423.16 \pm 5.38 Ω /cm², p<0.001) after 24h treatment (**Figure 5.6**). Cytokine addition in monolayers transfected with miR125b-M significantly reduced TEER values when compared not only to untreated and non-transfected controls (240.08 \pm 3.13 vs 423.16 \pm 5.38 Ω /cm², p<0.001) but also when compared with non-transfected monolayers exposed to cytokines (240.08 \pm 3.13 vs 281.30 \pm 1.98 Ω /cm², p<0.001) (**Figure 5.6**). Thus, this seems to suggest that an increase in miR125b levels could enhance cytokines-mediated barrier disruption. Interestingly, cytokine addition in monolayers transfected with miR125b-I not only was no longer capable of triggering a reduction in TEER values when compared with untreated monolayers (533.50 \pm 7.14 vs 423.16 \pm 5.38 Ω /cm², p<0.001), but had no effect on the previously observed miR125b-I driven increase in barrier stability (**Figure 5.6**). This observation could be suggesting that cytokines mediated effect on barrier stability in our BBB *in vitro* model could be miR125b-dependent. No differences in TEER values were reported after transfection with either miR125b-MC or miR125b-IC at any of the studied time points (**Figure 5.6**).

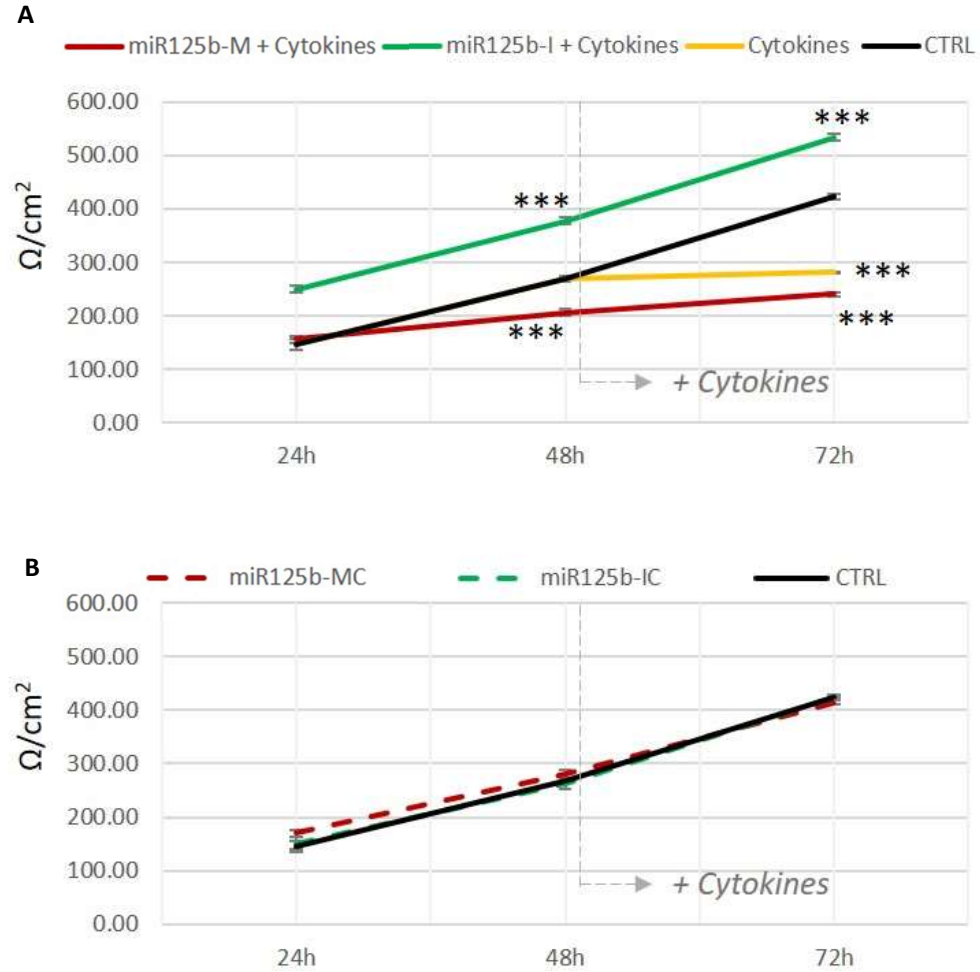


Figure 5.6 – miR125b may be underlying cytokine-driven loss of barrier integrity. hCMEC/D3 transfected with 200nM of either a miR125b mimic (miR125b-M), a miR125b inhibitor (miR125b-I) (A), a miR125b mimic control (miR125b-MC) or a miR125b inhibitor control (miR125b-IC) (B) were seeded onto cell inserts (0.3 μ m porous). An empty transfection was used as control (CTRL). After 48h, fresh media with or without a cytokine mixture (TNF α and IL1 α both at 10ng/ml) was added. Cells were cultured for further 24h. Transendothelial Electrical Resistance (TEER) was measured to assess barrier integrity every 24h and normalised to a cell-free coated-insert used as a negative control. Statistically significant differences were assessed via t-test. Each bar represents the mean \pm SEM for 3 wells. *** $p < 0.001$. Experiment replicated 5 times.

5.2.4. Microarray analysis of hCMEC/D3 confluent monolayers

hCMEC/D3 were transfected with miR125b-M, miR125b-I or run through an empty transfection and treated for 24h with cytokines (TNF α and IL1 α at 10ng/ml) (in the presence or absence of Shh (100ng/ml) and Vitamin D3 (100nM)). Total RNA was isolated, verified and sent for microarray analysis. Statistical analysis was performed by Cambridge Genomics. No significant changes in gene expression on the microarray were observed in miR125b-M or miR125b-I. In collaborative studies Dr Simon Moxon performed cumulative plot analysis for miR125 targets between mimic and inhibitor transfected cells (all treated with cytokines), although no differences were seen (**Appendix 5.A**). It is possible that more subtle miR125b driven changes were obscured by cytokine treatment, or miR125b driven changes in mRNA levels took place at earlier time-points.

As expected, microarray analysis showed a broad gene regulation in response to cytokines with 518 genes showing a significant change (adjusted p value <0.05) greater than 1.5-fold. Genomatix revealed a group of inter-related genes (dotted outlines in **Figure 5.7** and **Figure 5.8**) in the “cytokine signalling in immune system” pathway. Another pathway of interest emerging from this analysis was “Extracellular Matrix Remodelling” (dotted outline in **Figure 5.9**).

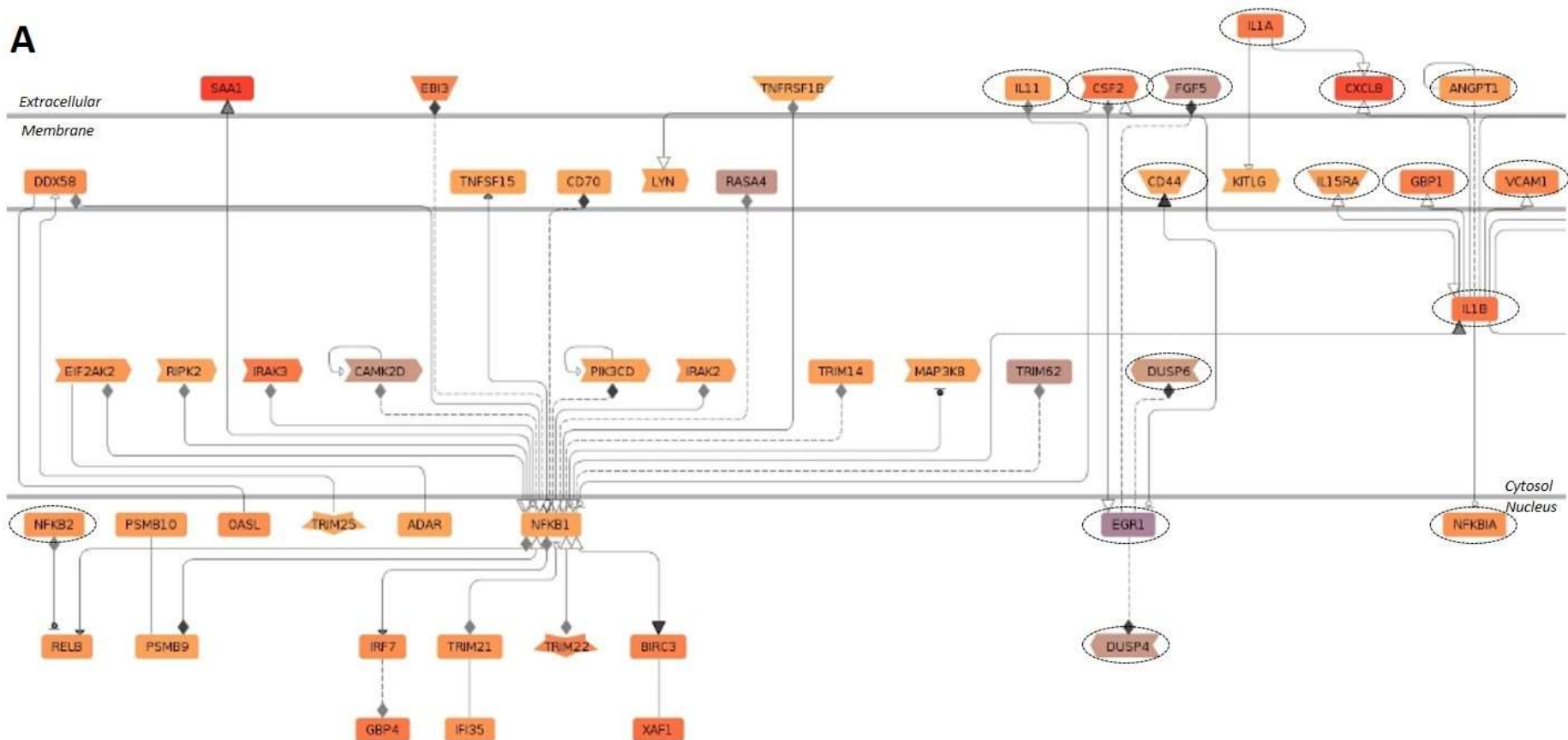


Figure 5.7 – Cytokine signalling in immune system pathway (A) retrieved by Genomatix. Cytokine responsive genes showing a significant change (adjusted p value < 0.05) greater than 1.5-fold in microarray analysis were imputed into Genomatix software. Changes in the “cytokines signalling in immune system” pathway are indicated as follow: red for up-regulated, blue for down-regulated and orange for not-regulated. Genes of interest are highlighted by a dotted outline.

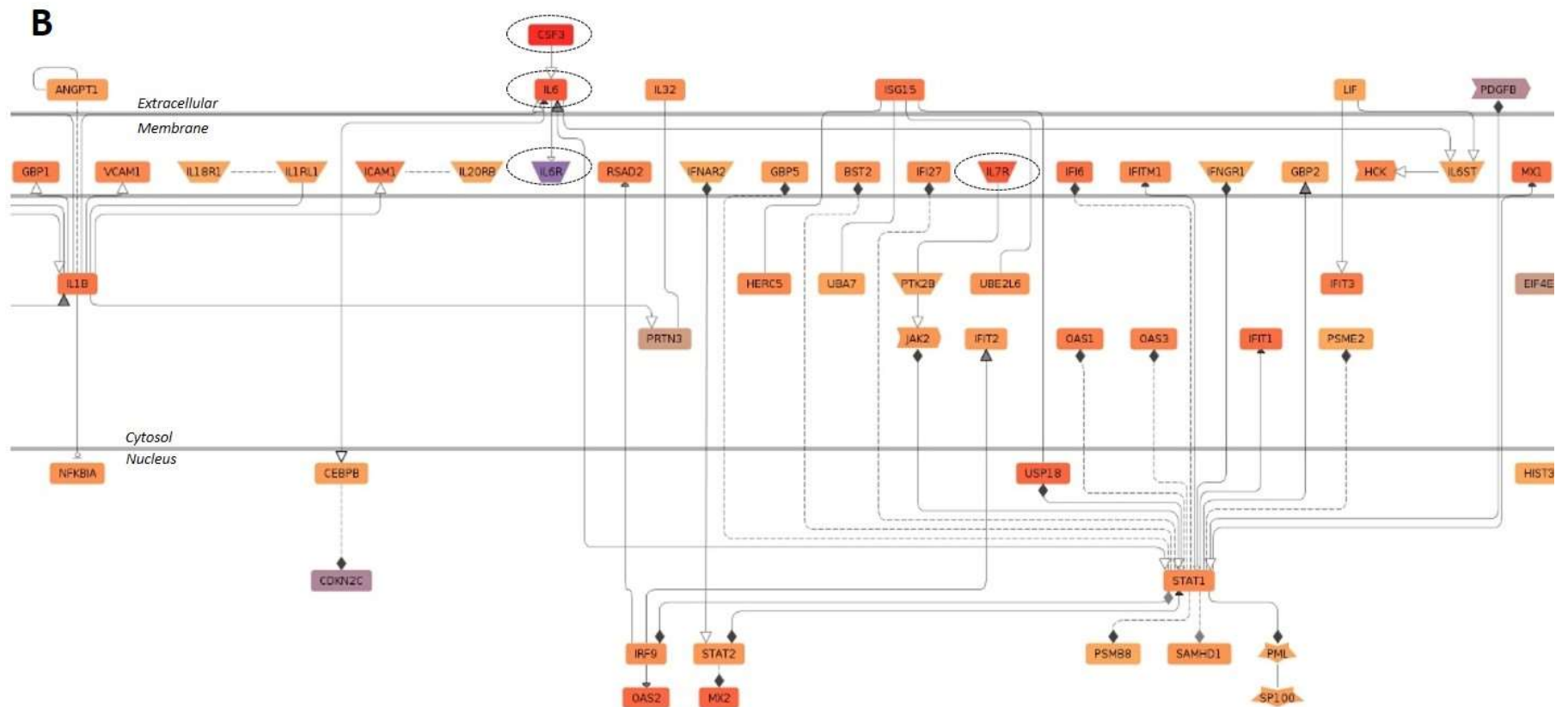


Figure 5.8 – Cytokine signalling in immune system pathway (B) retrieved by Genomatix. Cytokine responsive genes showing a significant change (adjusted p value < 0.05) greater than 1.5-fold in microarray analysis were imputed into Genomatix software. Changes in the “cytokines signalling in immune system” pathway are indicated as follow: red for up-regulated, blue for down-regulated and orange for not-regulated. Genes of interest are highlighted by a dotted outline.

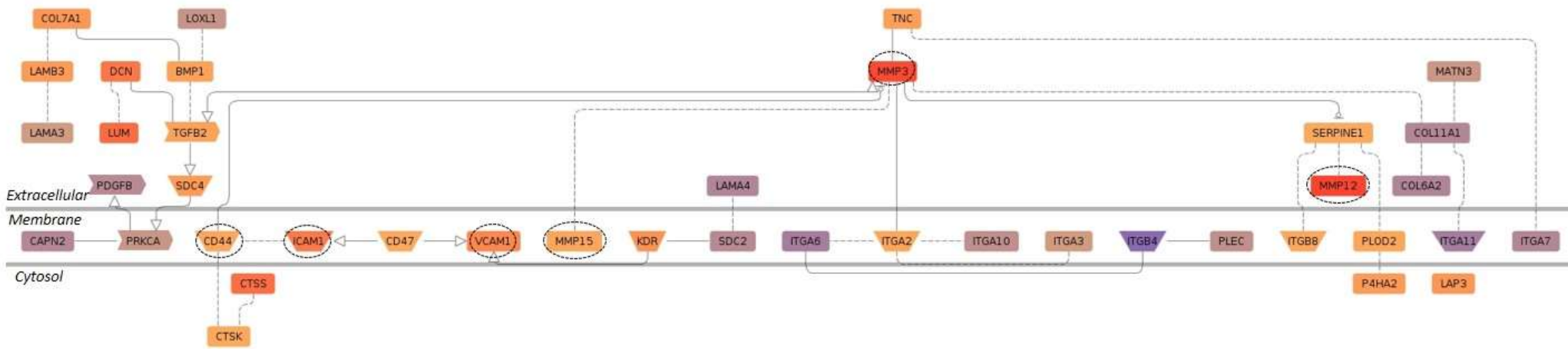


Figure 5.9 – Extracellular matrix remodelling pathway retrieved by Genomatix. Cytokine responsive genes showing a significant change (adjusted p value < 0.05) greater than 1.5-fold in microarray analysis were imputed into Genomatix software. Changes in the “Extracellular matrix remodelling” pathway are indicated as follow: red for up-regulated, blue for down-regulated and orange for no-regulated. Genes of interest are highlighted by a dotted outline.

Analysis of the literature revealed that some of the genes emerging from these pathways were previously associated in the literature with the pathogenesis of MS is shown (**Table 5.2** and **5.3**). Genes full names can be found in **Appendix 5.B**.

Table 5.2 – List of cytokine up-regulated genes associated with the pathogenesis of Multiple Sclerosis (MS) and retrieved from Genomatix pathway analysis.

	FOLD CHANGE	OBSERVATION	REFERENCE
MMP3	↑ 15.99	LPS intracerebral injection showed reduced BBB opening and neutrophil infiltration in MMP3 ^{-/-} mice	Esparza et al., 2004
		mRNA levels elevated in Relapsing Remitting MS patients and in a murine virus induced model of MS	Larochelle et al., 2011 Rosenberg et al., 2001
CXCL8	↑ 14.29	Promote neutrophil infiltration into the CNS through CXCR2 signalling	Semple et al., 2010
		Increased expression in stimulated (TNF α and IL1 β /INF γ) human cerebral microvascular ECs	De Laere et al., 2017; O'Carroll et al., 2015
CSF2	↑ 5.67	In a murine model of MS, CSF2 depletion resulted in disease resistance	Ponomarev et al., 2007
IL1β	↑ 5.60	Facilitates transendothelial migration of activated leukocytes into the CNS	Maghzi & Minagar, 2014
		Increased expression in peripheral blood mononuclear cells from MS patients	Heidary et al., 2014
		Mice lacking IL1B receptor (IL1R) show decreased disease severity and development in a model of MS	Schiffenbauer et al., 2000
		Enhances barrier permeability in BBB <i>in vitro</i> models	Ni et al., 2017

IL1α	↑ 5.29	Polymorphisms have been associated with early disease onset in peripheral blood from MS patients	Mirowska-Guzel et al., 2011
		Mice lacking IL1A receptor (IL1R) show decreased disease severity and development in a model of MS	Schiffenbauer et al., 2000
		Deletion of the IL1A gene did not impact disease onset or progression in a murine model of MS	Lévesque et al., 2016
ICAM1	↑ 4.85	Increased expression in the brain of a rat model of multiple sclerosis	Elo et al., 2018
		Increased expression on activated BBB under inflammatory conditions such as MS	Ortiz et al., 2014
		Increased expression at the inflamed BBB, contributing to increased leukocyte adhesion	Cerutti et al., 2016
GBP1	↑ 4.45	Upregulated in peripheral blood samples from MS patients treated with INF β	Goertsches et al., 2010
		Overexpression of GBP1 enhanced glioma cell invasion through MMP1 induction in mice brains	Li et al., 2011
VCAM1	↑ 3.43	Increased expression on activated BBB under inflammatory conditions such as MS	Ortiz et al., 2014
		Increased expression at the inflamed BBB, contributing to increased leukocyte adhesion	Cerutti et al., 2016 Cerutti et al., 2017
NFκBα	↑ 2.71	Polymorphisms in its inhibitor I κ B α are associated with increased susceptibility to MS	Balood et al., 2014
		A protecting allele has been found in the NFKBIA promoter in patients with primary progressive MS	Miterski et al., 2002

IL11	↑ 2.27	Increased serum levels during clinical relapses of MS patients. Additionally, the chromosomal region containing IL11 gene has been associated with MS susceptibility	Zhang & Zhang, 2015
ANGPT1	↑ 2.07	ANGPT1 treatment ameliorates inflammation-induced BBB leakage and cell infiltration into the CNS, reducing disease progression in a murine model of MS	Jiang et al., 2014
C/EBPβ	↑ 1.99	Myeloid C/EBPβ deficiency leads to disease attenuation in a murine model of MS	Pulido-Salgado et al., 2017
		CNS expression of C/EBPβ was upregulated in MS samples and a murine model of MS	Pulido-Salgado et al., 2017
		Microarray analysis indicate that EGR1 could be central in MS pathogenesis	Liu et al., 2013
IL15Rα	↑ 1.93	Inflammatory stimuli enhances IL5R gene expression in brain cerebral microvessels	Pan et al., 2011
		Increased gene expression in the brain of a murine model of MS	Wu et al., 2010
CD44	↑ 1.66	CD44 deletion leads to disease attenuation in a murine model of MS	Chitrala et al., 2017
		Hyaluronan triggers BBB breakdown through CD44 signalling in an <i>in vitro</i> model of the BBB	Al-Ahmad et al., 2018
SCF	↑ 1.52	Increased levels in cerebrospinal fluid of MS patients	Khaibullin et al., 2017

Table 5.3 – List of cytokine down-regulated genes associated with the pathogenesis of Multiple Sclerosis (MS) and retrieved from Genomatix pathway analysis.

	FOLD CHANGE	OBSERVATION	REFERENCE
EGR1	↓ 2.13	Increased in brain lesions of MS patients	Mycko et al., 2004
		Microarray analysis indicate that EGR1 could be central in MS pathogenesis	Liu et al., 2013
CDKN2C	↓ 2.09	Unknown	-
FGF5	↓ 1.67	Compromised BBB integrity and increased permeability in FGF2 ^{-/-} /FGF5 ^{-/-} double mutant mice, although the reported results seem to be mainly due to FGF2 depletion	Reuss et al., 2003
DUSP4	↓ 1.61	DUSP1 has been associated with enhanced innate immunity	Hendriks et al., 2013
DUSP6	↓ 1.51	DUSP1 has been associated with enhanced innate immunity	Hendriks et al., 2013

As it has been mentioned before, transfection with miR125b-M or miR125b-I did not trigger any major variation in gene expression levels. Similarly, no pathways were observed to be modulated. However, a closer analysis of more subtle variations (fold changes larger than 1.5) combined with a literature search for those genes previously associated with MS or BBB disruption retrieved a list of genes (**Appendix 5.C**) of interest to be validated through qRT-PCR. Once again, no effects were seen in miR125b-M or miR125b-I transfected samples after validation.

5.2.5. Effect of cytokines, Shh and Vitamin D3 on steady state mRNA levels in hCMEC/D3 cells

Steady state mRNA levels for several genes selected from the microarray were further explored with qRT-PCR. Changes observed are summarised together with the main observations from the literature in **Table 5.4**

Table 5.4 – Individual genes selected from microarray analysis associated with Multiple Sclerosis (MS) pathology and/or Blood Brain Barrier (BBB) disruption. Genes showing a significant change in microarray analysis greater than 1.5-fold (adjusted p value < 0.05) and associated with MS and/or BBB disruption in the literature were further analysed by qRT-PCR. Significant changes observed in 3 independent analysis are summarised in the table together with the most relevant observations from the literature. Vitamin D3 abbreviated as VitD3. (↑ for up-regulation; ↓ for down-regulation; - for unchanged).

Gene Name	Response to Treatments (n=3)			Observation	Reference
	Cytokines	Shh + VitD3	Cytokines + Shh + VitD3		
F3	↑	↓	↓	Increased expression in MS plaques	Reviewed in Wang et al., 2016
Notch3	↓	-	↓	Increased BBB permeability in Notch3 ^{-/-} mice	Henshall et al., 2015
RORC	↓	-	-	Vitamin D3 inhibits Th17 differentiation through RORC downregulation	Hamzaoui et al., 2014 Ikeda et al., 2010 Zhang et al., 2008
SMAD6	↓	-	↓	Inhibitor of SMAD4, whose decreased activity has been associated with BBB opening	Ronaldson et al., 2009

Thus, from the list of candidates, *Tissue Factor 3* (F3 or TF) was the only one consistently regulated by a combination of Shh and Vitamin D3 and other genes such as Notch3 (**Figure 5.10**) did not respond to Shh and Vitamin D3 addition. Thus, future analysis will focus on F3 variations.

Microarray analysis reported a cytokine-driven increase in F3 mRNA levels (adjusted p value = 0.04 and 1.77-fold increase). This cytokine effect was corroborated through validation by qRT-PCR of the same samples used in the microarray analysis (2.04 ± 0.36 vs 1.04 ± 0.16 , $p < 0.05$) (**Figure 5.11**). Additionally, microarray validation also revealed a Shh and Vitamin D3 driven reduction in F3 mRNA levels (0.48 ± 0.09 vs 1.04 ± 0.16 , $p < 0.05$) when compared with untreated samples (**Figure 5.11**). In the presence of a combination of Shh and Vitamin D3, cytokine-driven increase in F3 gene expression levels was maintained when compared with untreated cells (2.92 ± 0.49 vs 1.04 ± 0.16 , $p < 0.05$) (**Figure 5.11**).

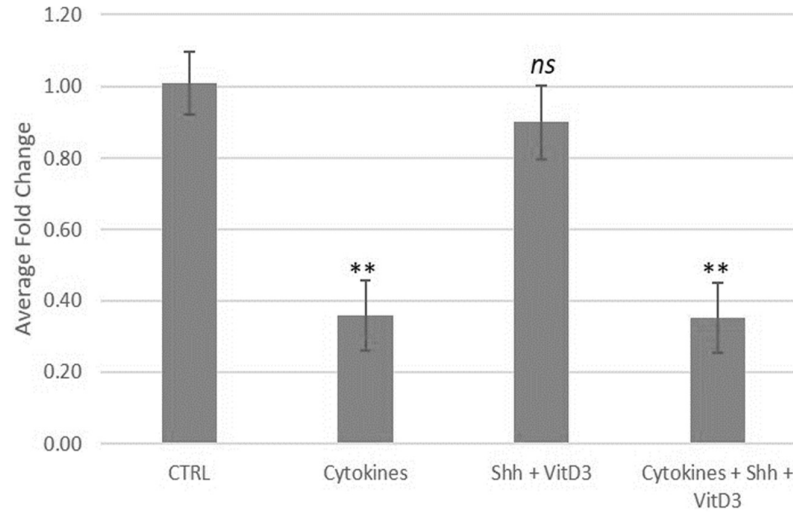


Figure 5.10 – Notch3 mRNA levels are modulated by cytokines but not by combination of Shh and Vitamin D3. hCMEC/D3 cells confluent monolayers were incubated with a mixture of cytokines (TNF α and IL1 α both at 10ng/ml) and/or a combination of Shh (100ng/ml) and Vitamin D3 (VitD3) (100nM) before being sent for microarray analysis. Microarray reported variations in F3 mRNA steady-state levels when then validated by qRT-PCR analysis of the same samples. All measurements were normalised to 18S endogenous control. Statistically significant differences were assessed via One-way ANOVA with post-hoc Tukey. Each bar represents the mean \pm SEM for 3 wells. ** $p < 0.01$; ns = $p > 0.5$. Experiment replicated three times.

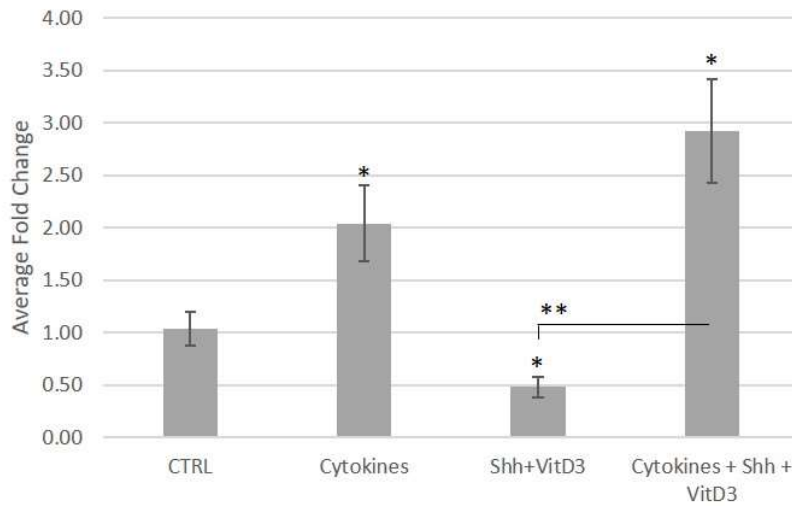


Figure 5.11 – F3 mRNA levels are modulated by cytokines and a combination of Shh and Vitamin D3. *hCMC/D3 cells confluent monolayers were incubated with a mixture of cytokines (TNF α and IL1 α both at 10ng/ml) and/or a combination of Shh (100ng/ml) and Vitamin D3 (VitD3) (100nM) before being sent for microarray analysis. Microarray reported variations in F3 mRNA steady-state levels when then validated by qRT-PCR analysis of the same samples. All measurements were normalised to 18S endogenous control. Statistically significant differences were assessed via One-way ANOVA with post-hoc Tukey. Each bar represents the mean \pm SEM for 3 wells. * $p < 0.5$; ** $p < 0.01$. Data from a single experiment.*

In order to gain some detailed knowledge of the observed *F3* regulation, hCMEC/D3 confluent monolayers were incubated with a mixture of cytokines (TNF α and IL1 α at 10ng/ml), Shh (100ng/ml) and/or Vitamin D3 (100nM) for 4h, 8h, 12h and 24h before measuring steady state mRNA levels by qRT-PCR. No variations in *F3* gene expression levels were detected in any of the different conditions at either 4h or 8h after treatment addition (**Figure 5.12**). Interestingly, at both 12h (2.64 ± 0.33 vs 1.01 ± 0.08 , $p<0.05$) and 24h (6.30 ± 1.06 vs 1.02 ± 0.15 , $p<0.01$), addition of cytokines caused a significant increase in *F3* mRNA levels when compared with untreated controls (**Figure 5.12**). A combination of Shh and Vitamin D3 triggered a significant downregulation on *F3* mRNA levels at 24h post-treatment (0.47 ± 0.05 vs 1.02 ± 0.15 , $p<0.01$) (**Figure 5.12**). However, Shh and Vitamin D3 could only partially protect against cytokine-induced increase in *F3* expression levels as, although significantly lower than the levels reported for cytokine-treated monolayers (2.39 ± 0.32 vs 6.30 ± 1.06 , $p<0.05$), *F3* levels were still significantly higher than those for untreated controls (2.39 ± 0.32 vs 1.02 ± 0.15 , $p<0.01$) (**Figure 5.12**). Interestingly, the Shh and Vitamin D3 partial protection against cytokine-driven increase in *F3* mRNA levels was not observed in previous analysis (**Figure 5.11**). Despite this disparity, Shh and Vitamin D3 combined ability to partially protect against cytokine-driven increase in *F3* mRNA levels was again confirmed in a third independent experiment (not shown), supporting the results presented in **Figure 5.12**. Cytokine-mediated induction of *F3* gene expression seemed to be time-dependent, as cytokine-induced *F3* levels became apparent between 12h and 24h after treatments (**Figure 5.12**).

Cytokine-, Shh- and Vitamin D3-mediated regulation of *F3* gene expression levels identify *F3* as a possible candidate that could be behind the observed effects in barrier modulation. Attempts were made to explore effects of cytokines, Shh and/or Vitamin D3 on *F3* protein levels. Unfortunately, Western Blot analysis could not be optimised and *F3* was not detectable.

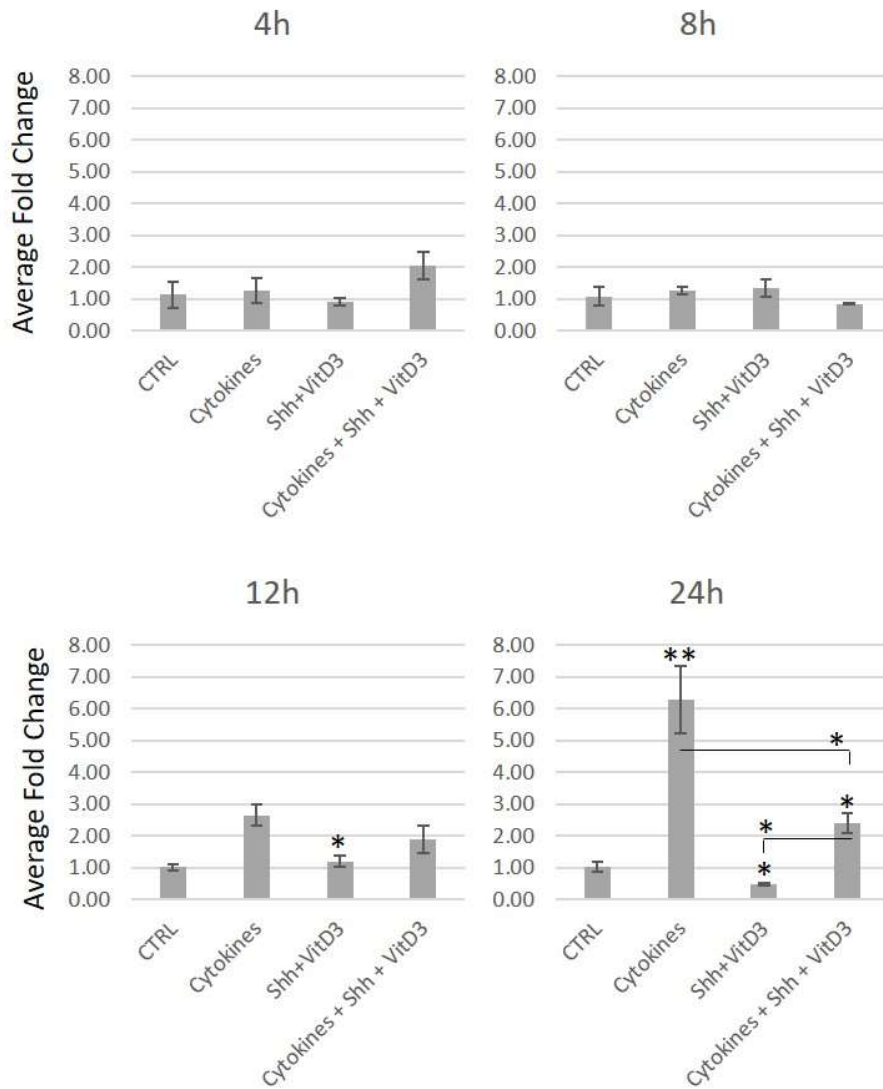


Figure 5.12 – A combination of Shh and Vitamin D3 can partially protect against cytokines-driven increase in F3 expression. hCMEC/D3 cells confluent monolayers were incubated with a mixture of cytokines (TNF α and IL1 α both at 10ng/ml) and/or a combination of Shh (100ng/ml) and Vitamin D3 (VitD3) (100nM) during 4h, 8h, 12h and 24h. After treatment, mRNA steady-state levels of F3 were determined by qRT-PCR. All measurements were normalised to 18S endogenous control. Statistically significant differences were assessed via One-way ANOVA with post-hoc Tukey. Each bar represents the mean \pm SEM for 3 wells. * $p < 0.5$; ** $p < 0.01$. Experiment replicated twice.

5.3. DISCUSSION

5.3.1. miR125b as a mediator of BBB stability

Both miRNAs (miR125b and miR326) were expressed in hCMEC/D3 cultured monolayers, but only miR125b seemed to be responsive to cytokine stimulation (**Figure 5.1**), at the time-point studied. The response of miR125b to inflammatory conditions has been previously reported in the literature since stimulation of isolated murine splenocytes with TNF α could trigger an acute increase in miR125b levels after 30min treatment (Tili et al., 2007). Regarding other miRNAs and BBB barrier function, Reijerkerk *et al.* reported a decrease in miR125a-5p levels in hCMEC/D3 monolayers in response to TNF α and INF γ -induced inflammation (Reijerkerk et al., 2013). These authors demonstrated a role for miR125a-5p in loss of junctional integrity as well as lower expression in MS lesions. The same group also explored the role of miR155 in hCMEC/D3 cell barrier function, and here demonstrated a negative effect of miR155 on dextran permeability.

The observed ability of miR125b to directly impact on hCMEC/D3 barrier integrity has not been previously reported, to our knowledge (**Figures 5.5** and **5.6**). However, recently a role for miR125b in intestinal barrier dysregulation through cingulin downregulation has been shown (Martínez et al., 2017) together with an ability to target VE-cadherin translation in human umbilical ECs (Muramatsu et al., 2013). Intriguingly, miR125b inhibition can completely abrogate cytokine effects on TEER in our model system. It remains to be determined whether miR125b regulates barrier integrity *in vitro* e.g. through analysis of dextran permeability or immune-cell transmigration (and indeed *in vivo*).

5.3.2. Microarray analysis of cytokine-mediated effects on hCMEC/D3 monolayers

Microarray analysis of cytokine-treated hCMEC/D3 monolayers revealed increased and decreased expression of several genes summarised in **Table 5.2** and **Table 5.3**, together with the most relevant observations related with MS pathogenesis. Interestingly, a previous study already reported cytokine-induced changes in hCMEC/D3 gene expression profile using a cytokine mixture of TNF α and INF γ (Lopez-Ramirez et al., 2013). Despite the fact that these authors used a different

cytokine combination, used, it is interesting to note that of the genes listed ICAM1, VCAM and IL15R α and CXCL5 (**Table 5.2**) were reported to be up-regulated in response to cytokines in both studies (Lopez-Ramirez et al., 2013). These observations suggest that genes common to both studies are regulated by TNF α . As it has been previously discussed in chapter 1, TNF α , INF γ and IL1 β are pro-inflammatory cytokines secreted during neuroinflammation capable of promoting BBB permeability and enhancing further infiltration of activated immune cells into the brain (reviewed in Noseworthy et al., 2000). However, in the context of Multiple Sclerosis (MS), INF γ 's role seems contradictory: INF γ has been reported to promote pathogenesis in EAE mice (a murine model of MS) (Goverman, 2009; Hirota et al., 2011); whereas studies with INF γ ^{-/-} or INF γ receptor (INF γ R)^{-/-} mice reported a more severe EAE pathogenesis (Ferber et al., 1996; Krakowski & Owens, 1996; Willenborg et al., 1996). Additionally, *in vitro* studies with endothelial cells isolated from INF γ R^{-/-} mice showed that leukocyte infiltration and BBB permeability could be prevented by reconstitution of INF γ R (Ni et al., 2014). Due to this controversial role of INF γ in the pathology of MS this cytokine was not used in this thesis.

5.3.3. Microarray analysis of miR125b-mediated effects of cytokines-treated hCMEC/D3 monolayers

To further clarify the underlying mechanisms of miR125b-mediated effects of barrier integrity under inflammatory conditions, Microarray analysis of cytokines-treated hCMEC/D3 monolayers transfected with miR125b mimic (also referred as miR125b overexpression) or inhibitor were performed.

As it has been previously discussed, no miR125b-dependent changes were reported by our Microarray analysis of cytokines-treated hCMEC/D3 monolayers. It is possible that cytokine treatment overruled any subtler changes derived from miR125b overexpression or inhibition and, as such, future studies should focus on miR125b-mediated effects under lower or absent inflammatory conditions. However, due to the major effects on cytokine-driven barrier TEER values observed by miR125b overexpression or inhibition (**Figure 5.6**), it is more likely that any miR125b-derived effects took place at earlier time-points. It seems unlikely that effects were on cell number given that total RNA isolated from cells transfected with miR125b mimic or inhibitor did not differ substantially from other treatments.

In order to explore possible miR125b effects, a closer analysis of more subtle variations (rather than whole pathways) retrieved a list of genes of interest previously related to MS in the published literature (**Table 5.3**). Validation by qRT-PCR revealed a cytokine-driven downregulation of Notch3, RAR Related Orphan Receptor C (RORC) and SMAD6 together with a consistent up-regulation of Tissue Factor or Coagulation Factor III (TF or F3) (**Table 5.3**). TNF α has been shown to induce Notch3 expression in periodontal ligament stem cells (Ma et al., 2018) and human oesophageal epithelial cells (Kasagi et al., 2018). Similarly, TNF α was shown to induce RORC gene expression in CD4⁺ cells (Zheng et al., 2014) and SMAD6 mRNA levels in a murine myoblast cell line (Mukai et al., 2007). Whilst Vitamin D3 has been shown to downregulate Notch3 in mammosphere cultures (Shan et al., 2016), RORC gene in human naïve CD4⁺ T cells (Ikeda et al., 2010) and peripheral blood CD4⁺ T cells from asthmatic patients (Hamzaoui et al., 2014); and SMAD6 gene expression levels in a breast epithelial cell line (Lee et al., 2006), no consistent effects of Vitamin D3 expression were observed in hCMEC/D3, suggesting cell-specific effects.

Interestingly, cell surface complement pathway proteinase tissue factor (F3) was not only consistently up-regulated by cytokines but its gene expression could also be downregulated by a combination of Shh and Vitamin D3 in 3 out of 3 experiments (**Figure 5.11** and **5.12**). Additionally, the cytokine effect could be partially reversed by addition of Shh and Vitamin D3, suggesting a possible protection (**Figure 5.11** and **5.12**). Of great relevance, F3 expression has been found to be increased in MS lesions, and pharmacologic inhibition of F3, as well as reduced expression in astrocytes, may ameliorate MS severity and progression in a murine model of MS (reviewed in Wang et al., 2016). TNF α was shown to increase F3 levels in isolated murine aortas and human HUVECs (Liang et al., 2014). On the other hand, Shh can induce F3 expression in cultured medulloblastoma cells (D'Asti et al., 2014). In vascular smooth muscle cells, the TNF α -induced increase in F3 expression and activity was inhibited by addition of the active form of Vitamin D3 (Martinez-Moreno et al., 2016).

Induction of F3 triggers the coagulation cascade, which will ultimately lead to the formation of thrombin (reviewed in Owens & Mackman, 2010). Puhlmann *et al.* (2005) provided in vitro evidence of a major role for F3 in HUVEC permeability to Evans Blue, speculating on the role of thrombin in barrier disruption (Puhlmann et al.,

2005). Thrombin's ability to induce BBB breakdown has been more recently described in several models (Hun Lee et al., 2015; Li et al., 2015; Festoff et al., 2016). Interestingly, Machida *et al.* suggested that thrombin could be mediating BBB damage through an increased MMP-9 release from brain pericytes in a PAR-1-dependent manner (Machida et al., 2015). Thus, it is possible that the observed effects of cytokines, Shh and Vitamin D3 on barrier integrity in our *in vitro* BBB model could be a response, in part, to a variation in F3 and the consequent effect on thrombin levels. However, the absence of pericytes in our *in vitro* BBB model suggests that, if the observed effects are due to modulations in the F3/thrombin pathway, alternative mechanisms may be involved. Supporting this idea, *in vitro* studies in HUVEC mono-culture showed that IL1 β -mediated barrier disruption was dependent on F3 activity (Puhlmann et al., 2005). In this sense, studies in a mono-culture of mouse brain ECs reported an overall decrease in TJ protein levels (ZO-1, occluding and claudin-5) and TEER values after thrombin treatment (Lee et al., 2015), supporting the idea of a thrombin-mediated mechanism exclusive to ECs. Thus, further research should elucidate if the F3/thrombin pathway is playing a role in the observed cytokines-mediated barrier dysfunction and the possibility of a Shh and Vitamin D3 driven protection in this context.

Overall these observations further support the protective effect of the Vitamin D3 axis in BBB integrity whilst future studies will refine the individual effects of Vitamin D3 and Shh in our model system.

5.4. KEY FINDINGS

- miR125b is expressed by hCMEC/D3 cells and its expression can be increased by a mixture of cytokines.
- Overexpression of miR125b triggers a reduction in BBB integrity (measured as TEER), whereas its inhibition promotes BBB integrity above control levels (measured as TEER).
- Cytokine-driven BBB breakdown can be further enhanced by miR125b overexpression (measured as TEER) whereas miR125b inhibition fully protect abrogates cytokine-driven effects, maintaining BBB integrity above control levels (measured as TEER).
- hCMEC/D3 changes in gene expression profile after cytokine stimulation (**Table 5.2** and **Table 5.3**).
- Cytokine-mediated increase in F3 expression levels can be partially blocked by a combination of Shh and Vitamin D3. In the absence of cytokines, a combination of Shh and Vitamin D3 can also reduce F3 gene expression levels.

5.5. FUTURE STUDIES

- Expression of miR326 should be explored at earlier time-points following hCMEC/D3 treatment with cytokines
- The effects of miR125b overexpression and inhibition on hCMEC/D3 gene expression profile should be assessed in the absence of cytokines
- The effects of miR125b overexpression and inhibition on hCMEC/D3 gene expression profile under inflammatory conditions should be assessed at earlier time-points.
- The effects of miR125b overexpression and inhibition in BBB stability (in the presence and absence of cytokines) should be assessed with an alternative method (e.g. fluorescently labelled dextran extravasation or activated immune-cell transmigration).
- Vitamin D3 effects on expression of Notch3, RORC and SMAD6 should be studied in our BB *in vitro* model at different time-points.
- The reported modulation of F3 should be also assessed at protein and activity (procoagulant activity assay) levels.
- The functional role of the F3/thrombin pathway in barrier integrity, and the effects of inflammation, Shh and Vitamin D3, should be assessed in our *in vitro* BBB model.

6. Discussion

The work presented in this thesis seems to indicate that both Hedgehog and Vitamin D3 pathways could be synergistically interacting in order to protect against the observed cytokine-driven loss in endothelial barrier stability. As previously discussed in Chapter 3 and 4, Shh and Vitamin D3 could be mediating their protection against cytokine-driven endothelial barrier disruption through regulation of metalloproteinase levels and/or activities. This and other alternative mechanisms by which Shh and Vitamin D3 could be synergistically protecting against cytokine's effects will be discussed below.

6.1. ZO-1 regulation and cytoskeletal rearrangements

The effects of inflammation on the integrity of endothelial barriers has been broadly reported in the literature (Forster et al., 2008; Aslam et al., 2012; Cohen et al., 2013; Labus et al., 2014). However, the mechanisms underlying this effect are not yet fully understood.

The most obvious manner in which cytokines could modulate BBB stability is through direct regulation of junctional proteins. In this regard, studies in mouse brain ECs described repressive elements in claudin-5 promoter responsive to TNF α -mediated NF κ B signalling (Aslam et al., 2012). Similarly, studies in HUVECs have reported a decrease in ZO-1 gene expression levels following TNF α stimulation (Zhang et al., 2017). Agreeing with this, stimulation with a mix of cytokines significantly reduced ZO-1 mRNA levels in our BBB *in vitro* model (Chapter 3). Interestingly both Shh and Vitamin D3 pathways can increase ZO-1 mRNA levels in brain endothelium (chapter 4; Xia et al., 2013; Won et al., 2015), offering a possible route for the observed Shh and Vitamin D3 synergistic protection against cytokine-driven loss in barrier integrity. However, the mechanisms by which cytokine, Shh and Vitamin D3 signals are integrated by the cell in order to modulate ZO-1 expression levels remain unclear. For example, *in vitro* studies using human tubular epithelial kidney cells have shown that Vitamin D3 can induce a direct interaction between VDR and one of NF κ B's subunit (p65) resulting in the sequestration of the latter (Tan et al., 2008). NF κ B's subunit p65 can be retained in the cytoplasm by direct binding with I κ B, leading to NF κ B repression (May & Ghosh, 1998). However, upon phosphorylation, I κ B is targeted for proteasomal degradation resulting in p65 nuclear translocation and consequent targeting of NF κ B's responsive genes (May & Ghosh, 1998). In this

regard, Vitamin D3 treatment has been shown to inhibit I κ B phosphorylation (and consequent degradation) in a brain microvascular endothelial cell line (Won et al., 2015). Additionally, studies in shVDR endothelial cells (endothelial cells in which VDR expression was blocked by shRNA) showed a reduction in I κ B levels accompanied by an increase in nuclear p65 (Bozic et al., 2015). Thus, these observations support the suggested Vitamin D3's inhibitory effect on NF κ B signalling.

Although not in the context of the BBB, a cross-talk between Shh and NF κ B has been also described in the literature, but its outcome is highly dependent on the studied cell type: cytokine-dependent NF κ B activation can be suppressed by exogenous addition of Shh in a pancreatic cell line (Umeda et al., 2010), whereas Shh can induce NF κ B transcriptional activity in a human renal cell carcinoma cell line (Dormoy et al., 2009). Interestingly, Akt phosphorylation (and consequent activation) is a shared element between the cytokine (reviewed in Alvarez et al., 2011), Shh (Kanda et al., 2003; Riobo et al., 2006) and Vitamin D3 (Zhang & Zanello, 2008; Datta Mitra et al., 2013) signalling routes, also pointing towards Akt as a possible molecular switch capable of integrating all these pathways.

6.2. ZO-1 phosphorylation: possible role in VitD3 and Shh effects on barrier integrity

Interestingly, ZO-1's phosphorylation signature can impact on its cellular localization: whereas tyrosine phosphorylation has been correlated with both increased and decreased barrier permeability, depending on the cell type, serine/threonine phosphorylation can promote ZO-1 endosomal internalization accompanied by an increase in permeability in epithelial cells (reviewed in Harhaj & Antonetti, 2004). In this regard, the PI3K/Akt pathway can mediate ZO-1 phosphorylation and consequent regulation of cellular distribution (Furuse et al., 1999). Thus, it is also possible that cytokine-, Shh- and Vitamin D3-driven regulation of barrier properties could be mediated by changes in ZO-1 phosphorylation signature, affecting its cellular distribution and its ability to form functional junctions. In this regard, the work presented in this thesis regarding Akt's inhibition effects on ZO-1

subcellular localization in MCEC-1 monolayers seem to indicate that all these pathways could be, at some point, regulated by Akt activity.

ZO-1 proteins act as adaptor proteins between the transmembrane junctional components (such as claudins and occludin) and the actin cytoskeleton (Fanning et al., 1998; Itoh et al., 1999). In this sense, ZO proteins work as adaptors between the dynamic cytoskeleton and the stable TJs, providing ECs with a barrier that can adjust to different cellular requirements. Under certain environmental conditions, actin filaments can change their usual conformation (distributed across the ECs as short filaments and monomers) and polymerise into large structures known as stress fibers (Burrige & Wittchen, 2013). *In vitro* studies using isolated mouse brain capillaries and human brain microvascular ECs have shown that the formation of stress fibers can increase cytoskeletal tension, leading to impaired TJ formation (McKenzie & Ridley, 2007; Shi et al., 2016). Interestingly, exposure of brain microvascular ECs to TNF α increases actin stress fibre formation, leading to a loss of ZO-1 immunostaining and an increase in barrier permeability (Wiggins-Dohlvik et al., 2014). Thus, it is possible that the cytokine-mediated increase in barrier permeability observed in our *in vitro* BBB model could be due to an enhanced formation of stress fibers and the consequent junctional disassembly.

6.3. Actin and junctional integrity

Actin contractility is induced by the phosphorylation of myosin light chain (MLC), which is in turn activated by the RhoA/ROCK/myosin-light chain kinase (MLCK) pathway (Hathaway et al., 1981). Interestingly, studies in human microvascular cardiac cells showed an ability for Shh to induce RhoA activation and the consequent formation of actin stress fibers (Chinchilla et al., 2010). This observation seems to contradict the observed protective effect of Shh against cytokine-mediated loss in barrier integrity, but it is possible that Shh effects could be cell type-specific. However, studies in brain microvascular ECs showed that Shh promotes angiogenesis after oxygen-glucose deprivation through an enhanced RhoA/ROCK pathway, suggesting that this mechanism could be conserved in the context of the BBB (He et al., 2013). Additionally, although no data is available in the context of the BBB, Vitamin D3 has been reported to reduce stress fibre formation in primary pancreatic stellate cells

(Wallbaum et al., 2018), offering another possible mechanism by which Vitamin D3 could be enhancing barrier formation in the presence of cytokines.

6.4. Roles of RhoA activation and CREB in barrier integrity

Studies in hCMEC/D3s show an actin-mediated nuclear translocation mechanism for ZO-1 following RhoA/ROCK/MLCK activation resulting in ZO-1 internalisation and TJ impairment (Zhong et al., 2012). This research also reported that Rho activation can trigger cAMP Response Element Binding Protein (CREB) phosphorylation, which in turn could enhance MLC activation (Zhong et al., 2012). CREB is a transcription factor that can recognise and bind to a CREB Responsive Element (CRE) present in the promoter region of many cAMP-responsive genes (Johannessen et al., 2004) including ZO-1 (Chen et al., 2008; Zhong et al., 2012). Akt can phosphorylate and activate CREB (Du & Montminy, 1998), so it could be proposed that Akt-mediated phosphorylation of CREB could enhance DNA binding activities leading to an increase in ZO-1 transcription, which would in turn enhance BBB integrity. However, Akt/CREB-dependent modulation of ZO-1 gene expression in the context of the BBB remains to be fully elucidated, but it seems that, overall, the Akt/CREB pathway could mediate opposing effects on BBB stability, inducing ZO-1 internalisation and TJ disruption or directly promoting ZO-1 gene expression.

The suggested Akt/CREB modulation of ZO-1 expression offers a new mechanism in which cytokine-, Shh- and Vitamin D3- pathways could converge, not only through regulation of Akt, but also through the modulation of CREB activities. Vitamin D3 promotes CREB binding in a monocytic cell line (Moeenrezakhanlou et al., 2007). In contrast, detailed studies of the renin promoter showed that Vitamin D3 (through VDR) can block renin gene expression by blocking CREB binding, a renin activator (Yuan et al., 2007); The role of the Akt/CREB pathway as a converging point for the cytokine, Shh and Vitamin D3 pathways needs to be further explored in the context of the BBB and inflammation, as the previous literature seems to suggest a wide variability depending on the studied cell type and integrated stimuli.

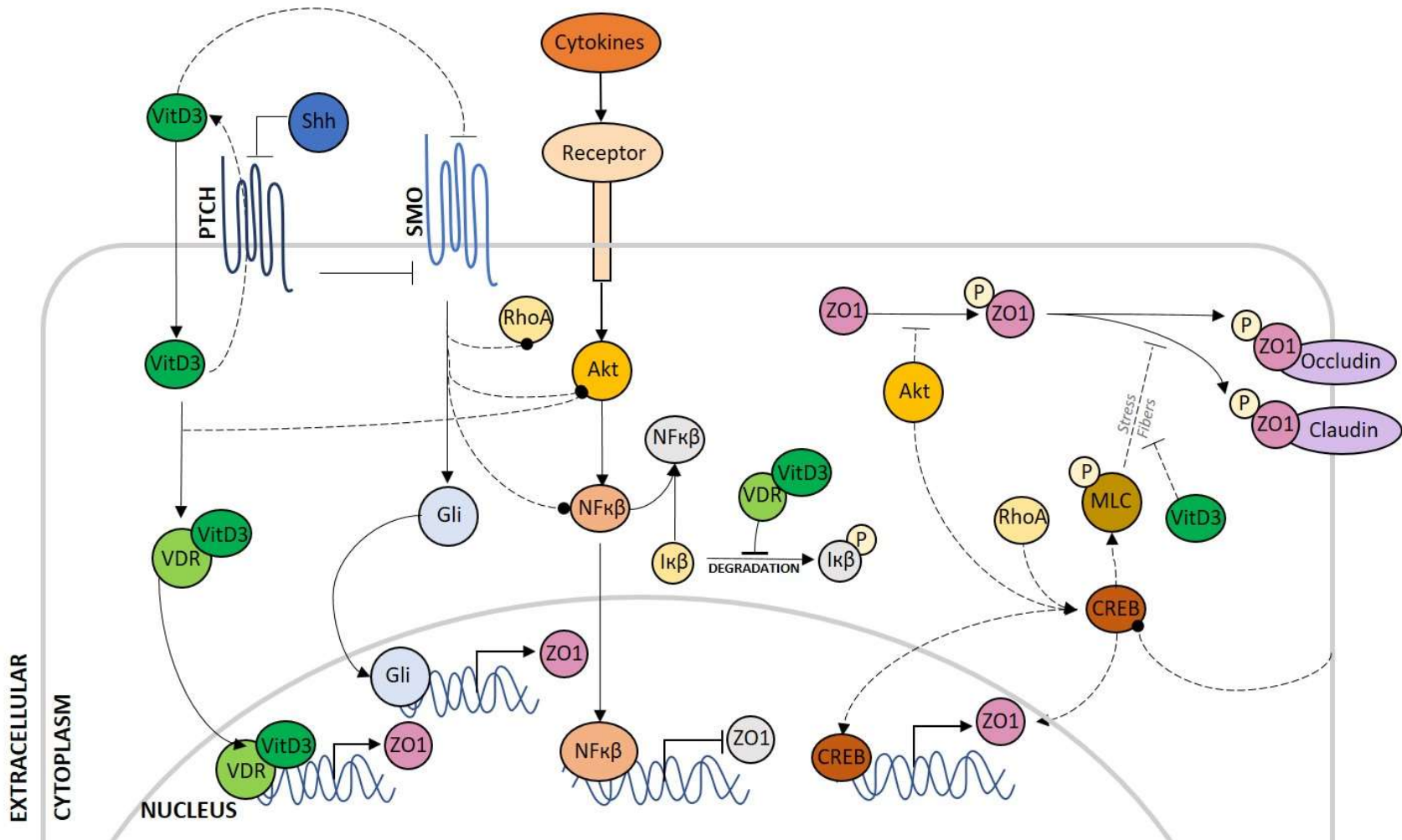


Figure 6.1 - Possible mechanisms underlying cytokine, Shh and Vitamin D3 interactions regulating junctional ZO-1 in the BBB. Interactions validated in the context of the BBB are represented by solid lines, while dotted lines refer to connections in a different cellular context. Arrowheads indicate activation, right-angle lines inhibition and filled circles an uncertain effect. See text for discussion of pathways depicted.

Actin-mediated disassembly of TJs could result in the opening of cell-to-cell contacts, exposing other junctional proteins and ECM components to the degradation by surrounding metalloproteinases. As discussed, NF κ B activation results in the transcription of several (M)MPs (such as MMP1, 3, -9, -10, -12 and -13 (Lee et al., 2007; Akhtar et al., 2010; Fanjul-Fernandez et al., 2010; Nakayama, 2013; Yun et al., 2014) and some ADAMTS proteinases (Li et al., 2015; Sun et al., 2015). Recent *in vitro* studies with a human brain microvascular EC line has shown that under hypoxic conditions NF κ B can mediate BBB disruption through enhanced MMP9 expression (Won et al., 2015). Thus, it is possible that the reported modulation of metalloproteinase levels seen in this thesis could be responding to a cytokine-, Shh- and/or Vitamin D3-dependent regulation of NF κ B. Future studies should assess the role of NF κ B in metalloproteinase expression in the context of our *in vitro* BBB model.

6.5. Regulation of metalloproteinase activity

Preliminary experiments with a broad inhibitor of endocytic processes revealed not only that endocytosis mechanisms could be regulating metalloproteinase (MMP3) extracellular levels endogenously but also that Shh and Vitamin D3 reduction in metalloproteinase (MMP3) secreted levels could be also mediated by an endocytic mechanism, perhaps involving LRP1. Cytokine suppression of LRP1 has been observed at the protein level in chondrocytes (Yamamoto et al., 2017) and in this thesis mRNA levels were reduced by cytokines in human endothelial cells (Chapter 4). In the context of neuroinflammation, LRP1 has been described to participate in the extracellular clearance of various metalloproteinases (MMP-2, -9, -14, -16 and -17) and their inhibitor TIMP1 (reviewed in Gonias & Campana, 2014). Additionally, LRP1 may be also playing an essential role in pathologies such as MS through the clearance of extracellular debris and degraded myelin, both important enhancers of the immune response (reviewed in Gonias & Campana, 2014). In this sense, LRP1 expression has been shown to be increased in patient's chronic active MS lesions (Hendrickx et al., 2013).

LRP proteins are not only known for participating in the extracellular clearance of secreted proteins but also to trigger intracellular signalling cascades (Suzuki et al., 2009; Zhang et al., 2007). In this regard, several studies have reported LRP ability to impact on NF κ B activity: in ECs, LRP mediates NF κ B-dependent activation of E-

selectin gene expression in an *in vitro* model of atherosclerosis (Yu et al., 2005); in an murine model of middle cerebral artery occlusion, tissue plasminogen (tPA)-mediated activation of LRP triggered NF κ B activation and the consequent inflammatory response (Zhang et al., 2007); however, studies in a macrophage cell line reported LRP1's ability to repress NF κ B activity in response to TNF α stimulation, pointing towards LRP1 as an anti-inflammatory agent (Gaultier et al., 2008). Thus, it is possible that LRP-mediated modulation of NF κ B depends on the studied cell type and/or the stimuli, indicating that further research is needed regarding LRP/NF κ B signalling under inflammatory conditions in the context of the BBB. In any case, Shh and Vitamin D3 seen ability to reverse cytokine-driven decrease in LRP1 gene expression levels (Chapter 4) should be also considered as an alternative mechanism by which cytokine, Shh and Vitamin D3 signalling pathways could be converging in the regulation of NF κ B activities and, consequently, BBB stability. Further studies should assess the role of LRP/NF κ B signalling cascade in BBB maintenance under inflammatory conditions and how Shh and/or Vitamin D3 could be modulating this mechanism in order to protect barrier integrity.

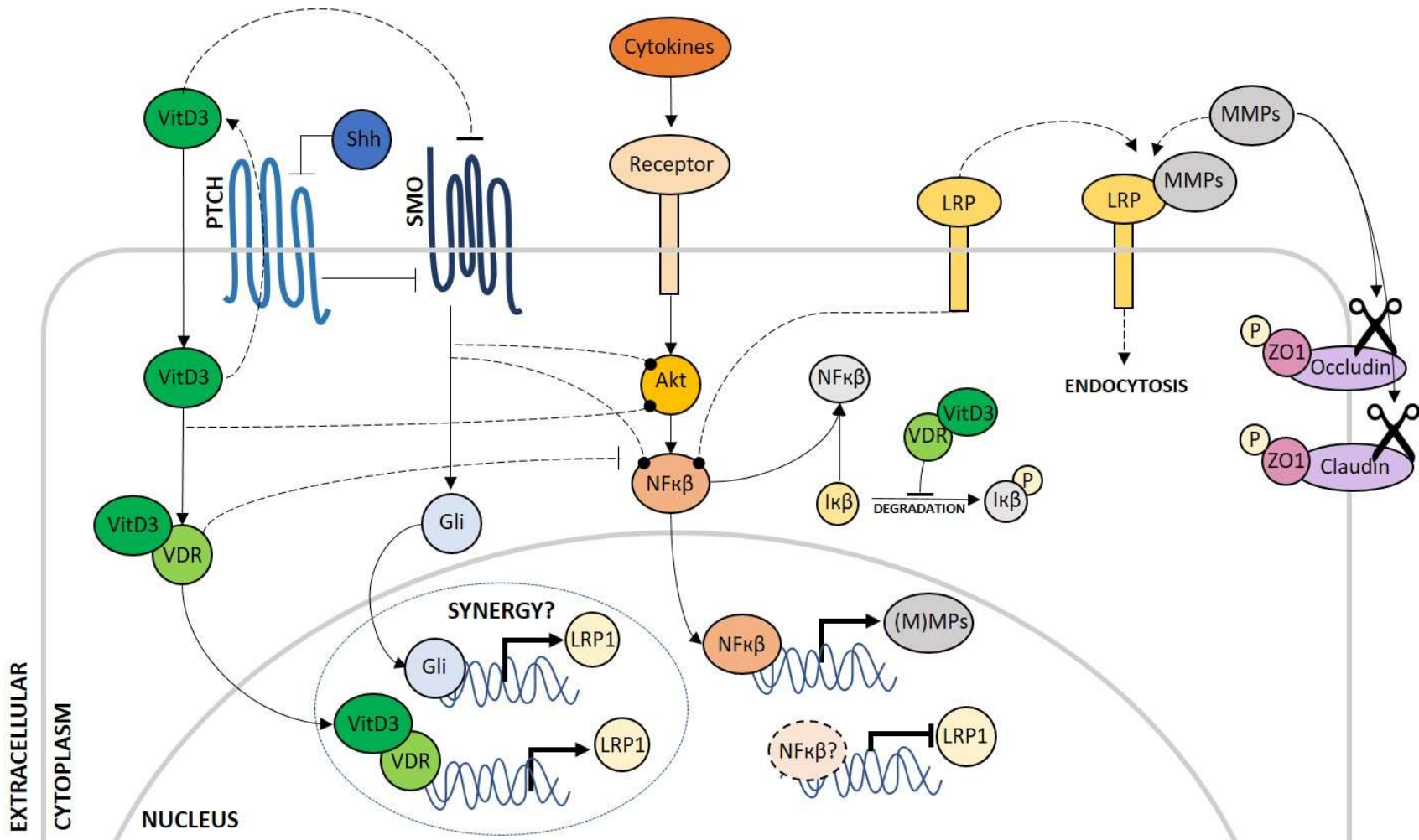


Figure 6.2 - Possible mechanisms underlying cytokine, Shh and Vitamin D3 interactions regulating metalloproteinase levels in the BBB. Cytokines reduce LRP1 expression. VitD3/VDR complex can target genes with a Vitamin D3 response element such as LRP1. In this thesis we see a combined ability of Shh and Vitamin D3 to induce LRP1 gene expression. LRP1 can mediate the endocytosis of secreted metalloproteinases and impact on NF κ B activity through its intracellular effects in other cell types. Interactions validated in the context of the BBB are represented by solid lines, while dotted lines refer to connexions described in a different cellular context. Arrowheads indicate activation, right-angle lines inhibition and filled circles an uncertain effect. See text for discussion of pathways depicted.

6.6. F3 as a regulator of BBB integrity

Interestingly, cell surface complement pathway proteinase tissue factor (F3) gene expression was up-regulated by and downregulated by a combination of Shh and Vitamin D3, also capable of partially reversing cytokine's effect (**Chapter 5, Figure 5.7**).

Induction of F3 triggers the coagulation cascade (**Figure 6.3**), which will ultimately lead to the formation of thrombin (reviewed in Owens & Mackman, 2010). Thrombin has been described to be capable of inducing cell contractility in lung endothelial barriers through MLC activation (reviewed in Kása et al., 2015) which, as it has been previously discussed, can lead to endothelial barrier disruption. Additionally, thrombin's ability to induce BBB breakdown has been recently described in the published literature (Hun Lee et al., 2015; Li et al., 2015; Festoff et al., 2016) as previously discussed. Treatment with coagulation inhibitors (such as heparin or dermatan sulfate) has been shown to reduce EAE severity and progression (Chelmicka-Szorc & Arnason, 1972; Inaba et al., 1999). Intriguingly, the levels of thrombin inhibitors were reported to be elevated during the course of acute EAE (a murine model of MS), although the authors speculate that this increase could be due to the EAE-associated increase in BBB permeability and the consequent entry of plasma components (including coagulation factors and their inhibitors) into the CNS (Beilin et al., 2005). In any case, the F3/thrombin pathway has been described in the literature to be cytokine-, Shh- and Vitamin D3- regulated: TNF α was shown to increase F3 levels in mouse isolated aortas and human HUVECs (Liang et al., 2014); Shh can induce F3 expression in cultured medulloblastoma cells (D'Asti et al., 2014); in vascular smooth muscle cells TNF α -induced increase in F3 expression and activity was inhibited by addition of Vitamin D3's active form (Martinez-Moreno et al., 2016); Vitamin D3 can down-regulate the expression of F3 in monocytic cells (Ohsawa et al., 2000) and studies in VDR knock-out mice have reported an increase in platelet aggregation through a down-regulation in the levels of anti-thrombin, suggesting a role for Vitamin D3 as a regulation of the coagulation cascade (Aihara et al., 2004) (**Figure 6.4**). Thus, Shh

and Vitamin D3 pathways could impact on each other in order to modulate BBB integrity through the F3/thrombin signalling cascade, the previously discussed literature points at the F3/thrombin pathway as a possible converging point for all these three pathways to exert their cross-talk.

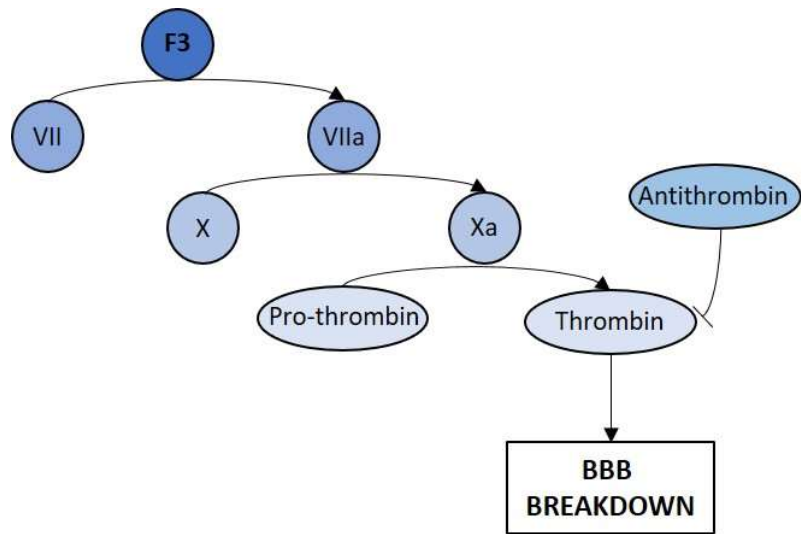


Figure 6.3 – Schematic representation of the Tissue Factor (F3) mediated pathway of the coagulation cascade. The coagulation cascade will eventually lead to the activation of thrombin and the consequent loss in Blood-Brain Barrier (BBB) integrity.

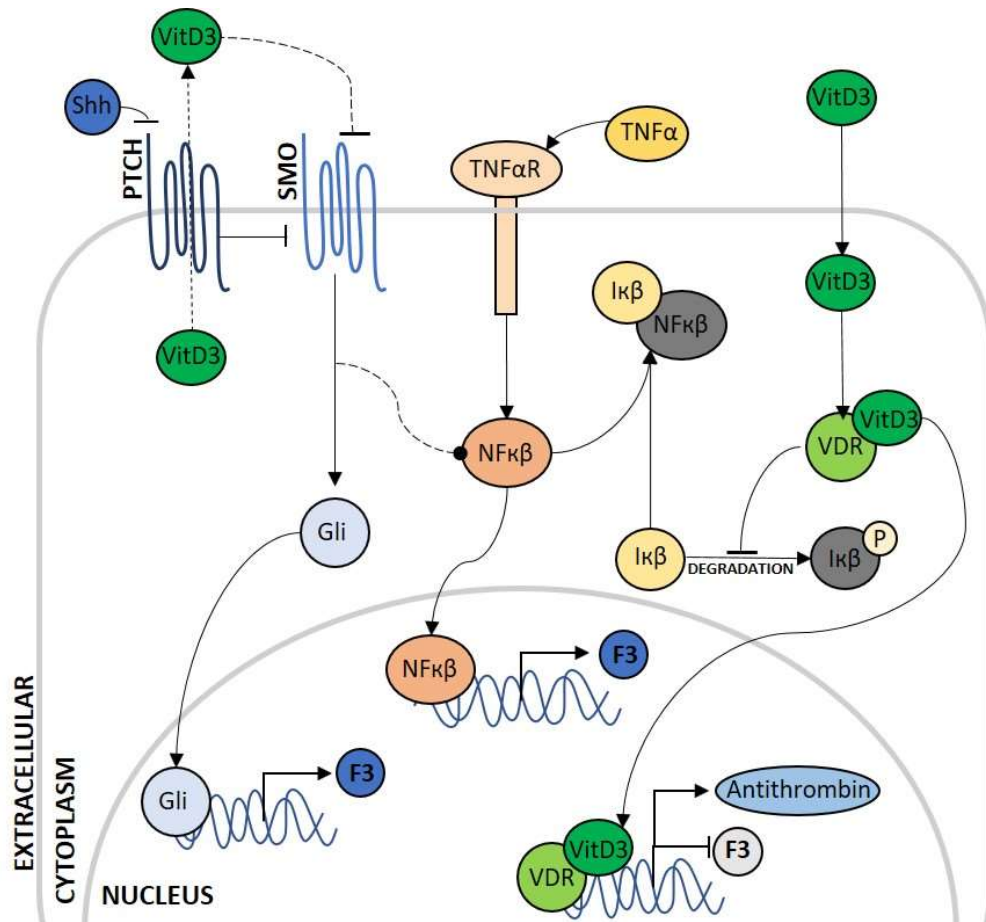


Figure 6.4 - Possible mechanisms underlying cytokine, Shh and Vitamin D3 interactions regulating F3 levels in the BBB. Interactions validated in the context of the BBB are represented by solid lines, while dotted lines refer to connections in a different cellular context. Arrowheads indicate activation, right-angle lines inhibition and filled circles an uncertain effect. See text for discussion of pathways depicted.

6.7. FUTURE STUDIES

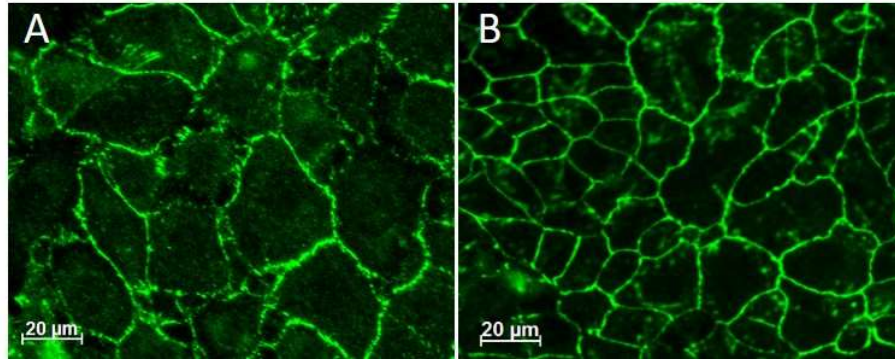
- Future studies should assess the role of NF κ B in the regulation of barrier functions in our *in vitro* model of the BBB. Additionally, the impact of cytokines, Shh and Vitamin D3 signalling on NF κ B regulation, on how all these three pathways could be integrated by NF κ B should be also studied. Assessing NF κ B nuclear translocation through immunostaining could be a suitable first approach. The potential synergistic effect of Shh and Vitamin D3 in BBB integrity and subsequent pathology could be assessed *in vivo* in the EAE mouse model for MS (a murine model of MS), with analysis of NF κ B translocation in endothelial cells *ex vivo*. NF κ B inhibitors have been successfully used as treatment for MS (Leibowitz & Yan, 2016) so their impact on disease severity and progression in combination with Shh and/or Vitamin D3 could be assessed in EAE mice. Additionally, EAE could be induced in a NF κ B reporter mouse system, monitoring NF κ B responses to EAE and eventually Shh and/or Vitamin D3 treatment. However, off-target effects of Shh treatment should be considered as it has been previously described to increase the migratory ability of activated monocytes (Dunaeva et al., 2010), pro-metastatic cells and in early stages of tumour development (reviewed in Skoda et al., 2017).
- Akt's potential role as a converging point for the cytokines, Shh and Vitamin D3 pathways in the context of our BBB *in vitro* model should also be assessed as it could be the start to elucidate the mechanism by which these pathways could impact on each other. The preliminary experiments in MCEC-1 cells presented in this thesis support Akt's involvement in all these three pathways and should be explored in our BBB *in vitro* system. However, since Akt plays a crucial role in a wide range of intracellular pathways, its inhibition could affect many cellular processes. As an alternative, the implication of Akt in the cytokine, Shh and Vitamin D3 pathways could be also studied through the assessment of Akt activation (phosphorylation).
- Previous literature suggests that ZO-1 phosphorylation could be regulating its cellular localisation and, consequently, junctional stability.

The impact of cytokines, Shh and Vitamin D3 signalling on ZO-1 phosphorylation pattern, together with its relevance in ZO-1 localization should be assessed. Additionally, Akt's suggested role as the kinase responsible for ZO-1 phosphorylation could be also explored.

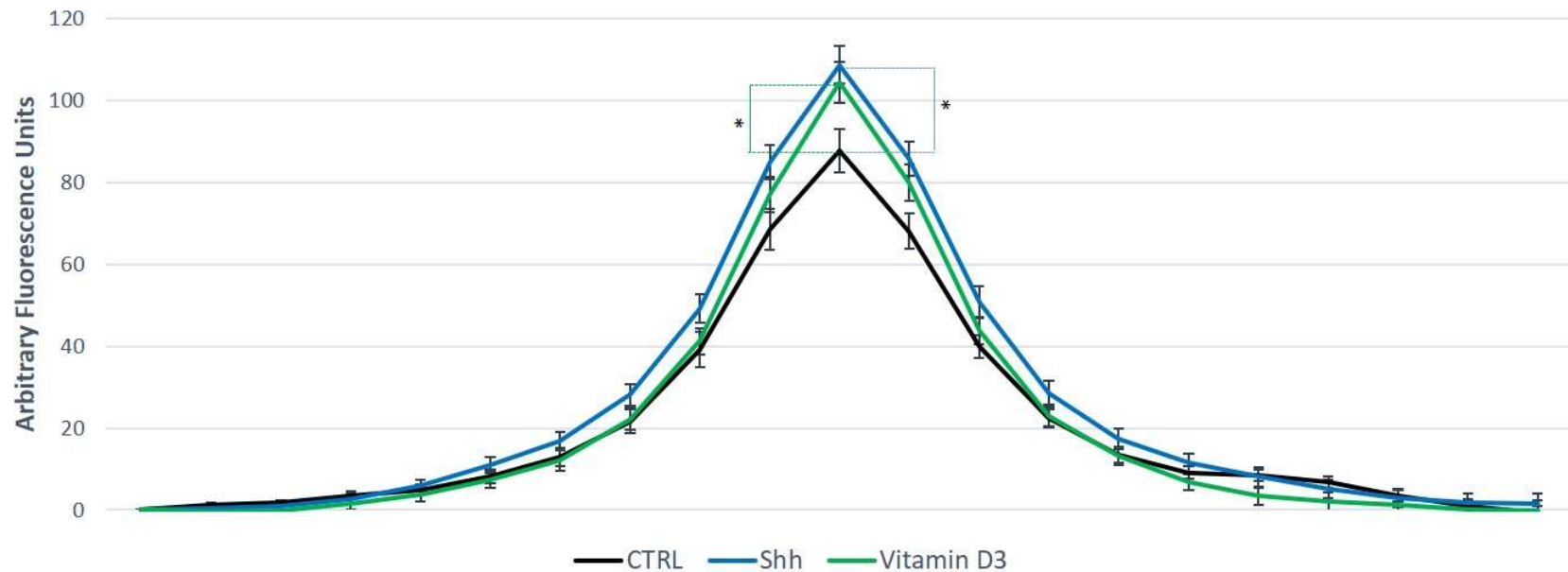
- If ZO-1 phosphorylation signature proved to be modulated by cytokines, the effects of targeted mutation of ZO-1 phosphorylatable residues in BBB maintenance could be explored.
- Alternatively, if Shh and/or Vitamin D3 treatment was shown to protect against cytokine-mediated changes in the ZO-1 phosphorylation pattern, the potentially protective effects of Shh and/or Vitamin D3 in BBB maintenance through ZO-1 phosphorylation could be studied in the EAE mouse model).
- Cytoskeletal reorganization mechanisms should also be considered as a mechanism underlying BBB modulation. Thus, cytokines, Shh and/or Vitamin D3 effects on cytoskeletal dynamics should be explored. However, as per Akt, actin remodelling is an essential step involved in many cellular processes. Thus, changes in cytoskeletal reorganization should be studied in combination with its effects on junctional proteins distribution. Additionally, if studied through a pharmacological approach, cell survival should be carefully monitored.
- LRP1 represents an exciting molecule for future study and, as such, *in vitro* studies with LRP1 specific inhibitors should be also performed. If LRP1 was shown to be involved in BBB maintenance in our *in vitro* system, future experiments should focus on exploring the role of LRP1 in BBB maintenance *in vivo*; the effects of LRP1 selective endothelial knockdown (LRP1^{-/-}) on BBB maintenance and disease progression could be explored in EAE mice (a murine model of MS).
- Further studies should assess the role of LRP/NFκβ signalling cascade in BBB maintenance under inflammatory conditions and how Shh and/or Vitamin D3 could be modulating this mechanism in order to protect barrier integrity.

- The effects of miR125b overexpression and inhibition on hCMEC/D3 gene expression profile under unstimulated conditions and also at earlier time-points under inflammatory conditions should be assessed.
- The role of F3/thrombin pathway in barrier stability, and the effects of inflammation, Shh and Vitamin D3 as modulators of this pathway should be assessed in our *in vitro* BBB model. If the F3/thrombin pathway proved to be BBB disruptive and/or responsive to any of the aforementioned stimuli future experiments should focus on F3/thrombin role in BBB maintenance *in vivo*; the effects of Shh and/or Vitamin D3 treatment in the F3/thrombin pathway, BBB maintenance and disease progression could be studied in EAE mice (a murine model of MS). Additionally, the effects of F3 selective endothelial deletion on BBB maintenance and disease progression could be also explored in the presence and absence of Shh and/or Vitamin D3. There is no evidence of F3^{-/-} mice viability on the published literature, but some work has been published with a TFPI (F3 pathway inhibitor) knockout mice (Wang et al., 2018) in which EAE could be induced and disease progression and severity could be studied in the context of an overactive F3 pathway. Additionally, the protective effects of Shh and/or Vitamin D3 could be tested in this context.

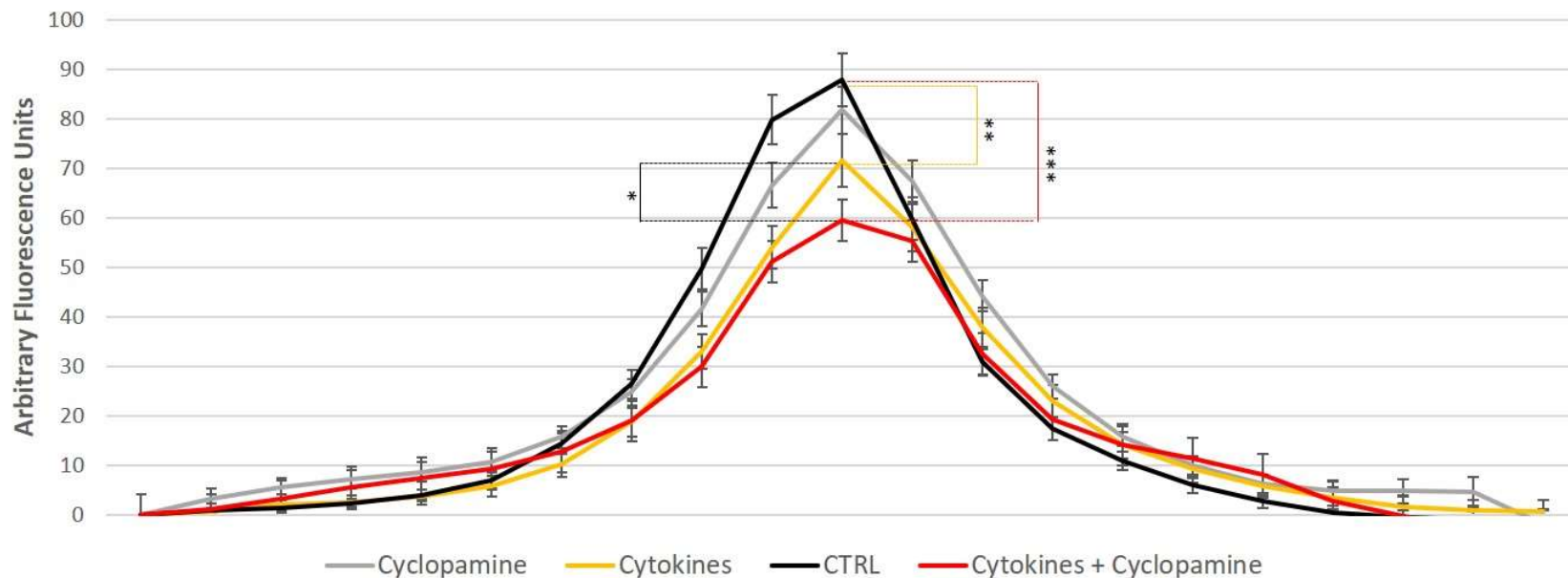
7. APPENDIX



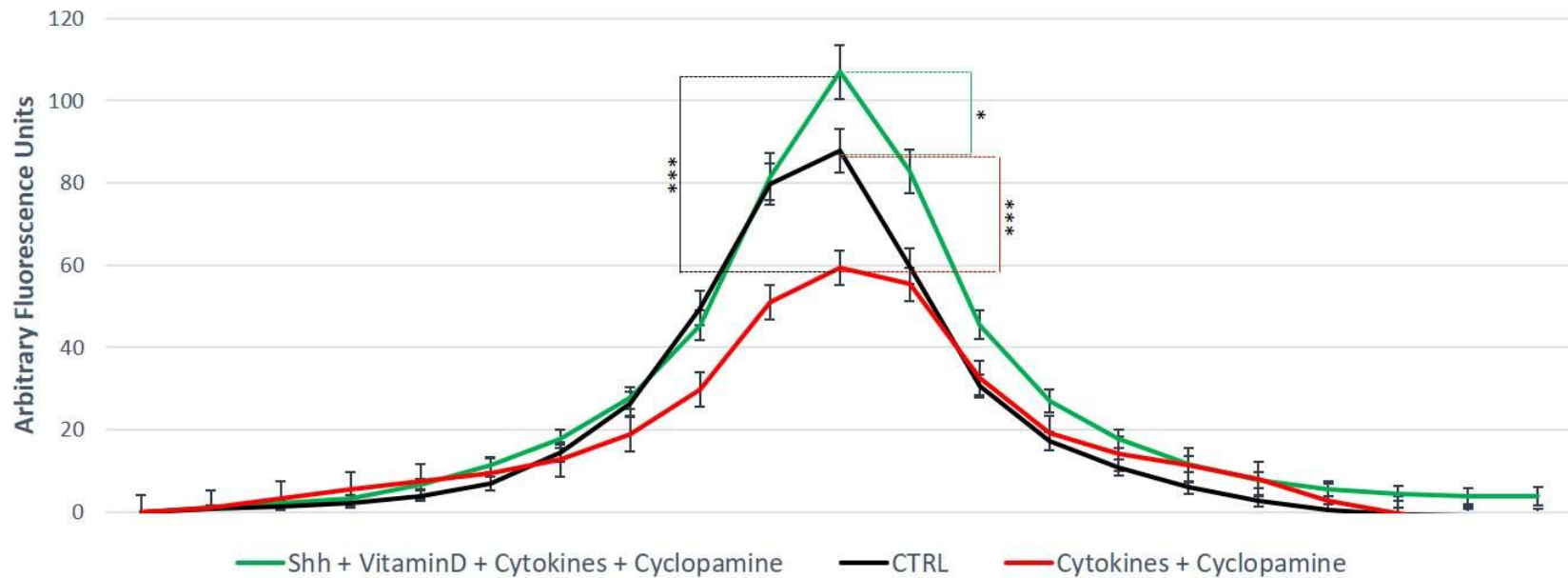
Appendix 3.A – Variations in MCEC-1 cell size. Cell size variations were not treatment-dependent but seems to be associated with the particular areas of the immunolabelled coverslip: peripheral (**A**) or central (**B**). Confluent MCEC-1 monolayers were immunolabelled for ZO-1 protein to visualise tight junctions.



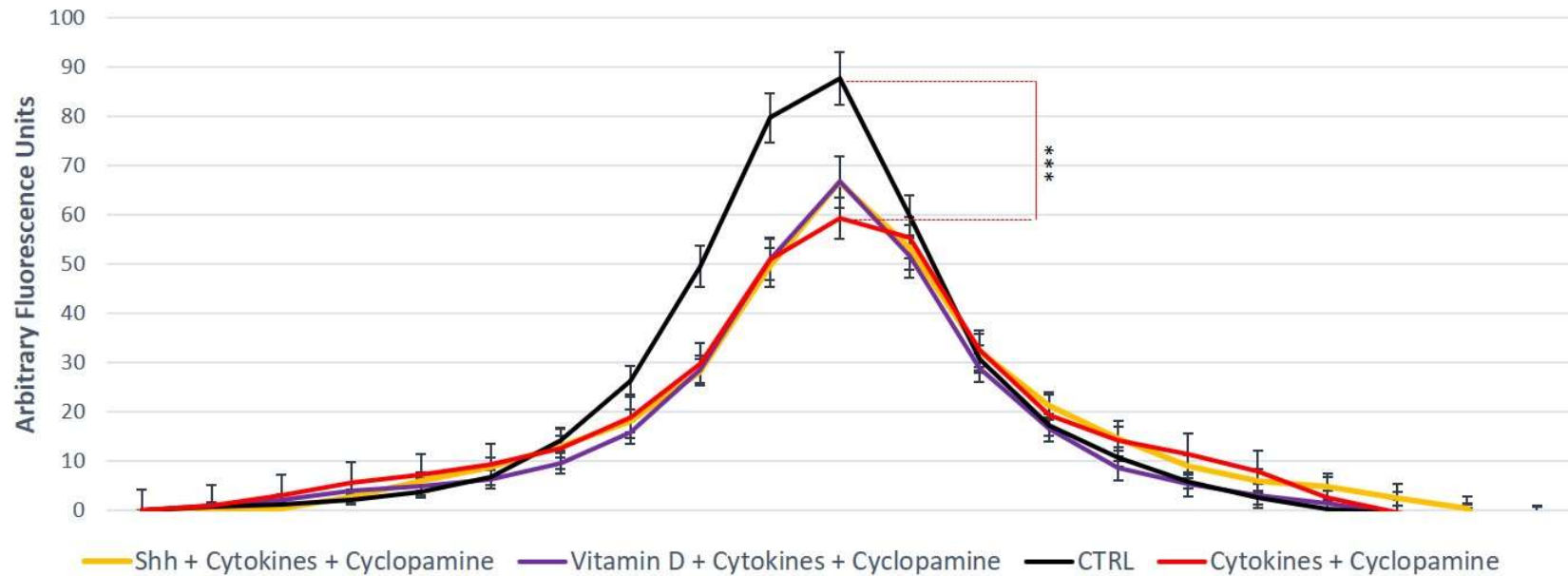
Appendix 3.B – Shh or Vitamin D3 increase junctional fluorescent intensity. Confluent MCEC-1 monolayers untreated (CTRL) and treated with either Shh (100ng/ml) or Vitamin D3 (100nM) for 24h. Cells were immunolabelled for ZO-1 to visualise tight junction integrity. Quantification of fluorescent intensity across the selected junction originated bell curves with a peak corresponding with the centre of a particular junction. Differences between peaks were used to quantify junctional integrity. Analysis performed with Andor IQ2 software. Statistically significant differences were assessed via One-way ANOVA with post-hoc Tukey. Each bar represents the mean \pm SEM for 3 independent experiments. * $p < 0.05$; ** $p < 0.01$; *** $p < 0.001$.



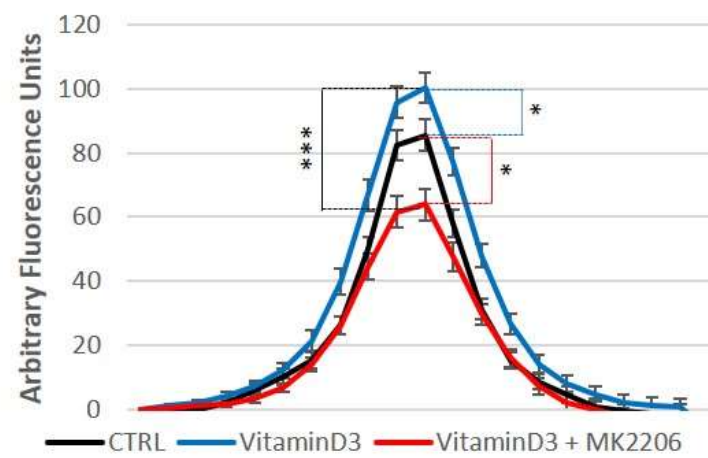
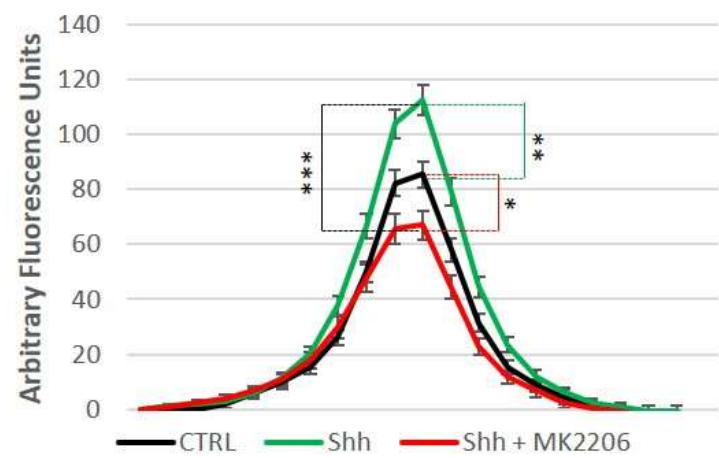
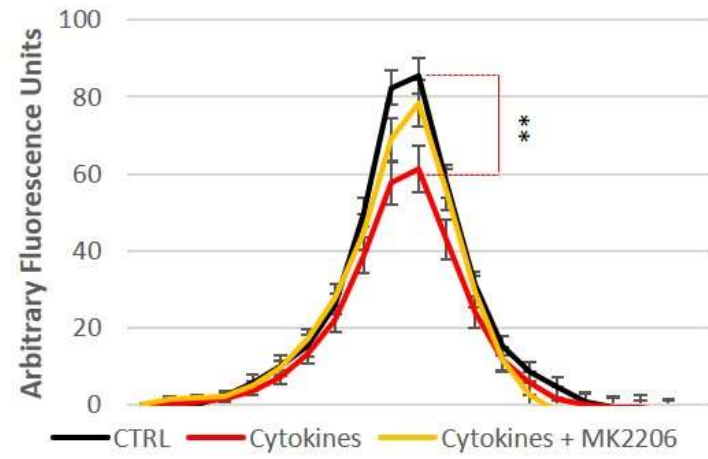
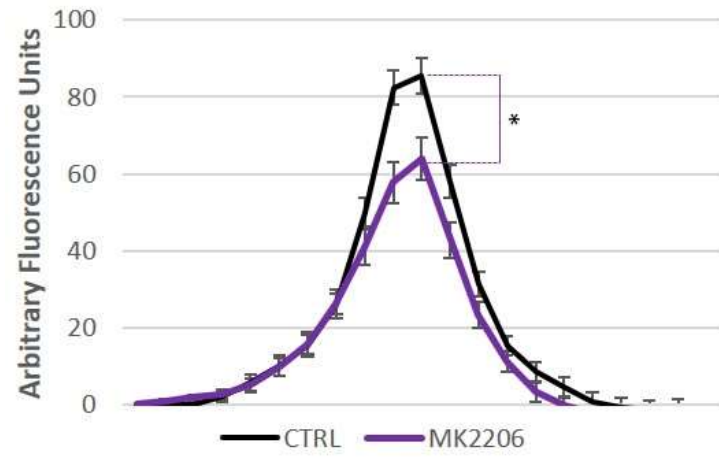
Appendix 3.C – Hedgehog pathway abrogation in the presence of cytokines can further reduce tight junction stability. MCEC-1 monolayers incubated with a mixture of cytokines (TNF α and IL1 α) (100pg/ml), the hedgehog pathway inhibitor cyclopamine (4 μ M) or a combination of both during 24h. CTRL, untreated cells. Cells immunolabelled for ZO-1 to visualise tight junction integrity. Quantification of fluorescent intensity across the selected junction originated bell curves with a peak corresponding with the centre of a particular junction. Differences between peaks were used to quantify junctional integrity. Analysis performed with Andor IQ2 software. Statistically significant differences were assessed via One-way ANOVA with post-hoc Tukey. Each bar represents the mean \pm SEM for 3 independent experiments. * p < 0.05; ** p < 0.01; *** p < 0.001.



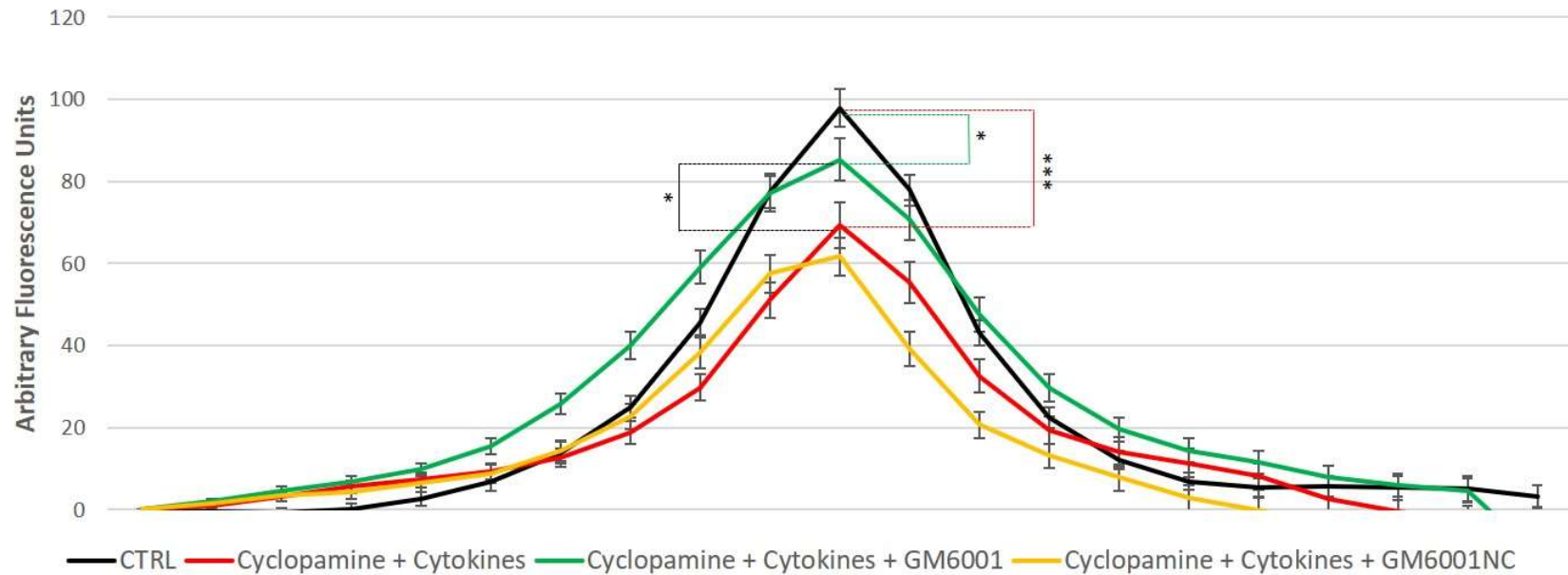
Appendix 3.D – A combination of Shh and Vitamin D3 rescues cytokines and cyclopamine driven loss of junctional stability. MCEC-1 monolayers incubated with a combination of Shh (100ng/ml) and/or Vitamin D3 (100nM) in the absence or presence of a mixture of cytokines (TNF α and IL1 α) (100pg/ml) and the hedgehog pathway inhibitor cyclopamine (4 μ M) for 24h. Untreated monolayers are represented as controls (CTRL). Cells were immunolabelled for ZO-1 to visualise tight junction integrity. Quantification of fluorescent intensity across the selected junction originated bell curves with a peak corresponding with the centre of a particular junction. Differences between peaks were used to quantify junctional integrity. Analysis performed with Andor IQ2 software. Statistically significant differences were assessed via One-way ANOVA with post-hoc Tukey. Each bar represents the mean \pm SEM for 2 independent experiments. * $p < 0.05$; ** $p < 0.01$; *** $p < 0.001$. Preliminary results.



Appendix 3.E – Shh or Vitamin D3 cannot rescue cytokines and cyclopamine driven loss of junctional stability individually. MCEC-1 monolayers incubated with a mixture of cytokines (TNF α and IL1 α) (100pg/ml) and the hedgehog pathway inhibitor cyclopamine (4 μ M) together with Shh (100ng/ml) or Vitamin D3 (100nM) for 24h. Untreated monolayers are represented as controls (CTRL). Cells were immunolabelled for ZO-1 to visualise tight junction integrity. Quantification of fluorescent intensity across the selected junction originated bell curves with a peak corresponding with the centre of a particular junction. Differences between peaks were used to quantify junctional integrity. Analysis performed with Andor IQ2 software. Statistically significant differences were assessed via One-way ANOVA with post-hoc Tukey. Each bar represents the mean \pm SEM for 2 independent experiments. * $p < 0.05$; ** $p < 0.01$; *** $p < 0.001$. Preliminary results.



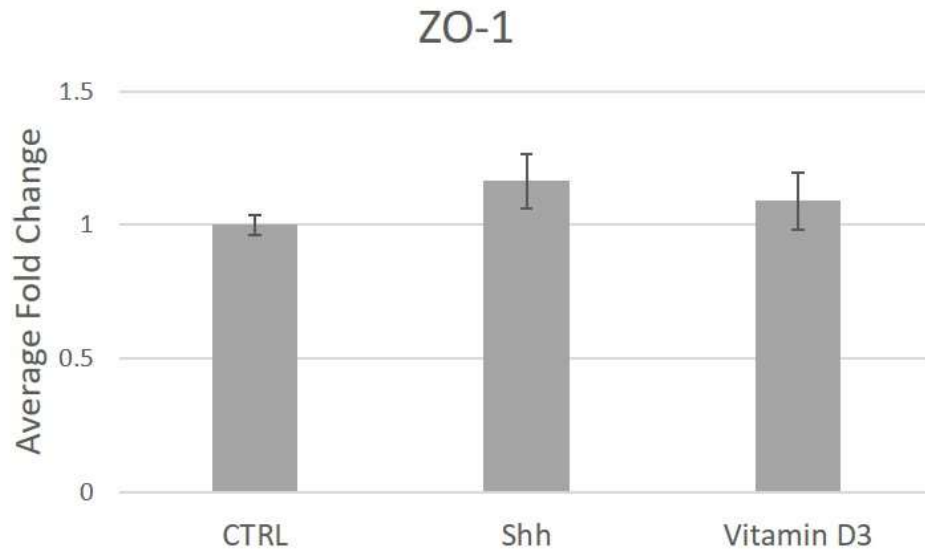
Appendix 3.F – Cytokines, Shh and Vitamin D3 driven modulation of junction stability is Akt dependent. MCEC-1 monolayers incubated with a mixture of cytokines (TNF α and IL1 α) (100pg/ml), Shh (100ng/ml) and Vitamin D3 (100nM) alone or in combination with the Akt inhibitor MK-22016 (5 μ M) for 24h. Untreated monolayers are represented as controls (CTRL). Cells were immunolabelled for ZO-1 to visualise tight junction integrity. Quantification of fluorescent intensity across the selected junction originated bell curves with a peak corresponding with the centre of a particular junction. Differences between peaks were used to quantify junctional integrity. Analysis performed with Andor IQ2 software. Statistically significant differences were assessed via One-way ANOVA with post-hoc Tukey. Each bar represents the mean \pm SEM for 3 independent experiments. * $p < 0.05$; ** $p < 0.01$; *** $p < 0.001$.



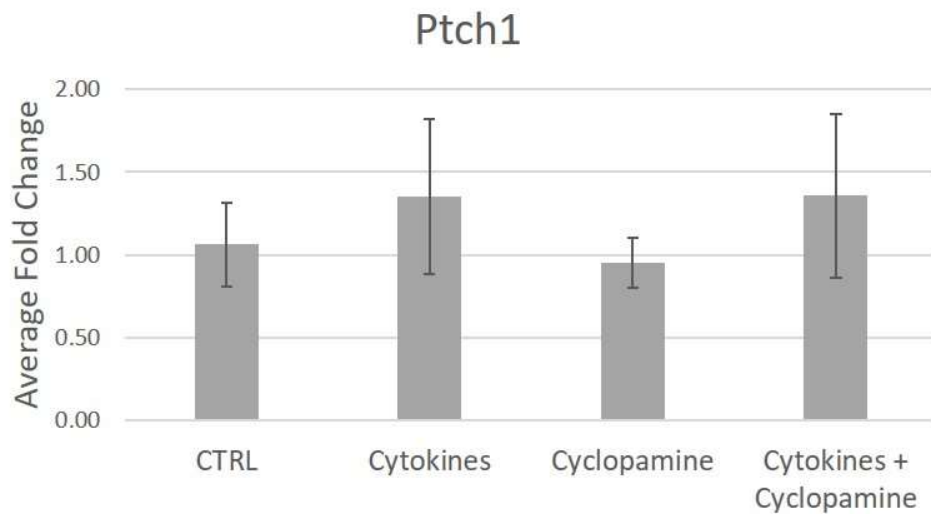
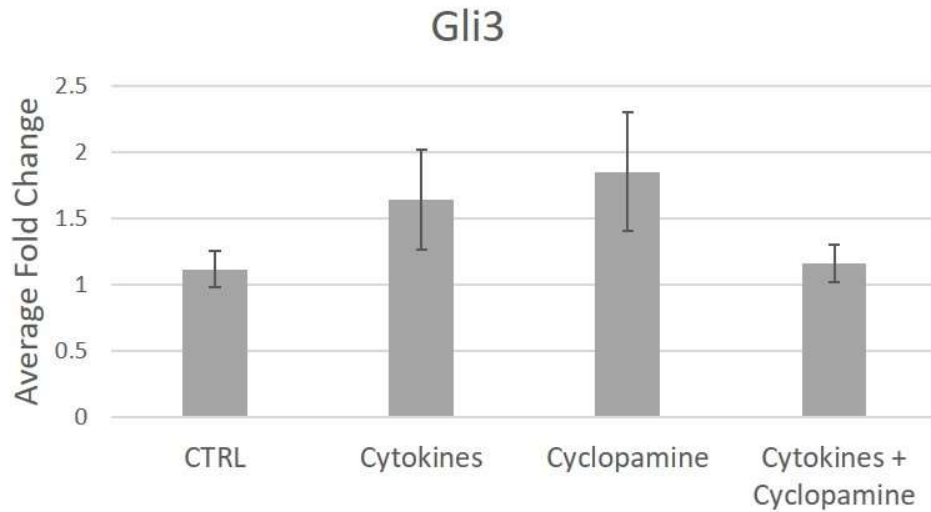
Appendix 3.G – Cytokines and cyclopamine driven loss of tight junction stability is metalloproteinase dependent MCEC-1 monolayers incubated with a mixture of cytokines (TNF α and IL1 α) (100pg/ml) and the hedgehog pathway inhibitor cyclopamine (4 μ M) in the presence or absence of a broad-spectrum metalloproteinase inhibitor (GM6001) for 24h. GM6001 negative control (NC) and untreated monolayers (CTRL) were used as controls. Cells were immunolabelled for ZO-1 to visualise tight junction integrity. Quantification of fluorescent intensity across the selected junction originated bell curves with a peak corresponding with the centre of a particular junction. Differences between peaks were used to quantify junctional integrity. Analysis performed with Andor IQ2 software. Statistically significant differences were assessed via One-way ANOVA with post-hoc Tukey. Each bar represents the mean \pm SEM for 3 independent experiments. * $p < 0.05$; *** $p < 0.001$.

		Treatment			
		CTRL	Cytokines	Cyclopamine	Cytokines + Cyclopamine
Raw Ct Values	MMP3	27.30	25.44	25.40	23.36
		27.96	25.86	24.66	23.62
		27.09	26.77	25.41	24.01
	MMP10	37.04	36.73	31.82	29.77
		36.75	36.12	31.57	26.42
		36.03	37.79	31.83	27.56
	MMP13	31.68	31.42	28.68	28.34
		32.06	31.82	28.76	25.25
		31.95	32.20	28.97	25.38
	TIMP1	26.94	25.65	26.97	25.88
		26.97	25.28	27.10	25.94
		26.79	25.73	26.98	25.76
	TIMP3	23.24	23.47	23.34	24.05
		22.98	23.45	23.07	24.09
		22.93	23.55	23.03	24.09
	ZO-1	28.88	29.13	28.97	29.50
		28.88	29.03	28.96	29.54
		29.03	29.31	28.98	29.37
	Smo	27.99	27.65	28.54	33.72
		28.18	27.71	28.35	28.84
		27.72	28.57	27.84	29.54
	Gli2	30.57	30.92	32.31	36.95
		31.05	30.52	31.96	33.60
		30.40	31.26	32.06	33.26

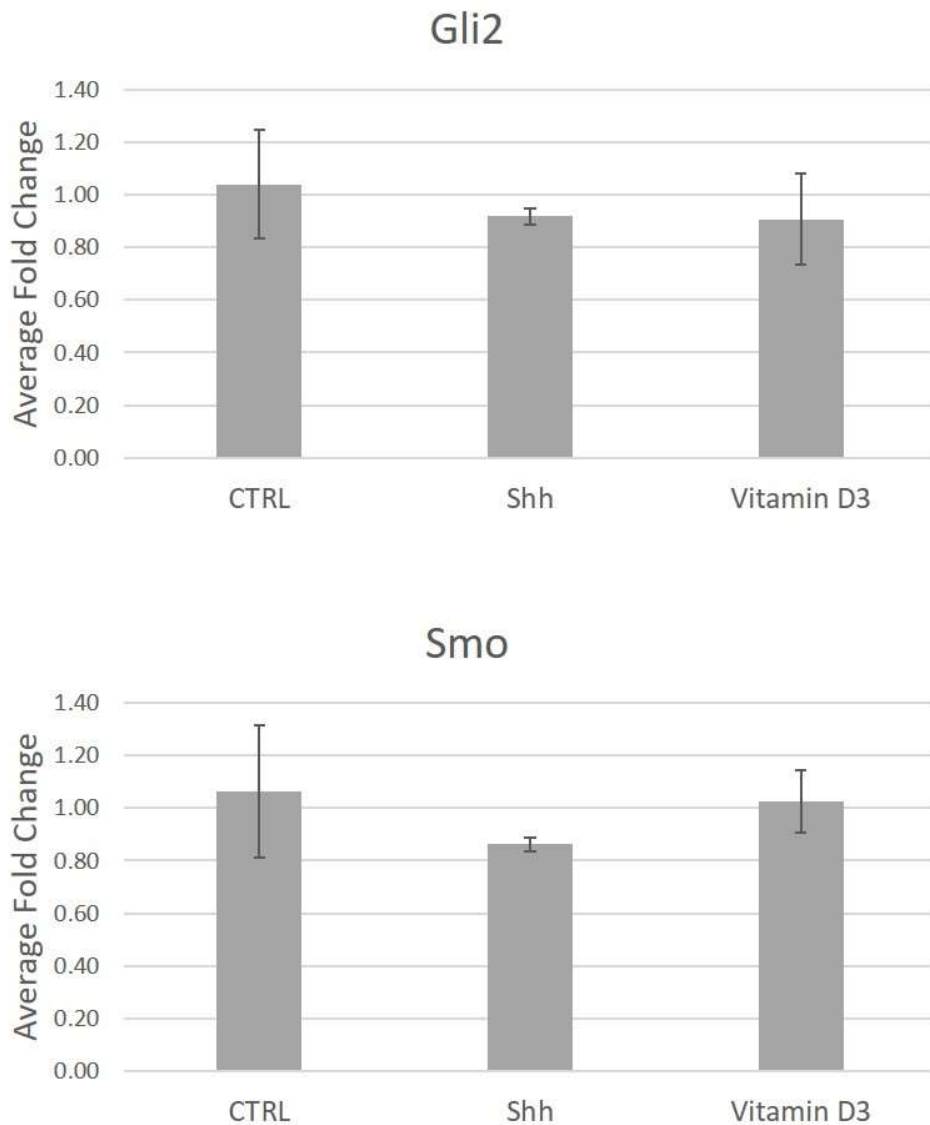
Appendix 3.H – Raw Ct Values for the measured genes in MCEC-1 monolayers. MCEC-1 cells confluent monolayers incubated with a mixture of cytokines (TNF α and IL1 α), cyclopamine alone or in combination. Untreated monolayers (CTRL) were used as controls. After 24h treatment, MMP3, 10 and 13 steady-state mRNA levels were determined by qRT-PCR. Raw Ct values for 3 replicates of the studied gene are shown.



Appendix 3.1 – Shh or Vitamin D3 addition had no effect in ZO-1 expression levels. MCEC-1 cells confluent monolayers incubated with Shh (100ng/ml) or Vitamin D3 (100nM) during 24h. Untreated monolayers (CTRL) were used as controls. After treatment, ZO-1 mRNA steady-state levels were determined by qRT-PCR with normalisation to 18s expression. Fold-change is depicted relative to untreated control. Statistically significant differences were assessed via One-way ANOVA with post-hoc Tukey. Each bar represents the mean \pm SEM for 3 wells. Representative experiment depicted. Experiment replicated 3 times.



Appendix 3.J – Gli3 or Ptch1 gene expression levels were not altered by addition of cytokines or Hedgehog pathway abrogation. MCEC-1 cells confluent monolayers incubated with a mixture of cytokines (TNF α and IL1 α) (100pg/ml), cyclopamine, or a combination of both during 24h. Untreated monolayers (CTRL) were used as control. After treatment, Gli3 and Ptch1 mRNA steady-state levels were determined by qRT-PCR with normalisation to 18s expression. Fold-change is depicted relative to untreated control. Statistically significant differences were assessed One-way ANOVA with post-hoc Tukey. Each bar represents the mean \pm SEM for 3 wells. Representative experiment depicted. Experiment replicated 3 times.



Appendix 3.K – Gli2 or Smo gene expression levels were not altered by addition of Shh or Vitamin D3. MCEC-1 cells confluent monolayers incubated with Shh (100ng/ml) or Vitamin D3 (100nM) during 24h. Untreated monolayers (CTRL) were used as controls. After treatment, Gli2 and Smo mRNA steady-state levels were determined by qRT-PCR with normalisation to 18s expression. Fold-change is depicted relative to untreated control. Statistically significant differences were assessed One-way ANOVA with post-hoc Tukey. Each bar represents the mean \pm SEM for 3 wells. Representative experiment depicted. Experiment replicated 3 times.

ZO-1		Treatment			
		CTRL	Cytokines	Shh + VitD3	Cytokines + Shh + VitD3
Raw Ct Values	4h	27.10	27.29	25.97	27.04
		27.52	27.20	26.16	27.98
		27.58	27.14	26.33	27.45
	8h	26.97	28.70	27.10	27.41
		27.06	28.60	27.73	27.68
		27.14	27.95	27.17	27.58
	12h	27.71	27.09	26.97	27.43
		27.39	27.21	26.87	27.36
		26.79	27.29	27.58	27.46
	24h	26.85	26.83	26.97	27.33
		26.94	26.98	26.57	27.14
		27.54	27.22	26.71	26.37

Appendix 4.A – ZO-1 Raw Ct Values in hCMEC/D3 monolayers. hCMEC/D3 cells confluent monolayers incubated with a mixture of cytokines (TNF α and IL1 α) (10ng/ml) in the presence or absence of a combination of Shh (100ng/ml) and Vitamin D3 (100nM). Untreated monolayers (CTRL) were used as controls. After 4h, 8h, 12h or 24h treatment, ZO-1 steady-state mRNA levels were determined by qRT-PCR. Raw Ct values for 3 wells are shown.

		Treatment	
		CTRL	Cytokines
Raw Ct Values	MMP1	34.21	28.54
		33.97	28.58
		34.63	28.46
	MMP2	31.82	32.94
		31.27	32.94
		31.65	33.03
	MMP3	33.19	32.35
		33.14	32.11
		33.40	32.89
	MMP10	Und	34.18
		34.60	
		34.48	
MMP12	33.37	31.75	
	33.42	31.75	
	34.20	32.01	
MMP14	31.64	30.13	
	30.32	29.62	
	30.80	29.89	
ADAM8	35.94	32.31	
	34.94	31.70	
	35.05	32.48	
TIMP1	26.95	25.66	
	26.33	25.74	
	26.20	25.49	
TIMP2	28.79	29.76	
	28.01	29.86	
	28.50	29.95	

Appendix 4.B – Raw Ct Values for the measured metalloproteinases and their inhibitors in response to cytokines. hCMEC/D3 cells confluent monolayers incubated with a mixture of cytokines (TNF α and IL1 α) (10ng/ml). Untreated monolayers (CTRL) were used as controls. After 24h treatment, steady-state mRNA levels for the indicated genes were determined by qRT-PCR. Raw Ct values for 3 wells are shown.

		Treatment			
		CTRL	Shh	VitD3	Shh + VitD3
Raw Ct Values	MMP1	34.21	34.91	35.02	34.87
		33.97	35.04	35.43	35.36
		34.63	34.56	35.48	34.93
	MMP2	31.82	31.43	31.97	32.26
		31.27	31.68	31.99	32.22
		31.65	31.43	31.77	31.94
	MMP3	33.19	33.76	33.52	33.71
		33.14	33.20	33.67	33.41
		33.40	33.47	33.91	34.23
	MMP10	Und	Und	Und	Und
MMP12	33.37	34.02	34.40	34.34	
	33.42	34.05	34.29	34.50	
	34.20	33.92	34.70	34.36	
MMP14	31.64	31.28	30.94	30.67	
	30.32	31.53	30.85	30.98	
	30.80	30.57	30.80	31.23	
ADAM8	35.94	36.28	37.27	35.04	
	34.94	36.79	35.25	35.52	
	35.05	35.66	36.04	36.07	
TIMP1	26.95	26.88	26.55	27.00	
	26.33	26.60	26.33	26.73	
	26.20	26.61	26.43	26.51	
TIMP2	28.79	28.99	28.82	29.06	
	28.01	28.88	28.69	29.21	
	28.50	28.43	28.75	28.74	

Appendix 4.C – Raw Ct Values for the measured metalloproteinases and their inhibitors in response to Shh and Vitamin D3. *hCMEC/D3* cells confluent monolayers were treated with Shh (100ng/ml) or Vitamin D3 (100nM). Untreated monolayers (CTRL) were used as controls. After 24h treatment, steady-state mRNA levels for the indicated genes were determined by qRT-PCR. Raw Ct values for 3 wells are shown.

MMP3		Treatment		
		CTRL	Cytokines	Cytokines + Shh + VitD3
Raw Ct Values	4h	31.14	26.09	25.37
		32.90	25.31	25.77
		35.92	25.85	25.86
	8h	30.54	25.77	26.15
		30.44	25.51	26.56
		31.34	25.14	26.05
	12h	30.40	25.30	26.56
		30.81	25.73	26.64
		30.98	25.27	25.98

MMP10		Treatment		
		CTRL	Cytokines	Cytokines + Shh + VitD3
Raw Ct Values	4h	38.11	30.22	29.96
		38.02	29.80	30.40
		Und	30.65	30.54
	8h	36.50	29.55	31.03
		37.70	29.95	30.29
		Und	29.46	30.46
	12h	Und	30.98	31.64
		Und	31.09	30.71
		Und	30.45	30.86

Appendix 4.D – Raw Ct Values for MMP3 and MMP10 in response to cytokines, Shh and Vitamin D3. hCMEC/D3 cells confluent monolayers were treated with a combination of Shh (100ng/ml) and Vitamin D3 (100nM) in the presence or absence of a mixture of cytokines (TNF α and IL1 α) (10ng/ml). Untreated monolayers (CTRL) were used as controls. After 4h, 8h and 12h treatments, steady-state mRNA levels for the indicated genes were determined by qRT-PCR. Raw Ct values for 3 wells

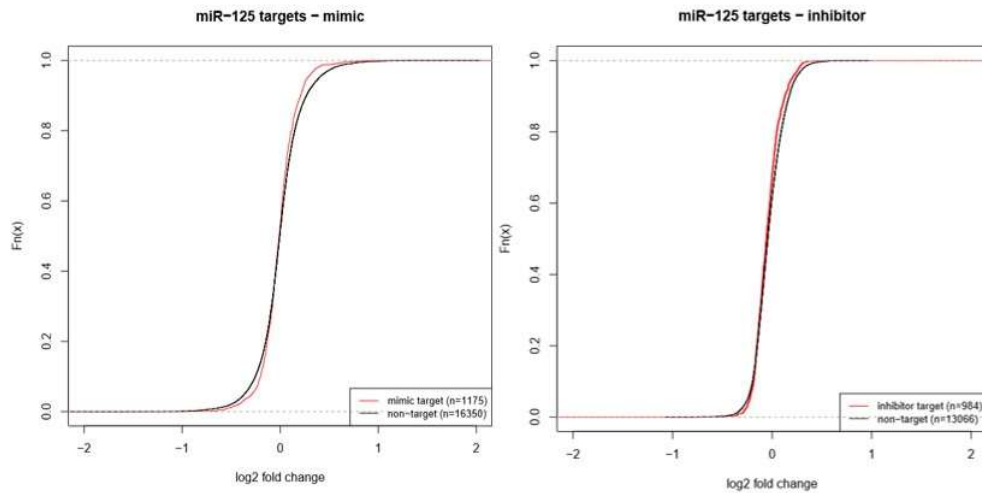
		Treatment			
		CTRL	Cytokines	Shh + VitD3	Cytokines + Shh + VitD3
Raw Ct Values	4h	30.98	30.40	29.21	29.39
		30.49	29.41	29.11	31.61
		30.11	29.80	29.26	30.07
	8h	29.44	31.50	29.64	30.77
		29.94	30.83	29.41	31.51
		30.33	31.20	30.31	31.12
	12h	29.78	30.45	29.85	30.74
		29.23	30.35	29.65	31.07
		29.53	31.27	29.50	30.17

		Treatment			
		CTRL	Cytokines	Shh + VitD3	Cytokines + Shh + VitD3
Raw Ct Values	4h	29.22	28.92	27.85	27.92
		29.99	28.99	28.59	30.08
		29.11	29.50	27.98	28.89
	8h	29.31	30.98	29.11	28.99
		29.24	30.23	28.89	30.32
		30.09	31.12	29.64	29.86
	12h	28.71	29.51	29.15	29.89
		28.97	29.52	29.40	29.76
		28.80	29.97	28.91	29.77

Appendix 4.E – Raw Ct Values for TIMP2 and TIMP4 in response to cytokines, Shh and Vitamin D3. hCMEC/D3 cells confluent monolayers were treated with a mixture of cytokines (TNF α and IL1 α) (10ng/ml) and/or a combination of Shh (100ng/ml) and Vitamin D3 (100nM). Untreated monolayers (CTRL) were used as controls. After 4h, 8h and 12h treatments, steady-state mRNA levels for the indicated genes were determined by qRT-PCR. Raw Ct values for 3 wells are shown.

LRP1		Treatment			
		CTRL	Cytokines	Shh + VitD3	Cytokines + Shh + VitD3
Raw Ct Values	4h	30.98	30.40	29.21	29.39
		30.49	29.41	29.11	31.61
		30.11	29.80	29.26	30.07
	8h	29.44	31.50	29.64	30.77
		29.94	30.83	29.41	31.51
		30.33	31.20	30.31	31.12
	12h	29.78	30.45	29.85	30.74
		29.23	30.35	29.65	31.07
		29.53	31.27	29.50	30.17
	24h	28.71	29.51	29.15	29.89
		28.97	29.52	29.40	29.76
		28.80	29.97	28.91	29.77

Appendix 4.F – LRP1 Raw Ct Values in hCMEC/D3 monolayers. hCMEC/D3 cells confluent monolayers incubated with a mixture of cytokines (TNF α and IL1 α) (10ng/ml) in the presence or absence of a combination of Shh (100ng/ml) and Vitamin D3 (100nM). Untreated monolayers (CTRL) were used as controls. After 4h, 8h, 12h or 24h treatment, LRP1 steady-state mRNA levels were determined by qRT-PCR. Raw Ct values for 3 wells are shown.



Appendix 5.A – Cumulative plot analysis for miR125 targets. Cumulative plot analysis in hCMEC/D3 monolayers for miR125 targets between mimic and inhibitor transfected cells in the presence of a cytokines mix (TNF α and IL1 α). Analysis performed in collaboration with Dr Simon Moxon.

Gene Symbol	Gene Name
MMP3	Matrix Metallopeptidase 3
CXCL8	C-X-C Motif Chemokine Ligand 8
CSF2	Colony Stimulating Factor 2
IL1 β	Interleukin 1 Beta
IL1 α	Interleukin 1 Alpha
ICAM1	Intercellular Adhesion Molecule 1
GBP1	Guanylate Binding Protein 1
VCAM1	Vascular Cell Adhesion Molecule 1
NF κ β α	Nuclear Factor Kappa B Subunit Alpha
IL11	Interleukin 11

Gene Symbol	Gene Name
ANGPT1	Angiopoietin 1
C/EBP β	CCAAT Enhancer Binding Protein Beta
IL15R α	Interleukin 15 Receptor Subunit Alpha
CD44	CD44 Molecule (Indian Blood Group)
SCF	Skp, Cullin, F-box containing complex
EGR1	Early Growth Response 1
CDKN2C	Cyclin Dependent Kinase Inhibitor 2C
FGF5	Fibroblast Growth Factor 5
DUSP4	Dual Specificity Phosphatase 4
DUSP6	Dual Specificity Phosphatase 6

Appendix 5.B – Gene symbol and full name of cytokine regulated genes and associated with the pathology of Multiple Sclerosis (MS) reported in table 5.2 and 5.3. Gene full names were retrieved from Gene Card.

8. REFERENCES

- Abbott, N. J., Patabendige, A. A., Dolman, D. E., Yusof, S. R., & Begley, D. J. (2010). Structure and function of the blood-brain barrier. *Neurobiol Dis*, 37(1), 13–25. <https://doi.org/10.1016/j.nbd.2009.07.030>
- Abdullah, Z., Rakkar, K., Bath, P. M. W., & Bayraktutan, U. (2015). Inhibition of TNF- α protects in vitro brain barrier from ischaemic damage. *Molecular and Cellular Neuroscience*. <https://doi.org/10.1016/j.mcn.2015.11.003>
- Abram, C. L., & Lowell, C. A. (2009). The Ins and Outs of Leukocyte Integrin Signaling. *Annual Review of Immunology*. <https://doi.org/10.1146/annurev.immunol.021908.132554>
- Abu-Rub, M., & Miller, R. H. (2018). Emerging Cellular and Molecular Strategies for Enhancing Central Nervous System (CNS) Remyelination. *Brain Sciences*, 8(6). <https://doi.org/10.3390/brainsci8060111>
- Afonso, P. V., Ozden, S., Prevost, M. C., Schmitt, C., Seilhean, D., Weksler, B., ... Ceccaldi, P. E. (2007). Human blood-brain barrier disruption by retroviral-infected lymphocytes: role of myosin light chain kinase in endothelial tight-junction disorganization. *J Immunol*, 179(4), 2576–2583. Retrieved from <http://www.jimmunol.org/content/179/4/2576.full.pdf>
- Agrawal, S., Anderson, P., Durbeej, M., van Rooijen, N., Ivars, F., Opendakker, G., & Sorokin, L. M. (2006). Dystroglycan is selectively cleaved at the parenchymal basement membrane at sites of leukocyte extravasation in experimental autoimmune encephalomyelitis. *J Exp Med*, 203(4), 1007–1019. <https://doi.org/10.1084/jem.20051342>
- Ahn, S. J., Rhim, E. M., Kim, J. Y., Kim, K. H., Lee, H. W., Kim, E. C., & Park, S. H. (2014). Tumor necrosis factor- α induces matrix metalloproteinases-3, -10, and -13 in human periodontal ligament cells. *J Periodontol*, 85(3), 490–497. <https://doi.org/10.1902/jop.2013.130063>
- Aihara, K. I., Azuma, H., Akaike, M., Ikeda, Y., Yamashita, M., Sudo, T., ... Matsumoto, T. (2004). Disruption of nuclear vitamin D receptor gene causes enhanced thrombogenicity in mice. *Journal of Biological Chemistry*. <https://doi.org/10.1074/jbc.M404865200>
- Akhtar, N., Rasheed, Z., Ramamurthy, S., Anbazhagan, A. N., Voss, F. R., & Haqqi, T. M. (2010). MicroRNA-27b regulates the expression of matrix metalloproteinase 13 in human osteoarthritis chondrocytes. *Arthritis Rheum*, 62(5), 1361–1371. <https://doi.org/10.1002/art.27329>
- Al-Ahmad, A. J., Patel, R., Palecek, S. P., & Shusta, E. V. (2018). Hyaluronan impairs the barrier integrity of brain microvascular endothelial cell through a CD44-dependent pathway. *Journal of Cerebral Blood Flow and Metabolism*. <https://doi.org/10.1177/0271678X18767748>

- Al-Obaidi, M. M. J., & Desa, M. N. M. (2018). Mechanisms of Blood Brain Barrier Disruption by Different Types of Bacteria, and Bacterial–Host Interactions Facilitate the Bacterial Pathogen Invading the Brain. *Cellular and Molecular Neurobiology*. <https://doi.org/10.1007/s10571-018-0609-2>
- Alluri, H., Wilson, R. L., Shaji, C. A., Wiggins-Dohlvik, K., Patel, S., Liu, Y., ... Tharakan, B. (2016). Melatonin preserves blood-brain barrier integrity and permeability via matrix metalloproteinase-9 inhibition. *PLoS ONE*. <https://doi.org/10.1371/journal.pone.0154427>
- Almutairi, M. M., Gong, C., Xu, Y. G., Chang, Y., & Shi, H. (2016). Factors controlling permeability of the blood-brain barrier. *Cell Mol Life Sci*, 73(1), 57–77. <https://doi.org/10.1007/s00018-015-2050-8>
- Altmann, D. M., & Boyton, R. J. (2004). Models of Multiple Sclerosis. *Drug Discovery Today: Disease Models*, 1(4), 6. <https://doi.org/doi:10.1016/j.ddmod.2004.11.004>
- Alvarez, J. I., Cayrol, R., & Prat, A. (2011). Disruption of central nervous system barriers in multiple sclerosis. *Biochim Biophys Acta*, 1812(2), 252–264. <https://doi.org/10.1016/j.bbadis.2010.06.017>
- Alvarez, J. I., Dodelet-Devillers, A., Kebir, H., Ifergan, I., Fabre, P. J., Terouz, S., ... Prat, A. (2011). The Hedgehog pathway promotes blood-brain barrier integrity and CNS immune quiescence. *Science*, 334(6063), 1727–1731. <https://doi.org/10.1126/science.1206936>
- Amantea, D., Micieli, G., Tassorelli, C., Cuartero, M. I., Ballesteros, I., Certo, M., ... Bagetta, G. (2015). Rational modulation of the innate immune system for neuroprotection in ischemic stroke. *Front Neurosci*, 9, 147. <https://doi.org/10.3389/fnins.2015.00147>
- An, J., Zhang, C., Polavarapu, R., Zhang, X., Zhang, X., Yepes, M., ... Ross, M. (2008). Tissue-type plasminogen activator and the low-density lipoprotein receptor-related protein induce Akt phosphorylation in the ischemic brain. *Blood*. <https://doi.org/10.1182/blood-2008-02-141630>
- Arpino, V., Mehta, S., Wang, L., Bird, R., Rohan, M., Pape, C., & Gill, S. E. (2016). Tissue inhibitor of metalloproteinases 3-dependent microvascular endothelial cell barrier function is disrupted under septic conditions. *Am J Physiol Heart Circ Physiol*, 310(11), H1455-67. <https://doi.org/10.1152/ajpheart.00796.2015>
- Asahi, M., Wang, X., Mori, T., Sumii, T., Jung, J. C., Moskowitz, M. A., ... Lo, E. H. (2001). Effects of matrix metalloproteinase-9 gene knock-out on the proteolysis of blood-brain barrier and white matter components after cerebral ischemia. *The Journal of Neuroscience : The Official Journal of the Society for Neuroscience*, 21(19), 7724–7732. <https://doi.org/21/19/7724> [pii]
- Aslam, M., Ahmad, N., Srivastava, R., & Hemmer, B. (2012). TNF-alpha induced NFkappaB signaling

- and p65 (RelA) overexpression repress Cldn5 promoter in mouse brain endothelial cells. *Cytokine*, 57(2), 269–275. <https://doi.org/10.1016/j.cyto.2011.10.016>
- Aveleira, C. A., Lin, C. M., Abcouwer, S. F., Ambrosio, A. F., & Antonetti, D. A. (2010). TNF-alpha signals through PKCzeta/NF-kappaB to alter the tight junction complex and increase retinal endothelial cell permeability. *Diabetes*, 59(11), 2872–2882. <https://doi.org/10.2337/db09-1606>
- Baker, N., Sharpe, P., Culley, K., Otero, M., Bevan, D., Newham, P., ... Gavrilovic, J. (2012). Dual regulation of metalloproteinase expression in chondrocytes by Wnt-1-inducible signaling pathway protein 3/CCN6. *Arthritis Rheum*, 64(7), 2289–2299. <https://doi.org/10.1002/art.34411>
- Balasa, R., Bianca, C., Septimiu, V., Iunius, S., Adina, H., Sebastian, A., ... Smaranda, M. (2018). The Matrix Metalloproteinases Panel in Multiple Sclerosis Patients Treated with Natalizumab: A Possible Answer to Natalizumab Non- Responders. *CNS & Neurological Disorders Drug Targets*, 17(6), 464–472. <https://doi.org/10.2174/1871527317666180703102536>
- Balashov, K. E., Rottman, J. B., Weiner, H. L., & Hancock, W. W. (1999). CCR5(+) and CXCR3(+) T cells are increased in multiple sclerosis and their ligands MIP-1alpha and IP-10 are expressed in demyelinating brain lesions. *Proc Natl Acad Sci U S A*, 96(12), 6873–6878. Retrieved from <http://www.ncbi.nlm.nih.gov/pubmed/10359806>
- Balood, M., Mesbah-Namin, S. A., Sanati, M. H., Zahednasab, H., Sahraian, M. A., & Ataei, M. (2014). Inhibitor IκBα promoter functional polymorphisms in patients with multiple sclerosis. *Molecular Biology Reports*. <https://doi.org/10.1007/s11033-013-2898-3>
- Barmina, O. Y., Walling, H. W., Fiacco, G. J., Freije, J. M. P., López-Otín, C., Jeffrey, J. J., & Partridge, N. C. (1999). Collagenase-3 binds to a specific receptor and requires the low density lipoprotein receptor-related protein for internalization. *Journal of Biological Chemistry*. <https://doi.org/10.1074/jbc.274.42.30087>
- Bartsch, J. W., Wildeboer, D., Koller, G., Naus, S., Rittger, A., Moss, M. L., ... Jockusch, H. (2010). Tumor Necrosis Factor- (TNF-) Regulates Shedding of TNF- Receptor 1 by the Metalloprotease-Disintegrin ADAM8: Evidence for a Protease-Regulated Feedback Loop in Neuroprotection. *Journal of Neuroscience*, 30(36), 12210–12218. <https://doi.org/10.1523/JNEUROSCI.1520-10.2010>
- Bauer, A. T., Bürgers, H. F., Rabie, T., & Marti, H. H. (2010). Matrix Metalloproteinase-9 Mediates Hypoxia-Induced Vascular Leakage in the Brain via Tight Junction Rearrangement. *Journal of Cerebral Blood Flow & Metabolism*, 30(4), 837–848. <https://doi.org/10.1038/jcbfm.2009.248>

- Bauer, H., Zweimueller-Mayer, J., Steinbacher, P., Lametschwandtner, A., & Bauer, H. C. (2010). The dual role of zonula occludens (ZO) proteins. *J Biomed Biotechnol*, 2010, 402593. <https://doi.org/10.1155/2010/402593>
- Beilin, O., Karussis, D. M., Korczyn, A. D., Gurwitz, D., Aronovich, R., Hantai, D., ... Chapman, J. (2005). Increased thrombin inhibition in experimental autoimmune encephalomyelitis. *Journal of Neuroscience Research*. <https://doi.org/10.1002/jnr.20270>
- Benson, R. A., Lowrey, J. A., Lamb, J. R., & Howie, S. E. (2004). The Notch and Sonic hedgehog signalling pathways in immunity. *Mol Immunol*, 41(6–7), 715–725. <https://doi.org/10.1016/j.molimm.2004.04.017>
- Bijlsma, M. F., Spek, C. A., Zivkovic, D., van de Water, S., Rezaee, F., & Peppelenbosch, M. P. (2006). Repression of smooth muscle cell growth by patched-dependent (pro-)vitamin D3 secretion. *PLoS Biol*, 4(8), e232. <https://doi.org/10.1371/journal.pbio.0040232>
- Bord, S., Horner, A., Hembry, R. M., & Compston, J. E. (1998). Stromelysin-1 (MMP-3) and stromelysin-2 (MMP-10) expression in developing human bone: potential roles in skeletal development. *Bone*, 23(1), 7–12.
- Bozic, M., Álvarez, Á., De Pablo, C., Sanchez-Niño, M. D., Ortiz, A., Dolcet, X., ... Valdivielso, J. M. (2015). Impaired Vitamin D signaling in endothelial cell leads to an enhanced leukocyte-endothelium interplay: Implications for atherosclerosis development. *PLoS ONE*. <https://doi.org/10.1371/journal.pone.0136863>
- Brew, K., & Nagase, H. (2010). The tissue inhibitors of metalloproteinases (TIMPs): An ancient family with structural and functional diversity. *Biochimica et Biophysica Acta - Molecular Cell Research*. <https://doi.org/10.1016/j.bbamcr.2010.01.003>
- Brown, A. J., Dusso, A., & Slatopolsky, E. (1999). Vitamin D. *Am J Physiol*, 277(2 Pt 2), F157-75. Retrieved from <http://www.ncbi.nlm.nih.gov/pubmed/10444570>
- Burridge, K., & Wittchen, E. S. (2013). The tension mounts: Stress fibers as force-generating mechanotransducers. *Journal of Cell Biology*. <https://doi.org/10.1083/jcb.201210090>
- Butterworth, R. F. (2015). Pathogenesis of hepatic encephalopathy and brain edema in acute liver failure. *J Clin Exp Hepatol*, 5(Suppl 1), S96–S103. <https://doi.org/10.1016/j.jceh.2014.02.004>
- Calabresi, P. A., Giovannoni, G., Confavreux, C., Galetta, S. L., Havrdova, E., Hutchinson, M., ... Investigators, S. (2007). The incidence and significance of anti-natalizumab antibodies: results from AFFIRM and SENTINEL. *Neurology*, 69(14), 1391–1403.

<https://doi.org/10.1212/01.wnl.0000277457.17420.b5>

- Caporro, M., Disanto, G., Gobbi, C., & Zecca, C. (2014). Two decades of subcutaneous glatiramer acetate injection: current role of the standard dose, and new high-dose low-frequency glatiramer acetate in relapsing-remitting multiple sclerosis treatment. *Patient Prefer Adherence*, *8*, 1123–1134. <https://doi.org/10.2147/ppa.s68698>
- Cerutti, C., Edwards, L. J., De Vries, H. E., Sharrack, B., Male, D. K., & Romero, I. A. (2017). MiR-126 and miR-126* regulate shear-resistant firm leukocyte adhesion to human brain endothelium. *Scientific Reports*. <https://doi.org/10.1038/srep45284>
- Cerutti, C., Soblechero-Martin, P., Wu, D., Lopez-Ramirez, M. A., de Vries, H., Sharrack, B., ... Romero, I. A. (2016). MicroRNA-155 contributes to shear-resistant leukocyte adhesion to human brain endothelium in vitro. *Fluids and Barriers of the CNS*. <https://doi.org/10.1186/s12987-016-0032-3>
- Chelmicka-Szorc, E., & Arnason, B. G. (1972). Partial suppression of experimental allergic encephalomyelitis with heparin. *Archives of Neurology*, *27*(2), 153–158.
- Chen, J. S., Huang, X. H., Wang, Q., Huang, J. Q., Zhang, L. J., Chen, X. L., ... Cheng, Z. X. (2013). Sonic hedgehog signaling pathway induces cell migration and invasion through focal adhesion kinase/AKT signaling-mediated activation of matrix metalloproteinase (MMP)-2 and MMP-9 in liver cancer. *Carcinogenesis*, *34*(1), 10–19. <https://doi.org/10.1093/carcin/bgs274>
- Chen, J., Xiao, L., Rao, J. N., Zou, T., Liu, L., Bellavance, E., ... Wang, J. Y. (2008). JunD represses transcription and translation of the tight junction protein zona occludens-1 modulating intestinal epithelial barrier function. *Mol Biol Cell*, *19*(9), 3701–3712. <https://doi.org/10.1091/mbc.E08-02-0175>
- Chen, P. L., & Easton, A. S. (2011). Anti-angiogenic effects of resveratrol on cerebral angiogenesis. *Curr Neurovasc Res*, *8*(1), 14–24.
- Chen, S.-W., Ma, Y.-Y., Zhu, J., Zuo, S., Zhang, J.-L., Chen, Z.-Y., ... Wang, P.-Y. (2015). Protective effect of 1,25-dihydroxyvitamin D₃ on ethanol-induced intestinal barrier injury both in vitro and in vivo. *Toxicology Letters*. <https://doi.org/10.1016/j.toxlet.2015.06.006>
- Chen, S., Wang, P., Zhu, J., Chen, G., Zhang, J., Chen, Z., ... Pan, Y. (2015). Protective Effect of 1,25-Dihydroxyvitamin D₃ on Lipopolysaccharide-Induced Intestinal Epithelial Tight Junction Injury in Caco-2 Cell Monolayers. *Inflammation*. <https://doi.org/10.1007/s10753-014-0041-9>
- Chen, S., Zhu, J., Chen, G., Zuo, S., Zhang, J., Chen, Z., ... Wang, P. (2015). 1,25-Dihydroxyvitamin D₃

- preserves intestinal epithelial barrier function from TNF- α induced injury via suppression of NF- κ B p65 mediated MLCK-P-MLC signaling pathway. *Biochem Biophys Res Commun*, 460(3), 873–878. <https://doi.org/10.1016/j.bbrc.2015.03.125>
- Chen, S., Zhu, J., Chen, G., Zuo, S., Zhang, J., Chen, Z., ... Wang, P. (2015). 1,25-Dihydroxyvitamin D₃ preserves intestinal epithelial barrier function from TNF- α induced injury via suppression of NF- κ B p65 mediated MLCK-P-MLC signaling pathway. *Biochemical and Biophysical Research Communications*. <https://doi.org/10.1016/j.bbrc.2015.03.125>
- Chen, T., Huang, Z., Wang, L., Wang, Y., Wu, F., Meng, S., & Wang, C. (2009). MicroRNA-125a-5p partly regulates the inflammatory response, lipid uptake, and ORP9 expression in oxLDL-stimulated monocyte/macrophages. *Cardiovasc Res*, 83(1), 131–139. <https://doi.org/10.1093/cvr/cvp121>
- Chinchilla, P., Xiao, L., Kazanietz, M. G., & Riobo, N. A. (2010). Hedgehog proteins activate pro-angiogenic responses in endothelial cells through non-canonical signaling pathways. *Cell Cycle*. <https://doi.org/10.4161/cc.9.3.10591>
- Chirayath, M. V., Gajdzik, L., Hulla, W., Graf, J., Cross, H. S., & Peterlik, M. (1998). Vitamin D increases tight-junction conductance and paracellular Ca²⁺ transport in Caco-2 cell cultures. *Am.J.Physiol*, 274(2 Pt 1), G389–G396.
- Chitralla, K. N., Guan, H., Singh, N. P., Busbee, B., Gandy, A., Mehrpouya-Bahrami, P., ... Nagarkatti, M. (2017). CD44 deletion leading to attenuation of experimental autoimmune encephalomyelitis results from alterations in gut microbiome in mice. *European Journal of Immunology*. <https://doi.org/10.1002/eji.201646792>
- Choudhry, Z., Rikani, A. A., Choudhry, A. M., Tariq, S., Zakaria, F., Asghar, M. W., ... Mobassarrah, N. J. (2014). Sonic hedgehog signalling pathway: a complex network. *Ann Neurosci*, 21(1), 28–31. <https://doi.org/10.5214/ans.0972.7531.210109>
- Christ, A., Christa, A., Kur, E., Lioubinski, O., Bachmann, S., Willnow, T. E., & Hammes, A. (2012). LRP2 Is an Auxiliary SHH Receptor Required to Condition the Forebrain Ventral Midline for Inductive Signals. *Developmental Cell*. <https://doi.org/10.1016/j.devcel.2011.11.023>
- Christakos, S., Ajibade, D. V., Dhawan, P., Fechner, A. J., & Mady, L. J. (2010). Vitamin D: metabolism. *Rheum Dis Clin North Am*, 38(1), 1–11, vii. <https://doi.org/10.1016/j.rdc.2012.03.003>
- Chuang, T. Y., Guo, Y., Seki, S. M., Rosen, A. M., Johanson, D. M., Mandell, J. W., ... Gaultier, A. (2016). LRP1 expression in microglia is protective during CNS autoimmunity. *Acta Neuropathologica Communications*. <https://doi.org/10.1186/s40478-016-0343-2>

- Chung, Y. C., Kim, Y. S., Bok, E., Yune, T. Y., Maeng, S., & Jin, B. K. (2013). MMP-3 contributes to nigrostriatal dopaminergic neuronal loss, BBB damage, and neuroinflammation in an MPTP mouse model of Parkinson's disease. *Mediators of Inflammation*. <https://doi.org/10.1155/2013/370526>
- Cohen, S. S., Min, M., Cummings, E. E., Chen, X., Sadowska, G. B., Sharma, S., & Stonestreet, B. S. (2013). Effects of interleukin-6 on the expression of tight junction proteins in isolated cerebral microvessels from yearling and adult sheep. *Neuroimmunomodulation*, *20*(5), 264–273. <https://doi.org/10.1159/000350470>
- Cooney, A. J., Leng, X., Tsai, S. Y., O'Malley, B. W., & Tsai, M. J. (1993). Multiple mechanisms of chicken ovalbumin upstream promoter transcription factor-dependent repression of transactivation by the vitamin D, thyroid hormone, and retinoic acid receptors. *J Biol Chem*, *268*(6), 4152–4160. Retrieved from <http://www.jbc.org/content/268/6/4152.full.pdf>
- Cortes, M., Liu, S. Y., Kwan, W., Alexa, K., Goessling, W., & North, T. E. (2015). Accumulation of the Vitamin D precursor cholecalciferol antagonizes hedgehog signaling to impair hemogenic endothelium formation. *Stem Cell Reports*. <https://doi.org/10.1016/j.stemcr.2015.08.010>
- Cox, M. B., Cairns, M. J., Gandhi, K. S., Carroll, A. P., Moscovis, S., Stewart, G. J., ... Lechner-Scott, J. (2010). MicroRNAs miR-17 and miR-20a inhibit T cell activation genes and are under-expressed in MS whole blood. *PLoS ONE*. <https://doi.org/10.1371/journal.pone.0012132>
- Cui, Q., Yu, Z., Purisima, E. O., & Wang, E. (2006). Principles of microRNA regulation of a human cellular signaling network. *Mol Syst Biol*, *2*, 46. <https://doi.org/10.1038/msb4100089>
- D'Asti, E., Kool, M., Pfister, S. M., & Rak, J. (2014). Coagulation and angiogenic gene expression profiles are defined by molecular subgroups of medulloblastoma: Evidence for growth factor-thrombin cross-talk. *Journal of Thrombosis and Haemostasis*. <https://doi.org/10.1111/jth.12715>
- Daneman, R. (2012). The blood-brain barrier in health and disease. *Ann Neurol*, *72*(5), 648–672. <https://doi.org/10.1002/ana.23648>
- Datta Mitra, A., Raychaudhuri, S. P., Abria, C. J., Mitra, A., Wright, R., Ray, R., & Kundu-Raychaudhuri, S. (2013). 1alpha,25-Dihydroxyvitamin-D3-3-bromoacetate regulates AKT/mTOR signaling cascades: a therapeutic agent for psoriasis. *J Invest Dermatol*, *133*(6), 1556–1564. <https://doi.org/10.1038/jid.2013.3>
- Davies, J. P., Chen, F. W., & Ioannou, Y. A. (2000). Transmembrane molecular pump activity of Niemann-Pick C1 protein. *Science*, *290*(5500), 2295–2298.

<https://doi.org/10.1126/science.290.5500.2295>

- De Bock, M., Van Haver, V., Vandenbroucke, R. E., Decrock, E., Wang, N., & Leybaert, L. (2016). Into rather unexplored terrain-transcellular transport across the blood-brain barrier. *GLIA*. <https://doi.org/10.1002/glia.22960>
- De Laere, M., Sousa, C., Meena, M., Buckinx, R., Timmermans, J. P., Berneman, Z., & Cools, N. (2017). Increased Transendothelial Transport of CCL3 Is Insufficient to Drive Immune Cell Transmigration through the Blood-Brain Barrier under Inflammatory Conditions In Vitro. *Mediators of Inflammation*. <https://doi.org/10.1155/2017/6752756>
- Dean, R. A., & Overall, C. M. (2007). Proteomics Discovery of Metalloproteinase Substrates in the Cellular Context by iTRAQ™ Labeling Reveals a Diverse MMP-2 Substrate Degradome. *Molecular & Cellular Proteomics*, 6(4), 611–623. <https://doi.org/10.1074/mcp.M600341-MCP200>
- Dehghani, L., Meamar, R., Etemadifar, M., Sheshde, Z. D., Shaygannejad, V., Sharifkhal, M., & Tahani, S. (2013). Can vitamin D suppress endothelial cells apoptosis in multiple sclerosis patients? *International Journal of Preventive Medicine*.
- Dejana, E., Lampugnani, M. G., Martinez-Estrada, O., & Bazzoni, G. (2000). The molecular organization of endothelial junctions and their functional role in vascular morphogenesis and permeability. *Int J Dev Biol*, 44(6), 743–748. Retrieved from <http://www.ncbi.nlm.nih.gov/pubmed/11061439>
- Dennler, S., André, J., Alexaki, I., Li, A., Magnaldo, T., Ten Dijke, P., ... Mauviel, A. (2007). Induction of sonic hedgehog mediators by transforming growth factor- β : Smad3-dependent activation of Gli2 and Gli1 expression in vitro and in vivo. *Cancer Research*. <https://doi.org/10.1158/0008-5472.CAN-07-0491>
- Dormoy, V., Danilin, S., Lindner, V., Thomas, L., Rothhut, S., Coquard, C., ... Massfelder, T. (2009). The sonic hedgehog signaling pathway is reactivated in human renal cell carcinoma and plays orchestral role in tumor growth. *Mol Cancer*, 8, 123. <https://doi.org/10.1186/1476-4598-8-123>
- Dreymueller, D., Pruessmeyer, J., Groth, E., & Ludwig, A. (2012). The role of ADAM-mediated shedding in vascular biology. *Eur J Cell Biol*, 91(6–7), 472–485. <https://doi.org/10.1016/j.ejcb.2011.09.003>
- Du, C., Liu, C., Kang, J., Zhao, G., Ye, Z., Huang, S., ... Pei, G. (2009). MicroRNA miR-326 regulates TH-17 differentiation and is associated with the pathogenesis of multiple sclerosis. *Nat Immunol*, 10(12), 1252–1259. <https://doi.org/10.1038/ni.1798>
- Du, J., Chen, Y., Shi, Y., Liu, T., Cao, Y., Tang, Y., ... Li, Y. C. (2015). 1,25-Dihydroxyvitamin D protects intestinal epithelial barrier by regulating the myosin light chain kinase signaling pathway.

Inflammatory Bowel Diseases. <https://doi.org/10.1097/MIB.0000000000000526>

- Du, K., & Montminy, M. (1998). CREB is a regulatory target for the protein kinase Akt/PKB. *Journal of Biological Chemistry*, 273(49), 32377–32379. <https://doi.org/10.1074/jbc.273.49.32377>
- Dubois, B., Masure, S., Hurtenbach, U., Paemen, L., Heremans, H., van den Oord, J., ... Arnold, B. (1999). Resistance of young gelatinase B-deficient mice to experimental autoimmune encephalomyelitis and necrotizing tail lesions. *J Clin Invest*, 104(11), 1507–1515. <https://doi.org/10.1172/jci6886>
- Dunaeva, M., Voo, S., van Oosterhoud, C., & Waltenberger, J. (2010). Sonic hedgehog is a potent chemoattractant for human monocytes: diabetes mellitus inhibits Sonic hedgehog-induced monocyte chemotaxis. *Basic Res Cardiol*, 105(1), 61–71. <https://doi.org/10.1007/s00395-009-0047-x>
- Dusso, A. S., Brown, A. J., & Slatopolsky, E. (2005). Vitamin D. *Am J Physiol Renal Physiol*, 289(1), F8–28. <https://doi.org/10.1152/ajprenal.00336.2004>
- Eadon, M. T., Jacob, A., Cunningham, P. N., Quigg, R. J., Garcia, J. G., & Alexander, J. J. (2014). Transcriptional profiling reveals that C5a alters microRNA in brain endothelial cells. *Immunology*, 143(3), 363–373. <https://doi.org/10.1111/imm.12314>
- Eigenmann, D. E., Xue, G., Kim, K. S., Moses, A. V., Hamburger, M., & Oufir, M. (2013). Comparative study of four immortalized human brain capillary endothelial cell lines, hCMEC/D3, hBMEC, TY10, and BB19, and optimization of culture conditions, for an in vitro blood-brain barrier model for drug permeability studies. *Fluids Barriers CNS*, 10(1), 33. <https://doi.org/10.1186/2045-8118-10-33>
- Eisenach, P. A., De Sampaio, P. C., Murphy, G., & Roghi, C. (2012). Membrane type 1 matrix metalloproteinase (MT1-MMP) ubiquitination at Lys581 increases cellular invasion through type I collagen. *Journal of Biological Chemistry*, 287(14), 11533–11545. <https://doi.org/10.1074/jbc.M111.306340>
- Elizondo, R. A., Yin, Z., Lu, X., & Watsky, M. A. (2014). Effect of vitamin D receptor knockout on cornea epithelium wound healing and tight junctions. *Invest Ophthalmol Vis Sci*, 55(8), 5245–5251. <https://doi.org/10.1167/iovs.13-13553>
- Elo, P., Tadayon, S., Liljenbäck, H., Teuho, J., Käkelä, M., Koskensalo, K., ... Roivainen, A. (2018). Vascular adhesion protein-1 is actively involved in the development of inflammatory lesions in rat models of multiple sclerosis. *Journal of Neuroinflammation*. <https://doi.org/10.1186/s12974-018-1152-2>

- Emonard, H., Bellon, G., De Diesbach, P., Mettlen, M., Hornebeck, W., & Courtoy, P. J. (2005). Regulation of matrix metalloproteinase (MMP) activity by the low-density lipoprotein receptor-related protein (LRP). A new function for an "old friend." *Biochimie*. <https://doi.org/10.1016/j.biochi.2004.11.013>
- Engelhardt, B. (2006). Molecular mechanisms involved in T cell migration across the blood-brain barrier. *J Neural Transm*, *113*(4), 477–485. <https://doi.org/10.1007/s00702-005-0409-y>
- Engelhardt, B., & Ransohoff, R. M. (2012). Capture, crawl, cross: the T cell code to breach the blood-brain barriers. *Trends Immunol*, *33*(12), 579–589. <https://doi.org/10.1016/j.it.2012.07.004>
- Enkhjargal, B., McBride, D. W., Manaenko, A., Reis, C., Sakai, Y., Tang, J., & Zhang, J. H. (2017). Intranasal administration of vitamin D attenuates blood-brain barrier disruption through endogenous upregulation of osteopontin and activation of CD44/P-gp glycosylation signaling after subarachnoid hemorrhage in rats. *Journal of Cerebral Blood Flow and Metabolism : Official Journal of the International Society of Cerebral Blood Flow and Metabolism*, *37*(7), 2555–2566. <https://doi.org/10.1177/0271678X16671147>
- Erickson, M. A., Hansen, K., & Banks, W. A. (2012). Inflammation-induced dysfunction of the low-density lipoprotein receptor-related protein-1 at the blood-brain barrier: Protection by the antioxidant N-acetylcysteine. *Brain, Behavior, and Immunity*. <https://doi.org/10.1016/j.bbi.2012.07.003>
- Esparza, J., Kruse, M., Lee, J., Michaud, M., & Madri, J. A. (2004). MMP-2 null mice exhibit an early onset and severe experimental autoimmune encephalomyelitis due to an increase in MMP-9 expression and activity. *FASEB J*, *18*(14), 1682–1691. <https://doi.org/10.1096/fj.04-2445com>
- Essa, S., Reichrath, S., Mahlknecht, U., Montenarh, M., Vogt, T., & Reichrath, J. (2012). Signature of VDR miRNAs and epigenetic modulation of vitamin D signaling in melanoma cell lines. *Anticancer Res*, *32*(1), 383–389. Retrieved from <http://ar.iiarjournals.org/content/32/1/383.full.pdf>
- Essandoh, K., Li, Y., Huo, J., & Fan, G.-C. (2016). Mirna-Mediated Macrophage Polarization and its Potential Role in the Regulation of Inflammatory Response. *Shock (Augusta, Ga.)*. <https://doi.org/10.1097/SHK.0000000000000604>
- Fan, H. X., Wang, S., Zhao, H., Liu, N., Chen, D., Sun, M., & Zheng, J. H. (2014). Sonic hedgehog signaling may promote invasion and metastasis of oral squamous cell carcinoma by activating MMP-9 and E-cadherin expression. *Medical Oncology*. <https://doi.org/10.1007/s12032-014-0041-5>
- Fanjul-Fernandez, M., Folgueras, A. R., Cabrera, S., & Lopez-Otin, C. (2010). Matrix metalloproteinases:

- evolution, gene regulation and functional analysis in mouse models. *Biochim Biophys Acta*, 1803(1), 3–19. <https://doi.org/10.1016/j.bbamcr.2009.07.004>
- Fanning, A. S., Jameson, B. J., Jesaitis, L. A., & Anderson, J. M. (1998). The tight junction protein ZO-1 establishes a link between the transmembrane protein occludin and the actin cytoskeleton. *J Biol Chem*, 273(45), 29745–29753. Retrieved from <http://www.jbc.org/content/273/45/29745.full.pdf>
- Fazi, F., & Nervi, C. (2008). MicroRNA: basic mechanisms and transcriptional regulatory networks for cell fate determination. *Cardiovasc Res*, 79(4), 553–561. <https://doi.org/10.1093/cvr/cvn151>
- Feinstein, A., Freeman, J., & Lo, A. C. (2015). Treatment of progressive multiple sclerosis: what works, what does not, and what is needed. *Lancet Neurol*, 14(2), 194–207. [https://doi.org/10.1016/s1474-4422\(14\)70231-5](https://doi.org/10.1016/s1474-4422(14)70231-5)
- Feng, P., Li, X., Chen, W., He, R., & Wang, X. (2016). [Effects of Tumor Necrosis Factor Alpha on the Expression of Matrix Metalloproteinases and Tissue Inhibitors of Matrix Metalloproteinases in Keratoconus Fibroblasts]. *Sheng wu yi xue gong cheng xue za zhi = Journal of biomedical engineering = Shengwu yixue gongchengxue zazhi*, 33(6), 1139–1144.
- Ferber, I. a, Brocke, S., Taylor-Edwards, C., Ridgway, W., Dinisco, C., Steinman, L., ... Fathman, C. G. (1996). Mice with a disrupted IFN-gamma gene are susceptible to the induction of experimental autoimmune encephalomyelitis (EAE). *Journal of Immunology (Baltimore, Md. : 1950)*.
- Fernandez-Castaneda, A., Arandjelovic, S., Stiles, T. L., Schlobach, R. K., Mowen, K. A., Gonias, S. L., & Gaultier, A. (2013). Identification of the low density lipoprotein (LDL) receptor-related protein-1 interactome in central nervous system myelin suggests a role in the clearance of necrotic cell debris. *Journal of Biological Chemistry*. <https://doi.org/10.1074/jbc.M112.384693>
- Ferretti, E., De Smaele, E., Miele, E., Laneve, P., Po, A., Pelloni, M., ... Gulino, A. (2008). Concerted microRNA control of Hedgehog signalling in cerebellar neuronal progenitor and tumour cells. *EMBO J*, 27(19), 2616–2627. <https://doi.org/10.1038/emboj.2008.172>
- Festoff, B. W., Sajja, R. K., van Dreden, P., & Cucullo, L. (2016). HMGB1 and thrombin mediate the blood-brain barrier dysfunction acting as biomarkers of neuroinflammation and progression to neurodegeneration in Alzheimer's disease. *Journal of Neuroinflammation*. <https://doi.org/10.1186/s12974-016-0670-z>
- Fiotti, N., Zivadinov, R., Altamura, N., Nasuelli, D., Bratina, A., Tommasi, M. A., ... Zorzon, M. (2004). MMP-9 microsatellite polymorphism and multiple sclerosis. *J Neuroimmunol*, 152(1–2), 147–

153. <https://doi.org/10.1016/j.jneuroim.2004.03.009>

- Forster, C., Burek, M., Romero, I. A., Weksler, B., Couraud, P. O., & Drenckhahn, D. (2008). Differential effects of hydrocortisone and TNF α on tight junction proteins in an in vitro model of the human blood-brain barrier. *J Physiol*, 586(Pt 7), 1937–1949. <https://doi.org/10.1113/jphysiol.2007.146852>
- Friedman, R. C., Farh, K. K., Burge, C. B., & Bartel, D. P. (2009). Most mammalian mRNAs are conserved targets of microRNAs. *Genome Res*, 19(1), 92–105. <https://doi.org/10.1101/gr.082701.108>
- Fujita, H., Sugimoto, K., Inatomi, S., Maeda, T., Osanai, M., Uchiyama, Y., ... Chiba, H. (2008). Tight junction proteins claudin-2 and -12 are critical for vitamin D-dependent Ca²⁺ absorption between enterocytes. *Mol Biol Cell*, 19(5), 1912–1921. <https://doi.org/10.1091/mbc.E07-09-0973>
- Fujita, K., Ando, T., Ohba, T., Wako, M., Sato, N., Nakamura, Y., ... Haro, H. (2012). Age-related expression of MCP-1 and MMP-3 in mouse intervertebral disc in relation to TWEAK and TNF- α stimulation. *Journal of Orthopaedic Research*. <https://doi.org/10.1002/jor.21560>
- Furuse, M., Sasaki, H., & Tsukita, S. (1999). Manner of interaction of heterogeneous claudin species within and between tight junction strands. *Journal of Cell Biology*, 147(4), 891–903. <https://doi.org/10.1083/jcb.147.4.891>
- Gandhi, R., Healy, B., Gholipour, T., Egorova, S., Musallam, A., Hussain, M. S., ... Weiner, H. L. (2013). Circulating MicroRNAs as biomarkers for disease staging in multiple sclerosis. *Annals of Neurology*. <https://doi.org/10.1002/ana.23880>
- Garcia, L. A., Ferrini, M. G., Norris, K. C., & Artaza, J. N. (2013). 1,25(OH)₂vitamin D₃ enhances myogenic differentiation by modulating the expression of key angiogenic growth factors and angiogenic inhibitors in C2C12 skeletal muscle cells. *Journal of Steroid Biochemistry and Molecular Biology*. <https://doi.org/10.1016/j.jsbmb.2012.09.004>
- Garton, K. J., Gough, P. J., Philalay, J., Wille, P. T., Blobel, C. P., Whitehead, R. H., ... Raines, E. W. (2003). Stimulated shedding of vascular cell adhesion molecule 1 (VCAM-1) is mediated by tumor necrosis factor- α -converting enzyme (ADAM 17). *Journal of Biological Chemistry*, 278(39), 37459–37464. <https://doi.org/10.1074/jbc.M305877200>
- Gaultier, A., Arandjelovic, S., Li, X., Janes, J., Dragojlovic, N., Zhou, G. P., ... Campana, W. M. (2008). A shed form of LDL receptor-related protein-1 regulates peripheral nerve injury and neuropathic pain in rodents. *Journal of Clinical Investigation*. <https://doi.org/10.1172/JCI32371>

- Gaultier, A., Wu, X., Le Moan, N., Takimoto, S., Mukandala, G., Akassoglou, K., ... Gonias, S. L. (2009). Low-density lipoprotein receptor-related protein 1 is an essential receptor for myelin phagocytosis. *Journal of Cell Science*. <https://doi.org/10.1242/jcs.040717>
- Giangreco, A. A., Vaishnav, A., Wagner, D., Finelli, A., Fleshner, N., Van der Kwast, T., ... Nonn, L. (2013). Tumor suppressor microRNAs, miR-100 and -125b, are regulated by 1,25-dihydroxyvitamin D in primary prostate cells and in patient tissue. *Cancer Prev Res (Phila)*, *6*(5), 483–494. <https://doi.org/10.1158/1940-6207.CAPR-12-0253>
- Gijbels, K., Galardy, R. E., & Steinman, L. (1994). Reversal of experimental autoimmune encephalomyelitis with a hydroxamate inhibitor of matrix metalloproteases. *Journal of Clinical Investigation*, *94*(6), 2177–2182. <https://doi.org/10.1172/JCI117578>
- Giraudon, P., Buart, S., Bernard, A., Thomasset, N., & Belin, M. F. (1996). Extracellular matrix-remodeling metalloproteinases and infection of the central nervous system with retrovirus human T-lymphotropic virus type I (HTLV-I). *Progress in Neurobiology*. [https://doi.org/10.1016/0301-0082\(96\)00017-2](https://doi.org/10.1016/0301-0082(96)00017-2)
- Goertsches, R., Comabella, M., Navarro, A., Perkal, H., & Montalban, X. (2005). Genetic association between polymorphisms in the ADAMTS14 gene and multiple sclerosis. *J Neuroimmunol*, *164*(1–2), 140–147. <https://doi.org/10.1016/j.jneuroim.2005.04.005>
- Goertsches, R. H., Hecker, M., Koczan, D., Serrano-Fernandez, P., Moeller, S., Thiesen, H. J., & Zettl, U. K. (2010). Long-term genome-wide blood RNA expression profiles yield novel molecular response candidates for IFN- γ -1b treatment in relapsing remitting MS. *Pharmacogenomics*. <https://doi.org/10.2217/pgs.09.152>
- Gomez, J. P., Gonçalves, C., Pichon, C., & Midoux, P. (2017). Effect of IL-1 β , TNF- α and IGF-1 on trans-endothelial passage of synthetic vectors through an in vitro vascular endothelial barrier of striated muscle. *Gene Therapy*. <https://doi.org/10.1038/gt.2017.40>
- Gomez, J. P., Pichon, C., & Midoux, P. (2013). Ability of plasmid DNA complexed with histidinylated IPEI and IPEI to cross in vitro lung and muscle vascular endothelial barriers. *Gene*, *525*(2), 182–190. <https://doi.org/10.1016/j.gene.2013.03.055>
- Gonias, S. L., & Campana, W. M. (2014). LDL receptor-related protein-1: A regulator of inflammation in atherosclerosis, cancer, and injury to the nervous system. *American Journal of Pathology*. <https://doi.org/10.1016/j.ajpath.2013.08.029>
- Goverman, J. (2009). Autoimmune T cell responses in the central nervous system. *Nature Reviews*

Immunology. <https://doi.org/10.1038/nri2550>

- Graesser, D., Mahooti, S., & Madri, J. A. (2000). Distinct roles for matrix metalloproteinase-2 and alpha4 integrin in autoimmune T cell extravasation and residency in brain parenchyma during experimental autoimmune encephalomyelitis. *J Neuroimmunol*, *109*(2), 121–131. Retrieved from <http://www.ncbi.nlm.nih.gov/pubmed/10996214>
- Grishkan, I. V., Fairchild, A. N., Calabresi, P. A., & Gocke, A. R. (2013). 1,25-Dihydroxyvitamin D3 selectively and reversibly impairs T helper-cell CNS localization. *Proc Natl Acad Sci U S A*, *110*(52), 21101–21106. <https://doi.org/10.1073/pnas.1306072110>
- Guo, Y. X., He, L. Y., Zhang, M., Wang, F., Liu, F., & Peng, W. X. (2016). 1,25-Dihydroxyvitamin D3 regulates expression of LRP1 and RAGE in vitro and in vivo, enhancing Aβ1-40 brain-to-blood efflux and peripheral uptake transport. *Neuroscience*. <https://doi.org/10.1016/j.neuroscience.2016.01.041>
- Gurney, K. J., Estrada, E. Y., & Rosenberg, G. A. (2006). Blood-brain barrier disruption by stromelysin-1 facilitates neutrophil infiltration in neuroinflammation. *Neurobiology of Disease*, *23*(1), 87–96. <https://doi.org/10.1016/j.nbd.2006.02.006>
- Hafler, D. A. (2004). Multiple sclerosis. *J Clin Invest*, *113*(6), 788–794. <https://doi.org/10.1172/JCI21357>
- Hamzaoui, A., Berraies, A., Hamdi, B., Kaabachi, W., Ammar, J., & Hamzaoui, K. (2014). Vitamin D reduces the differentiation and expansion of Th17 cells in young asthmatic children. *Immunobiology*. <https://doi.org/10.1016/j.imbio.2014.07.009>
- Hansmann, F., Herder, V., Kalkuhl, A., Haist, V., Zhang, N., Schaudien, D., ... Ulrich, R. (2012). Matrix metalloproteinase-12 deficiency ameliorates the clinical course and demyelination in Theiler's murine encephalomyelitis. *Acta Neuropathologica*, *124*(1), 127–142. <https://doi.org/10.1007/s00401-012-0942-3>
- Harhaj, N. S., & Antonetti, D. A. (2004). Regulation of tight junctions and loss of barrier function in pathophysiology. *Int J Biochem Cell Biol*, *36*(7), 1206–1237. <https://doi.org/10.1016/j.biocel.2003.08.007>
- Hathaway, D. R., Eaton, C. R., & Adelstein, R. S. (1981). Regulation of human platelet myosin light chain kinase by the catalytic subunit of cyclic AMP-dependent protein kinase. *Nature*, *291*(5812), 252–256. Retrieved from <https://www.ncbi.nlm.nih.gov/pubmed/6894484>
- Hatherell, K., Couraud, P. O., Romero, I. A., Weksler, B., & Pilkington, G. J. (2011). Development of a

- three-dimensional, all-human in vitro model of the blood-brain barrier using mono-, co-, and tri-cultivation Transwell models. *Journal of Neuroscience Methods*. <https://doi.org/10.1016/j.jneumeth.2011.05.012>
- Hauser, S. L., & Goodin, D. S. (2008). *Harrison's Principles of Internal Medicine* (17th ed., Vol. 1). McGraw-Hill Medical.
- He, Q. W., Xia, Y. P., Chen, S. C., Wang, Y., Huang, M., Huang, Y., ... Hu, B. (2013). Astrocyte-derived sonic hedgehog contributes to angiogenesis in brain microvascular endothelial cells via RhoA/ROCK pathway after oxygen-glucose deprivation. *Molecular Neurobiology*. <https://doi.org/10.1007/s12035-013-8396-8>
- He, Y., Yao, Y., Tsirka, S. E., & Cao, Y. (2014). Cell-culture models of the blood-brain barrier. *Stroke*, *45*(8), 2514–2526. <https://doi.org/10.1161/STROKEAHA.114.005427>
- Heidary, M., Rakhshi, N., Pahlevan Kakhki, M., Behmanesh, M., Sanati, M. H., Sanadgol, N., ... Nikraves, A. (2014). The analysis of correlation between IL-1B gene expression and genotyping in multiple sclerosis patients. *Journal of the Neurological Sciences*. <https://doi.org/10.1016/j.jns.2014.05.013>
- Hellström, M., Kalén, M., Lindahl, P., Abramsson, A., & Betsholtz, C. (1999). Role of PDGF-B and PDGFR-beta in recruitment of vascular smooth muscle cells and pericytes during embryonic blood vessel formation in the mouse. *Development (Cambridge, England)*, *126*(14), 3047–3055. Retrieved from <http://www.ncbi.nlm.nih.gov/pubmed/10375497>
- Hendrickx, D. A. E., Koning, N., Schuurman, K. G., Van Strien, M. E., Van Eden, C. G., Hamann, J., & Huitinga, I. (2013). Selective upregulation of scavenger receptors in and around demyelinating areas in multiple sclerosis. *Journal of Neuropathology and Experimental Neurology*. <https://doi.org/10.1097/NEN.0b013e31827fd9e8>
- Hendriks, W. J. a J., Elson, A., Harroch, S., Pulido, R., Stoker, A., & den Hertog, J. (2013). Protein tyrosine phosphatases in health and disease. *The FEBS Journal*. <https://doi.org/10.1111/febs.12000>
- Henshall, T. L., Keller, A., He, L., Johansson, B. R., Wallgard, E., Raschperger, E., ... Lendahl, U. (2015). Notch3 is necessary for blood vessel integrity in the central nervous system. *Arterioscler Thromb Vasc Biol*, *35*(2), 409–420. <https://doi.org/10.1161/ATVBAHA.114.304849>
- Hill, J., Rom, S., Ramirez, S. H., & Persidsky, Y. (2014). Emerging Roles of Pericytes in the Regulation of the Neurovascular Unit in Health and Disease. *Journal of Neuroimmune Pharmacology*. <https://doi.org/10.1007/s11481-014-9557-x>

- Hirota, K., Duarte, J. H., Veldhoen, M., Hornsby, E., Li, Y., Cua, D. J., ... Stockinger, B. (2011). Fate mapping of IL-17-producing T cells in inflammatory responses. *Nature Immunology*. <https://doi.org/10.1038/ni.1993>
- Hosokawa, Y., Hosokawa, I., Shindo, S., Ozaki, K., & Matsuo, T. (2015). Calcitriol Suppressed Inflammatory Reactions in IL-1 β -Stimulated Human Periodontal Ligament Cells. *Inflammation*. <https://doi.org/10.1007/s10753-015-0209-y>
- Hosseini, A., Estiri, H., Akhavan Niaki, H., Alizadeh, A., Abdolhossein Zadeh, B., Ghaderian, S. M. H., ... Fallah, A. (2017). Multiple Sclerosis Gene Therapy with Recombinant Viral Vectors: Overexpression of IL-4, Leukemia Inhibitory Factor, and IL-10 in Wharton's Jelly Stem Cells Used in EAE Mice Model. *Cell Journal*, 19(3), 361–374. <https://doi.org/10.22074/cellj.2017.4497>
- Hu, J., Zhang, Z., Xie, H., Chen, L., Zhou, Y., Chen, W., & Liu, Z. (2013). Serine protease inhibitor A3K protects rabbit corneal endothelium from barrier function disruption induced by TNF- α . *Investigative Ophthalmology and Visual Science*. <https://doi.org/10.1167/iovs.12-10145>
- Hun Lee, J., Won, S., & Stein, D. G. (2015). Progesterone attenuates thrombin-induced endothelial barrier disruption in the brain endothelial cell line bEnd.3: The role of tight junction proteins and the endothelial protein C receptor. *Brain Research*. <https://doi.org/10.1016/j.brainres.2015.04.002>
- Hyc, A., Osiecka-Iwan, A., Niderla-Bielinska, J., & Moskalewski, S. (2011). Influence of LPS, TNF, TGF- β 1 and IL-4 on the expression of MMPs, TIMPs and selected cytokines in rat synovial membranes incubated in vitro. *International Journal of Molecular Medicine*. <https://doi.org/10.3892/ijmm.2010.550>
- Ikeda, U., Wakita, D., Ohkuri, T., Chamoto, K., Kitamura, H., Iwakura, Y., & Nishimura, T. (2010). 1 α ,25-Dihydroxyvitamin D3 and all-trans retinoic acid synergistically inhibit the differentiation and expansion of Th17 cells. *Immunology Letters*. <https://doi.org/10.1016/j.imlet.2010.07.002>
- Inaba, Y., Ichikawa, M., Koh, C. S., Inoue, A., Itoh, M., Kyogashima, M., & Komiyama, A. (1999). Suppression of experimental autoimmune encephalomyelitis by dermatan sulfate. *Cellular Immunology*, 198(2), 96–102. <https://doi.org/10.1006/cimm.1999.1588>
- Incardona, J. P., Gaffield, W., Kapur, R. P., & Roelink, H. (1998). The teratogenic Veratrum alkaloid cyclopamine inhibits sonic hedgehog signal transduction. *Development*, 125(18), 3553–3562. Retrieved from <http://www.ncbi.nlm.nih.gov/pubmed/9716521>
- Itoh, M., Furuse, M., Morita, K., Kubota, K., Saitou, M., & Tsukita, S. (1999). Direct binding of three

- tight junction-associated MAGUKs, ZO-1, ZO-2, and ZO-3, with the COOH termini of claudins. *Journal of Cell Biology*, 147(6), 1351–1363. <https://doi.org/10.1083/jcb.147.6.1351>
- Itoh, Y. (2015). Membrane-type matrix metalloproteinases: Their functions and regulations. *Matrix Biology*. <https://doi.org/10.1016/j.matbio.2015.03.004>
- Jackson, C. J., & Nguyen, M. (1997). Human microvascular endothelial cells differ from macrovascular endothelial cells in their expression of matrix metalloproteinases. *The International Journal of Biochemistry & Cell Biology*. [https://doi.org/10.1016/S1357-2725\(97\)00061-7](https://doi.org/10.1016/S1357-2725(97)00061-7)
- Jaeger, L. B., Dohgu, S., Sultana, R., Lynch, J. L., Owen, J. B., Erickson, M. A., ... Banks, W. A. (2009). Lipopolysaccharide alters the blood-brain barrier transport of amyloid β protein: A mechanism for inflammation in the progression of Alzheimer's disease. *Brain, Behavior, and Immunity*. <https://doi.org/10.1016/j.bbi.2009.01.017>
- Jayakumar, A. R., Rama Rao, K. V., & Norenberg, M. D. (2015). Neuroinflammation in hepatic encephalopathy: mechanistic aspects. *J Clin Exp Hepatol*, 5(Suppl 1), S21-8. <https://doi.org/10.1016/j.jceh.2014.07.006>
- Jiang, H., Zhang, F., Yang, J., & Han, S. (2014). Angiopoietin-1 ameliorates inflammation-induced vascular leakage and improves functional impairment in a rat model of acute experimental autoimmune encephalomyelitis. *Experimental Neurology*. <https://doi.org/10.1016/j.expneurol.2014.05.013>
- Johannessen, M., Delghandi, M. P., & Moens, U. (2004). What turns CREB on? *Cellular Signalling*. <https://doi.org/10.1016/j.cellsig.2004.05.001>
- Joshi, S., Pantalena, L. C., Liu, X. K., Gaffen, S. L., Liu, H., Rohowsky-Kochan, C., ... Youssef, S. (2011). 1,25-dihydroxyvitamin D(3) ameliorates Th17 autoimmunity via transcriptional modulation of interleukin-17A. *Mol Cell Biol*, 31(17), 3653–3669. <https://doi.org/10.1128/MCB.05020-11>
- Junker, A., Krumbholz, M., Eisele, S., Mohan, H., Augstein, F., Bittner, R., ... Meinl, E. (2009). MicroRNA profiling of multiple sclerosis lesions identifies modulators of the regulatory protein CD47. *Brain*, 132(Pt 12), 3342–3352. <https://doi.org/10.1093/brain/awp300>
- Kanda, S., Mochizuki, Y., Suematsu, T., Miyata, Y., Nomata, K., & Kanetake, H. (2003). Sonic hedgehog induces capillary morphogenesis by endothelial cells through phosphoinositide 3-kinase. *J Biol Chem*, 278(10), 8244–8249. <https://doi.org/10.1074/jbc.M210635200>
- Kása, A., Csontos, C., & Verin, A. D. (2015). Cytoskeletal mechanisms regulating vascular endothelial barrier function in response to acute lung injury. *Tissue Barriers*.

<https://doi.org/10.4161/21688370.2014.974448>

- Kasagi, Y., Chandramouleeswaran, P. M., Whelan, K. A., Tanaka, K., Giroux, V., Sharma, M., ... Nakagawa, H. (2018). The Esophageal Organoid System Reveals Functional Interplay Between Notch and Cytokines in Reactive Epithelial Changes. *CMGH*. <https://doi.org/10.1016/j.jcmgh.2017.12.013>
- Kasper, L. H., & Reder, A. T. (2014). Immunomodulatory activity of interferon-beta. *Ann Clin Transl Neurol*, *1*(8), 622–631. <https://doi.org/10.1002/acn3.84>
- Keller, A., Leidinger, P., Steinmeyer, F., Stähler, C., Franke, A., Hemmrich-Stanisak, G., ... Ruprecht, K. (2014). Comprehensive analysis of microRNA profiles in multiple sclerosis including next-generation sequencing. *Multiple Sclerosis (Houndmills, Basingstoke, England)*. <https://doi.org/10.1177/1352458513496343>
- Kelwick, R., Desanlis, I., Wheeler, G. N., & Edwards, D. R. (2015). The ADAMTS (A Disintegrin and Metalloproteinase with Thrombospondin motifs) family. *Genome Biol*, *16*, 113. <https://doi.org/10.1186/s13059-015-0676-3>
- Khaibullin, T., Ivanova, V., Martynova, E., Cherepnev, G., Khabirov, F., Granatov, E., ... Khaiboullina, S. (2017). Elevated levels of proinflammatory cytokines in cerebrospinal fluid of multiple sclerosis patients. *Frontiers in Immunology*. <https://doi.org/10.3389/fimmu.2017.00531>
- Kieseier, B. C. (2011). The mechanism of action of interferon-beta in relapsing multiple sclerosis. *CNS Drugs*, *25*(6), 491–502. <https://doi.org/10.2165/11591110-000000000-00000>
- Kim, S.-H., Pei, Q.-M., Jiang, P., Yang, M., Qian, X.-J., & Liu, J.-B. (2017). Effect of active vitamin D3 on VEGF-induced ADAM33 expression and proliferation in human airway smooth muscle cells: implications for asthma treatment. *Respiratory Research*. <https://doi.org/10.1186/s12931-016-0490-9>
- Kipp, M., & Amor, S. (2012). FTY720 on the way from the base camp to the summit of the mountain: relevance for remyelination. *Mult Scler*, *18*(3), 258–263. <https://doi.org/10.1177/1352458512438723>
- Kipp, M., Van der Star, B. J., Vogel, D. Y., Puentes, F., Van der Valk, P., Baker, D., & Amor, S. (2012). Experimental in vivo and in vitro models of multiple sclerosis: EAE and beyond. *Multiple Sclerosis and Related Disorders*, *1*(1), 14. <https://doi.org/10.1016/j.msard.2011.09.002>
- Kniesel, U., & Wolburg, H. (2000). Tight junctions of the blood-brain barrier. *Cell Mol Neurobiol*, *20*(1), 57–76. Retrieved from <http://www.ncbi.nlm.nih.gov/pubmed/10690502>

- Kong, J., Zhang, Z., Musch, M. W., Ning, G., Sun, J., Hart, J., ... Li, Y. C. (2008). Novel role of the vitamin D receptor in maintaining the integrity of the intestinal mucosal barrier. *Am J Physiol Gastrointest Liver Physiol*, 294(1), G208-16. <https://doi.org/10.1152/ajpgi.00398.2007>
- Krakowski, M., & Owens, T. (1996). Interferon-gamma confers resistance to experimental allergic encephalomyelitis. *European Journal of Immunology*. <https://doi.org/10.1002/eji.1830260735>
- Krishnan, V., Pereira, F. A., Qiu, Y., Chen, C. H., Beachy, P. A., Tsai, S. Y., & Tsai, M. J. (1997). Mediation of Sonic hedgehog-induced expression of COUP-TFII by a protein phosphatase. *Science*, 278(5345), 1947–1950. Retrieved from <http://www.ncbi.nlm.nih.gov/pubmed/9395397>
- Kulczar, C., Lubin, K. E., Lefebvre, S., Miller, D. W., & Knipp, G. T. (2017). Development of a direct contact astrocyte-human cerebral microvessel endothelial cells blood–brain barrier coculture model. *Journal of Pharmacy and Pharmacology*. <https://doi.org/10.1111/jphp.12803>
- Kuruville, L., & Kartha, C. C. (2003). Molecular mechanisms in endothelial regulation of cardiac function. *Molecular and Cellular Biochemistry*. <https://doi.org/10.1023/A:1026061507004>
- Labus, J., Hackel, S., Lucka, L., & Danker, K. (2014). Interleukin-1beta induces an inflammatory response and the breakdown of the endothelial cell layer in an improved human THBMEC-based in vitro blood-brain barrier model. *J Neurosci Methods*, 228, 35–45. <https://doi.org/10.1016/j.jneumeth.2014.03.002>
- Larochelle, C., Alvarez, J. I., & Prat, A. (2011). How do immune cells overcome the blood-brain barrier in multiple sclerosis? *FEBS Lett*, 585(23), 3770–3780. <https://doi.org/10.1016/j.febslet.2011.04.066>
- Lassmann, H., Bruck, W., & Lucchinetti, C. F. (2007). The immunopathology of multiple sclerosis: an overview. *Brain Pathol*, 17(2), 210–218. <https://doi.org/10.1111/j.1750-3639.2007.00064.x>
- Lee, C. W., Lin, C. C., Lin, W. N., Liang, K. C., Luo, S. F., Wu, C. B., ... Yang, C. M. (2007). TNF-alpha induces MMP-9 expression via activation of Src/EGFR, PDGFR/PI3K/Akt cascade and promotion of NF-kappaB/p300 binding in human tracheal smooth muscle cells. *Am J Physiol Lung Cell Mol Physiol*, 292(3), L799-812. <https://doi.org/10.1152/ajplung.00311.2006>
- Lee, H. J., Wislocki, A., Goodman, C., Ji, Y., Ge, R., Maehr, H., ... Suh, N. (2006). A novel vitamin D derivative activates bone morphogenetic protein signaling in MCF10 breast epithelial cells. *Molecular Pharmacology*. <https://doi.org/10.1124/mol.105.022079>
- Lee, M.-H., Dodds, P., Verma, V., Maskos, K., Knäuper, V., & Murphy, G. (2003). Tailoring tissue inhibitor of metalloproteinases-3 to overcome the weakening effects of the cysteine-rich

- domains of tumour necrosis factor-alpha converting enzyme. *The Biochemical Journal*.
<https://doi.org/10.1042/BJ20021538>
- Lee, M. A., Palace, J., Stabler, G., Ford, J., Gearing, A., & Miller, K. (1999). Serum gelatinase B, TIMP-1 and TIMP-2 levels in multiple sclerosis. A longitudinal clinical and MRI study. *Brain*, *122* (Pt 2, 191–197.
- Lee, Y. A., Choi, H. M., Lee, S. H., Hong, S. J., Yang, H. I., Yoo, M. C., & Kim, K. S. (2012). Hypoxia differentially affects IL-1 β -stimulated MMP-1 and MMP-13 expression of fibroblast-like synoviocytes in an HIF-1 α -dependent manner. *Rheumatology*.
<https://doi.org/10.1093/rheumatology/ker327>
- Lehmann, W., Edgar, C. M., Wang, K., Cho, T. J., Barnes, G. L., Kakar, S., ... Einhorn, T. A. (2005). Tumor necrosis factor alpha (TNF- α) coordinately regulates the expression of specific matrix metalloproteinases (MMPS) and angiogenic factors during fracture healing. *Bone*.
<https://doi.org/10.1016/j.bone.2004.10.010>
- Leibowitz, S. M., & Yan, J. (2016). NF- κ B Pathways in the Pathogenesis of Multiple Sclerosis and the Therapeutic Implications. *Frontiers in Molecular Neuroscience*.
<https://doi.org/10.3389/fnmol.2016.00084>
- Lemire, J. M., & Archer, D. C. (1991). 1,25-dihydroxyvitamin D3 prevents the in vivo induction of murine experimental autoimmune encephalomyelitis. *J Clin Invest*, *87*(3), 1103–1107.
<https://doi.org/10.1172/JCI115072>
- Leppert, D., Lindberg, R. L., Kappos, L., & Leib, S. L. (2001). Matrix metalloproteinases: multifunctional effectors of inflammation in multiple sclerosis and bacterial meningitis. *Brain Res Brain Res Rev*, *36*(2–3), 249–257. Retrieved from <http://www.ncbi.nlm.nih.gov/pubmed/11690622>
- Lévesque, S. A., Paré, A., Mailhot, B., Bellver-Landete, V., Kébir, H., Lécuyer, M.-A., ... Lacroix, S. (2016). Myeloid cell transmigration across the CNS vasculature triggers IL-1 β -driven neuroinflammation during autoimmune encephalomyelitis in mice. *The Journal of Experimental Medicine*.
<https://doi.org/10.1084/jem.20151437>
- Li, L., Tao, Y., Tang, J., Chen, Q., Yang, Y., Feng, Z., ... Chen, Z. (2015). A Cannabinoid Receptor 2 Agonist Prevents Thrombin-Induced Blood–Brain Barrier Damage via the Inhibition of Microglial Activation and Matrix Metalloproteinase Expression in Rats. *Translational Stroke Research*.
<https://doi.org/10.1007/s12975-015-0425-7>
- Li, M., Mukasa, A., del-Mar Inda, M., Zhang, J., Chin, L., Cavenee, W., & Furnari, F. (2011). Guanylate

- binding protein 1 is a novel effector of EGFR-driven invasion in glioblastoma. *The Journal of Experimental Medicine*. <https://doi.org/10.1084/jem.20111102>
- Li, Y. P., Wei, X. C., Li, P. C., Chen, C. W., Wang, X. H., Jiao, Q., ... Wei, L. (2015). The Role of miRNAs in Cartilage Homeostasis. *Current Genomics*, 16(6), 393–404. <https://doi.org/10.2174/1389202916666150817203144>
- Li, Y., Xia, Y., Wang, Y., Mao, L., Gao, Y., He, Q., ... Hu, B. (2013). Sonic hedgehog (Shh) regulates the expression of angiogenic growth factors in oxygen-glucose-deprived astrocytes by mediating the nuclear receptor NR2F2. *Mol Neurobiol*, 47(3), 967–975. <https://doi.org/10.1007/s12035-013-8395-9>
- Liang, Y., Li, X., Zhang, X., Li, Z., Wang, L., Sun, Y., ... Ma, X. (2014). Elevated levels of plasma TNF- α are associated with microvascular endothelial dysfunction in patients with sepsis through activating the NF- κ B and p38 mitogen-activated protein kinase in endothelial cells. *Shock (Augusta, Ga.)*. <https://doi.org/10.1097/SHK.0000000000000116>
- Lidington, E. A., Rao, R. M., Marelli-Berg, F. M., Jat, P. S., Haskard, D. O., & Mason, J. C. (2002). Conditional immortalization of growth factor-responsive cardiac endothelial cells from H-2K(b)-tsA58 mice. *American Journal of Physiology. Cell Physiology*, 282(1), C67-74. <https://doi.org/10.1152/ajpcell.2002.282.1.C67>
- Liebner, S., Corada, M., Bangsow, T., Babbage, J., Taddei, A., Czapalla, C. J., ... Dejana, E. (2008). Wnt/beta-catenin signaling controls development of the blood-brain barrier. *The Journal of Cell Biology*, 183(3), 409–417. <https://doi.org/10.1083/jcb.200806024>
- Lim, L. P., Lau, N. C., Garrett-Engele, P., Grimson, A., Schelter, J. M., Castle, J., ... Johnson, J. M. (2005). Microarray analysis shows that some microRNAs downregulate large numbers of target mRNAs. *Nature*, 433(7027), 769–773. <https://doi.org/10.1038/nature03315>
- Limb, G. A., Matter, K., Murphy, G., Cambrey, A. D., Bishop, P. N., Morris, G. E., & Khaw, P. T. (2005). Matrix metalloproteinase-1 associates with intracellular organelles and confers resistance to lamin A/C Degradation during apoptosis. *American Journal of Pathology*. [https://doi.org/10.1016/S0002-9440\(10\)62371-1](https://doi.org/10.1016/S0002-9440(10)62371-1)
- Lin, R., Amizuka, N., Sasaki, T., Aarts, M. M., Ozawa, H., Goltzman, D., ... White, J. H. (2002). 1 α ,25-dihydroxyvitamin D3 promotes vascularization of the chondro-osseous junction by stimulating expression of vascular endothelial growth factor and matrix metalloproteinase 9. *J Bone Miner Res*, 17(9), 1604–1612. <https://doi.org/10.1359/jbmr.2002.17.9.1604>

- Lindberg, R. L., De Groot, C. J., Montagne, L., Freitag, P., van der Valk, P., Kappos, L., & Leppert, D. (2001). The expression profile of matrix metalloproteinases (MMPs) and their inhibitors (TIMPs) in lesions and normal appearing white matter of multiple sclerosis. *Brain*, *124*(Pt 9), 1743–1753. Retrieved from <http://brain.oxfordjournals.org/content/brain/124/9/1743.full.pdf>
- Lindberg, R. L., Hoffmann, F., Mehling, M., Kuhle, J., & Kappos, L. (2010). Altered expression of miR-17-5p in CD4+ lymphocytes of relapsing-remitting multiple sclerosis patients. *Eur J Immunol*, *40*(3), 888–898. <https://doi.org/10.1002/eji.200940032>
- Liu, J., Jin, X., Liu, K. J., & Liu, W. (2012). Matrix Metalloproteinase-2-Mediated Occludin Degradation and Caveolin-1-Mediated Claudin-5 Redistribution Contribute to Blood-Brain Barrier Damage in Early Ischemic Stroke Stage. *Journal of Neuroscience*, *32*(9), 3044–3057. <https://doi.org/10.1523/JNEUROSCI.6409-11.2012>
- Liu, M., Hou, X., Zhang, P., Hao, Y., Yang, Y., Wu, X., ... Guan, Y. (2013). Microarray gene expression profiling analysis combined with bioinformatics in multiple sclerosis. *Molecular Biology Reports*. <https://doi.org/10.1007/s11033-012-2449-3>
- Liu, W., Wang, P., Shang, C., Chen, L., Cai, H., Ma, J., ... Xue, Y. (2014). Endophilin-1 regulates blood-brain barrier permeability by controlling ZO-1 and occludin expression via the EGFR-ERK1/2 pathway. *Brain Res*, *1573*, 17–26. <https://doi.org/10.1016/j.brainres.2014.05.022>
- Lopez-Ramirez, M. A., Fischer, R., Torres-Badillo, C. C., Davies, H. A., Logan, K., Pfizenmaier, K., ... Romero, I. A. (2012). Role of caspases in cytokine-induced barrier breakdown in human brain endothelial cells. *J Immunol*, *189*(6), 3130–3139. <https://doi.org/10.4049/jimmunol.1103460>
- Lopez-Ramirez, M. A., Male, D. K., Wang, C., Sharrack, B., Wu, D., & Romero, I. A. (2013). Cytokine-induced changes in the gene expression profile of a human cerebral microvascular endothelial cell-line, hCMEC/D3. *Fluids and Barriers of the CNS*. <https://doi.org/10.1186/2045-8118-10-27>
- Lopez-Ramirez, M. A., Wu, D., Pryce, G., Simpson, J. E., Reijerkerk, A., King-Robson, J., ... Romero, I. A. (2014). MicroRNA-155 negatively affects blood-brain barrier function during neuroinflammation. *FASEB J*, *28*(6), 2551–2565. <https://doi.org/10.1096/fj.13-248880>
- Lu, D. Y., Yu, W. H., Yeh, W. L., Tang, C. H., Leung, Y. M., Wong, K. L., ... Fu, W. M. (2009). Hypoxia-induced matrix metalloproteinase-13 expression in astrocytes enhances permeability of brain endothelial cells. *J Cell Physiol*, *220*(1), 163–173. <https://doi.org/10.1002/jcp.21746>
- Luissint, A. C., Artus, C., Glacial, F., Ganeshamoorthy, K., & Couraud, P. O. (2012). Tight junctions at the blood brain barrier: physiological architecture and disease-associated dysregulation. *Fluids*

Barriers CNS, 9(1), 23. <https://doi.org/10.1186/2045-8118-9-23>

- Luissint, A. C., Federici, C., Guillonneau, F., Chretien, F., Camoin, L., Glacial, F., ... Couraud, P. O. (2012). Guanine nucleotide-binding protein Galphai2: a new partner of claudin-5 that regulates tight junction integrity in human brain endothelial cells. *J Cereb Blood Flow Metab*, 32(5), 860–873. <https://doi.org/10.1038/jcbfm.2011.202>
- Luu, V. Z., Chowdhury, B., Al-Omran, M., Hess, D. A., & Verma, S. (2018). Role of endothelial primary cilia as fluid mechanosensors on vascular health. *Atherosclerosis*. <https://doi.org/10.1016/j.atherosclerosis.2018.06.818>
- Ma, X., Zhou, J., Zhong, Y., Jiang, L., Mu, P., Li, Y., ... Nagarkatti, P. (2014). Expression, regulation and function of microRNAs in multiple sclerosis. *Int J Med Sci*, 11(8), 810–818. <https://doi.org/10.7150/ijms.8647>
- Ma, Y., Li, S.-H., Ding, X.-X., & Wu, P.-L. (2018). [Effects of tumor necrosis factor-alpha on osteogenic differentiation and Notch signaling pathway in human periodontal ligament stem cells]. *Hua xi kou qiang yi xue za zhi = Huaxi kouqiang yixue zazhi = West China journal of stomatology*, 36(2), 184–189. <https://doi.org/10.7518/hxkq.2018.02.013>
- Machida, T., Takata, F., Matsumoto, J., Takenoshita, H., Kimura, I., Yamauchi, A., ... Kataoka, Y. (2015). Brain pericytes are the most thrombin-sensitive matrix metalloproteinase-9-releasing cell type constituting the blood-brain barrier in vitro. *Neuroscience Letters*. <https://doi.org/10.1016/j.neulet.2015.05.028>
- Maghzi, A. H., & Minagar, A. (2014). IL1- β expression in multiple sclerosis. *Journal of the Neurological Sciences*. <https://doi.org/10.1016/j.jns.2014.05.009>
- Mahad, D. H., Trapp, B. D., & Lassmann, H. (2015). Pathological mechanisms in progressive multiple sclerosis. *Lancet Neurol*, 14(2), 183–193. [https://doi.org/10.1016/s1474-4422\(14\)70256-x](https://doi.org/10.1016/s1474-4422(14)70256-x)
- Man, S., Ubogu, E. E., & Ransohoff, R. M. (2007). Inflammatory cell migration into the central nervous system: a few new twists on an old tale. *Brain Pathol*, 17(2), 243–250. <https://doi.org/10.1111/j.1750-3639.2007.00067.x>
- Mark, K. S., & Miller, D. W. (1999). Increased permeability of primary cultured brain microvessel endothelial cell monolayers following TNF-alpha exposure. *Life Sciences*, 64(21), 1941–1953. [https://doi.org/10.1016/S0024-3205\(99\)00139-3](https://doi.org/10.1016/S0024-3205(99)00139-3)
- Marrie, R. A. (2004). Environmental risk factors in multiple sclerosis aetiology. *Lancet Neurol*, 3(12), 709–718. [https://doi.org/10.1016/S1474-4422\(04\)00933-0](https://doi.org/10.1016/S1474-4422(04)00933-0)

- Martinesi, M., Bruni, S., Stio, M., & Treves, C. (2006). 1,25-Dihydroxyvitamin D3 inhibits tumor necrosis factor- α -induced adhesion molecule expression in endothelial cells. *Cell Biology International*. <https://doi.org/10.1016/j.cellbi.2006.01.004>
- Martinez-Moreno, J. M., Herencia, C., Montes de Oca, A., Muñoz-Castañeda, J. R., Rodríguez-Ortiz, M. E., Díaz-Tocados, J. M., ... Almaden, Y. (2016). Abstract - Vitamin D modulates tissue factor and protease-activated receptor 2 expression in vascular smooth muscle cells. *FASEB Journal : Official Publication of the Federation of American Societies for Experimental Biology*, 30(3), 1367–1376. <https://doi.org/10.1096/fj.15-272872>
- Martínez, C., Rodinõ-Janeiro, B. K., Lobo, B., Stanifer, M. L., Klaus, B., Granzow, M., ... Santos, J. (2017). MiR-16 and miR-125b are involved in barrier function dysregulation through the modulation of claudin-2 and cingulin expression in the jejunum in IBS with diarrhoea. *Gut*. <https://doi.org/10.1136/gutjnl-2016-311477>
- Mastronardi, F. G., daCruz, L. A., Wang, H., Boggs, J., & Moscarello, M. A. (2003). The amount of sonic hedgehog in multiple sclerosis white matter is decreased and cleavage to the signaling peptide is deficient. *Mult Scler*, 9(4), 362–371. Retrieved from <http://www.ncbi.nlm.nih.gov/pubmed/12926841>
- May, M. J., & Ghosh, S. (1998). Signal transduction through NF-kappa B. *Immunology Today*. [https://doi.org/10.1016/S0167-5699\(97\)01197-3](https://doi.org/10.1016/S0167-5699(97)01197-3)
- McCarthy, D. P., Richards, M. H., & Miller, S. D. (2012). Mouse models of multiple sclerosis: experimental autoimmune encephalomyelitis and Theiler's virus-induced demyelinating disease. *Methods Mol Biol*, 900, 381–401. https://doi.org/10.1007/978-1-60761-720-4_19
- McCormack, P. L. (2013). Natalizumab: A review of its use in the management of relapsing-remitting multiple sclerosis. *Drugs*. <https://doi.org/10.1007/s40265-013-0102-7>
- McKenzie, J. A., & Ridley, A. J. (2007). Roles of Rho/ROCK and MLCK in TNF-alpha-induced changes in endothelial morphology and permeability. *J Cell Physiol*, 213(1), 221–228. <https://doi.org/10.1002/jcp.21114>
- McQuibban, G. A., Gong, J. H., Tam, E. M., McCulloch, C. A., Clark-Lewis, I., & Overall, C. M. (2000). Inflammation dampened by gelatinase A cleavage of monocyte chemoattractant protein-3. *Science*, 289(5482), 1202–1206. Retrieved from <http://www.ncbi.nlm.nih.gov/pubmed/10947989>
- Meira, M., Sievers, C., Hoffmann, F., Rasenack, M., Kuhle, J., Derfuss, T., ... Lindberg, R. L. P. (2014).

- Unraveling natalizumab effects on deregulated miR-17 expression in CD4+ T cells of patients with relapsing-remitting multiple sclerosis. *Journal of Immunology Research*. <https://doi.org/10.1155/2014/897249>
- Miao, Y. S., Zhao, Y. Y., Zhao, L. N., Wang, P., Liu, Y. H., Ma, J., & Xue, Y. X. (2015). MiR-18a increased the permeability of BTB via RUNX1 mediated down-regulation of ZO-1, occludin and claudin-5. *Cell Signal*, 27(1), 156–167. <https://doi.org/10.1016/j.cellsig.2014.10.008>
- Minagar, A., & Alexander, J. S. (2003). Blood-brain barrier disruption in multiple sclerosis. *Mult Scler*, 9(6), 540–549.
- Mirowska-Guzel, D., Gromadzka, G., Mach, A., Czlonkowski, A., & Czlonkowska, A. (2011). Association of IL1A, IL1B, ILRN, IL6, IL10 and TNF- α polymorphisms with risk and clinical course of multiple sclerosis in a Polish population. *Journal of Neuroimmunology*. <https://doi.org/10.1016/j.jneuroim.2011.04.014>
- Miterski, B., Böhringer, S., Klein, W., Sindern, E., Haupts, M., Schimrigk, S., & Epplen, J. T. (2002). Inhibitors in the NF κ B cascade comprise prime candidate genes predisposing to multiple sclerosis, especially in selected combinations. *Genes and Immunity*. <https://doi.org/10.1038/sj.gene.6363846>
- Moeenrezakhanlou, A., Nandan, D., Shephard, L., & Reiner, N. E. (2007). 1 α ,25-dihydroxycholecalciferol activates binding of CREB to a CRE site in the CD14 promoter and drives promoter activity in a phosphatidylinositol-3 kinase-dependent manner. *J Leukoc Biol*, 81(5), 1311–1321. <https://doi.org/10.1189/jlb.1106681>
- Mohieldin, A. M., Zubayer, H. S. M., Al Omran, A. J., Saternos, H. C., Zarban, A. A., Nauli, S. M., & AbouAlaiwi, W. A. (2016). Vascular endothelial primary cilia: Mechanosensation and hypertension. *Current Hypertension Reviews*. <https://doi.org/10.2174/1573402111666150630140615>
- Mohri, T., Nakajima, M., Takagi, S., Komagata, S., & Yokoi, T. (2009). MicroRNA regulates human vitamin D receptor. *Int J Cancer*, 125(6), 1328–1333. <https://doi.org/10.1002/ijc.24459>
- Molinari, C., Rizzi, M., Squarzanti, D. F., Pittarella, P., Vacca, G., & Renò, F. (2013). 1 α ,25-dihydroxycholecalciferol (vitamin D3) induces NO-dependent endothelial cell proliferation and migration in a three-dimensional matrix. *Cellular Physiology and Biochemistry*. <https://doi.org/10.1159/000350099>
- Mukai, T., Otsuka, F., Otani, H., Yamashita, M., Takasugi, K., Inagaki, K., ... Makino, H. (2007). TNF- α

inhibits BMP-induced osteoblast differentiation through activating SAPK/JNK signaling. *Biochemical and Biophysical Research Communications*.
<https://doi.org/10.1016/j.bbrc.2007.03.099>

Munger, K. L., Levin, L. I., Hollis, B. W., Howard, N. S., & Ascherio, A. (2006). Serum 25-hydroxyvitamin D levels and risk of multiple sclerosis. *JAMA*, *296*(23), 2832–2838.
<https://doi.org/10.1001/jama.296.23.2832>

Muramatsu, F., Kidoya, H., Naito, H., Sakimoto, S., & Takakura, N. (2013). MicroRNA-125b inhibits tube formation of blood vessels through translational suppression of VE-cadherin. *Oncogene*.
<https://doi.org/10.1038/onc.2012.68>

Murugaiyan, G., Beynon, V., Mittal, A., Joller, N., & Weiner, H. L. (2011). Silencing microRNA-155 ameliorates experimental autoimmune encephalomyelitis. *J Immunol*, *187*(5), 2213–2221.
<https://doi.org/10.4049/jimmunol.1003952>

Mycko, M. P., Papoian, R., Boschert, U., Raine, C. S., & Selmaj, K. W. (2004). Microarray gene expression profiling of chronic active and inactive lesions in multiple sclerosis. *Clinical Neurology and Neurosurgery*. <https://doi.org/10.1016/j.clineuro.2004.02.019>

Naeini, A., Moeinzadeh, F., Vahdat, S., Ahmadi, A., Hedayati, Z., & Shahzeidi, S. (2017). The effect of Vitamin D administration on intracellular adhesion molecule-1 and vascular cell adhesion molecule-1 levels in hemodialysis patients: A placebo-controlled, double-blinded clinical trial. *Journal of Research in Pharmacy Practice*. <https://doi.org/10.4103/2279-042X.200994>

Naik, P., & Cucullo, L. (2012). In vitro blood-brain barrier models: current and perspective technologies. *J Pharm Sci*, *101*(4), 1337–1354. <https://doi.org/10.1002/jps.23022>

Nakayama, K. (2013). cAMP-response element-binding protein (CREB) and NF-kappaB transcription factors are activated during prolonged hypoxia and cooperatively regulate the induction of matrix metalloproteinase MMP1. *J Biol Chem*, *288*(31), 22584–22595.
<https://doi.org/10.1074/jbc.M112.421636>

Nelson, P. T., Wang, W. X., & Rajeev, B. W. (2008). MicroRNAs (miRNAs) in neurodegenerative diseases. In *Brain Pathology*. <https://doi.org/10.1111/j.1750-3639.2007.00120.x>

Ni, C., Wang, C., Zhang, J., Qu, L., Liu, X., Lu, Y., ... Qin, Z. (2014). Interferon- γ safeguards blood-brain barrier during experimental autoimmune encephalomyelitis. *American Journal of Pathology*.
<https://doi.org/10.1016/j.ajpath.2014.08.019>

Ni, J., Zhu, Y. N., Zhong, X. G., Ding, Y., Hou, L. F., Tong, X. K., ... Zuo, J. P. (2009). The chemokine

receptor antagonist, TAK-779, decreased experimental autoimmune encephalomyelitis by reducing inflammatory cell migration into the central nervous system, without affecting T cell function. *Br J Pharmacol*, 158(8), 2046–2056. Retrieved from <http://www.ncbi.nlm.nih.gov/pubmed/20050195>

Ni, Y., Teng, T., Li, R., Simonyi, A., Sun, G. Y., & Lee, J. C. (2017). TNF α alters occludin and cerebral endothelial permeability: Role of p38MAPK. *PLoS ONE*, 12(2). <https://doi.org/10.1371/journal.pone.0170346>

Niino, M., Fukazawa, T., Yabe, I., Kikuchi, S., Sasaki, H., & Tashiro, K. (2000). Vitamin D receptor gene polymorphism in multiple sclerosis and the association with HLA class II alleles. *J Neurol Sci*, 177(1), 65–71. Retrieved from <http://www.ncbi.nlm.nih.gov/pubmed/10967184>

Noseworthy, J. H., Lucchinetti, C., Rodriguez, M., & Weinshenker, B. G. (2000). Multiple sclerosis. *N Engl J Med*, 343(13), 938–952. <https://doi.org/10.1056/nejm200009283431307>

Nylander, A., & Hafler, D. A. (2012). Multiple sclerosis. *J Clin Invest*, 122(4), 1180–1188. <https://doi.org/10.1172/JCI58649>

O'Carroll, S. J., Kho, D. T., Wiltshire, R., Nelson, V., Rotimi, O., Johnson, R., ... Graham, E. S. (2015). Pro-inflammatory TNF α and IL-1 β differentially regulate the inflammatory phenotype of brain microvascular endothelial cells. *Journal of Neuroinflammation*. <https://doi.org/10.1186/s12974-015-0346-0>

O'Connell, R. M., Kahn, D., Gibson, W. S., Round, J. L., Scholz, R. L., Chaudhuri, A. A., ... Baltimore, D. (2010). MicroRNA-155 promotes autoimmune inflammation by enhancing inflammatory T cell development. *Immunity*, 33(4), 607–619. <https://doi.org/10.1016/j.immuni.2010.09.009>

Ohsawa, M., Koyama, T., Yamamoto, K., Hirosawa, S., Kamei, S., & Kamiyama, R. (2000). 1 α ,25-Dihydroxyvitamin D₃ and its potent synthetic analogs downregulate tissue factor and upregulate thrombomodulin expression in monocytic cells, counteracting the effects of tumor necrosis factor and oxidized LDL. *Circulation*. <https://doi.org/10.1161/01.CIR.102.23.2867>

Oksenberg, J. R., Baranzini, S. E., Barcellos, L. F., & Hauser, S. L. (2001). Multiple sclerosis: genomic rewards. *J Neuroimmunol*, 113(2), 171–184. Retrieved from <http://www.ncbi.nlm.nih.gov/pubmed/11164900>

Ono, M., Masaki, A., Maeda, A., Kilts, T. M., Hara, E. S., Komori, T., ... Young, M. F. (2018). CCN4/WISP1 controls cutaneous wound healing by modulating proliferation, migration and ECM expression in dermal fibroblasts via α 5 β 1 and TNF α . *Matrix Biology*.

<https://doi.org/10.1016/j.matbio.2018.01.004>

- Ortiz, G. G., Pacheco-Moisés, F. P., Macías-Islas, M. Á., Flores-Alvarado, L. J., Mireles-Ramírez, M. A., González-Renovato, E. D., ... Alatorre-Jiménez, M. A. (2014). Role of the Blood-Brain Barrier in Multiple Sclerosis. *Archives of Medical Research*. <https://doi.org/10.1016/j.arcmed.2014.11.013>
- Owens, A. P., & Mackman, N. (2010). Tissue factor and thrombosis: The clot starts here. *Thrombosis and Haemostasis*. <https://doi.org/10.1160/TH09-11-0771>
- Palmer, A. M. (2013). Multiple sclerosis and the blood-central nervous system barrier. *Cardiovasc Psychiatry Neurol*, 2013, 530356. <https://doi.org/10.1155/2013/530356>
- Palmer, H. G., Gonzalez-Sancho, J. M., Espada, J., Berciano, M. T., Puig, I., Baulida, J., ... Munoz, A. (2001). Vitamin D(3) promotes the differentiation of colon carcinoma cells by the induction of E-cadherin and the inhibition of beta-catenin signaling. *J Cell Biol*, 154(2), 369–387. Retrieved from <http://www.ncbi.nlm.nih.gov/pubmed/11470825>
- Pan, W., Wu, X., Kastin, A. J., Zhang, Y., Hsuchou, H., Halberg, F., ... Cornelissen-Guillaume, G. G. (2011). Potential protective role of IL15R α during inflammation. *Journal of Molecular Neuroscience*. <https://doi.org/10.1007/s12031-010-9459-1>
- Panizo, S., Barrio-Vazquez, S., Naves-Diaz, M., Carrillo-Lopez, N., Rodriguez, I., Fernandez-Vazquez, A., ... Cannata-Andia, J. B. (2013). Vitamin D receptor activation, left ventricular hypertrophy and myocardial fibrosis. *Nephrol Dial Transplant*, 28(11), 2735–2744. <https://doi.org/10.1093/ndt/gft268>
- Park, J. A., Choi, K. S., Kim, S. Y., & Kim, K. W. (2003). Coordinated interaction of the vascular and nervous systems: From molecule- to cell-based approaches. *Biochemical and Biophysical Research Communications*. <https://doi.org/10.1016/j.bbrc.2003.09.129>
- Paul, R., Lorenzl, S., Koedel, U., Sporer, B., Vogel, U., Frosch, M., & Pfister, H. W. (1998). Matrix metalloproteinases contribute to the blood-brain barrier disruption during bacterial meningitis. *Annals of Neurology*, 44(4), 592–600. <https://doi.org/10.1002/ana.410440404>
- Pedersen, L. B., Mogensen, J. B., & Christensen, S. T. (2016). Endocytic Control of Cellular Signaling at the Primary Cilium. *Trends in Biochemical Sciences*. <https://doi.org/10.1016/j.tibs.2016.06.002>
- Pedersen, L. B., Nashold, F. E., Spach, K. M., & Hayes, C. E. (2007). 1,25-dihydroxyvitamin D3 reverses experimental autoimmune encephalomyelitis by inhibiting chemokine synthesis and monocyte trafficking. *J Neurosci Res*, 85(11), 2480–2490. <https://doi.org/10.1002/jnr.21382>

- Peluso, M. O., Campbell, V. T., Harari, J. A., Tibbitts, T. T., Proctor, J. L., Whitebread, N., ... Faia, K. L. (2014). Impact of the smoothed inhibitor, IPI-926, on smoothed ciliary localization and hedgehog pathway activity. *PLoS ONE*. <https://doi.org/10.1371/journal.pone.0090534>
- Petersen, E. R., Sondergaard, H. B., Oturai, A. B., Jensen, P., Sorensen, P. S., Sellebjerg, F., & Bornsen, L. (2016). Soluble serum VCAM-1, whole blood mRNA expression and treatment response in natalizumab-treated multiple sclerosis. *Mult Scler Relat Disord*, *10*, 66–72. <https://doi.org/10.1016/j.msard.2016.09.001>
- Pfefferkorn, T., & Rosenberg, G. A. (2003). Closure of the blood-brain barrier by matrix metalloproteinase inhibition reduces rtPA-mediated mortality in cerebral ischemia with delayed reperfusion. *Stroke*, *34*(8), 2025–2030. <https://doi.org/10.1161/01.STR.0000083051.93319.28>
- Pilz, G., Harrer, A., Oppermann, K., Wipfler, P., Golaszewski, S., Afazel, S., ... Kraus, J. (2012). Molecular evidence of transient therapeutic effectiveness of natalizumab despite high-titre neutralizing antibodies. *Mult Scler*, *18*(4), 506–509. <https://doi.org/10.1177/1352458511423650>
- Pla-Navarro, I., Bevan, D., Hajihosseini, M. K., Lee, M., & Gavrilovic, J. (2018). Interplay between metalloproteinases and cell signalling in blood brain barrier integrity. *Histology and Histopathology*, 18003. <https://doi.org/10.14670/HH-18-003>
- Plumb, J., McQuaid, S., Cross, A. K., Surr, J., Haddock, G., Bunning, R. A., & Woodroffe, M. N. (2006). Upregulation of ADAM-17 expression in active lesions in multiple sclerosis. *Mult Scler*, *12*(4), 375–385.
- Ponomarev, E. D., Shriver, L. P., Maresz, K., Pedras-Vasconcelos, J., Verthelyi, D., & Dittel, B. N. (2007). GM-CSF Production by Autoreactive T Cells Is Required for the Activation of Microglial Cells and the Onset of Experimental Autoimmune Encephalomyelitis. *The Journal of Immunology*. <https://doi.org/10.4049/jimmunol.178.1.39>
- Prendergast, C., & Anderton, S. (2009). Immune cell entry to central nervous system--current understanding and prospective therapeutic targets. *Endocrine, Metabolic & Immune Disorders Drug Targets*. <https://doi.org/EMID-DT-ABS-00007> [pii]
- Puhlmann, M., Weinreich, D. M., Farma, J. M., Carroll, N. M., Turner, E. M., & Alexander, H. R. (2005). Interleukin-1 β induced vascular permeability is dependent on induction of endothelial tissue factor (TF) activity. *Journal of Translational Medicine*. <https://doi.org/10.1186/1479-5876-3-37>
- Pulido-Salgado, M., Vidal-Taboada, J. M., Garcia Diaz-Barriga, G., Serratosa, J., Valente, T., Castillo, P., ... Saura, J. (2017). Myeloid C/EBP β deficiency reshapes microglial gene expression and is

protective in experimental autoimmune encephalomyelitis. *Journal of Neuroinflammation*.
<https://doi.org/10.1186/s12974-017-0834-5>

Quagliarello, V. J., Wispelwey, B., Long, W. J., & Scheld, W. M. (1991). Recombinant human interleukin-1 induces meningitis and blood-brain barrier injury in the rat: Characterization and comparison with tumor necrosis factor. *Journal of Clinical Investigation*, 87(4), 1360–1366.
<https://doi.org/10.1172/JCI115140>

R&D. (n.d.). Cytokine-related Mechanisms of Apoptosis. Retrieved September 20, 2001, from
<https://www.rndsystems.com/resources/articles/cytokine-related-mechanisms-apoptosis>

Raab, S., Beck, H., Gaumann, A., Yüce, A., Gerber, H. P., Plate, K., ... Breier, G. (2004). Impaired brain angiogenesis and neuronal apoptosis induced by conditional homozygous inactivation of vascular endothelial growth factor. *Thrombosis and Haemostasis*, 91(3), 595–605.
<https://doi.org/10.1160/TH03-09-0582>

Radaelli, M., Merlini, A., Greco, R., Sangalli, F., Comi, G., Ciceri, F., & Martino, G. (2014). Autologous bone marrow transplantation for the treatment of multiple sclerosis. *Current Neurology and Neuroscience Reports*. <https://doi.org/10.1007/s11910-014-0478-0>

Ravindran, J., Agrawal, M., Gupta, N., & Lakshmana Rao, P. V. (2011). Alteration of blood brain barrier permeability by T-2 toxin: Role of MMP-9 and inflammatory cytokines. *Toxicology*.
<https://doi.org/10.1016/j.tox.2010.11.006>

Reddy, P., Slack, J. L., Davis, R., Cerretti, D. P., Kozlosky, C. J., Blanton, R. a, ... Black, R. a. (2000). Functional analysis of the domain structure of tumor necrosis factor-alpha converting enzyme. *The Journal of Biological Chemistry*, 275(19), 14608–14614.
<https://doi.org/10.1074/jbc.275.19.14608>

Reddycherla, A. V., Meinert, I., Reinhold, A., Reinhold, D., Schraven, B., & Simeoni, L. (2015). MiR-20a Inhibits TCR-Mediated signaling and cytokine production in human Naïve CD4⁺ T Cells. *PLoS ONE*.
<https://doi.org/10.1371/journal.pone.0125311>

Reeson, P., Tennant, K. A., Gerrow, K., Wang, J., Weiser Novak, S., Thompson, K., ... Brown, C. E. (2015). Delayed Inhibition of VEGF Signaling after Stroke Attenuates Blood-Brain Barrier Breakdown and Improves Functional Recovery in a Comorbidity-Dependent Manner. *Journal of Neuroscience*.
<https://doi.org/10.1523/JNEUROSCI.2810-14.2015>

Reijerkerk, A., Lopez-Ramirez, M. A., van Het Hof, B., Drexhage, J. A., Kamphuis, W. W., Kooij, G., ... de Vries, H. E. (2013). MicroRNAs regulate human brain endothelial cell-barrier function in

- inflammation: implications for multiple sclerosis. *J Neurosci*, 33(16), 6857–6863.
<https://doi.org/10.1523/jneurosci.3965-12.2013>
- Reiss, K., & Saftig, P. (2009). The “a disintegrin and metalloprotease” (ADAM) family of sheddases: physiological and cellular functions. *Semin Cell Dev Biol*, 20(2), 126–137.
<https://doi.org/10.1016/j.semcdb.2008.11.002>
- Rempe, R. G., Hartz, A. M., & Bauer, B. (2016). Matrix metalloproteinases in the brain and blood-brain barrier: Versatile breakers and makers. *J Cereb Blood Flow Metab*, 36(9), 1481–1507.
<https://doi.org/10.1177/0271678X16655551>
- Renault, M. A., Roncalli, J., Tongers, J., Thorne, T., Klyachko, E., Misener, S., ... Losordo, D. W. (2010). Sonic hedgehog induces angiogenesis via Rho kinase-dependent signaling in endothelial cells. *J Mol Cell Cardiol*, 49(3), 490–498. <https://doi.org/10.1016/j.yjmcc.2010.05.003>
- Reuss, B., Dono, R., & Unsicker, K. (2003). Functions of fibroblast growth factor (FGF)-2 and FGF-5 in astroglial differentiation and blood-brain barrier permeability: evidence from mouse mutants. *The Journal of Neuroscience: The Official Journal of the Society for Neuroscience*.
<https://doi.org/23/16/6404> [pii]
- Ribes, V., & Briscoe, J. (2009). Establishing and interpreting graded Sonic Hedgehog signaling during vertebrate neural tube patterning: the role of negative feedback. *Cold Spring Harb Perspect Biol*, 1(2), a002014. <https://doi.org/10.1101/cshperspect.a002014>
- Riobo, N. A., Lu, K., Ai, X., Haines, G. M., & Emerson Jr., C. P. (2006). Phosphoinositide 3-kinase and Akt are essential for Sonic Hedgehog signaling. *Proc Natl Acad Sci U S A*, 103(12), 4505–4510.
<https://doi.org/10.1073/pnas.0504337103>
- Rivera, S., Khrestchatisky, M., Kaczmarek, L., Rosenberg, G. A., & Jaworski, D. M. (2010). Metzincin proteases and their inhibitors: foes or friends in nervous system physiology? *J Neurosci*, 30(46), 15337–15357. <https://doi.org/10.1523/JNEUROSCI.3467-10.2010>
- Rodriguez, A., Vigorito, E., Clare, S., Warren, M. V, Couttet, P., Soond, D. R., ... Bradley, A. (2007). Requirement of bic/microRNA-155 for normal immune function. *Science*, 316(5824), 608–611.
<https://doi.org/10.1126/science.1139253>
- Rodriguez, D., Morrison, C. J., & Overall, C. M. (2010). Matrix metalloproteinases: what do they not do? New substrates and biological roles identified by murine models and proteomics. *Biochimica et Biophysica Acta*, 1803(1), 39–54. <https://doi.org/10.1016/j.bbamcr.2009.09.015>
- Ronaldson, P. T., Demarco, K. M., Sanchez-Covarrubias, L., Solinsky, C. M., & Davis, T. P. (2009).

Transforming growth factor-beta signaling alters substrate permeability and tight junction protein expression at the blood-brain barrier during inflammatory pain. *Journal of Cerebral Blood Flow and Metabolism : Official Journal of the International Society of Cerebral Blood Flow and Metabolism*. <https://doi.org/10.1038/jcbfm.2009.32>

Rosenberg, G. A., Cunningham, L. A., Wallace, J., Alexander, S., Estrada, E. Y., Grossetete, M., ... Gearing, A. (2001). Immunohistochemistry of matrix metalloproteinases in reperfusion injury to rat brain: Activation of MMP-9 linked to stromelysin-1 and microglia in cell cultures. *Brain Research*, 893(1–2), 104–112. [https://doi.org/10.1016/S0006-8993\(00\)03294-7](https://doi.org/10.1016/S0006-8993(00)03294-7)

Roy, S., Khanna, S., Krishnaraju, A. V., Subbaraju, G. V., Yasmin, T., Bagchi, D., & Sen, C. K. (2006). Regulation of vascular responses to inflammation: inducible matrix metalloproteinase-3 expression in human microvascular endothelial cells is sensitive to antiinflammatory Boswellia. *Antioxid Redox Signal*. <https://doi.org/10.1089/ars.2006.8.653>

Sajja, R. K., Prasad, S., & Cucullo, L. (2014). Impact of altered glycaemia on blood-brain barrier endothelium: an in vitro study using the hCMEC/D3 cell line. *Fluids Barriers CNS*, 11(1), 8. <https://doi.org/10.1186/2045-8118-11-8>

Savarin, C., Bergmann, C. C., Hinton, D. R., & Stohlman, S. A. (2013). MMP-independent role of TIMP-1 at the blood brain barrier during viral encephalomyelitis. *ASN Neuro*. <https://doi.org/10.1042/AN20130033>

Schiffenbauer, J., Streit, W. J., Butfiloski, E., Labow, M., Edwards, C., & Moldawer, L. L. (2000). The induction of EAE is only partially dependent on TNF receptor signaling but requires the IL-1 type I receptor. *Clinical Immunology*. <https://doi.org/10.1006/clim.2000.4851>

Schlomann, U., Rathke-Hartlieb, S., Yamamoto, S., Jockusch, H., & Bartsch, J. W. (2000). Tumor necrosis factor alpha induces a metalloprotease-disintegrin, ADAM8 (CD 156): implications for neuron-glia interactions during neurodegeneration. *The Journal of Neuroscience : The Official Journal of the Society for Neuroscience*, 20(21), 7964–7971.

Schumacher, N., Meyer, D., Mauermann, A., Von Der Heyde, J., Wolf, J., Schwarz, J., ... Rabe, B. (2015). Shedding of endogenous interleukin-6 receptor (IL-6R) is governed by a disintegrin and metalloproteinase (ADAM) proteases while a full-length IL-6R isoform localizes to circulating microvesicles. *Journal of Biological Chemistry*, 290(43), 26059–26071. <https://doi.org/10.1074/jbc.M115.649509>

Scilabra, S. D., Troebergs, L., Yamamoto, K., Emonard, H., Thgøersen, I., Enghild, J. J., ... Nagases, H.

- (2013). Differential regulation of extracellular tissue inhibitor of metalloproteinases-3 levels by cell membrane-bound and shed low density lipoprotein receptor-related protein 1. *Journal of Biological Chemistry*. <https://doi.org/10.1074/jbc.M112.393322>
- Sebastiani, G., Grieco, F. A., Spagnuolo, I., Galleri, L., Cataldo, D., & Dotta, F. (2011). Increased expression of microRNA miR-326 in type 1 diabetic patients with ongoing islet autoimmunity. *Diabetes Metab Res Rev*, 27(8), 862–866. <https://doi.org/10.1002/dmrr.1262>
- Semple, B. D., Kossman, T., & Morganti-Kossmann, M. C. (2010). Role of chemokines in CNS health and pathology: A focus on the CCL2/CCR2 and CXCL8/CXCR2 networks. *Journal of Cerebral Blood Flow and Metabolism*. <https://doi.org/10.1038/jcbfm.2009.240>
- Seo, J. H., Guo, S., Lok, J., Navaratna, D., Whalen, M. J., Kim, K. W., & Lo, E. H. (2012). Neurovascular matrix metalloproteinases and the blood-brain barrier. *Curr Pharm Des*, 18(25), 3645–3648. Retrieved from <http://www.ncbi.nlm.nih.gov/pmc/articles/PMC3814178/pdf/nihms-510077.pdf>
- Shan, N. L., Wahler, J., Lee, H. J., Bak, M. J., Gupta, S. Das, Maehr, H., & Suh, N. (2016). Vitamin D compounds inhibit cancer stem-like cells and induce differentiation in triple negative breast cancer. *The Journal of Steroid Biochemistry and Molecular Biology*. <https://doi.org/10.1016/j.jsbmb.2016.12.001>
- Sheng, W. H., Sheng, K. T., Zhao, Y. X., Li, H., Zhou, J. L., Yao, H. Y., & Li, X. H. (2015). Identifying the biomarkers of multiple sclerosis based on non-coding RNA signature. *European Review for Medical and Pharmacological Sciences*.
- Shi, Y., Zhang, L., Pu, H., Mao, L., Hu, X., Jiang, X., ... Chen, J. (2016). Rapid endothelial cytoskeletal reorganization enables early blood–brain barrier disruption and long-term ischaemic reperfusion brain injury. *Nature Communications*, 7, 10523. <https://doi.org/10.1038/ncomms10523>
- Simpson, J. E., Newcombe, J., Cuzner, M. L., & Woodroffe, M. N. (2000). Expression of the interferon-gamma-inducible chemokines IP-10 and Mig and their receptor, CXCR3, in multiple sclerosis lesions. *Neuropathol Appl Neurobiol*, 26(2), 133–142. Retrieved from <http://www.ncbi.nlm.nih.gov/pubmed/10840276>
- Singh, R. J., Mason, J. C., Lidington, E. A., Edwards, D. R., Nuttall, R. K., Khokha, R., ... Gavrilovic, J. (2005). Cytokine stimulated vascular cell adhesion molecule-1 (VCAM-1) ectodomain release is regulated by TIMP-3. *Cardiovasc Res*, 67(1), 39–49. <https://doi.org/10.1016/j.cardiores.2005.02.020>

- Singh, V. B., Singh, M. V., Gorantla, S., Poluektova, L. Y., & Maggirwar, S. B. (2016). Smoothened Agonist Reduces Human Immunodeficiency Virus Type-1-Induced Blood-Brain Barrier Breakdown in Humanized Mice. *Scientific Reports*, 6(February), 26876. <https://doi.org/10.1038/srep26876>
- Skoda, A. M., Simovic, D., Karin, V., Kardum, V., Vranic, S., & Serman, L. (2017). The role of the Hedgehog signaling pathway in cancer: A comprehensive review. *Bosnian Journal of Basic Medical Sciences*. <https://doi.org/10.17305/bjbms.2018.2756>
- Søndergaard, H. B., Hesse, D., Krakauer, M., Sørensen, P. S., & Sellebjerg, F. (2013). Differential microRNA expression in blood in multiple sclerosis. *Multiple Sclerosis (Houndmills, Basingstoke, England)*. <https://doi.org/10.1177/1352458513490542>
- Song, H.-L., Lv, S., & Liu, P. (2009). The roles of tumor necrosis factor-alpha in colon tight junction protein expression and intestinal mucosa structure in a mouse model of acute liver failure. *BMC Gastroenterology*. <https://doi.org/10.1186/1471-230X-9-70>
- Song, J., Wu, C., Korpos, E., Zhang, X., Agrawal, S. M., Wang, Y., ... Sorokin, L. (2015). Focal MMP-2 and MMP-9 Activity at the Blood-Brain Barrier Promotes Chemokine-Induced Leukocyte Migration. *Cell Rep*, 10(7), 1040–1054. <https://doi.org/10.1016/j.celrep.2015.01.037>
- Sporici, R., & Issekutz, T. B. (2010). CXCR3 blockade inhibits T-cell migration into the CNS during EAE and prevents development of adoptively transferred, but not actively induced, disease. *Eur J Immunol*, 40(10), 2751–2761. <https://doi.org/10.1002/eji.200939975>
- Stach, K., Kalsch, A. I., Nguyen, X. D., Elmas, E., Kraleov, S., Lang, S., ... Kalsch, T. (2011). 1alpha,25-dihydroxyvitamin D3 attenuates platelet activation and the expression of VCAM-1 and MT1-MMP in human endothelial cells. *Cardiology*, 118(2), 107–115. <https://doi.org/10.1159/000327547>
- Stach, K., Nguyen, X. D., Lang, S., Elmas, E., Weiß, C., Borggrefe, M., ... Kalsch, T. (2012). Simvastatin and atorvastatin attenuate VCAM-1 and uPAR expression on human endothelial cells and platelet surface expression of CD40 ligand. *Cardiology Journal*. <https://doi.org/10.5603/CJ.2012.0005>
- Stamatovic, S. M., Johnson, A. M., Keep, R. F., & Andjelkovic, A. V. (2016). Junctional proteins of the blood-brain barrier: New insights into function and dysfunction. *Tissue Barriers*, 4(1), e1154641. <https://doi.org/10.1080/21688370.2016.1154641>
- Sun, Z., Yin, Z., Liu, C., Liang, H., Jiang, M., & Tian, J. (2015). IL-1 β promotes ADAMTS enzyme-mediated aggrecan degradation through NF- κ B in human intervertebral disc. *Journal of Orthopaedic*

Surgery and Research, 10(1), 159. <https://doi.org/10.1186/s13018-015-0296-3>

- Suzuki, Y., Nagai, N., Yamakawa, K., Kawakami, J., Lijnen, H. R., & Umemura, K. (2009). Tissue-type plasminogen activator (t-PA) induces stromelysin-1 (MMP-3) in endothelial cells through activation of lipoprotein receptor-related protein. *Blood*. <https://doi.org/10.1182/blood-2009-02-203919>
- Szalay, G., Sauter, M., Haberland, M., Zuegel, U., Steinmeyer, A., Kandolf, R., & Klingel, K. (2009). Osteopontin: A fibrosis-related marker molecule in cardiac remodeling of enterovirus myocarditis in the susceptible host. *Circulation Research*. <https://doi.org/10.1161/CIRCRESAHA.109.193805>
- Tai, L. M., Holloway, K. A., Male, D. K., Loughlin, A. J., & Romero, I. A. (2010). Amyloid-beta-induced occludin down-regulation and increased permeability in human brain endothelial cells is mediated by MAPK activation. *J Cell Mol Med*, 14(5), 1101–1112. <https://doi.org/10.1111/j.1582-4934.2009.00717.x>
- Taipale, J., Cooper, M. K., Maiti, T., & Beachy, P. A. (2002). Patched acts catalytically to suppress the activity of Smoothed. *Nature*, 418(6900), 892–897. <https://doi.org/10.1038/nature00989>
- Tajouri, L., Ovcarić, M., Curtain, R., Johnson, M. P., Griffiths, L. R., Csurhes, P., ... Lea, R. A. (2005). Variation in the vitamin D receptor gene is associated with multiple sclerosis in an Australian population. *J Neurogenet*, 19(1), 25–38. <https://doi.org/10.1080/01677060590949692>
- Tan, X., Wen, X., & Liu, Y. (2008). Paricalcitol inhibits renal inflammation by promoting vitamin D receptor-mediated sequestration of NF-kappaB signaling. *J Am Soc Nephrol*, 19(9), 1741–1752. <https://doi.org/10.1681/ASN.2007060666>
- Tetlow, L. C., & Woolley, D. E. (1999). Effects of 1 alpha,25dihydroxyvitaminD3 on matrix metalloproteinase expression by rheumatoid synovial cells and articular chondrocytes in vitro. *Annals of the New York Academy of Sciences*, 878, 615–618.
- Thai, T. H., Calado, D. P., Casola, S., Ansel, K. M., Xiao, C., Xue, Y., ... Rajewsky, K. (2007). Regulation of the germinal center response by microRNA-155. *Science*, 316(5824), 604–608. <https://doi.org/10.1126/science.1141229>
- Thevenard, J., Verzeaux, L., Devy, J., Etique, N., Jeanne, A., Schneider, C., ... Emonard, H. (2014). Low-density lipoprotein receptor-related protein-1 mediates endocytic clearance of tissue inhibitor of metalloproteinases-1 and promotes its cytokine-like activities. *PLoS ONE*. <https://doi.org/10.1371/journal.pone.0103839>

- Tien, W. S., Chen, J. H., & Wu, K. P. (2017). SheddomeDB: the ectodomain shedding database for membrane-bound shed markers. *BMC Bioinformatics*, *18*(Suppl 3), 42. <https://doi.org/10.1186/s12859-017-1465-7>
- Tili, E., Michaille, J.-J., Cimino, A., Costinean, S., Dumitru, C. D., Adair, B., ... Croce, C. M. (2007). Modulation of miR-155 and miR-125b Levels following Lipopolysaccharide/TNF- α Stimulation and Their Possible Roles in Regulating the Response to Endotoxin Shock. *The Journal of Immunology*. <https://doi.org/10.4049/jimmunol.179.8.5082>
- Timms, P. M., Mannan, N., Hitman, G. A., Noonan, K., Mills, P. G., Syndercombe-Court, D., ... Boucher, B. J. (2002). Circulating MMP9, vitamin D and variation in the TIMP-1 response with VDR genotype: mechanisms for inflammatory damage in chronic disorders? *QJM*, *95*(12), 787–796. Retrieved from <http://www.ncbi.nlm.nih.gov/pubmed/12454321>
- Toft-Hansen, H., Nuttall, R. K., Edwards, D. R., & Owens, T. (2004). Key metalloproteinases are expressed by specific cell types in experimental autoimmune encephalomyelitis. *J Immunol*, *173*(8), 5209–5218. Retrieved from <http://www.jimmunol.org/content/173/8/5209.full.pdf>
- Trenova, A. G., Slavov, G. S., Draganova-Filipova, M. N., Mateva, N. G., Manova, M. G., Miteva, L. D., & Stanilova, S. A. (2018). Circulating levels of interleukin-17A, tumor necrosis factor-alpha, interleukin-18, interleukin-10, and cognitive performance of patients with relapsing-remitting multiple sclerosis. *Neurological Research*, 1–7. <https://doi.org/10.1080/01616412.2017.1420522>
- Trickler, W. J., Mayhan, W. G., & Miller, D. W. (2005). Brain microvessel endothelial cell responses to tumor necrosis factor-alpha involve a nuclear factor kappa B (NF-kappaB) signal transduction pathway. *Brain Research*, *1048*(1–2), 24–31. <https://doi.org/10.1016/j.brainres.2005.04.028>
- Uberti, F., Lattuada, D., Morsanuto, V., Nava, U., Bolis, G., Vacca, G., ... Molinari, C. (2014). Vitamin D protects human endothelial cells from oxidative stress through the autophagic and survival pathways. *Journal of Clinical Endocrinology and Metabolism*. <https://doi.org/10.1210/jc.2013-2103>
- Uhmann, A., Niemann, H., Lammering, B., Henkel, C., Hess, I., Rosenberger, A., ... Hahn, H. (2012). Calcitriol inhibits hedgehog signaling and induces vitamin d receptor signaling and differentiation in the patched mouse model of embryonal rhabdomyosarcoma. *Sarcoma*, *2012*, 357040. <https://doi.org/10.1155/2012/357040>
- Umeda, H., Ozaki, N., Mizutani, N., Fukuyama, T., Nagasaki, H., Arima, H., & Oiso, Y. (2010). Protective

effect of hedgehog signaling on cytokine-induced cytotoxicity in pancreatic beta-cells. *Exp Clin Endocrinol Diabetes*, 118(10), 692–698. <https://doi.org/10.1055/s-0030-1254151>

- Unemori, E. N., Bair, M. J., Bauer, E. A., & Amento, E. P. (1991). Stromelysin expression regulates collagenase activation in human fibroblasts. Dissociable control of two metalloproteinases by interferon-gamma. *J Biol Chem*, 266(34), 23477–23482. Retrieved from <http://www.ncbi.nlm.nih.gov/pubmed/1660474>
- Van den Steen, P. E., Van Aelst, I., Hvidberg, V., Piccard, H., Fiten, P., Jacobsen, C., ... Opendakker, G. (2006). The hemopexin and O-glycosylated domains tune gelatinase B/MMP-9 bioavailability via inhibition and binding to cargo receptors. *The Journal of Biological Chemistry*, 281(27), 18626–18637. <https://doi.org/10.1074/jbc.M512308200>
- van der Star, B. J., Vogel, D. Y., Kipp, M., Puentes, F., Baker, D., & Amor, S. (2012). In vitro and in vivo models of multiple sclerosis. *CNS Neurol Disord Drug Targets*, 11(5), 570–588.
- Vestweber, D. (2015). How leukocytes cross the vascular endothelium. *Nature Reviews Immunology*, 15(11), 692–704. <https://doi.org/10.1038/nri3908>
- Wallbaum, P., Rohde, S., Ehlers, L., Lange, F., Hohn, A., Bergner, C., ... Jaster, R. (2018). Antifibrogenic effects of Vitamin D derivatives on mouse pancreatic stellate cells. *World Journal of Gastroenterology*. <https://doi.org/10.3748/wjg.v24.i2.170>
- Wang, B. Q., Shi, M., Zhang, J. P., Wu, X., Chang, M. J., Chen, Z. H., ... Bai, C. X. (2018). Knockdown of Tfp1-Anchored Endothelial Cells Exacerbates Lipopolysaccharide-Induced Acute Lung Injury via NF-kappaB Signaling Pathway. *Shock (Augusta, Ga.)*. <https://doi.org/10.1097/SHK.0000000000001120>
- Wang, J., Zhang, X., Mu, L., Zhang, M., Gao, Z., Zhang, J., ... Li, H. (2014). T-PA acts as a cytokine to regulate lymphocyte-endothelium adhesion in experimental autoimmune encephalomyelitis. *Clinical Immunology*. <https://doi.org/10.1016/j.clim.2014.03.004>
- Wang, L., Fan, W., Cai, P., Fan, M., Zhu, X., Dai, Y., ... Zhao, B. Q. (2013). Recombinant ADAMTS13 reduces tissue plasminogen activator-induced hemorrhage after stroke in mice. *Ann Neurol*, 73(2), 189–198. <https://doi.org/10.1002/ana.23762>
- Wang, S., Reeves, B., & Pawlinski, R. (2016). Astrocyte tissue factor controls CNS hemostasis and autoimmune inflammation. *Thrombosis Research*. [https://doi.org/10.1016/S0049-3848\(16\)30369-3](https://doi.org/10.1016/S0049-3848(16)30369-3)
- Wang, X., Wang, H., Yang, H., Li, J., Cai, Q., Shapiro, I. M., & Risbud, M. V. (2014). Tumor necrosis

factor- α - and interleukin-1 β -dependent matrix metalloproteinase-3 expression in nucleus pulposus cells requires cooperative signaling via syndecan 4 and mitogen-activated protein kinase-NF- κ B axis: Implications in inflammatory disc disease. *American Journal of Pathology*. <https://doi.org/10.1016/j.ajpath.2014.06.006>

Wang, Y. H., Sui, X. M., Sui, Y. N., Zhu, Q. W., Yan, K., Wang, L. S., ... Zhou, J. H. (2015). BRD4 induces cell migration and invasion in HCC cells through MMP-2 and MMP-9 activation mediated by the Sonic hedgehog signaling pathway. *Oncol Lett*, *10*(4), 2227–2232. <https://doi.org/10.3892/ol.2015.3570>

Wang, Y., Jin, S., Sonobe, Y., Cheng, Y., Horiuchi, H., Parajuli, B., ... Suzumura, A. (2014). Interleukin-1 β induces blood-brain barrier disruption by downregulating sonic hedgehog in astrocytes. *PLoS ONE*, *9*(10), e110024. <https://doi.org/10.1371/journal.pone.0110024>

Waschbisch, A., Atiya, M., Linker, R. A., Potapov, S., Schwab, S., & Derfuss, T. (2011). Glatiramer acetate treatment normalizes deregulated microRNA expression in relapsing remitting multiple sclerosis. *PLoS One*, *6*(9), e24604. <https://doi.org/10.1371/journal.pone.0024604>

Waubant, E., Goodkin, D. E., Gee, L., Bacchetti, P., Sloan, R., Stewart, T., ... Miller, K. (1999). Serum MMP-9 and TIMP-1 levels are related to MRI activity in relapsing multiple sclerosis. *Neurology*, *53*(7), 1397–1401. Retrieved from <http://www.ncbi.nlm.nih.gov/pubmed/10534241>

Weaver, A., Goncalves da Silva, A., Nuttall, R. K., Edwards, D. R., Shapiro, S. D., Rivest, S., & Yong, V. W. (2005). An elevated matrix metalloproteinase (MMP) in an animal model of multiple sclerosis is protective by affecting Th1/Th2 polarization. *FASEB J*, *19*(12), 1668–1670. <https://doi.org/10.1096/fj.04-2030fje>

Wekerle, H., & Kurschus, F. C. (2006). Animal models of multiple sclerosis. *Drug Discovery Today: Disease Models*, *3*(4), 9. <https://doi.org/10.1016/j.ddmod.2006.11.004>

Weksler, B. B., Subileau, E. A., Perriere, N., Charneau, P., Holloway, K., Leveque, M., ... Couraud, P. O. (2005). Blood-brain barrier-specific properties of a human adult brain endothelial cell line. *FASEB J*, *19*(13), 1872–1874. <https://doi.org/10.1096/fj.04-3458fje>

Weksler, B., Romero, I. A., & Couraud, P. O. (2013). The hCMEC/D3 cell line as a model of the human blood brain barrier. *Fluids Barriers CNS*, *10*(1), 16. <https://doi.org/10.1186/2045-8118-10-16>

Wiggins-Dohlvik, K., Merriman, M., Shaji, C. A., Alluri, H., Grimsley, M., Davis, M. L., ... Tharakan, B. (2014). Tumor necrosis factor- α disruption of brain endothelial cell barrier is mediated through matrix metalloproteinase-9. *Am J Surg*, *208*(6), 954–60; discussion 960.

<https://doi.org/10.1016/j.amjsurg.2014.08.014>

Willenborg, D. O., Fordham, S., Bernard, C. C., Cowden, W. B., & Ramshaw, I. A. (1996). IFN-gamma plays a critical down-regulatory role in the induction and effector phase of myelin oligodendrocyte glycoprotein-induced autoimmune encephalomyelitis. *Journal of Immunology (Baltimore, Md. : 1950)*.

Won, S., Sayeed, I., Peterson, B. L., Wali, B., Kahn, J. S., & Stein, D. G. (2015). Vitamin D prevents hypoxia/reoxygenation-induced blood-brain barrier disruption via vitamin D receptor-mediated NF-kB signaling pathways. *PLoS One*, *10*(3), e0122821. <https://doi.org/10.1371/journal.pone.0122821>

Wu, K., Fukuda, K., Xing, F., Zhang, Y., Sharma, S., Liu, Y., ... Watabe, K. (2015). Roles of the cyclooxygenase 2 matrix metalloproteinase 1 pathway in brain metastasis of breast cancer. *J Biol Chem*, *290*, 9842–9854. <https://doi.org/10.1074/jbc.M114.602185>

Wu, X., Pan, W., Stone, K. P., Zhang, Y., Hsueh, H., & Kastin, A. J. (2010). Expression and signaling of novel IL15R?? splicing variants in cerebral endothelial cells of the blood-brain barrier. *Journal of Neurochemistry*. <https://doi.org/10.1111/j.1471-4159.2010.06729.x>

Xia, Y. peng, He, Q. wei, Li, Y. nan, Chen, S. cai, Huang, M., Wang, Y., ... Hu, B. (2013). Recombinant human sonic hedgehog protein regulates the expression of ZO-1 and occludin by activating angiopoietin-1 in stroke damage. *PLoS ONE*, *8*(7), e68891. <https://doi.org/10.1371/journal.pone.0068891>

Xie, S., Issa, R., Sukkar, M. B., Oltmanns, U., Bhavsar, P. K., Papi, A., ... Chung, K. F. (2005). Induction and regulation of matrix metalloproteinase-12 in human airway smooth muscle cells. *Respiratory Research*, *6*, 148. <https://doi.org/10.1186/1465-9921-6-148>

Xing, Y., Shepherd, N., Lan, J., Li, W., Rane, S., Gupta, S. K., ... Yu, Q. (2017). MMPs/TIMPs imbalances in the peripheral blood and cerebrospinal fluid are associated with the pathogenesis of HIV-1-associated neurocognitive disorders. *Brain, Behavior, and Immunity*. <https://doi.org/10.1016/j.bbi.2017.04.024>

Yamamoto, K., Murphy, G., & Troeberg, L. (2015). Extracellular regulation of metalloproteinases. *Matrix Biology*. <https://doi.org/10.1016/j.matbio.2015.02.007>

Yamamoto, K., Owen, K., Parker, A. E., Scilabra, S. D., Dudhia, J., Strickland, D. K., ... Nagase, H. (2014). Low density lipoprotein receptor-related protein 1 (LRP1)-mediated endocytic clearance of a disintegrin and metalloproteinase with thrombospondin motifs-4 (ADAMTS-4): functional

- differences of non-catalytic domains of ADAMTS-4 and ADAMTS-5 in LRP1 binding. *The Journal of Biological Chemistry*, 289(10), 6462–6474. <https://doi.org/10.1074/jbc.M113.545376>
- Yamamoto, K., Santamaria, S., Botkjaer, K. A., Dudhia, J., Troeberg, L., Itoh, Y., ... Nagase, H. (2017). Inhibition of Shedding of Low-Density Lipoprotein Receptor-Related Protein 1 Reverses Cartilage Matrix Degradation in Osteoarthritis. *Arthritis & Rheumatology*. <https://doi.org/10.1002/art.40080>
- Yamamoto, K., Troeberg, L., Scilabra, S. D., Pelosi, M., Murphy, C. L., Strickland, D. K., & Nagase, H. (2013). LRP-1-mediated endocytosis regulates extracellular activity of ADAMTS-5 in articular cartilage. *FASEB Journal*. <https://doi.org/10.1096/fj.12-216671>
- Yang, Q., Pan, W., & Qian, L. (2017). Identification of the miRNA–mRNA regulatory network in multiple sclerosis. *Neurological Research*. <https://doi.org/10.1080/01616412.2016.1250857>
- Yang, Y., Estrada, E. Y., Thompson, J. F., Liu, W., & Rosenberg, G. A. (2007). Matrix Metalloproteinase-Mediated Disruption of Tight Junction Proteins in Cerebral Vessels is Reversed by Synthetic Matrix Metalloproteinase Inhibitor in Focal Ischemia in Rat. *Journal of Cerebral Blood Flow & Metabolism*, 27(4), 697–709. <https://doi.org/10.1038/sj.jcbfm.9600375>
- Yang, Z., Strickland, D. K., & Bornstein, P. (2001). Extracellular Matrix Metalloproteinase 2 Levels are Regulated by the Low Density Lipoprotein-related Scavenger Receptor and Thrombospondin 2. *Journal of Biological Chemistry*. <https://doi.org/10.1074/jbc.M008925200>
- Yao, R., Ma, Y. L., Liang, W., Li, H. H., Ma, Z. J., Yu, X., & Liao, Y. H. (2012). MicroRNA-155 modulates Treg and Th17 cells differentiation and Th17 cell function by targeting SOCS1. *PLoS One*, 7(10), e46082. <https://doi.org/10.1371/journal.pone.0046082>
- Yednock, T. A., Cannon, C., Fritz, L. C., Sanchez-Madrid, F., Steinman, L., & Karin, N. (1992). Prevention of experimental autoimmune encephalomyelitis by antibodies against alpha 4 beta 1 integrin. *Nature*, 356(6364), 63–66. <https://doi.org/10.1038/356063a0>
- Yepes, M., Sandkvist, M., Moore, E. G., Bugge, T. H., Strickland, D. K., & Lawrence, D. A. (2003). Tissue-type plasminogen activator induces opening of the blood-brain barrier via the LDL receptor-related protein. *Journal of Clinical Investigation*. <https://doi.org/10.1172/JCI200319212>
- Yi, J., Zhu, Y., Jia, Y., Jiang, H., Zheng, X., Liu, D., ... Wang, K. (2016). The Annexin a2 Promotes Development in Arthritis through Neovascularization by Amplification Hedgehog Pathway. *PLoS One*, 11(3), e0150363. <https://doi.org/10.1371/journal.pone.0150363>
- Yildirim, B., Guler, T., Akbulut, M., Oztekin, O., & Sariiz, G. (2014). 1-alpha,25-dihydroxyvitamin D3

regresses endometriotic implants in rats by inhibiting neovascularization and altering regulation of matrix metalloproteinase. *Postgraduate Medicine*.
<https://doi.org/10.3810/pgm.2014.01.2730>

Yin, Z., Pinteá, V., Lin, Y., Hammock, B. D., & Watsky, M. A. (2011). Vitamin D enhances corneal epithelial barrier function. *Invest Ophthalmol Vis Sci*, 52(10), 7359–7364.
<https://doi.org/10.1167/iovs.11-7605>

Yong, V. W. (2005). Metalloproteinases: mediators of pathology and regeneration in the CNS. *Nat Rev Neurosci*, 6(12), 931–944. <https://doi.org/10.1038/nrn1807>

Yoo, Y. A., Kang, M. H., Lee, H. J., Kim, B. H., Park, J. K., Kim, H. K., ... Oh, S. C. (2011). Sonic hedgehog pathway promotes metastasis and lymphangiogenesis via activation of Akt, EMT, and MMP-9 pathway in gastric cancer. *Cancer Res*, 71(22), 7061–7070. <https://doi.org/10.1158/0008-5472.CAN-11-1338>

Yu, G., Rux, A. H., Ma, P., Bdeir, K., & Sachais, B. S. (2005). Endothelial expression of E-selectin is induced by the platelet-specific chemokine platelet factor 4 through LRP in an NF- κ B-dependent manner. *Blood*. <https://doi.org/10.1182/blood-2004-07-2617>

Yuan, W., Pan, W., Kong, J., Zheng, W., Szeto, F. L., Wong, K. E., ... Li, Y. C. (2007). 1,25-dihydroxyvitamin D3 suppresses renin gene transcription by blocking the activity of the cyclic AMP response element in the renin gene promoter. *The Journal of Biological Chemistry*.
<https://doi.org/10.1074/jbc.M705495200>

Yun, S. P., Lee, S. J., Oh, S. Y., Jung, Y. H., Ryu, J. M., Suh, H. N., ... Han, H. J. (2014). Reactive oxygen species induce MMP12-dependent degradation of collagen 5 and fibronectin to promote the motility of human umbilical cord-derived mesenchymal stem cells. *Br J Pharmacol*, 171(13), 3283–3297. <https://doi.org/10.1111/bph.12681>

Zhang, R., Dong, H., Zhao, H., Zhou, L., Zou, F., & Cai, S. (2016). 1, 25-Dihydroxyvitamin D3 targeting VEGF pathway alleviates house dust mite (HDM)-induced airway epithelial barrier dysfunction. *Cellular Immunology*, 312, 1–10. <https://doi.org/10.1016/j.cellimm.2016.11.004>

Zhang, X., Jin, J., Peng, X., Ramgolam, V. S., & Markovic-Plese, S. (2008). Simvastatin Inhibits IL-17 Secretion by Targeting Multiple IL-17-Regulatory Cytokines and by Inhibiting the Expression of IL-17 Transcription Factor RORC in CD4+ Lymphocytes. *The Journal of Immunology*.
<https://doi.org/10.4049/jimmunol.180.10.6988>

Zhang, X., Polavarapu, R., She, H., Mao, Z., & Yepes, M. (2007). Tissue-type plasminogen activator and

the low-density lipoprotein receptor-related protein mediate cerebral ischemia-induced nuclear factor-kappaB pathway activation. *The American Journal of Pathology*. <https://doi.org/10.2353/ajpath.2007.070472>

Zhang, X., & Zanello, L. P. (2008). Vitamin D receptor-dependent 1 alpha,25(OH)₂ vitamin D₃-induced anti-apoptotic PI3K/AKT signaling in osteoblasts. *J Bone Miner Res*, 23(8), 1238–1248. <https://doi.org/10.1359/jbmr.080326>

Zhang, Y. G., Wu, S., & Sun, J. (2013). Vitamin D, Vitamin D Receptor, and Tissue Barriers. *Tissue Barriers*, 1(1). <https://doi.org/10.4161/tisb.23118>

Zhang, Y., Han, Y., Zhao, Y., Lv, Y., Hu, Y., Tan, Y., ... Kou, J. (2017). DT-13 ameliorates TNF- α -induced vascular endothelial hyperpermeability via non-muscle myosin IIA and the Src/PI3K/Akt signaling pathway. *Frontiers in Immunology*. <https://doi.org/10.3389/fimmu.2017.00925>

Zhang, Z., & Zhang, R. (2015). Epigenetics in autoimmune diseases: Pathogenesis and prospects for therapy. *Autoimmunity Reviews*. <https://doi.org/10.1016/j.autrev.2015.05.008>

Zhao, M., Tang, S.-N., Marsh, J. L., Shankar, S., & Srivastava, R. K. (2013). Ellagic acid inhibits human pancreatic cancer growth in Balb c nude mice. *Cancer Letters*. <https://doi.org/10.1016/j.canlet.2013.05.009>

Zhao, X., Tang, Y., Qu, B., Cui, H., Wang, S., Wang, L., ... Shen, N. (2010). MicroRNA-125a contributes to elevated inflammatory chemokine RANTES levels via targeting KLF13 in systemic lupus erythematosus. *Arthritis Rheum*, 62(11), 3425–3435. <https://doi.org/10.1002/art.27632>

Zhen, H., Zhao, L., Ling, Z., Kuo, L., Xue, X., & Feng, J. (2018). Wip1 regulates blood-brain barrier function and neuro-inflammation induced by lipopolysaccharide via the sonic hedgehog signaling pathway. *Molecular Immunology*, 93, 31–37. <https://doi.org/10.1016/j.molimm.2017.09.020>

Zheng, Y., Sun, L., Jiang, T., Zhang, D., He, D., & Nie, H. (2014). TNF α promotes th17 cell differentiation through il-6 and il-1 β produced by monocytes in rheumatoid arthritis. *Journal of Immunology Research*. <https://doi.org/10.1155/2014/385352>

Zhong, Y., Zhang, B., Eum, S. Y., & Toborek, M. (2012a). HIV-1 Tat triggers nuclear localization of ZO-1 via Rho signaling and cAMP response element-binding protein activation. *J Neurosci*, 32(1), 143–150. <https://doi.org/10.1523/jneurosci.4266-11.2012>

Zhong, Y., Zhang, B., Eum, S. Y., & Toborek, M. (2012b). HIV-1 Tat Triggers Nuclear Localization of ZO-1 via Rho Signaling and cAMP Response Element-Binding Protein Activation. *Journal of*

Neuroscience. <https://doi.org/10.1523/JNEUROSCI.4266-11.2012>

Zhou, X., Zhao, H., & Cai, S. (2011). [25-hydroxyvitamin D3-induced increases of normal human airway epithelial cell permeability is not mediated by upregulated ZO-1 expression]. *Nan fang yi ke da xue xue bao = Journal of Southern Medical University*, 31(7), 1187–1189.

Zhu, S. L., Luo, M. Q., Peng, W. X., Li, Q. X., Feng, Z. Y., Li, Z. X., ... Huang, J. L. (2014). Sonic hedgehog signalling pathway regulates apoptosis through Smo protein in human umbilical vein endothelial cells. *Rheumatology (Oxford)*. <https://doi.org/10.1093/rheumatology/keu421>

Zhu, S. L., Luo, M. Q., Peng, W. X., Li, Q. X., Feng, Z. Y., Li, Z. X., ... Huang, J. L. (2015). Sonic hedgehog signalling pathway regulates apoptosis through Smo protein in human umbilical vein endothelial cells. *Rheumatology (United Kingdom)*. <https://doi.org/10.1093/rheumatology/keu421>